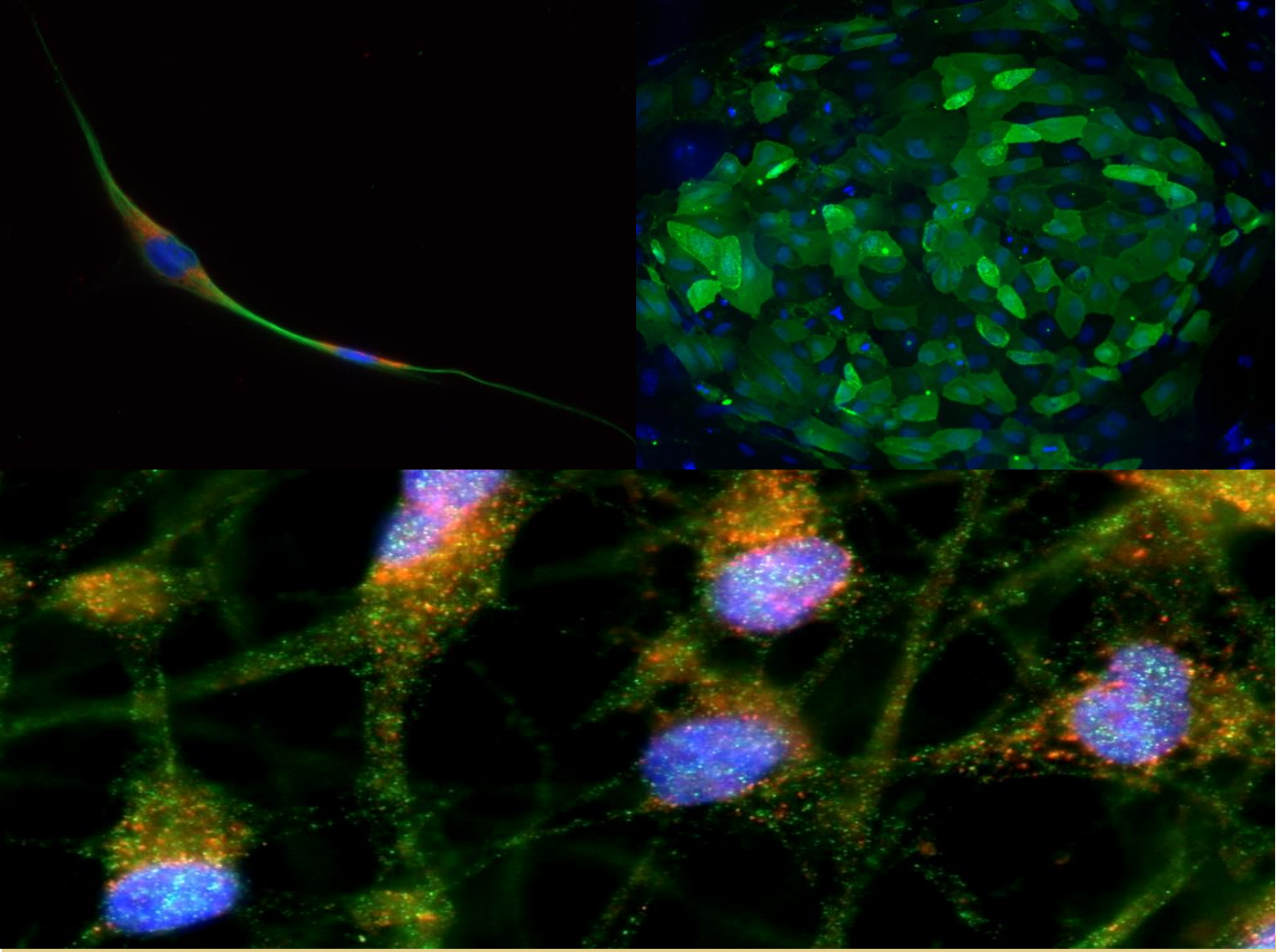

Isabel Maria dos Santos Onofre

Dissecting the pathogenesis of Machado-Joseph Disease in a new human disease model derived from induced pluripotent stem cells

Tese de doutoramento em Ciências Farmacêuticas, na área de especialização em Biotecnologia Farmacêutica, orientada pelo Doutor Luís Fernando Morgado Pereira de Almeida e Doutor Henry Paulson apresentada à Faculdade de Farmácia da Universidade de Coimbra

Dezembro de 2015

· U C ·

UNIVERSIDADE DE COIMBRA

Dissecting the pathogenesis of Machado-Joseph Disease in a new human disease model derived from induced pluripotent stem cells

Isabel Maria dos Santos Onofre

Universidade de Coimbra

2015

Dissecting the pathogenesis of Machado-Joseph Disease in a new human disease model derived from induced pluripotent stem cells

Isabel Maria dos Santos Onofre

Thesis submitted to the Faculty of Pharmacy of the University of Coimbra for the attribution of the Doctor degree in Pharmaceutical Sciences, in the specialty field of Pharmaceutical Biotechnology.

Tese apresentada à Faculdade de Farmácia da Universidade de Coimbra para prestação de provas de doutoramento em Ciências Farmacêuticas, na área de especialização de Biotecnologia Farmacêutica.

Universidade de Coimbra

2015

Dissecting the pathogenesis of Machado-Joseph Disease in a new human disease model derived from induced pluripotent stem cells

The research work presented in this thesis was performed at the Center for Neuroscience and Cell Biology of Coimbra, University of Coimbra, Portugal and at the Hubrecht Institute, The Netherlands under supervision of Dr. Luís Pereira de Almeida and Dr Niels Giejsen.

O trabalho experimental apresentado nesta tese foi realizado no Centro de Neurociências e Biologia Celular de Coimbra, Portugal e no Hubrecht Institute, Holanda sob supervisão do Professor Doutor Luis Pereira de Almeida e do Doutor Niels Geijsen.

This work was supported by the Portuguese Foundation for Science and Technology, fellowship SFRH/BD/61461/ 2009 and by funds FEDER through Programa Mais Centro (CENTRO-07-ST24-FEDER-002006) and the Competitive Factors Operational Program–COMPETE; grants PTDC/SAU-NMC/116512/2010) and PEst-C/SAU/LA0001/2013-2014; by the Richard Chin and Lily Lock Machado Joseph Disease Research Fund; and the National Ataxia Foundation.

Este trabalho foi financiado pela Fundação para a Ciência e a Tecnologia (FCT), bolsa de doutoramento com a referência, SFRH/BD/61461/ 2009, Programa Mais Centro e Programa Operacional Factores de Competitividade (COMPETE), Projectos PTDC/SAU-NMC/116512/2010 e PEst-C/SAU/LA0001/2013-2014, pelo *Richard Chin and Lily Lock Machado-Joseph research fund* e a *National Ataxia Foundation.*

Front Cover:

Fluorescence Immunocytochemistry-from fibroblasts to neurons.
Top left: microscope image of fibroblasts stained for ataxin-3 (green), TE-7 (red) and DAPI; top right: microscope image of an iPS cell colony stained for TRA-1-60 (green) and DAPI (blue); bottom: microscope image of a neuronal culture stained for ataxin- 3 (green), ubiquitin (red) and DAPI (blue).

“Nothing is more powerful than an idea whose time has come.”

- Victor Hugo

A minha Mãe

e a meus Avós

Acknowledgements/Agradecimentos

"As pessoas sonhavam nesses tempos com os microscópios ainda melhores que viriam a seguir, que revelariam ainda mais universos ocultos. E com esses microscópios, disse Senebier, um dia chegaríamos a ver "o presente grávido de todo o futuro. "O presente grávido de todo o futuro! Não gostavam vocês de ver isto um dia? Então estudem. Estudem muito. Não há outra maneira de se chegar lá."

Clara Pinto Correia, *in prefácio* de Oliveira E, Pedrosa C e Pires R. *Da Célula ao Universo: Ciências da Terra e da Vida*: 11.ºano.Texto Editora. Lisboa (2002).

Ao Professor Doutor Luís Pereira de Almeida agradeço a sua orientação científica, o seu total apoio e confiança no decurso deste trabalho de doutoramento, que em muito contribuiram para a minha formação e cultura científicas. Agradeço ainda a sua amizade e generosidade que sempre demonstrou. Foi um enorme privilégio o de poder contar sempre com a sua elevada capacidade científicas e dimensão humana ao longo deste percurso! Um profundo muito obrigada!

To Dr. Niels Geijsen for accepting me in his laboratory and for the strong encouragement, support and friendship during my PhD.

À Professora Doutora Maria Conceição Pedroso de Lima agradeço a oportunidade de poder desenvolver este trabalho no Grupo de Vectores e Terapia Génica.

À Professora Doutora Catarina Resende de Oliveira agradeço a oportunidade de poder desenvolver este trabalho no Centro de Neurociências e Biologia Celular de Coimbra.

À Fundação para a Ciência e Tecnologia agradeço o seu financiamento sem o qual esta tese não teria sido possível.

To all my lab colleagues at the Hubrecht Institute, Nune Schelling-Kazaryan, Diego D'Astolfo, Nicolas Rivron, Maaike Welling and Manda Auberbach for all the great scientific and non-scientific moments that we shared. Thanks for all the support and friendship! It was a fantastic experience for me!

A todos os meus colegas e amigos no do Grupo de Vectores e Terapia Génica do Centro de Neurociências e Biologia Celular da Universidade de Coimbra, especialmente à Isabel Ferreira, Clévio Nóbrega e Lígia Ferreira, que foram os meus mentores na iniciação científica. Um agradecimento muito especial ao Manuel Garrido, pela infinita paciência e inesgotável fonte de conselhos e truques científicos; e aos que serão sempre os meus eternos "colegas de bancada": Ana Teresa Simões e Nélio Gonçalves, por todos os momentos partilhados, por terem sido o modelo a seguir.

Agradeço também a todos os meus colegas, Mariana Conceição, Joana Neves, Vitor Carmona, Patricia Rosado, Ana Cristina Ferreira, Dina Pereira, Janete Santos, Sara Lopes, Geetha Vijayakumar, Liliana Mendonça, Rui Nobre, Catarina Miranda e Sónia Duarte pelo companheirismo e amizade.

Um agradecimento especial ao “gang JN”, ao Nuno Fonseca pela partilha de ideias e combates “científico-futebolisticos”;à Ângela Fernandes a parceira de diabruras e de um uso muito peculiar de diminutivos; à Ana Gregório, pelo seu bom-humor e “boletim de notícias extraordinárias”, que só ela poderia encontrar; à Sarah Pagliaro pelo seu entusiasmo e parcerias em organização de eventos no nosso laboratório; à Carla Gomes e à Ligia Silva pela sua amizade e atitude *no-nonsense*!

Não poderia deixar de agradecer ao Pedro Costa e ao Carlos Custódia, pela co-fundação e pelas generosas contribuições para o “GVTG,enterranços, calinadas e outras cientifidades tais!”

Às Joaníssimas, Joana Fernandes e Joana Vindeirinho, pela amizade, pelo carinho, pelas inúmeras tertúlias acerca de tudo e mais alguma coisa, pelo apoio e pela boa disposição!

Aos meus amigos de “fora do laboratório”, à Elsa Silva, ao Gustavo Costa, ao Pedro Gouveia e à Sónia Pereira, pelas viagens, as férias, D&D e todo o convivio e amizade ao longo destes anos!

Finalmente, à minha família, em particular à minha mãe e avós por sempre terem acreditado em mim e por terem sido pilares na minha vida.

Obrigada pelo carinho, compreensão e amizade durante todos estes anos.

Esta tese é-vos dedicada

Table of contents

Abbreviations

ABCG2	ATP-binding cassette sub-family G member 2
AFP	Alpha-fetoprotein
ALK	Activin receptor-like kinase
ALS	Amyotrophic lateral sclerosis
BDNF	Brain-derived neurotrophic factor
bFGF	Basic fibroblast growth factor
BSA	bovine serum albumin
Ca^{2+}	Calcium ion
CDX2	Caudal Type Homeobox
Ck 5/6	Cytokeratin 5/6
c-MYC	v-myc avian myelocytomatosis viral oncogene homolog
CQ	Chloroquine
DAPI	4',6-diamidino-2-phenylindole
DMEM	Dulbecco's Modified Eagle Medium
DNMT3B	DNA (cytosine-5-)-methyltransferase 3 beta
DRPLA	Dentatorubral and Pallidoluysian Atrophy
EBs	Embryoid bodies
EGF	Epidermal growth factor
EOMES	Eomesodermin
ER	Endoplasmic reticulum
ES cells	Embryonic stem cells
FBS	Fetal bovine serum
FD	Familial dysautonomia
GABA	γ-Amino-butyric Acid
GCTs	germ cell tumors
GDF3	growth and differentiation factor 3
GDNF	Glial cell line-derived neurotrophic factor
GFAP	Glial fibrillary acidic protein
GSK-3β	Glycogen synthase kinase-3 beta
HD	Huntington’s Disease

HDAC	Histone deacetylase
HEK 293T	Human embryonic kidney 293 T cell line
hES cells	Human embryonic stem cells
hESC	Human embryonic stem cells
HIF	Hypoxia-inducible factor
hiPS cells	Human induced pluripotent stem cells
hiPSCs	human induced pluripotent stem cells
ICM	Inner cell mass
iPS cell	Induced pluripoten stem cells
KCL	Potassium chloride
KLF4	Kruppel-like factor 4
LC3	Microtubule-associated protein 1A/1B-light chain 3
L-Glu	L-Glutamine
LSD1	Lysine-specific demethylase 1
MAP2	Microtubule-associated protein 2
MEFs	Mouse embryonic fibroblasts
MEK/ERK	Mitogen-activated protein kinase kinase/extracellular signal-regulated kinase
MJD	Machado Joseph Disease
MOI	Multiplicity of infection
NDM	Neuronal differentiation medium
NEAA	Non-Essential Amino Acid
NIM	Neural induction culture medium
NSCs	Neural stem cell
NSE	Neuron specific enolase
OCT4	Octamer-binding transcription factor 4 or POU5F1-POU domain, class 5, transcription factor 1
p62/SQSTM	p62/Sequestosome 1
PBS	Phosphate-buffered saline
PCR	Polymerase chain reaction
PD	Parkinson’s Disease
PFA	Paraformaldehyde
PFK1	Phosphofructokinase 1
PHD	Prolyl-hydroxylase s
PI3 kinase com	Phosphoinositide 3-kinase complex

PolyQ	Polyglutamine
qRT-PCR	Quantitative reverse transcriptase - polymerase chain reaction
REX1	Reduced Expressed 1/Zinc finger protein 42
s100	S100 calcium-binding protein
SBMA	Spinal and Bulbar Atrophy
SCA	Spinocerebellar Ataxia
SMA	Spinal muscular atrophy
SNP	Single-nucleotide polymorphism
SOX2	Sex determining region Y-box 2
SSEA4	Stage-specific embryonic antigen-4
TDGF1	Teratocarcinoma-derived growth factor 1
TERT	Telomerase reverse transcriptase
TF	Transcription factor
TRA-1-60	Tumor-related Antigen-1-60
TTF1	Thyroid transcription factor-1
UPS	Ubiquitin-proteosome system
Vit C	Vitamin C
VPA	Valproic acid
α-SMA	α-Smooth Muscle Actin

Resumo

A doença de Machado-Joseph, também conhecida por ataxia espinocerebelosa tipo 3, é a ataxia autossómica dominante mais comum a nível mundial. A DMJ é uma doença neurodegenerativa de início tardio causado por uma expansão de CAGs na região codificante do gene *ATXN3* localizado no cromossoma 14q32.1, sendo a mutação traduzida numa cadeia de poliglutaminas anormalmente longa na proteína ataxina-3.

Com o desenvolvimento das células estaminais pluripotentes induzidas (iPSCs), o estudo da patologia da MJD deixou de estar restrito a modelos de doença artificiais, tais como modelos animais ou linhas celulares, que apresentam limitações como modelos de doenças neurodegenerativas. Nesse sentido, nesta tese, o nosso objectivo foi o de desenvolver um novo modelo in vitro humano para estudar a DMJ.

Esta tese está organizada em 4 capítulos. No capítulo 1, é feita uma revisão acerca das principais características patológicas da MJD e também uma revisão acerca de modelos *in vitro* derivados de células estaminais pluripotentes induzidas.

No capítulo 2 é descrito o desenvolvimento e investigação do fenótipo DMJ em fibroblastos adultos da derme de doentes. As culturas foram caracterizadas geneticamente e o fenótipo DMJ foi estudado neste tipo particular de células não-neuronais, atendendo à disfunção autofágica. Foi encontrada uma disfunção da autofagia relacionada com o fenótipo DMJ, em particular, níveis reduzidos de beclina-1 e redução de formação de autofagossomas.

No capítulo 3, reportamos o sucesso da geração de iPSCs a partir das culturas de fibroblastos da derme previamente estabelecidas. Foi utilizado um vector lentiviral para expressar os 4 factores de reprogramação (Sox2, Oct4, Klf4 e c-Myc) na reprogramação dos fibroblastos humanos adultos da derme. A pluripotência destas células foi totalmente caracterizada, atendendo aos critérios de morfologia, marcadores moleculares, como a actividade da fosfatase alcalina, expressão de marcadores de superfície e de factores de transcrição nucleares e de genes associados à pluripotência celular; e de ensaios funcionais, particularmente os ensaios de diferenciação *in vitro* e *in vivo.* Verificámos ainda que estas células mantiveram o cariótipo diploide e o genótipo da doença, apresentando-se em perfeitas condições para serem diferenciadas em culturas neuronais de DMJ.

No capítulo 4 é descrita a diferenciação das iPSCs em neurónios específicos de doentes e um estudo da patogénese da DMJ. Verificámos que a autofagia está comprometida em culturas precoces de neurónios DMJ, fornecendo evidência de que a desregulação dos mecanismos de clearance de proteínas é um evento precoce na DMJ. Verificámos ainda que a localização subcelular da ataxina-3 é alterada na presença de níveis aumentados de Ca^{2+} em neurónios MJD, deslocando-se do citoplasma para o núcleo, onde foi detectada na forma de pequenos agregados.

Em conclusão, esta tese evidencia que as iPSCs obtidas de doentes DMJ são uma ferramenta poderosa no contexto de modelação da doença, criando a oportunidade única de gerar neurónios específicos de doentes DMJ e o estudo da doença. Além disso, os nossos resultados demonstram ainda que os neurónios humanos obtidos por diferenciação são uma plataforma para estudos futuros de novas terapêuticas e desenvolvimento de fármacos.

Abstract

Machado-Joseph disease, also called spinocerebellar ataxia type 3 (MJD/SCA3), is the most frequent autosomal dominantly-inherited ataxia worldwide. MJD is a late onset neurogenerative disease caused by a CAG expansion within the coding region of the *ATXN3* gene mapped to chromosome 14q32.1, resulting in an abnormal polyglutamine tract within the ataxin-3 protein.

With the development of induced pluripotent stem cells (iPS) cells, the study of the pathology of MJD is no longer restricted to artificial disease models, such as animal models or cell lines, which present limitations as models for neurogenerative disorder. Therefore, in this thesis we aimed at developing a new human *in vitro* model to study MJD.

The thesis is organized in 4 chapters. In chapter 1, a review of the MJD main pathogenesis characteristics is presented, along with a review of iPSCs-derived *in vitro* models.

In chapter 2, we describe the generation and investigation of the MJD phenotype in patient adult dermal fibroblasts. We characterized genetically those cultures and studied the MJD phenotype on this particular type of non-neuronal cells, regarding autophagy dysfunction. We found autophagy impairments related with MJD phenotype in these cells, particularly a decrease in beclin-1 levels and reduction of autophagosome formation.

In chapter 3, we report the successful generation of iPS cells from the previous established cultures of dermal fibroblasts. We used a lentiviral vector encoding for the 4 reprogramming factors (Sox2, Oct4, Klf4 and c-Myc) for reprogramming the human adult dermal fibroblasts into iPS cells. We fully characterized the pluripotency of those cells regarding the criteria of morphology, molecular markers, such as the alkaline phosphatase activity and expression of cell surface markers, nuclear transcription factors and pluripotency related genes; and functional assays, particularly the *in vitro* and *in vivo* differentiation potential. We found that these cells retained a diploid karyotype and the disease genotype, being in the perfect conditions to be differentiated in MJD neuronal cultures.

In chapter 4, we describe the differentiation of iPS cells in patient-specific neurons and the study of the pathogenesis of MJD. We found that autophagy is impaired in early cultures of MJD neurons, providing evidence that the initial

pathogenesis of MJD concerning the deregulation of protein clearance mechanisms is an early event. Also ataxin-3 subcellular localization changed in the presence of increased intracellular levels of Ca^{2+} in MJD neurons, from the cytoplasm to the nucleus, where it was detected in the form of small aggregates.

In conclusion, this thesis provides evidence that MJD patient derived iPS cells are a powerful tool in the context of disease modeling. They provide a unique opportunity to generate MJD patient-specific neurons, allowing the study of the disease. Furthermore, our results show that MJD can be robustly modeled and the derived human MJD neurons are a platform for the investigation of new therapeutics and drug development.

Chapter 1

Introduction

1.1- Neurodegenerative diseases-Polyglutamine diseases

Aggregation and deposition of misfolded proteins in neurons is a common hallmark in most neurodegenerative disorders (Holmberg et al., 2004), including Alzheimer's disease (AD), Parkinson's disease (PD) and hereditary diseases including those caused by expansions of polyglutamine (PolyQ) tracts, such as Huntington's disease (HD) and the autosomic dominant spinocerebellar ataxias (SCAs). Pathology and death of specific neuronal populations have been found in parallel to this accumulation of specific polypeptides, which form aggregated intracellular inclusions.

The aggregates are composed of normal or mutated, soluble proteins or peptides that differ among the various neurodegenerative diseases, and are typically ubiquitously expressed throughout the organism, but accumulate and cause dysfunctions in the CNS. Such accumulation occurs early in the lifetime of the individual, but only manifest clinically as neurodegenerative disease in middle or late life. Most of these disorders are sporadic, but genetic forms can be caused by mutations in the gene encoding the amyloidogenic protein that make it more prone to misfolding and aggregation (Skovronsky et al., 2006).

Table I- Neurodegenerative diseases: proteins and pathology.

Disease	Aggregated protein	Type of inclusion	Intracellular localization of inclusions
AD	Amyloid-β (Aβ) Tau	Amyloid plaque Neurofibrilatory tangles	Extracellular Intracytoplasmic (neurons)
ALS	SOD, TDP-43, FUS	Skein and Bunina bodies	Nuclear, cytoplasmic (neurons and astrocytes)
PD	α-synuclein	Lewy body	Intracytoplasmic (neurons)
Polyglutamine diseases			
DRPLA	Atrophin-1	Neuronal inclusions	Nuclear
HD	Huntingtin	Neuronal inclusions	Nuclear, cytoplasmic
SBMA	Androgen receptor	Neuronal inclusions	Nuclear
SCA1	Ataxin-1	Neuronal inclusions	Nuclear
SCA2	Ataxin-2	Neuronal inclusions	Nuclear, cytoplasmic
MJD/SCA3	Ataxin-3	Neuronal inclusions	Nuclear
SCA6	Voltage-dependent P/Q-type calcium channel subunit alpha-1A	Neuronal inclusions	Nuclear, cytoplasmic
SCA7	Ataxin-7	Neuronal inclusions	Nuclear
SCA17	TATA box binding protein	Neuronal inclusions	Nuclear

Neurodegenerative diseases characterized by deposition of aggregated proteins. The aggregated proteins present in inclusions and its intracellular localization are listed. Adapted from (Shao and Diamond, 2007).

Polyglutamine diseases are a family of nine neurodegenerative disorders (see Table I) that are caused by over-repeated CAG triplets in specific genes, which translate into expanded tracts of glutamines that confer pathogenicity to the carrying proteins (Shao

and Diamond, 2007). These include Spinal and Bulbar Atrophy (SBMA), the first to be discovered (La Spada et al., 1991), Huntington's disease (HD) (MacDonald et al., 1993), Dentatorubral and Pallidoluysian Atrophy (DRPLA) (Koide et al., 1994; Nagafuchi et al., 1994); and several forms of spinocerebellar ataxias (SCAs), specifically SCA1 (Orr et al., 1993), SCA2 (Imbert et al., 1996; Pulst et al., 1996; Sanpei et al., 1996), Machado-Joseph disease or SCA3 (Kawaguchi et al., 1994), SCA6 (Zhuchenko et al., 1997), SCA7 (David et al., 1997), and SCA17 (Nakamura et al., 2001). All of these disorders are progressive neurodegenerative diseases in which the disease protein misfolds, resulting in the formation of abnormal protein inclusions in neurons and each disorder is characterized by selective neuronal cell death in specific regions of the brain (Gatchel and Zoghbi, 2005).

There is an inverse correlation of CAG repeat length with the age at onset of the disease and the disease severity. The age of onset decreases and disease severity increases with longer glutamine repeats, although the threshold polyQ length for developing disease is different for each disease (Chen et al., 2001; Maciel et al., 1995). The CAG repetition is unstable and relates with the phenomenon of anticipation, where the CAG repeat length expands from one generation to the next, leading to an earlier and severe manifestation of the disease (Coutinho and Sequeiros, 1981; Myers et al., 1982).

1.1.1- Pathogenesis of polyglutamine diseases

A common feature of the mutant protein in polyglutamine diseases is the formation of nuclear aggregates within the neurons of human patients (post mortem tissues) and animal models (Havel et al., 2009; Ichikawa et al., 2001), containing the disease protein, ubiquitin (Donaldson et al., 2003) and important homeostatic proteins such as heat shock proteins (Muchowski et al., 2000) and proteasomal subunits (Chai et al., 1999; Paulson et al., 1997b), implying that the ubiquitin-proteasome system (UPS) is involved in polyQ pathogenesis, as there is a recruitment of cellular components that protect cells against protein misfolding and aggregation (Ciechanover and Brundin, 2003; Gatchel and Zoghbi, 2005; Weber et al., 2014). PolyQ-expanded proteins are structurally unstable and tend to aggregate into β-rich structures, exposing hydrophobic surfaces (Perutz, 1999; Perutz et al., 1994; Scherzinger et al., 1997), leading to a loss of normal protein function and disturbance of the normal cellular functions, as abnormal protein-protein interactions are formed trapping several functional proteins in the aggregates.

Although the strong evidence that perturbations in protein homeostasis are central to disease and protein inclusions are the hallmark of polyQ diseases, it is not clear whether these aggregates are toxic or a cytoprotective response that sequesters abnormal proteins, (Shao and Diamond, 2007; Williams and Paulson, 2008). Currently, it is believed that

aggregation is a complex process, involving several intermediates that contribute to the toxic gain-of-function properties of the mutated proteins (Ross and Poirier, 2004). Aggregates are not considered the primary pathogenic identity, based on the evidence that the distribution of aggregates does not perfectly match with neuronal loss (Kuemmerle et al., 1999; Paulson et al., 1997b; Saudou et al., 1998; Slow et al., 2005; Trottier et al., 1998) and that small aggregates, oligomers (soluble species) and fragments containing the polyQ expansion are more toxic and may underlie the neuronal dysfunction and neurological phenotype (Chen et al., 2001; DiFiglia et al., 1997; Ikeda et al., 1996; Sanchez et al., 2003).

The nucleus is considered a primary site of neuronal dysfunction caused by polyQ proteins (Ross et al., 1999; Yang et al., 2002), where they initiate several events as aggregation and sequestration of transcription factors, perturbing gene expression and transcriptional regulation (Lin et al., 2000; McCampbell et al., 2000; Nucifora et al., 2001; Schaffar et al., 2004). Mitochondrial dysfunction also contributes to polyQ neurodegeneration and neuronal death, by affecting the bioenergetics balance and mitochondrial calcium homeostasis (Antonini et al., 1996; Brouillet et al., 1995; Weber et al., 2014)

1.1.2- Machado-Joseph Disease/ Spinocerebellar ataxia type 3

Machado-Joseph disease (MJD) or Spinocerebellar ataxia type 3 (SCA3) is the most common dominantly inherited spinocerebellar ataxia in the world (Costa Mdo and Paulson, 2012; Durr et al., 1996; Maciel et al., 1995; Schöls et al., 1995) and was first described among Northern American families of Portuguese Azorean ancestry, namely in the descendants of William Machado (from São Miguel island) (Nakano et al., 1972). Later one, the disorder was reported in other families of Azorean origin living in Massachusetts, the Thomas family (Woods and Schaumburg, 1972) and the Sousa family (Romanul et al., 1977) and also in Joseph family (from Flores island) in California (Rosenberg et al., 1976). In 1977, Romanul suggested that the previously described families represented variations of the same clinical disorder and it was defined that Machado-Joseph Disease was a single genetic disease with variable phenotypic expression (Barbeau et al., 1984; Coutinho and Andrade, 1978).

Nowadays, MJD is considered the most frequent form among the autosomal dominantly inherited cerebellar ataxias in Europe, Japan and United States (Riess et al., 2008), reaching the highest prevalence of 1/239 in Flores island (Bettencourt and Lima, 2011).

1.1.3- Neuropathological and clinical features

Pathologically, MJD neurodegeneration and neuronal loss involves selective brain regions, particularly the cerebellum (spinocerebellar pathways, pontine and dentate nucleus), brainstem (medulla oblongata and pons), basal ganglia (globus pallidus, caudate and putamen), midbrain and spinal cord (Durr et al., 1996; Klockgether et al., 1998; Paulson et al., 1997b; Rosenberg, 1992; Rub et al., 2006; Sudarsky and Coutinho, 1995).

MJD is classified as a late-onset and progressive neurodegenerative disease, the first symptoms appear when patients are in their 40s and survival after disease onset ranges from ~20 to 25 years (Kieling et al., 2007; Klockgether et al., 1998; Paulson, 2012). The first symptoms are usually gait ataxia and patients present several features such as cerebellar ataxia, spasticity, progressive external ophthalmoplegia, dystonia, facial and lingual fasciculation bulging eyes and peripheral neuropathy (Matsumura et al., 1996a; Paulson, 2012; Riess et al., 2008; Takiyama et al., 1997). Four distinct clinical subtypes of MJD (Coutinho and Andrade, 1978; Lima and Coutinho, 1980; Rosenberg, 1992) have been reported based on the variability of age of onset and neurological signs, and more recently, an additional MJD type V has been proposed (Sakai and Kawakami, 1996), as presented in Table II.

Table II- Classification of MJD according with age of onset and clinical characteristics.

Classification	Age of onset	Clinical Characteristics
Type I	10-30 years old	Rapid progression of symptoms Cerebellar ataxia Rigidity and distonya Progressive ophtalmoplegia Proeminent pyramidal signs (rigidity and spasticity) Extrapyramidal signs (bradykinesia and dystonia)
Type II	20-50 years old	The most common type Cerebellar ataxia Progressive ophtalmoplegia With or without pyramidal signs
Type III	40-75 old	Milder ataxia peripheral neuropathy and muscle atrophy
Type IV	Variable onset	Rare Mild cerebellar deficits Distal motor sensory neuropathy or amyotrophy Parkinsonism responsive to dopamine
Type V		Very rare Spastic paraplegia Shares many features with those in other subtypes.

Adapted from (Costa Mdo and Paulson, 2012) and (D'Abreu et al., 2010)

There is currently no cure for MJD and only symptomatic treatment strategies are available. Parkinsonian features, dystonia and restless legs syndrome can be treated with levodopa or dopamine agonists (Buhmann et al., 2003; Schols et al., 2004; Tuite et al., 1995); tremors and muscle cramps can be alleviated with magnesium, chinine, mexiletine and carbamazepine (Franca et al., 2008; Kanai et al., 2003; Schols et al., 2004) and spasticity can be treated with injections of botulinum toxin (Freeman and Wszolek, 2005). Urinary urgency and frequency are usually treated with spasmolytics or adrenergic α-receptor blockers; sleep disturbances are mostly treated with hypnotic drugs and depression can be treated with antidepressants and occupational therapy (Monte et al., 2003).

Ataxia is one of the most difficult symptoms to treat by pharmacological approaches and it has been suggested that physical and occupational therapy are helpful strategies (Schols et al., 2004). Patients with symptoms of dysarthria and dysphagia can be enrolled in regular speech and swallowing therapies. Non-pharmacological interventions as prism glasses may help with diplopia and strollers and wheelchairs are physical aids that together with occupational therapy help patients to cope with the disabilities and assist them in their everyday activities (D'Abreu et al., 2010; Saute and Jardim, 2015).

1.1.4- *ATXN3* gene

In 1994, Kawaguchi and colleagues (Kawaguchi et al., 1994) identified the mutation in MJD/SCA3 as an unstable CAG repeat motif in the coding region of *MJD1* (now termed as *ATXN3*) gene on the long arm of chromosome 14 (14q24.3-q32) (St George-Hyslop et al., 1994; Takiyama et al., 1993). This 11 exon gene encodes the disease protein ataxin-3, a 42 kDa protein (Ichikawa et al., 2001) and the CAG repeat resides in the exon 10, where it encodes a polyglutamine tract near the carboxyl terminus of ataxin-3 (Ichikawa et al., 2001; Schmitt et al., 2003) (Fig 1.1). In normal individuals the gene contain 12-44 CAGs, whereas most of the patients exhibit an expansion of the repeat number ranging from 61 to 87 CAGs (Lima et al., 2005; Maciel et al., 2001). Rare alleles of intermediate repeat length that fall between the normal and mutant ranges of CAG repeats (45-56 CAGs) are rare and are not associated with classical clinical features of the disease (Maciel et al., 1995; Maruyama et al., 1995; Padiath et al., 2005; Takiyama et al., 1997; van Alfen et al., 2001).

MJD presents four haplotypes, based on the analysis of three intragenic single base pair polymorphisms (SNPs) (A669TG/G669TG- rs1048755, C987GG/G987GG- rs12895357 and TAA1118/TAC1118- rs7158733) (Gaspar et al., 2001; Goto et al., 1997; Maciel et al., 1999; Martins et al., 2007; Martins et al., 2006).

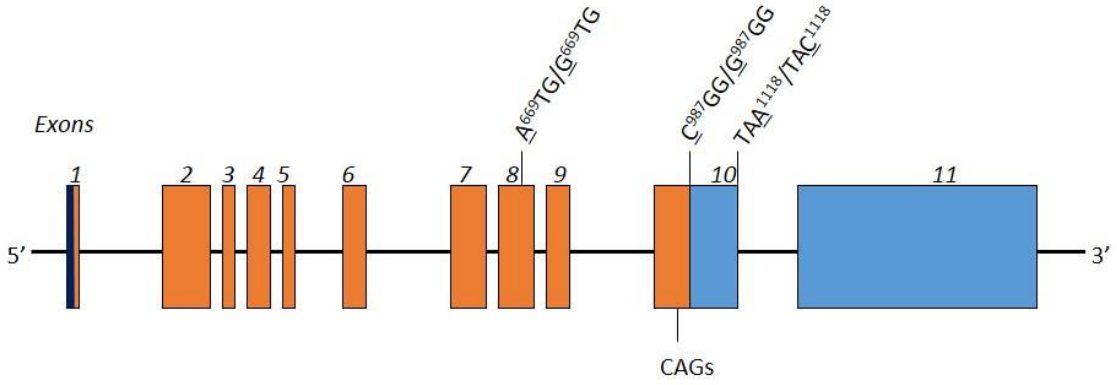

Figure 1.1-Schematic representation of *ATXN3* gene structure and SNPs studied to define MJD haplotypes.

Exons are presented as boxes and numbered from 1 to 11. Dark blue box represents the 5'UTR and light blue boxes represent the 3' UTR. Recently a 13 exons composition of the gene has been suggested (11 exons plus 6a and 9a) (Bettencourt et al., 2010). The main SNPs considered to define the MJD haplotypes are also presented, regarding its localization on the gene. Adapted from (Bettencourt and Lima, 2011) and (Martins et al., 2007).

The most common haplotypes are the GGC haplotype related to island of São Miguel and the ACA related to Flores island (Lima et al., 1998) that are present in 94% of the MJD families. Both haplotypes can be found in Portugal mainland and the most prevalent haplotype worldwide is the ACA, with 72% of the families sharing this haplotype (Gaspar et al., 1996; Gaspar et al., 2001). Both the SNPs TA$\underline{A}^{1118}$/TA$\underline{C}^{1118}$ and $\underline{C}^{987}$GG/$\underline{G}^{987}$GG that neighbors the CAG repetition affects the CAG repeat instability (Igarashi et al., 1996; Maciel et al., 1999; Matsumura et al., 1996b) but it is still unknown the contribution to the pathogenesis of the disease. The SNP $\underline{C}^{987}$GG/$\underline{G}^{987}$GG has been used in RNAi studies to selectively suppress the expression of the mutant allele while sparing expression of the normal allele, (Alves et al., 2008a; Miller et al., 2003; Nobrega et al., 2014; Nobrega et al., 2013), demonstrating to be a promising clinical target.

1.1.5- Ataxin-3

Ataxin-3 is a widely distributed protein among eukaryotic organisms (Albrecht et al., 2003) and despite the localized neuronal degeneration observed in MJD patients, ataxin-3 is ubiquitously expressed in different tissues and cell types (Costa et al., 2004; Ichikawa et al., 2001; Paulson et al., 1997a; Schmidt et al., 1998; Trottier et al., 1998). Ataxin-3 is constituted by a catalytic conserved N-terminal Josephin domain with deubiquitinating protease activity (Albrecht et al., 2004; Burnett et al., 2003; Masino et al., 2003; Nicastro et al., 2005) and a flexible C-terminal containing the polyQ sequence of variable length and two or three ubiquitin interacting motifs (UIM), depending on the protein isoform (Goto et al., 1997) (Fig 1.2). Fifty-six alternative splicing variants of the *ATXN3* gene were identified

(Bettencourt et al., 2013; Bettencourt et al., 2010) and the most predominant isoform expressed in brain has a third UIM domain after the polyQ sequence (Harris et al., 2010).

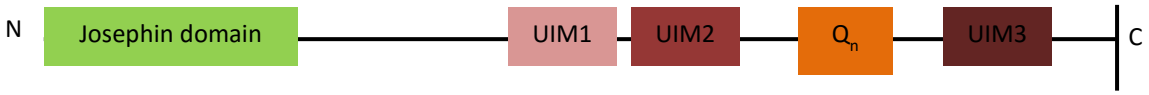

Figure 1.2-Schematic representation of ataxin-3 promary structure.
Ataxin-3 protein is composed by the Josephin domain and the c-terminal tail containing two or three ubiquitin interacting motifs (UIMs) and a polyQ sequence of variable length (Q_n).

Ataxin-3 is a DUB enzyme that cleaves ubiquitin or poly-ubiquitin chains from substrates (Warrick et al., 2005; Winborn et al., 2008), recognizing preferentially chains of 4 or greater ubiquitin molecules (Burnett et al., 2003; Chai et al., 2004). Ataxin-3 plays a major role in the ubiquitin-proteosome pathway (UPS) due to the ubiquitin binding properties, it binds to ubiquitinated proteins targeted for degradation through the UIMs and translocates those substrates to the proteasome for degradation (Donaldson et al., 2003; Doss-Pepe et al., 2003). Ataxin-3 also appears to be implicated in transcriptional regulation (Evert et al., 2006; Li et al., 2002), cellular response to heat and oxidative stress (Araujo et al., 2011; Reina et al., 2010; Rodrigues et al., 2011; Zhou et al., 2013) and aggresome and cytoskeleton organization (Burnett and Pittman, 2005; do Carmo Costa et al., 2010; Mazzucchelli et al., 2009; Rodrigues et al., 2010). Although several studies enlighten ataxin-3 functions, as presented above, the precise cellular role of ataxin-3 is still unknown as also how it is altered upon polyglutamine expansion, with contrary reports stating its essential role for normal cellular functioning (Rodrigues et al., 2010; Rodrigues et al., 2011). Ataxin-3 participates in several cellular pathways but its absence does not compromise cellular viability or fertility in knockout models of ataxin-3 and only mild phenotypes were described (Boy et al., 2009; Schmitt et al., 2007; Switonski et al., 2011).

Regarding subcellular localization, ataxin-3 is predominantly a cytoplasmic protein but is also present in the nucleus (Paulson et al., 1997a; Schmidt et al., 1998; Tait, 1998; Trottier et al., 1998) and in mitochondria (Pozzi et al., 2008). Nucleocytoplasmic shuttling is mediated by one nuclear localization signal (NLS), RKRR, aminoacid 282-285 (Albrecht et al., 2004; Tait, 1998), and two nuclear export signals (NES), NES77 (177-Y99) and NES141 (E141-E258) (Antony et al., 2009); ataxin-3 is also transported to the nucleus by diffusion across the nuclear membrane (Chai et al., 2002). In summary, the subcellular localization of ataxin-3 is a highly regulated process and understanding of the events that modulate intracellular localization may help to elucidate the disease pathogenesis, as mutant ataxin-3 tends to accumulate in the nucleus, and being the nucleus the preferential site for poly-Q induced toxicity (Costa Mdo and Paulson, 2012; Yang et al., 2002).

1.1.6- Mutant ataxin-3 and disease pathogenesis

Mutant ataxin-3 is involved in several mechanisms that are implicated in MJD pathogenesis, particularly the formation of aggregates, proteolytic cleavage, transcriptional deregulation, mitochondrial dysfunction, axonal transport impairment, dysregulation of intracellular Ca^{2+} homeostasis and impairment of protein degradation (Fig 1.3).

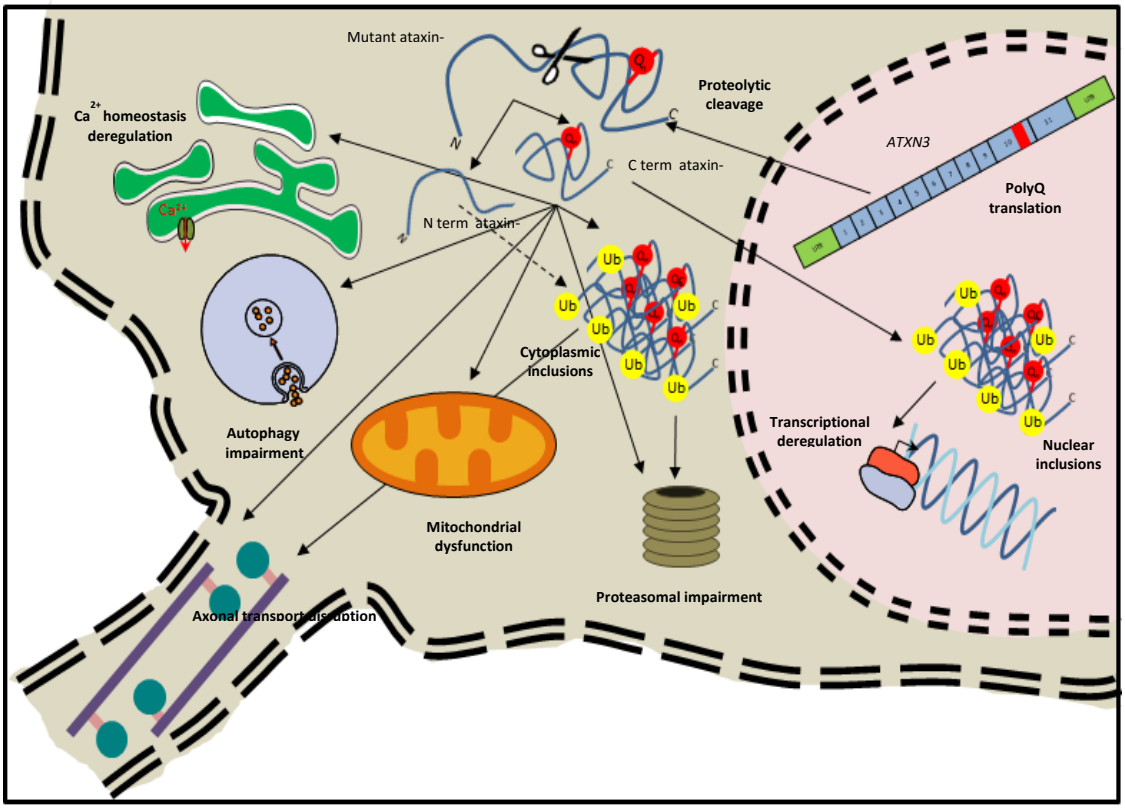

Figure 1.3-Cellular mechanisms in the pathogenesis in MJD.

The *ATXN3* gene is translated into mutant ataxin-3, containing an expanded the polyQ tract. The polyQ tract triggers conformational changes, resulting in abnormally folded mutant ataxin-3. Mutant ataxin-3 can be proteolytically cleaved giving rise to N-terminal and C-terminal fragments that are prone to aggregate. Full length and cleaved forms of mutant ataxin-3 produce ubiquitinated inclusions in the nucleus and in the cytoplasm, contributing to transcriptional desregulation, proteosomal and autophagy impairment, mitochondrial dysfunction, compromised axonal transport and Ca^{2+} homeostasis desregulation. Adapted from (Evers et al., 2014)

1.1.6.1- Aggregation of mutant ataxin-3

Neuronal intranuclear inclusions (NIIs) formed by ubiquitinated mutant ataxin-3 represent a pathological hallmark of MJD, found in MJD patients (Paulson et al., 1997b; Schmidt et al., 1998) and reproduced in cellular and animal models overexpressing mutant ataxin-3 (Alves et al., 2008a; Bichelmeier et al., 2007; Ikeda et al., 1996; Schmidt et al., 2002), but their role in the pathogenesis of MJD is still unclear and controversial, as they may present a pathologic structure or a cytoprotective one (Paulson, 2012; Shao and Diamond, 2007; Trottier et al., 1998). The absence of direct correlation between the presence of NIIs and neurodegeneration suggests that other species of mutant ataxin-3, such as monomers (Nagai et al., 2007) and oligomers (Bevivino and Loll, 2001; Takahashi et al., 2008) may play a role as cytotoxic species during the multistep process of aggregation (Williams and Paulson, 2008).

These findings are corroborated by similar observations in other neurodegenerative and polyQ diseases (Arrasate et al., 2004; Kayed et al., 2003; Ross and Poirier, 2005) reinforcing the hypothesis that polyglutamine oligomerization may have a crucial role in neuronal dysfunction.

1.1.6.2- Proteolytic cleavage of mutant ataxin-3

The toxic fragment hypothesis, regarding the proteolytic cleavage of polyQ expanded protein is considered a major contributor mechanism to the polyQ disorders pathogenesis. The proteolytic cleavage of mutant ataxin-3 may produce smaller fragments, containing the polyQ repeat that are more toxic and prone to aggregate than full-length ataxin-3 (Berke et al., 2004; Goti et al., 2004; Haacke et al., 2006; Koch et al., 2011; Takahashi et al., 2008). Those fragments are more easily translocated to the nucleus where they aggregate and exert toxic effects (Bichelmeier et al., 2007; Breuer et al., 2010; Goti et al., 2004; Ikeda et al., 1996). There is some controversy regarding the identification of the proteolytic fragments of mutant ataxin-3, as they were not found to contribute to the MJD phenotype in some MJD models (Berke et al., 2004; Jung et al., 2009), but those divergent results might be explained by variations on the experimental conditions.

These proteolytic fragments have been proposed to be a product of autolytic cleavage (Mauri et al., 2006), of caspase activity (Berke et al., 2004; Jung et al., 2009; Wellington et al., 1998) or of calpain-mediated cleavage (Haacke et al., 2007; Hubener et al., 2013; Koch et al., 2011; Simoes et al., 2012; Simoes et al., 2014). Inhibiting calpains by overexpression of calpastatin or administration of the calpain inhibitor BDA-410 alleviated

the phenotype in mouse models of MJD. It is clear that proteolytic enzymes may play a major role in MJD pathogenesis, by triggering cleavage aggregation and toxicity of mutant ataxin-3 fragments and are a promising target for modification of disease progression.

1.1.6.3- Transcription dysregulation

Mutant ataxin-3 is responsible for transcriptional deregulation by forming aberrant interactions with transcriptional regulators and compromising their function as co-repressors or activators (Araujo et al., 2011; Evert et al., 2006; Perez et al., 1998). It was found on both cell and mouse models that transcription of genes involved in inflammation and neuronal cell death were upregulated and genes involved in glutamatergic and gabaergic neurotransmission and intracellular calcium signaling were downregulated (Chou et al., 2008; Evert et al., 2001; Evert et al., 2003).

The altered expression of these genes suggests that transcriptional dysregulation might be one of the initiating processes underlying MJD pathogenesis, but further studies are needed to elucidate its specific role in MJD neurological phenotype.

1.1.6.4-Mitochondrial dysfunction

It has been suggested that mitochondrial dysfunction could be implicated in the pathogenesis of MJD. Recently, some studies in cellular and mouse models of MJD revealed that mitochondrial DNA damage was increased and ATP and antioxidant enzyme levels were reduced (Kazachkova et al., 2013; Laco et al., 2012b; Yu et al., 2009b), suggesting impairment of mitochondrial function. Those findings are in line with the hypothesis that oxidative stress, induced by reactive oxygen species (ROS) and free radicals are one of the main causes of neuronal death in neurodegenerative diseases (Emerit et al., 2004).

1.1.6.5- Axonal transport impairment

Axonal transport dysfunction has been presented as a hypothesis that might explain the neuropathy observed in polyQ diseases (Caviston et al., 2007; Gunawardena et al., 2003). Mutant ataxin-3 aggregates were found in axons of affected brain regions of MJD patients (Seidel et al., 2010) and it was shown in animal models of MJD that mutant ataxin-

3 aggregates impaired synaptic transmission by contributing to aberrant formation of neuronal processes and destabilization of cytoskeletal organization and transport (Burnett and Pittman, 2005; do Carmo Costa et al., 2010; Khan et al., 2006; Rodrigues et al., 2010). Together these studies support the hypothesis that axonal dysfunction may play an important role in MJD pathogenesis.

1.1.6.6-Dysregulation of intracellular Ca^{2+} homeostasis

The homeostatic mechanisms to maintain low intracellular Ca^{2+} levels are very important to the function and survival of neurons and its failure can cause neuronal death by triggering apoptosis and oxidative stress (Bezprozvanny, 2009; Mattson, 2007). Abnormal Ca^{2+} signaling has been reported for polyQ diseases (Bezprozvanny, 2010; Gatchel and Zoghbi, 2005) and in the specific case of MJD, a study in a mouse model showed that mutant ataxin-3 specifically bound and activated the calcium channel $InsP_3R1$, increasing the intracellular Ca^{2+} levels on neurons and causing neuronal loss (Chen et al., 2008a). Recently, it was demonstrated in an MJD neuronal model derived from iPSCs, that the increased intracellular Ca^{2+} levels mediated by glutamate promoted aggregation and calpain mediated proteolysis of mutant ataxin-3, contributing to neuronal dysfunction (Koch et al., 2011). These findings also suggest that the deranged Ca^{2+}signalling plays an important role in pathology progression and neurodegeneration.

1.1.6.7-Impairment of protein degradation

The loss of the DUB activity (Chai et al., 2004; Winborn et al., 2008) of mutant ataxin-3 and also the loss of ability to guide substrates to be degraded in the proteasome (Doss-Pepe et al., 2003; Laco et al., 2012a) together with the sequestration of proteasomal components (Chai et al., 1999; Paulson et al., 1997b) and molecules involved in autophagy, such as beclin-1 and the chaperone HSP27 (Chang et al., 2009; Nascimento-Ferreira et al., 2013; Nascimento-Ferreira et al., 2011; Teixeira-Castro et al., 2011) in aggregates contributes to the failure of the cellular protein quality control system in MJD.

The abnormal accumulation of mutant ataxin-3 verified in MJD patient's brains and mouse models (Nascimento-Ferreira et al., 2011) is indicated as a consequence of UPS system disruption and autophagy impairment as previously described for other neurodegenerative disorders (Ravikumar et al., 2004; Wong and Cuervo, 2010b) and may

support the idea that the underlying mechanism of neuronal dysfunction in MJD is the impairment of neuronal proteostasis.

1.1.7-Potential therapeutic strategies

An advantage of monogenic diseases, as MJD is that silencing of the responsible gene should result in alleviation of the disease phenotype. So far, two strategies for allele-specific silencing of mutant ataxin-3 have been reported, based on targeting a unique SNP to the mutant ataxin-3 (Alves et al., 2008a) or targeting the CAG repetition (Hu et al., 2011). The silencing of both wild-type and mutant ataxin-3 (Alves et al., 2010) and the lack of harmful effects of *ATXN3* knockout in mice (Schmitt et al., 2007) indicate that therapeutic strategies involving non-allele specific silencing to treat MJD patients may be effective (Nóbrega and de Almeida, 2012).

Transcriptional dysregulation, specifically the activity of mutant ataxin-3 as a co-repressor of transcription (Li et al., 2002), has been targeted by using HDAC inhibitors, particularly sodium butyrate and valproic acid, that reverse histone hypoacetylation and transcriptional downregulation (Chou et al., 2011; Teixeira-Castro et al., 2011), resulting in improvement in locomotor activity in mouse and *C.elegans* transgenic models of MJD. These compounds may be useful as a preventive therapy for MJD (Evers et al., 2014).

Mutant ataxin-3 misfolding, oligomerization and aggregation has been reduced in *Drosophila* and *C.elegans* models of MJD using Hsp90 inhibitors (Fujikake et al., 2008; Teixeira-Castro et al., 2011), which induce endogenous molecular chaperones, contributing to the modulation and stabilization of ataxin-3 in native conformation (Nagai et al., 2010). Also, the overexpression of chaperones such as Hsp40 and Hsp70 (Chai et al., 1999; Warrick et al., 1999), or chemical-like chaperones (Yoshida et al., 2002) has been shown to reduce cytotoxicity and aggregates formation by handling misfolded mutant ataxin-3. Y-27632, an inhibitor of Rho kinases also contributed to reduce the levels of mutant ataxin-3 aggregates in a cellular MJD model (Bauer et al., 2009). Preventing the proteolytic cleavage of mutant ataxin-3 is also another strategy to reduce toxic entities, more precisely, the mutant ataxin-3 fragments. The use of caspase inhibitors (Berke et al., 2004; Jung et al., 2009) and calpain inhibitors (Haacke et al., 2007; Koch et al., 2011; Simoes et al., 2012) are interesting approaches but the lack of specificity targeting the proteolytic enzymes may be a problem to overcome before move it to the clinics (Evers et al., 2014)

Another strategy that targets directly mutant ataxin-3, more specifically its clearance, is the activation of the UPS system and autophagy. The overexpression of UPS-related proteins increases the degradation rate of mutant ataxin-3 and alleviates cytotoxicity (Jana et al., 2005; Matsumoto et al., 2004; Miller et al., 2005), as also the

overexpression of autophagy related molecules, particularly Beclin-1 (Nascimento-Ferreira et al., 2011) or autophagy inducers such as rapamycin (Menzies et al., 2010; Ravikumar et al., 2004). The reposition of the protein quality control system represents a very promising therapeutic option for MJD as well as for other polyQ diseases (Wong and Cuervo, 2010b).

Targeting mitochondrial dysfunction in MJD (Yu et al., 2009b) by using antioxidants may also be a good strategy to alleviate the pathology, as suggested for other polyQ diseases as HD (Hersch et al., 2006; Huntington Study Group Pre et al., 2010). Another potential therapeutic strategy is the modulation of calcium homeostasis, by targeting the calcium release from the ER (Chen et al., 2008a) or indirectly by preventing glutamatergic mediated excitotoxicity through the normalization of glutamatergic transmission associated with adenosine A_{2A} receptor antagonism (Goncalves et al., 2013).

In conclusion, there are several lines of investigation in the search for safe and efficacious therapies for MJD but it is still challenging to successfully transpose the results found in MJD disease models to clinical trials in MJD. There is no perfect model to predict the efficacy of a molecule or genetic therapeutic approach in a clinical trial by itself. Nevertheless, a combination of better human neuronal models, to further understand pathogenesis mechanisms, combined with animal models, that provide a readout of *in vivo* phenotype alterations seem to be the best methodology to validate and accelerate the delivery of new therapies into clinics.

1.2- Induced Pluripotent Stem Cells (iPS cells)

1.2.1- Pluripotent stem cells

Pluripotent stem cells (PSCs) are characterized by their capability of extensive self-renewal (the ability to symmetrically duplicate in culture) and differentiation in all the cell types of the body (deriving from the three germ layers: endoderm, mesoderm and ectoderm), while maintaining an undifferentiated state indefinitely (Wilmut et al., 2011). The property of cell pluripotency was first described by Hans Driesch in 1891 (Driesch, 1891) when he isolated two cells of an early sea urchin blastocyst and observed the development of two complete sea urchins (Robinton and Daley, 2012). But it was several decades later in 1981 that the first PSCs, mouse embryonic stem cells were isolated and cultured by Martin Evans and Matthew Kaufman (Evans and Kaufman, 1981). Seventeen years later the first human embryonic stem cell (hESC) lines were established by James Thomson and colleagues (Thomson et al., 1998) by isolation and expansion *in vitro* of the inner cell mass (ICM) of pre-implantation embryos at blastocyst stage (Fig 1.4).

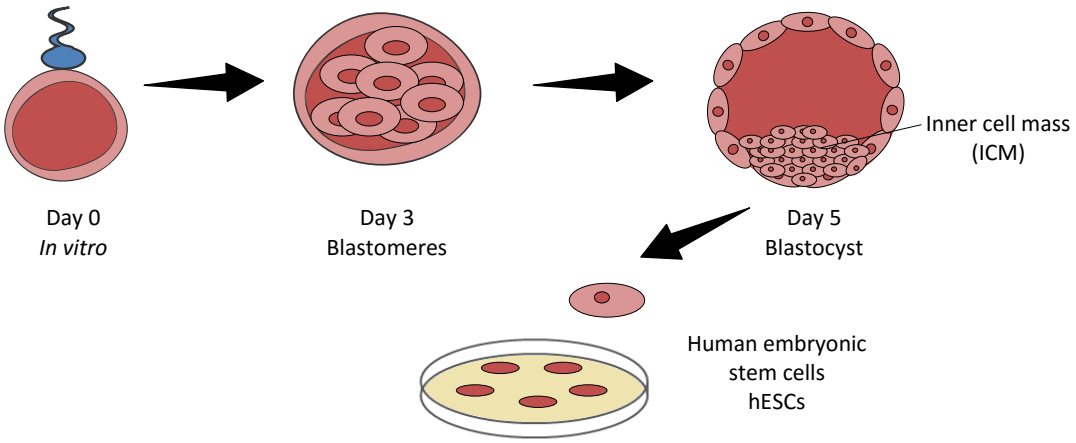

Figure 1.4- Derivation of human embryonic stem cells

Human embryonic stem cells are derived from the inner cell mass (ICM) of day 5 blastocyst. The ICM cells have the potential to generate any cell type of the body and when removed from its normal embryonic environment and cultured under appropriate conditions, the ICM-derived cells can continue to proliferate and replicate themselves indefinitely and still maintaining the developmental potential to form any cell type of the body. Adapted from, September 2015.

The derivation of hES cells opened a new avenue for disease modeling (Gearhart, 1998) by using embryos with mutations identified by pre-implantation genetic diagnosis (PGD) and hES cell lines derived from these (Mateizel et al., 2006; Sermon et al., 2009). Moreover, hES cell lines carrying mutations were created by homologous recombination (Giudice and Trounson, 2008) of a normal hES cell line, enabling the generation of cell

lines that could be used to study mechanisms of disease. Nevertheless, both of those approaches in many cases failed to fulfill the purpose due to significant barriers, such as the lack of PGD for most diseases, inefficiency of gene targeting in hES cell lines and ethical concerns regarding the required destruction of human embryos in order to generate hES cells for research (Tiscornia et al., 2011).

1.2.2- Induced pluripotent stem cells

When in 2006 Takashi and Yamanaka (Takahashi and Yamanaka, 2006) announced the successful derivation of induced pluripotent stem cells (iPS cells) from adult mouse fibroblasts through the ectopic co-expression of only 4 reprogramming factors (TFs): Octamer-binding transcription factor 4 (OCT4 also known as Pou5f1), Sex determining region Y-box 2 (SOX2), Krüppel-like factor 4 (KLF4) and v-myc avian myeolocytomatosis viral oncogene homolog (c-MYC) it revolutionized the field of pluripotent stem cells. In an elegant experiment, Takahashi and Yamanaka tested twenty-four genes selected for their pivotal roles in the maintenance of ES cells identity and found that the overexpression of a combination of 4 TFs was sufficient to trigger a cascade of events that gave rise to pluripotent stem cells, the so-called induced pluripotent stem cells (iPS cells) (Fig 1.5).

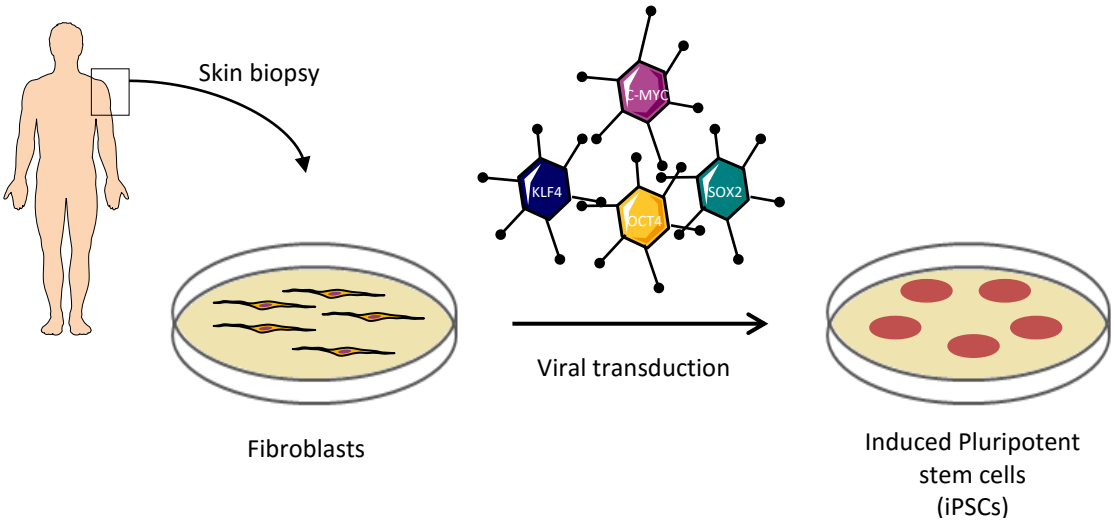

Figure 1.5 Schematic representation of the generation of induced pluripotent stem cells by overexpression of Oct4, Sox2, Klf4 and c-Myc in fibroblasts using a retroviral mediated strategy.

Adult fibroblasts from human donors were exposed to retroviral vectors expressing a cocktail of four transgenes encoding the reprogramming factors Oct4, Sox2, Klf4, and c-Myc. Approximately, thirty days after transduction and further cultivation under human ES cell growth conditions, human induced pluripotent stem (iPS) cell colonies can be isolated and expanded. Adapted from (Zaehres and Scholer, 2007)

The perception of cellular reprogramming changed as it was shown that plasticity of somatic cells was much greater than had been previously thought and that differentiation was a reversible process, abolishing a long standing biology dogma of one-way differentiation in somatic cells (Weismann, 1885). The historic contribution of nuclear reprogramming for the stem cell and developmental biology fields was the confirmation of cellular identity and plasticity corroborating previous seminal studies of pluripotency induction pioneered in the 50's by Briggs and King (Briggs and King, 1952), and Gurdon in the 60's (Gurdon, 1962; Gurdon et al., 1958), that included demonstrations of reversibility of the differentiated state of the nucleus of terminally differentiated somatic cells (nuclei of an intestinal epithelial cell of *Xenopus*) after somatic cell nuclear transfer (SCNT) to an enucleated egg resulting in the generation of whole and viable organisms (tadpoles). This technique was further used in mammals, being the most recognized study the cloning of Dolly the sheep (Wilmut et al., 1997). Together both nuclear and epigenetic cellular reprogramming were considered groundbreaking techniques and were distinguished by the attribution of the Nobel prize in Physiology or Medicine to Shinya Yamanaka and John Gurdon in 2012 for their major contributions in the field.

Reprogramming was quickly applied to human cells, and in 2007 human iPS cells were first generated by the same group (Takahashi et al., 2007) transducing human dermal fibroblasts with retroviral vectors carrying the same TFs (OSKM). In the same year, Yu and colleagues (Yu et al., 2007) also generated human iPS cells by transducing human fibroblasts with lentiviral vectors encoding the factors OCT4, SOX2, NANOG and LIN28 (OSNL). The iPS cells generated by both groups shared the main properties of hES cells, including the unlimited self-renewal and the potential to differentiate into cells of the three germ layers, being molecularly and functionally very similar.

hiPS cells can be derived from any individual offering a solution to problems related to hES cells and its derivatives, circumventing the ethical concern of embryo destruction and immune rejection. Also the simplicity of the method in generating isogenic and autologous pluripotent stem cells enabled avoiding SCNT, a very demanding technique (Lako et al., 2010) and opened new opportunities for patient-specific cell therapies, and generation of *in vitro* systems to study pathogenesis and drug screening in differentiated human cell types (potential human iPS cells applications are schematically represented in Fig 1.6).

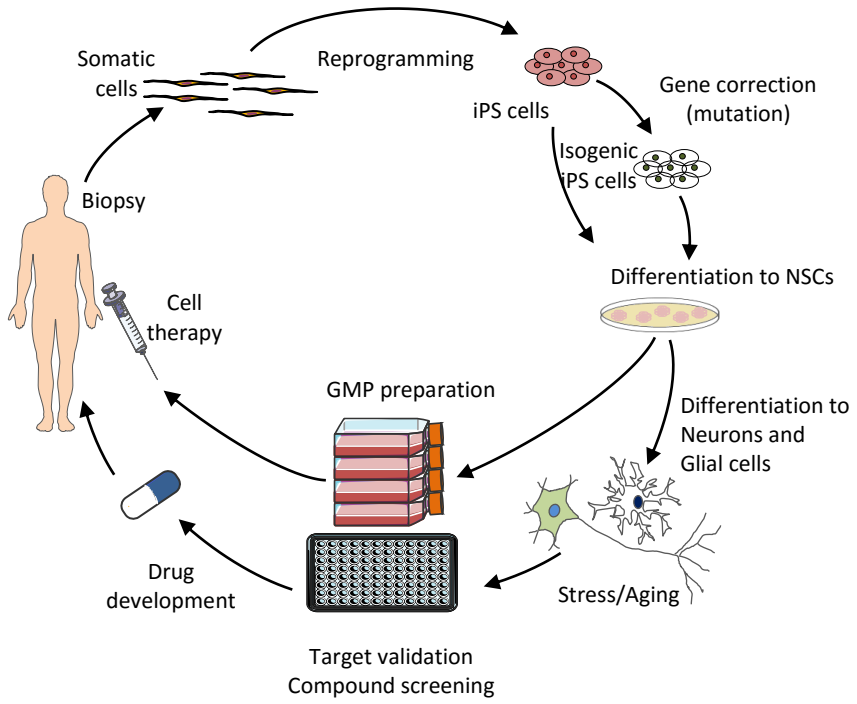

Figure 1.6- Overview of the use of induced pluripotent stem cells research for neurodegenerative diseases.
Adult somatic cells can be reprogrammed into iPS cells. The iPS cells derived from a donor carrying a mutation in a disease risk gene can be genetically corrected using homologous recombination, ZFN, TALEN or CRISPR/Cas9. The resulting isogenic cells can be used as normal controls or potentially for cell transplantation therapy. iPSC-derived specific neurons can be used in drug screening and new drug discovery, toxicity tests, models for studying the neurodegenerative diseases and for self-transplantation therapy. Adapted from (Ross and Akimov, 2014).

1.2.2.1- Cell reprogramming

iPS cells can be generated mainly by two different protocols, OSKM or OSNL that combine the exogenous expression of a combination of 4 genes, the pluripotency transcription factors and core transcription factors OCT4, SOX2 and NANOG (Boyer et al., 2005; Chen et al., 2008b; Jaenisch and Young, 2008; Kim et al., 2008a; Loh et al., 2006) and LIN28 (Okita and Yamanaka, 2011) and the proto-oncogenes KLF4 and c-MYC that provide a cellular growth boost during the reprogramming process (Jaenisch and Young, 2008). These two factors can be replaced or excluded from the reprogramming cocktail, especially c-MYC, but with some loss in reprogramming efficiency (Nakagawa et al., 2008; Wernig et al., 2008).

The successful reprogramming technique employed firstly in fibroblasts was quickly applied to a wide variety of other cell types such as pancreatic β-cells (Stadtfeld et al., 2008a), oral fibroblasts (Miyoshi et al., 2010), keratinocytes (Aasen et al., 2008), bone marrow (Park et al., 2008b), cord and peripheral blood (Giorgetti et al., 2009; Loh et al., 2009), neural stem cells (Kim et al., 2009b), adipose stem cells (Sun et al., 2009) and

dental-derived mesenchymal stem cells (Yan et al., 2010) demonstrating the universal application of the cellular reprogramming process and capacity to alter cell identity.

1.2.2.2- Enhancing cell reprogramming safety

Despite the potential of iPS cells in human disease research some limitations remain for application of iPS cells in the clinic, particularly the slow reprogramming process, low reprogramming efficiency and safety issues linked to the use of TF delivery methods that may involve genome integration.

In Table III are listed the methods used so far to reprogram several different somatic cell types to pluripotency. The protocol employing the original 4 RFs, delivered by integrating viral vectors is still the preferred option due to the higher reprogramming efficiencies (Bellin et al., 2012). But many methods have been developed to avoid genome integration, ranging from excisable and non-integrating viral vectors, to transfection of modified mRNAs transcripts, protein transduction or even chemical compounds. Compared to the traditional integrating viral methods, the non-viral approaches can be used to generate qualified iPS cells without the risk of insertional mutagenesis, apt to be used in the clinics. Thanks to the evolution of safer reprogramming methods it was possible to initiate in 2014 (just seven years after the generation of the first human iPS cells) the first human clinical trial using retinal pigment epithelium derived from a AMD (Age-related macular degeneration) patient to perform an autologous transplant proving the feasibility of clinical translation and use of patient-specific cellular therapies (Kamao et al., 2014).

Table III- Reprogramming methods used to derive human induced pluripotent stem cells.

Vector type	Cell types	Factors	Efficiency (%)	Advantages	Disadvantages	References
Integrating strategies						
Retrovirus	Fibroblasts, Keratinocytes, Blood, adipose, liver and neuronal cells	OSKM OSK miR 302/367	~0.01-1	High efficiency	Genomic integration Incomplete proviral silencing Insertional mutagenesis	(Lowry et al., 2008; Takahashi et al., 2007) (Anokye-Danso et al., 2011)
Lentivirus	Fibroblasts Keratinocytes Pancreatic β cells	OSNL OSKM	~0.1-1.1	High efficiency Transduce dividing and non-dividing cells	Incomplete proviral silencing Insertional mutagenesis	(Sommer et al., 2009; Stadtfeld et al., 2008a; Yu et al., 2007)
Inducible lentivirus	Fibroblasts, keratinocytes, blood cells	OSKM OSKMN	~0.1-2	Controlled expression of transgenes	Requires transactivator expression	(Maherali et al., 2008; Stadtfeld et al., 2008b)

Excisable strategies						
Lentivirus-Cre exscisable	Fibroblasts	OSK OSKM	~0.1-1	Transgene-free	Labor-intensive screening of excised lines and loxP sites retained in the genome	(Zhou et al., 2009) (Soldner et al., 2009; Sommer et al., 2010)
Transposon	Fibroblasts	OSKM	~0.1	Transgene-free	Labor-intensive screening of excised lines	Woltjen et al., 2009)
Non-integrating strategies						
Adenoviral	Fibroblasts and liver cells	OSKM	~0.001	Integration-free	Slow and inefficient	(Stadtfeld et al., 2008c) (Zhou and Freed, 2009)
Plasmid	Fibroblast	OSNL	~0.001	Integration-free	Very low efficiency Requirement for multiple rounds of transfection	(Kaji et al., 2009) (Okita et al., 2008; Si-Tayeb et al., 2010)
Episomal	Fibroblasts, dental pulp cells, mononuclear bone marrow and cord blood cells	OSNL OSKMLN	~0.001	High efficiency after only one transfection	Rare genomic integration event Need to check genomic integration	(Yu et al., 2009a) (Okita et al., 2011)
DNA free strategies						
Sendai virus	Fibroblasts, T cells	OSKM	~1	Free of viral gene integration	Slow process	(Ban et al., 2011; Fusaki et al., 2009; Nishimura et al., 2011; Seki et al., 2010)
Minicircle DNA	Adipose stem cells	OSNL	~0.005	Nonviral Transgene-free Single vector	Requirement for sorting of transfected cells, low efficiency	(Narsinh et al., 2011)
synthetic mRNA	Newborn and adult fibroblasts	OSKM/G OSKML OSLN	~1-4.4	Bypasses innate antiviral response Faster reprogramming kinetics, controllable and high efficiency	Requirement for multiple rounds of transfection, technically complex	(Yoshioka et al., 2013) Warren, Manos et al. 2010) (Yakubov et al., 2010)
miRNAs	Adipose stromal cells and fibroblasts	miR-200c miR-302s miR-369 or miR-302 miR-372	~0.1	No exogenous transcription factors and integration-free	Lower efficiency than other commonly used methods, labor-intensive	(Subramanyam et al., 2011) (Miyoshi et al., 2011)
Protein	Fibroblasts	OS	~0.001	Direct delivery of transcription factors and free of gene materials	Very low efficiency, short half-life and requirement for large quantities of pure protein and multiple applications	(Kim et al., 2009a) (Zhou et al., 2009) (Cho et al., 2010)
Chemicals	Fibroblasts	O	~0.2	Less risk of mutating the genes and free of gene materials	Unknown side effects and toxicity of chemicals	(Hou et al., 2013) (Desponts and Ding, 2010; Li and Ding, 2010)

Reprogramming factors can be delivered to patient cells using one or a combination of the listed strategies. DNA free reprogramming strategies are currently the best candidates for clinical use. Adapted from (Jang et al., 2014).
G-GLIS1,K-KLF4, L-LIN28, M-CMYC, N-NANOG, O-OCT4 and S-SOX2.

1.2.2.3- Enhancing cell reprogramming efficiency

Cellular reprogramming is a stochastic process (Hanna et al., 2009; Yamanaka, 2009), which explains the slowness and inefficiency of the process as just a minority of the somatic cells are in fact reprogrammed. Several small molecules have been identified and characterized to either enhance reprogramming efficiencies or substitute specific reprogramming factors (Table IV). Among the reported molecules used to enhance human iPS cells generation are chromatin/epigenetic modifiers, modulators of signal transduction pathways as kinase inhibitors, mesenchymal-to-epithelial transition (MET) regulators such as TGF β inhibitors, cell senescence alleviators and modulators of metabolism.

These chemical approaches are very important to uncover the molecular mechanisms involved in cellular reprogramming and to better regulate and control cell fate during the process (Nie et al., 2012)

Table IV- Compounds used in combination with OSKM factors (Oct4, Sox2, Klf4 and c-Myc) to facilitate human iPS cells reprogramming.

Molecule	Function	Yamanaka factors used	Cell type	Effect on reprograming	References
Epigenetic modifiers					
Tranylcypromine Parnate	LSD1 inhibitor	Oct4 Klf4	Keratinocyte	In combination with CHIR99021, enables reprogramming of human keratinocytes induced by Oct4 and Klf4	(Li et al., 2009b)
Valproic acid (VPA)	HDAC inhibitor	Oct4 Sox2	Fibroblast	Enables reprogramming of human fibroblasts induced by Oct4 and Sox2.	(Huangfu et al., 2008a; Huangfu et al., 2008b)
Sodium butyrate	HDAC inhibitor	Oct4	Fibroblast	In combination with A-83-01, PD0325901, and PS48, enables reprogramming of human somatic cells transduced with Oct4 only	(Mali et al., 2010)
RSC133	DMNT inhibitor, histone deacetylase inhibitor	Oct4 Sox2 Klf4 cMYC	Fibroblast	Enhances reprogramming of human somatic cells and maintenance of iPS cells.	(Lee et al., 2012b)
BIX	H3K9 protein methyltransferases (PMTs)	Oct4 Sox2	Fibroblast NSCs	Combination eliminates the need for Oct4, NPCs express endogenous SOX2	(Kim et al., 2008b)
Kinase inhibitors					
SB431542	ALK4,ALK5,ALK7 inhibitor	Oct4 Sox2 Klf4 cMYC	Fibroblast	Enhances and accelerates reprogramming of human somatic cells.	(Lin et al., 2009)
PD0325901	Selective MEK/ERK inhibitor	Oct4 Sox2 Klf4 cMYC	Fibroblast	Enhances and accelerates reprogramming of somatic cells	(Lin et al., 2009)
Thiazovivin	Rho-associated protein kinase inhibitor	Oct4 Sox2 Klf4 cMYC	Fibroblast	Enhances and accelerates reprogramming of somatic cells	(Lin et al., 2009)
LiCl	GSK-3β inhibitor		Fibroblast		(Wang et al., 2011)
MET regulators					

A83-01	TGFβ inhibitor	Oct4 Sox2 Klf4	Fibroblast	Together with LIF and 2i maintain mESC-like human iPS cells	(Li et al., 2009a)
Senescence alleviator					
Vitamin C	Antioxidant and co-factor for several metabolic enzymes	Oct4 Sox2 Klf4 cMYC	Fibroblast	Promotes iPSC generation from both mouse and human somatic cells	(Esteban et al., 2010)
Metabolism modulator					
N-Oxalylglycine	HIF,PHD1 and PHD2 inhibitor	Oct4 Sox2 Klf4 cMYC	Fibroblast	Enhances efficiency of reprogramming to iPSC	(Zhu et al., 2010)
Fructose 2,6-bisphosphate	PFK1 activator	Oct4 Sox2 Klf4 cMYC	Fibroblast	Enhances efficiency of reprogramming to iPSC	(Zhu et al., 2010)
Quercetin	Hypoxia-inducible factor pathway activator	Oct4 Sox2 Klf4 cMYC	Fibroblast	Enhances efficiency of reprogramming to iPSC	(Zhu et al., 2010)
DNP	Oxidative phosphorylation uncoupler	Oct4 Sox2 Klf4 cMYC	Fibroblast	Enhances efficiency of reprogramming to iPSC	(Zhu et al., 2010)
Miscellaneous					
8 Br-cAMP	cAMP-dependent kinase	Oct4 Sox2 Klf4 cMYC	Fibroblast	Improves the reprogramming efficiency of human neonatal foreskin fibroblasts transduced with all 4 iPSC TFs	Wang et al., 2011)
PS48	PDK1 activator	Oct4	Fibroblast	In combination with A-83-01, PD0325901 and sodium butyrate, enables reprogramming of human somatic cells transduced with Oct4 only	(Zhu et al., 2010)

Several strategies have been developed to use in combination with OSKM factors or to replace one or more to factors and to increase the cell reprogramming efficiencies. The class of the molecule, its function and effect on reprogramming are listed as well the somatic cell type and reprogramming method used. Adapted from (Feng et al., 2009) and (Federation et al., 2014)

1.2.3-Assessment of pluripotency

The characteristics of human iPS cells are very similar to those of hES cells in many aspects including cell morphology, expression of pluripotent markers, epigenetic changes, and potential to differentiate into cells of the three germ layers (endoderm, mesoderm and ectoderm) both *in vitro* (EBs formation) and *in vivo* (teratoma formation). Consistent standards for the identification and evaluation of iPS cells have become widely accepted in an effort to harmonize the generation and characterization of iPS cells among different laboratories (Chan et al., 2009; Maherali and Hochedlinger, 2008).

1.2.3.1-Molecular assays for pluripotency

Assessing reprogramming begins with the identification of compact colonies with well-defined borders that are composed by cells with large nucleus and nucleoli and scant cytoplasm. Those cells also stain positively for alkaline phosphatase activity, however this marker has been shown to be insufficient to test true iPS cells (Chan et al., 2009) and should be used to complement other pluripotency assays. Fully reprogrammed iPS cells express a network of pluripotency genes including OCT4, SOX2 and NANOG, TERT, REX1 and DNMT3B in similar levels to hES cells (Stadtfeld et al., 2008b). For iPS cells generated by integrating virus-mediated reprogramming strategies, silencing of proviral genes is essential to happen before the activation of the endogenous pluripotency genes; this event is complemented by the expression of embryonic antigens SSEA4, TRA-1-60A and TRA-1-81 at the cell surface (Robinton and Daley, 2012).

The verification of these *bona fide* molecular pluripotency markers is a clear indication that iPS cells generated are true iPS cells and can be further tested in functional assays of pluripotency (Table V).

Table V- Summary of pluripotency testing methods.

Pluripotency assay		Purpose	Nature of the assay	Strength/definitiveness of assay
Molecular	Colony morphology	Verify ES cells colony-like morphology of clustered, border-defined colonies	*In vitro*	Low
	Immunohistochemistry	Stain for alkaline phosphatase activity and standard pluripotency markers such as TRA-1-60,TRA-1-81 and SSEA4	*In vitro*	Medium
	Real time qPCR	Detect and quantify expression levels of selected pluripotency genes and silencing of proviral genes	*In vitro*	Medium-high
Functional	EB formation and analysis	Test differentiation capacity into all 3 germ layers in vitro	*In vitro*	Medium-high
	Teratoma formation	Test differentiation capacity into all 3 germ layers in vivo	*In vivo*	High

The molecular and functional assays more currently used to evaluate pluripotency are listed as also the relative contribution of each assay to the determination of the pluripotency.
Adapted from Stembook online (http://www.ncbi.nlm.nih.gov/books/NBK27044/), September 2015

1.2.3.2-Functional assays for pluripotency

Characterization of the functional abilities of iPS cells begins with *in vitro* differentiation and the differentiation in embryoid bodies (EBs), which are compact cell aggregates composed by several cell types and resemble the gastrulating embryo. These cultures are then assessed for markers of each of the three germ layers after a short period of differentiation (Karbanova and Mokry, 2002; Pekkanen-Mattila et al., 2010; Sheridan et al., 2012). The highest stringent assay for human iPS cells is the *in vivo* differentiation and the formation of teratomas, being this assay the current functional gold standard for human iPS cells (Muller et al., 2010).

In this assay immune-deficient mice are injected subcutaneously or intramuscularly with human iPS cells and if the cells are truly pluripotent, they will form well-differentiated tumors comprising tissues from each of the three germ layers. This assay provides information about the spontaneous differentiation potential of the injected iPS cells and although it is the most stringent assay available for human iPS cells, it is not powerful enough to assess whether iPS cells can produce all the cell types of the human body. Nevertheless, together with DNA methylation and gene expression profiles (Bock et al., 2011; Daley et al., 2009), the teratoma assay can help to adopt a set of standards that can be applied uniformly worldwide and accelerate the use of iPS cells for therapy (Zhang, 2014).

1.3- New *in vitro* models derived from induced pluripotent stem cells

1.3.1- Neurodegenerative disease models: animal and *in vitro* models

Disease models are indispensable tools for understanding the pathogenesis of disease and for enabling the development of novel therapeutics. Traditionally, human diseases have been modeled in mouse models and derived primary cultures or in transformed cell lines (Tiscornia et al., 2011), given that primary patient cells are only available in very small quantities. In fact, human tissues other than blood are usually unavailable in sufficient amounts for research. In the particular case of live brain tissue, availability of tissue is even more scarce as it can be obtained only in specific pathologies treated by surgical approaches and always in extremely low amounts. Postmortem samples are also difficult to obtain and the quality of the material may impair analysis.

A substantial amount of the current knowledge about the molecular mechanisms of disease development has been derived from the study of mouse models. Biological systems that allow the analysis of *in vivo* context of whole organisms are considered more informative than cell-based *in vitro* approaches, as they can be used to examine disease progression over time, starting even at early time points when human patients are presymptomatic and enable the study of behavioral phenotypes (Merkle and Eggan, 2013). However these advantages are offset by species-specific differences between mice and humans in their physiological and anatomical characteristics that fail to accurately reproduce human pathology (Dolmetsch and Geschwind, 2011; Hackam and Redelmeier, 2006; van der Worp et al., 2010). Specifically in the case of brain, neurogenesis, patterning during neurodevelopment (Clowry et al., 2010), ratio of glia to neurons and subtypes of neurons (Oberheim et al., 2006), exhibit fundamental differences between humans and rodents (Kaye and Finkbeiner, 2013). Also, the development of these models is often time consuming and expensive. Faster and more human-relevant model systems are needed to complement animal models and to accurately recapitulate the natural processes that occur in human patients.

Transformed cell lines are accessible in large quantities and can be engineered to express a disease-causing gene of interest, but the immortal growth of these cultures typically entails selection for genetic alterations that may influence the cells response and performance. The physiology of animal models and transformed cell lines is different from that of patient cells, which may explain why many drug candidates have not been effective in patients when tested in clinical trials (Scannell et al., 2012; Sterneckert et al., 2014). The clear rationale would be the use of human primary cells but most primary cells are difficult to access and have a finite lifespan in culture, a shared characteristic with adult stem cells that hinder their broadly use as *in vitro* models. Human adult neural stem cells (NSCs) were

isolated for the first time in the late 90's (Eriksson et al., 1998; Kukekov et al., 1999) proving that human neurogenesis was present in adult brain. Since then several improvements have been made in human NSCs culture and expansion (Reynolds and Weiss, 1992; Skogh et al., 2001) but it is still a challenge to isolate these cells from *post mortem* tissues due to technical
difficulties and low availability of samples.

The other source of *in vitro* models are the ones derived from pluripotent stem cells that have many favorable attributes, given that human pluripotent stem cells (hPSCs) can theoretically be differentiated into any desired cell type and the molecular and cellular phenotypes can be studied in any target cell.

Cultured cells can be produced in a relatively rapid way and in large quantities, allowing the development of large-scale genetic and chemical screens for phenotypic modifiers (Merkle and Eggan, 2013). In Table VI are listed advantages and disadvantages of the main *in vitro* models used to study human neurodegenerative diseases.

Table VI- Advantages and disadvantages of human cells available for human disease modeling.

Cell Type		Advantages	Disadvantages
Immortalized cell lines		Stable, standardized and reproducible Economical Ethically unbiased	Lack important aspects of native function Not representative of all cell types No comprehensive reflection of organism/systems biology No comprehensive disease modelling
Primary cell lines		Fully differentiated cell types Close approximation of native function	Not easily accessible or available for all cell types Require fresh preparation Questionable reproducibility
Adult stem cells		Realistic model of human disease Patient-specific cells Ethically unbiased	Partially immature phenotype Supply very limited Isolation and expansion in culture very difficult Capacity of unlimited self-renewal and plasticity unclear
Pluripotent stem cells	hES cells	High quantity Readily available source of all cell types Fully differentiated cell types Close approximation of native function Realistic model of human disease	Growth and maintenance expensive A lot of time needed to obtain fully differentiated cell types Ethical concerns Partially immature phenotype
	hiPS cells	Realistic model of human disease Patient-specific cells Pluripotent and unlimited supply Ethically unbiased	Partially immature phenotype Uncontrolled viral integration into genome during iPSC derivation poses limitations for comprehensive conclusions, non-viral derivation methods required

The most relevant advantages and disadvantages of the human cells available for disease modeling are listed. Adapted from (Ebert and Svendsen, 2010)

1.3.2- Neuronal patterning and differentiation

The iPS cells neuronal differentiation recapitulates early *in vivo* neurodevelopment, producing embryonic-like neurons that proceed through the neurodevelopmental stages of neural progenitor cell proliferation, regionalization, terminal neuronal differentiation and maturation (Purves, 2004). During normal neurodevelopment, neural induction begins immediately after gastrulation when the neural plate forms; the neural plate is a flat sheet of neuroepithelium that evaginates over time and fuses dorsally to form a cylinder of cells, the neural tube. The neural tube contains multipotent NSCs that proliferate extensively in neurogenic zones lining the ventricles, the ventricular (VZ) and subventricular zones (SVZ) and generate intermediate progenitors (IPCs), neurons and glia of the central nervous system (CNS) (Gage and Temple, 2013; Sergiu et al., 2014). Three primary vesicles develop in the rostral part of the neural tube giving rise to forebrain, midbrain and hindbrain, whereas the caudal part of the neurotube remains undifferentiated and will form the spinal cord.

Through the actions of morphogens, cells acquire positional identity and specified neural fates (Altmann and Brivanlou, 2001; Le Dreau and Marti, 2012). Two opposed signaling centers: the ventral floor plate and the dorsal roof plate are responsible for the secretion of signals with patterning activity, including the Sonic hedgehog (Shh) secreted from the ventral floor plate and members of the Wingless-type MMTV integration site (Wnt); and the Bone Morphogenetic Protein (BMP) families (Liem et al., 1995) secreted from the RP (roof plate). Those main signaling pathways are required for dorsal-ventral patterning and anterior-posterior patterning is assigned to non-BMP members of the transforming growth factor-beta (TGF- β) superfamily (Liem et al., 1997) and Retinoic Acids (Diez del Corral et al., 2003) (Fig 1.7).

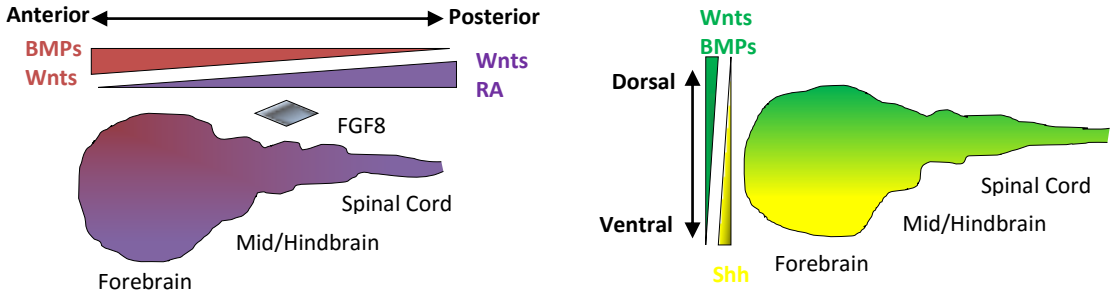

Figure 1.7- Schematic representation of signalling factor families that are expressed as gradients along the anterior-posterior axis and dorsal-ventral axis.

A coronal section of the developing telencephalon is depicted and the gradients of signalling factors: BMP-bone morphogenetic protein; FGF-fibroblast growth factor; RA-retinoic acid and Shh-sonic hedgehog. Adapted from (Petros et al., 2011).

TGF-β family members are factors that suppress the neural induction of ectoderm and promote an epidermal lineage, thus neural induction requires in its early step the inhibition of non-neural fates by blocking neural inhibitors (Munoz-Sanjuan and Brivanlou, 2002). Particularly the influence of BMPs on neural differentiation can be modulated by endogenous BMP antagonists as Noggin (Smith and Harland, 1992; Valenzuela et al., 1995), Chordin (Pappano et al., 1998; Sasai et al., 1994), Follistatin (Hemmati-Brivanlou et al., 1994) and other antagonists for TGF-β family members as Activin (Hemmati-Brivanlou and Melton, 1994) and Nodal (Camus et al., 2006), that promote the inhibition of SMAD proteins that act as ligand-inducible inhibitors of signal transduction (Heldin et al., 1997). The transcriptional regulation by SMADs is concentration-dependent on TGF-β family members induction levels, being the nuclear levels a direct readout of ligand induced receptor activation (Nishimura et al., 2003; Wilson et al., 1997) (Fig 1.8), which makes SMAD signaling a crucial target in neural induction.

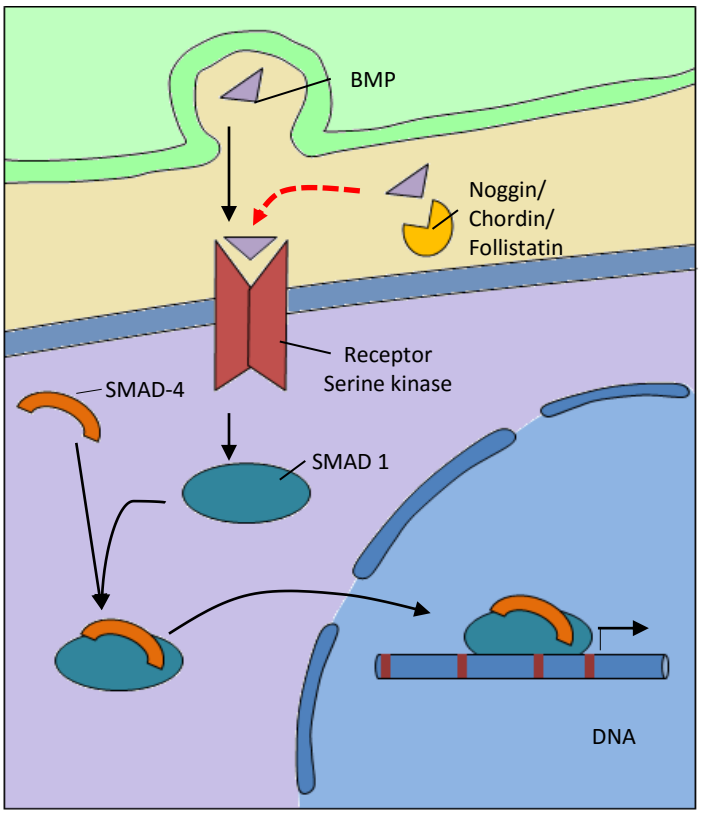

Figure 1.8- Schematics of ligands, receptors and primary intracellular signalling molecules for BMP (Bone morphogenetic protein), as an example of the inductive signalling pathway of TGF-β superfamily.

BMP ligands bind to heteromeric type I and type II receptors and induce the autophosphorylation of the receptors. The active receptor complex phosphorylates the Smad1 protein, which associates with the Smad4 and translocates to the nucleus where it activates the transcription of genes that promote dorsal fates and inhibit ventral fates. Adapted from (Purves, 2004).

In vitro neural induction of human iPS cells is the first step in most protocols of neuronal differentiation, mimicking the *in vivo* neurodevelopment process by progressively restricting the differentiation potential of pluripotent cells to obtain specified neural progenitors (Chambers et al. 2009).This step can be accomplished by using spontaneous differentiation, stromal feeder co-culture (Aubry et al., 2008; Kawasaki et al., 2000; Perrier et al., 2004), treatment with retinoic acid (Maden, 2002, 2007), culture in defined media containing the FGF mitogens (Murry and Keller, 2008; Zhang, 2006) and more recently by dual inhibition of BMP and Activin/Nodal/TGF-β signaling pathways, also known as dual SMAD inhibition (dSMADi) (Chambers et al., 2009). DSMADi can be achieved by using recombinant endogenous inhibitors as Noggin or small molecule antagonists of BMP-dorsomorphin (Zhou et al., 2010) and its derivative LDN-193189 (Chambers et al., 2012) and endogenous antagonists of Nodal as Lefty (Meno et al., 1999) and Cerberus (Belo et al., 1997) or the small molecule SB431542 (Smith et al., 2008).

These neural progenitors can then be patterned along the anterior-posterior and dorso-ventral axes using specific morphogens and growth factors which activate or inhibit the key developmental pathways of Wnt, Shh, RA and FGF. The use of small molecules to replace the expensive recombinant protein factors has been employed providing higher potency, efficacy and scalability in neuronal differentiation, as in the case of purmorphamine (PMA) (Sinha and Chen, 2006) and cyclopamine (Incardona et al., 2000), respectively an agonist and antagonist of Shh, XAV 939 a tankyrase inhibitor (Huang et al., 2009) that can replace Dkk-1(Watanabe et al., 2005) as an antagonist of Wnt; and CHIR99021, an Wnt activator that selectively inhibits the GSK-3β (Kirkeby et al., 2012; Lyashenko et al., 2011).

On this basis, a wide variety of protocols have been described for hES cells and hiPS cells specification to various disease-relevant neuronal subtypes, such as cerebral cortex neurons, midbrain neurons, cerebellar neurons or spinal cord motoneurons, as summarized in Table VII.

Table VII- Protocols for human PS cells differentiation towards neuronal fate

Neuronal type	Key patterning factors	Brain region	References
Cortical pyramidal neurons	Cyclopamine, FGF2,RA	Forebrain	(Espuny-Camacho et al., 2013; Gaspard et al., 2008; Murashov et al., 2005; Zeng et al., 2010)
Cortical interneurons	Shh, FGF2, PMA, XAV939	Forebrain	(Goulburn et al., 2012; Li et al., 2009c; Maroof et al., 2013; Nicholas et al.,

			2013; Nicoleau et al., 2013)
Dopaminergic neurons	Shh, AA, FGF8, FGF2 PMA,CHIR99021	Midbrain	(Chambers et al., 2009; Kawasaki et al., 2000; Kirkeby et al., 2012; Kriks et al., 2011; Morizane et al., 2013; Perrier et al., 2004; Sonntag et al., 2007; Swistowski et al., 2010; Yan et al., 2005)
Striatal medium spiny neurons	Shh,BDNF,DKK-1, cAMP, valproic acid	Midbrain	(Aubry et al., 2008; Delli Carri et al., 2013a)
Cerebellar neurons	WNT1/3, BMP4/6/7,Shh,FGF8/4,JAG1	Hindbrain	(Erceg et al., 2012; Erceg et al., 2010; Salero and Hatten, 2007; Wang et al., 2015)

The table lists the principal neuronal types derived from human pluripotent stem cells, specifying the key exogenous signaling factors: FGF- fibroblast growth factor, RA-retinoic acid, PMA-purmorphamine, Shh-sonic hedgehog, AA-ascorbic acid, BDNF-brain-derived neurotrophic factor, DKK-1-Dickkopf-1, cAMP-cyclic adenosine monophosphate, WNT-wingless-related integration site, JAG-1-jagged1. Adapted from (Petros et al., 2011) and (Srikanth and Young-Pearse, 2014)

Motor neurons	Shh, RA, SB431542	Spinal cord	(Amoroso et al., 2013; Chambers et al., 2009; Dimos et al., 2008; Hu and Zhang, 2009; Karumbayaram et al., 2009; Nizzardo et al., 2010)

1.3.3- Neurodegenerative diseases modeled with iPS cells

Many neuronal iPS cells-derived models have been developed to study and characterize monogenic neurodegenerative diseases in the last seven years. The first iPSCs-based disease models for neurodegenerative disorders were generated for amyotrophic lateral sclerosis (ALS) (Dimos et al., 2008) and spinal muscular atrophy (SMA) (Ebert et al., 2009) and since then many other mendelian neurodegenerative disorders have been modelled, as presented in Table VIII.

All the neuronal models established from differentiation of diseased iPS cells prove to be accurate human *in vitro* models as the expression of the mutant protein associated with the genetic mutation linked to the disease pathogenesis was conserved. Most of the disease phenotypes reported were early phenotypes, associated with increased neuronal sensivity to cellular stress, failure of survival pathways as autophagy and apoptosis and impaired maturation and complexity of neuronal processes.

Table VIII- Overview of the iPS cell-derived models for monogenic neurodegenerative diseases.

Neurodegenerative disease	Types of affected neurons	Histopathology	Gene (mutation)	Reprogramming method	iPSC-derived cell subtype	Reported phenotype	References
Alzheimer's disease (AD)	Basal forebrain cholinergic neurons, cortical neurons	Neurofibrilliary tangles, amyloid plaque, Loss of neurons and synapses	PS1 and PS2	RV: OSKLN/ SF	Neurons	Increased amyloid β42 generation	(Yagi et al., 2011)
			Sporadic and APP duplication	RV: OSKM/ SF	Neurons	Increased amyloid β42 secretion; Tau phosphorylation and GSK3β phosphorylation	(Israel et al., 2012)(Hossini et al., 2015)
			APP E693Δ	Episomal OSKML siRNA p53/SF RV: OSKM/ SF	Cortical neurons	Increased amyloid β42 generation and oligomerization, increased levels of cellular stress	(Kondo et al., 2013; Mertens et al., 2013)
			PS1	RV: OSKM/ SF Episomal OSKMLNT/ SF	Neural progenitor cells and neurosn	Increased amyloid β42 generation	(Sproul et al., 2014)(Mahairaki et al., 2014)
Amyotrophic lateral sclerosis (ALS)	Upper and lower motor neurons	Ubiquitinated inclusion bodies, loss of motor neurons	SOD1	RV: OSKM, OSK/ SF	Motor neurons	NA Neurofilament misregulation and aggregation Neurite degeneration	(Boulting et al., 2011; Chen et al., 2014; Dimos et al., 2008; Kiskinis et al., 2014; Wainger et al., 2014)
			TDP-43	RV: OSKM SF	Motor neurons and glia	TDP-43 aggregates	(Bilican et al., 2012)
			C9ORF72	RV: OSKM SF	Neurons and motor neurons	Sensivity to glutamate neurotoxicity	(Donnelly et al., 2013; Sareen et al., 2012)
			VAPB	RV: OSKM SF	Motor neurons	VAPB aggregates	(Mitne-Neto et al., 2011)
			FUS	LV: OSKM/ SF	Motor neurons	Incorporation of mutant FUS in stress granules	(Lenzi et al., 2015)
			Sporadic	RV: OSKM SF	Motor neurons	TDP-43 intranuclear aggregates	(Burkhardt et al., 2013)
Familial dysautonomia (FD)	Sensory and autonomic neurons	Reduced size of DRG neurons, reduced number of non-myellinated small fibers and intermediolateral column neurons	IKGKAB	RV: OSKM/ SF and FLB	Neural crest cells	Defects in IKBKAP splicing,neurogenesis and migration	(Lee et al., 2009; Lee et al., 2012a)
Friedreich's Ataxia (FA)	Dorsal root ganglia (DRG) peripheral neurons and cerebellar neurons	Reduced size of DRG neurons,iron misdistribution, decreased myelination	FXN (GAA expansion)	RV: OSKM/ SF LV: OSLN/ SF	Neural crest cells, peripheral sensory neurons	FXN GAA repeat instability; Impaired electrophysiological properties and mitochondria defects	(Ku et al., 2010; Liu et al., 2011);(Hick et al., 2013)
Frontotemporal dementia (FTD)	Cortical neurons of frontal and temporal lobes	Neuronal loss	Sporadic and GNR mutation	RV: OSKM/ SF	Neurons	Increased sensivity to cellular stress	Almeida et al., 2012
			C9ORF72 (GGGGCC repeat expansion)	RV: OSKM/ SF	Neurons	Decreased neuronal viability upon treatment with chloroquine	(Almeida et al., 2013; Almeida et al., 2012)
Huntington's disease (HD)	Striatal GABAergic medium spiny neurons, cortical neurons	Neural inclusion bodies, loss of striatal/cortical neurons	HTT (CAG repeats)	RV: OSKM/ SF Episomal OSKML siRNA p53/ SF	NPCs, neurons, Striatal neurons	Increased lysosomal activity and susceptibility to stress and toxicity Huntingtin aggregates upon proteasome inhibition,	(An et al., 2012; Camnasio et al., 2012; Consortium, 2012; Jeon et al., 2012; Juopperi et al., 2012; Mattis et al., 2015; Zhang et al., 2010)
Parkinson's disease	Midbrain nigro-striatal dopaminergic neurons	Lewy-bodies, loss of dopaminergic neurons	Idiopathic	LV: Cre-excisable, DOX-inducible OSKM or OSK/ SF	Dopaminergic neurons	NA	(Hargus et al., 2010; Soldner et al., 2009)

			LRRK2	RV: OSK (M)/ SF	Dopaminergic neurons	Increased caspase-3 activation and dopaminergic neuron death with various cell stress conditions; Mitochondrial DNA damage; Accumulation of autophagosomes	(Cooper et al., 2012b; Nguyen et al., 2011; Orenstein et al., 2013; Reinhardt et al., 2013; Sanchez-Danes et al., 2012; Sanders et al., 2014; Su and Qi, 2013)
			PARK2	LV: OSKMN/ SF	Dopaminergic neurons	Reduced DAT expression, low dopamine uptake, Susceptibility to oxidative stress; Reduced length and complexity of neuronal processes	(Imaizumi et al., 2012; Jiang et al., 2012; Ren et al., 2014)
			PINK1	RV: OSKM/ SF	dopaminergic neurons	Impaired stress-induced mitochondrial translocation of parkin; Susceptibility to oxidative stress	(Cooper et al., 2012b; Rakovic et al., 2013; Seibler et al., 2011)
			SCNA	RV: OSKM/ SF LV: Cre-excisable, DOX-inducible OSKM or OSK/ SF	Neurons	Increased neural α-synuclein protein levels sensivity to oxidative stress	(Byers et al., 2011; Devine et al., 2011; Soldner et al., 2011)
SBMA	Anterior horn cells and dorsal root ganglion cells	Intranuclear inclusion bodies, neuronal loss	Androgen Receptor (CAG expansion)	LV: OSKM/ SF	Motor neurons	Increased acetylated α-tubulin AR aggregation	(Grunseich et al., 2014; Nihei et al., 2013)
Spinal muscular atrophy (SMA)	Spinal motor neurons	Loss of anterior horn cells	SMN1 deletion	RV: OSNL Episomal plasmid OSKMNL combinations/ SF	Neurons and astrocytes, Mature motor neurons	Reduced number of motor neurons, decreased soma size, and axon length, synaptic defects; Increased activation of apoptotic markers	(Corti et al., 2012; Ebert et al., 2009; Sareen et al., 2012)
SCA2	Cerebellar and thalamic neurons,	Cytoplasmic inclusion bodies, neuronal loss	ATAXIN2 (CAG expansion)	RV: OSKM/ SF	Neurons	Decreased survival of neurons	(Xia et al., 2013)
(SCA3/ /MJD)	Cerebellar neurons, striatal and cortical neurons	Intranuclear inclusion bodies, neuronal loss	ATAXIN3 (CAG expansion)	RV: OSKM/ SF	Neurons	Insoluble ataxin-3 aggregates upon glutamate excitation	(Koch et al., 2011)
SCA7	Cerebellar, thalamic, midbrain and retinal neurons,	Intranuclear inclusion bodies, neuronal loss	ATAXIN7 (CAG expansion)	RV: OSKM/ SF	Neurons	NA	(Luo et al., 2012)

Adapted from (Han et al., 2011) and (Bellin et al., 2012)
S-SOX2, O-OCT4, K-KLF4, M-MYC, N-NANOG, L-LIN28, T-SV40LT, SF-skin fibroblasts, FLB-fetal lung fibroblasts and NPCs-neural progenitor cells.

These models prove to be very useful as *in vitro* platforms for testing strategies to reverse the disease phenotype with either drugs or molecular therapy approaches involving gene silencing, overexpression or correction. Several compounds have been tested in neuronal iPS cells derived models, as in the cases of AD (Hossini et al., 2015; Israel et al., 2012; Kondo et al., 2013; Mertens et al., 2013; Yagi et al., 2011), ALS (Bilican et al., 2012; Burkhardt et al., 2013; Egawa et al., 2012; Mitne-Neto et al., 2011; Wainger et al., 2014),

FD (Lee et al., 2009; Lee et al., 2012a), PD (Cooper et al., 2012b),SBMA (Grunseich et al., 2014; Nihei et al., 2013) SCA3/MJD (Koch et al., 2011) and SMA (Ebert et al., 2009). Drug screening along with disease modelling are the most immediate applications of these models as they prove to be valuable human *in vitro* predictive tools to elucidate disease mechanisms and to obtain drug efficacy and toxicity data in preclinical testing of candidate compounds, accelerating the delivery of therapeutics to patients (Grskovic et al., 2011; Merkle and Eggan, 2013; Pankevich et al., 2014).

With the advent of new techniques for gene editing, especially the development of engineered nucleases, including Zinc Finger Nucleases (ZFNs) (Zou et al., 2009), Transcription Activator-Like Effector Nucleases (TALENs) (Hockemeyer et al., 2011) and Clustered Regularly Interspaced Short Palindromic repeats (CRISPR)-associated Cas9 nucleases (Cong et al., 2013; Jinek et al., 2012; Mali et al., 2013) it is now possible and easier to generate isogenic controls, as compared with classical approaches as homologous recombination. Isogenic controls are genotyped matched iPS cell lines where the gene mutation has been corrected by removing the gene mutation and are ideal controls, as they allow the perfect matched comparison of disease-specific genotypes and have been widely used in several neuronal iPS cells derived models of monogenic diseases: ALS (Chen et al., 2014; Kiskinis et al., 2014; Wainger et al., 2014), FA (Li et al., 2015), HD (An et al., 2012) and PD (Reinhardt et al., 2013; Ryan et al., 2013; Sanders et al., 2014; Soldner et al., 2011). The correction of the genetic mutation underlying the disease pathogenesis dramatically reduces the effect of phenotypic alterations that might be attributed to genotypic variability and eliminates the influence of the genetic background in the molecular perturbations that are essential to define the disease phenotype (Merkle and Eggan, 2013).

1.3.4- *In vitro* ageing: a strategy to trigger late onset neurodegenerative diseases

HiPSCs-derived neurons used to study mechanisms of disease are often differentiated from two weeks up to thirty weeks (Chambers et al., 2009; Nicholas et al., 2013) and represent the first trimester stage of human development (Mariani et al., 2012). The prolonged time in culture and the co-culture of neurons and astrocytes are well-known strategies that accelerate maturation and synapse formation (Christopherson et al., 2005; Johnson et al., 2007) but time in culture may not have a direct relationship with the state of maturity and “age” of the neuronal population (Hester et al., 2011). Therefore, it is still a challenge to predict when an age-dependent phenotype may emerge as the relation between long-term culture and aging is not clear.

Neurons derived from patients with late onset disorders can reveal early mechanisms prior to the development of "downstream" phenotypes, such as the altered gene expression and protein processing/aggregation that may only be observed in fully mature and aged neurons. Several methods are employed to accelerate the maturation and aging of hiPSCs-derived neurons enabling the study of disease phenotypes in more manageable time frames. The use of stressors, the overexpression of proteins implicated in cellular aging regulation (Liu et al., 2012) and the induction of excitotoxicity are the most common techniques that have been successfully used in several studies (Sandoe and Eggan, 2013).

Ageing is associated with increased oxidative stress (Ward et al., 2014) and in an effort to mimic stress-induced changes that occur during normal aging, oxidative stressors were used in several neuronal iPSCs-derived models of late-onset diseases to produce the ageing effect *in vitro* and to induce age-dependent phenotypes. The use of hydrogen peroxide and sodium arsenite are the most common approaches to induce the production of reactive oxygen species (ROS) in ALS (Egawa et al., 2012; Lenzi et al., 2015), HD (Consortium, 2012) and PD (Cooper et al., 2012b; Nguyen et al., 2011) neuronal models derived from iPS cells. In these studies, disease-related susceptibility phenotypes were uncovered, where patient-specific neurons were more susceptible to stress-induced death than control neurons.

Other classes of stressors used to unveil late-onset neuronal phenotypes are the proteasome inhibitors such as MG132 (Cooper et al., 2012b; Jeon et al., 2012; Mitne-Neto et al., 2011; Nguyen et al., 2011) and autophagy inhibitors such as 3-Methyladenine (Consortium, 2012), chloroquine (Camnasio et al., 2012) and ammonium chloride (Sanchez-Danes et al., 2012) that contribute to protein aggregation and proteotoxicity, hallmarks of neurodegeneration in the established neuronal models.

Progerin is a truncated form of lamin A that causes premature ageing in humans (Scaffidi and Misteli, 2006). The expression of progerin in iPS cells-derived dopaminergic neurons of Parkinson's patients harboring the *PINK1* and *PARK2* mutations (Miller et al., 2013) induced dendrite degeneration and production of ROS, causing oxidative stress in a similar way to oxidative stress inducers (Reinhardt et al., 2013). The effects of progerin expression can be compared to those of chemically induced oxidative stress, but it is still unclear whether the verified cellular alterations are due to the induced programmed aging, were dependent on the progerin expression, or to the PD genotype (Studer et al., 2015; Vera and Studer, 2015).

Excitotoxicity is a pathological hallmark of neurodegenerative diseases and neurotoxicity can be induced by excessive concentrations of glutamate, the major excitatory neurotransmitter in the CNS (Mattson and Magnus, 2006). The actions of glutamate are mostly mediated by AMPA and NMDA receptors that flux Na^+ and Ca^{2+} and

the overactivation of these receptors results in sustained Ca^{2+} influx. Therefore, one method to mimic *in vivo* ageing *in vitro* is the exposure of iPSCs-derived neurons to high extracellular concentrations of glutamate, as demonstrated using iPS cells derived from ALS (Donnelly et al., 2013), HD (Consortium, 2012; Mattis et al., 2015) and MJD patients (Koch et al., 2011) The neurons derived from these iPS cells presented higher sensitivity and cell death dependent on glutamate treatment as compared to controls. In the MJD model, it was demonstrated that glutamate-induced excitotoxicity mediated by increased levels of Ca^{2+} activated proteolysis and aggregation of the ataxin-3 protein, reinforcing an important insight about MJD pathogenesis.

For future research, it is important to improve the assessment of the *in vitro* maturation and aging of neurons to further define the disease-specific molecular signature and correlate it with emerging disease phenotypes. The improved predictability of these iPS cell-derived neuronal models is an essential requirement and will help to support these models as essential tools to provide significant understanding of disease mechanisms and to identify new therapies for patients.

1.4- Objectives

In this work we aimed at generating a new human neuronal *in vitro* model derived from iPS cells to investigate the MJD pathogenesis.

The specific objectives of this work were the following:

- To establish and characterize primary human adult fibroblast cultures of MJD (chapter 2) to be used as the somatic cell type used in reprogramming (chapter 3).

- To study impairment of the autophagy pathway in MJD patient's fibroblasts (Chapter 2).

- To generate and characterize a set of human MJD iPS cell lines, regarding its pluripotency, and genetic stability (Chapter 3).

- To generate and investigate a neuronal *in vitro* model to study the early events of the pathogenesis of MJD in patient-specific neurons derived from iPS cells (Chapter 4).

Chapter 2

Fibroblasts of Machado Joseph Disease patients reveal autophagy impairment

2.1- Abstract

Machado Joseph Disease (MJD) is the most frequent autosomal dominantly inherited cerebellar ataxia caused by the over-repetition of a CAG trinucleotide in the *ATXN3* gene. This expansion translates into a polyglutamine tract within the ataxin-3 protein that confers a toxic gain-of-function to the mutant protein ataxin-3, contributing to protein misfolding and intracellular accumulation of aggregates and neuronal degeneration.

Autophagy impairment has been shown to be one of the mechanisms that contribute for the MJD phenotype. Here we investigated whether this phenotype was present in patient-derived fibroblasts, a common somatic cell type used in the derivation of induced pluripotent stem cells and subsequent differentiation into neurons, for *in vitro* disease modeling.

We generated and studied adult dermal fibroblasts from 5 MJD patients and 4 healthy individuals and we found that early passage MJD fibroblasts exhibited autophagy impairments with an underlying mechanism of decreased autophagosome production.

Our results provide a well-characterized MJD fibroblast resource for neurodegenerative disease research and contribute for the understanding of mutant ataxin-3 biology and its molecular consequences.

2.2- Introduction

Machado Joseph Disease (MJD) also known as Spinocerebellar Ataxia Type 3 (SCA3) is an autosomal dominant inherited cerebellar ataxia and a progressive, adult-onset neurodegenerative disease (Durr et al., 1996; Paulson et al., 1997b). SCA3 is caused by a CAG-repeat expansion in the *ATXN3* gene on chromosome 14q24.3–q32.2, which results in an abnormally long polyglutamine tract in the ataxin-3 protein (Kawaguchi et al., 1994).

There is strong evidence that proteins with an overlong mutant polyglutamine tract are inefficiently degraded by the ubiquitin-proteosome system (UPS) but may be cleared by macroautophagy (hereafter referred to as autophagy), an intracellular degradation pathway with a crucial role in degradation of insoluble aggregate-prone proteins (Levine and Kroemer, 2008) such as the polyglutamine proteins involved in neurodegenerative diseases (Sridhar et al., 2012). Our group previously provided evidence of an impairment of the autophagy pathway in a MJD rodent model and decreased levels of Beclin-1/ATG6, a component of the class III PI3 kinase complex required for autophagy initiation and autophagosome formation, in human fibroblasts from two MJD patients (Nascimento-Ferreira et al., 2011).

Adult dermal fibroblasts are an accessible source of patient cells, easy to grow in culture and currently the most suitable somatic cell type for reprogramming giving an efficient yield of induced pluripotent stem cells (iPSCs) (Grskovic et al., 2011). Studying patient-derived fibroblasts, as somatic cell type of origin can give new insights in the establishment of diseased phenotype of patient-derived neurons resulting from iPSCs differentiation, taking in account that fibroblasts hold the native genetic background of the patient without further genetic manipulation (Schwartz et al., 2014; Wray et al., 2012).

Therefore, in this work we collected and studied a cohort of human primary fibroblast cultures obtained from MJD patients and healthy controls in order to elucidate whether this type of peripheral cells presents a MJD related phenotype, at molecular, cellular or functional level. For this purpose, we examined the levels of i) Beclin-1/ATG6 and ii) p62/SQSTM, a protein with an ubiquitin-associated domain that is involved in interaction with ubiquitinated proteins and transport to autophagosomes. p62/SQSTM interacts with LC3, a protein present in autophagic membranes, through its LC3 recognition sequence (LRS) allowing the incorporation of ubiquitinated proteins in autophagosomes to be subsequently degraded in autolysosomes (Mizushima, 2007). To clarify whether a) autophagosome formation is impaired or b) the autophagic flux (rate of autophagosome delivery to lysosomes) is compromised we investigated the levels of LC3-II (Menzies et al., 2012).

We used primary skin fibroblasts as an extraneural disease model to study the underlying mechanism of molecular autophagic dysfunction associated to MJD. This strategy has been used for other neurodegenerative disorders such as Parkinson's disease, Huntington's disease and Alzheimer's disease (Auburger et al., 2012; Connolly, 1998; Mazzola and Sirover, 2001) to complement studies in animal models, transformed cell lines and patient tissues. Therefore, in this work we aimed at evaluating the MJD phenotype in human adult fibroblasts and to further use it as starting material for reprogramming and implementation of disease models.

2.3-Material and Methods

2.3.1- Cell culture

MJD and control fibroblasts were generated from 3 mm forearm and thigh dermal biopsies following informed consent under protocols approved by the Hospital Center of the University of Coimbra and the Medical Faculty of the University of Coimbra. All the fibroblasts were cultured in complete culture medium (DMEM (Gibco), supplemented with 10% FBS (Gibco), 2mM L-Glu (Gibco), 1% penicillin/streptomycin (Gibco) and 1% NEAA (Sigma-Aldrich)) (Rittie and Fisher, 2005; Takashima, 2001).

Briefly, skin explants were washed in PBS and subcutaneous tissue was excised. Epidermis was removed either mechanically or enzymatically (0.05% dispase/PBS, 1h at 37ºC) and resulting dermal samples were cut in small pieces and placed in 0.1% gelatin coated tissue culture dishes.

Fibroblasts outgrowths were detected within a week and allowed to grow upon confluency in complete culture medium. Human fibroblasts were harvested with trypsin 0.05% and transferred to culture flasks for further expansion. Cell subculture was done when confluence was reached and using a 1:3 split ratio.

2.3.2- Karyotype analysis

The karyotype analysis was performed using standard G-banding techniques (Rooney DE, 1992). Cells cultured in a T25 flask were treated with 0.2µg/ml Colcemid for up to 3 hours, followed by dissociation with trypsin/EDTA. The cells were pelleted via centrifugation and re-suspended in pre-warmed 0.05M KCl hypotonic solution and incubated for 20 minutes. Following centrifugations the cells were re-suspended in fixative. Metaphase spreads were prepared on glass microscope slides and GTG-banded by brief exposure to trypsin and stained with Giemsa. A minimum of 10 metaphase spreads were analysed for the fibroblasts. Karyotypes were established according to the International System for Human Cytogenetic Nomenclature (ISCN) 2013 (Shaffer LG, 2013).

2.3.3- Immunocytochemistry

Cells were briefly fixed in a 50/50 mixture of ice cold acetone-methanol or PFA 4% for 10 min and then blocked in PBS containing 0.3% Triton X-100 and 5% FBS for 1 hr before incubation with primary antibodies (Ataxin-3 1:1000 Immunostep, TE-7 1:100 Millipore, Vimentin 1:100 Cell Signaling and LC3B 1:400 Cell Signaling) overnight at 4ºC, in PBS containing 0.3% Triton X-100 and 1% BSA. After three washes with PBS, cells were incubated with Alexa Fluor® 488 and 594 secondary antibodies (1:200, Invitrogen) for 2 h at room temperature. Additionally, cells were stained with DAPI in order to visualize cell nuclei and, after washing, mounted in Fluoroshield (Sigma-Aldrich Aldrich). Fluorescent signals were detected using a Zeiss inverted microscope (Zeiss Axio Observer Z1).

2.3.4- Cell counts and quantification of ataxin-3 and LC3-II

LC3-II and Ataxin-3 fluorescence were measured using a semiautomated image-analysis software package (Zen Observer, Germany). At least 100 cells for each condition were analyzed, using an x40 objective.

2.3.5- Cell treatment

Fibroblasts were incubated with 100 μM chloroquine diphosphate (Sigma-Aldrich) dissolved in water in the treated group and with vehicle in non-treated group, during 2 h at 37ºC before protein extraction or immunocytochemistry.

2.3.6- Protein Isolation and Western Blot Analysis

The cells were lysed with RIPA buffer (50 mM Tris-Cl, pH 7.5, 150 mM NaCl, 1% Nonidet P-40, 0.5% sodium deoxycholate and 0.1% SDS, 1 mM PMSF and 1mM DTT) supplemented with a protease inhibitor cocktail (Roche), triturated and centrifuged at 12,000 rpm for 20 min at 4ºC. The cell lysates were collected after centrifugation. The protein concentration in the lysates was determined using the Bradford protein assay reagent (Bio-Rad). Approximately 30 μg of protein were separated on SDS-PAGE gels (4% stacking and 10% or 12% running) and transferred to a PVDF membrane (Immobilon®-P

Millipore). The blots were then incubated with primary antibodies against Beclin-1 (1:1000, BD Biosciences), LC3B (1:1000, Cell Signaling), p62/SQSTM1 (1:1000, Cell Signaling), Ataxin-3 (clone 1H9 1:3000, Millipore) and actin (clone AC-74 1:5000, Sigma-Aldrich). As a control, membranes were re-probed for β-actin or α–tubulin. The protein bands were visualized by using the corresponding alkaline phosphatase-linked secondary antibodies and ECF substrate (GE Healthcare) in a chemifluorescence device (VersaDoc Imaging System Model 3000, BioRad). For semiquantitative analysis, a partition ratio with actin was calculated following quantification with Quantity-one 1-D image analysis software version 4.5.

2.3.7- DNA extraction and genotyping

Genomic DNA was isolated from fibroblasts cultures using the Quick-gDNA Miniprep Genomic DNA Purification kit (Zymo® Research Corporation). All DNA samples were considered pure regarding the A260/A280 ratio that was comprised between1.8–2.0.

Two fragments of approximately 473 base pairs (bp) were generated by PCR reaction for allele 1 and allele 2, with customized primers for exon 10 of *ATXN3* gene. Those fragments were resolved in an agarose gel and further purified using the MiniElute Gel Extraction Kit (Qiagen).

A cloning reaction of the PCR fragments was performed with Zero Blunt® TOPO® PCR Cloning kit for Sequencing (Invitrogen) following the manufacturer indications. After transformation of competent *E. coli* cells, the resulting colonies were selected and analysed by colony PCR using the universal primers of the vector (M13 forward and T3 or alternatively M13 reverse and T7). Positive colonies were sent to sequence (Eurofins MWG Operon, Germany).

Information regarding primers and PCR parameters used will be provided upon request.

2.3.8- RNA extraction and cDNA synthesis

Total RNA was isolated using NucleoSpin RNA II kit (Macherey-Nagel) from all primary fibroblast cultures at early and later cell passages, according to the manufacturer's instructions. Total amount of RNA was quantified by optical density (OD) using a Nanodrop 2000 Spectrophotometer (Thermo Scientific) and the purity was evaluated by measuring the ratio of OD at 260 and 280 nm. 1 μg of DNAse-I treated RNA was converted to cDNA by iScript cDNA synthesis kit (BioRad) following the manufacturer's instructions and stored

at -20ºC. A portion of the RT reaction (1/20 volume) was used to amplify the various genes with specific primer sets.

2.3.9- Quantitative real-time polymerase chain reaction (qRT-PCR)

Quantitative PCR was performed in a thermocycler (StepOne Plus Real Time PCR System, Applied Biosystems) using the SSO Advanced Universal SYBR Green PCR Supermix (Biorad). The primers for the target human gene (ATXN3, NM_004993 and BECN1, NM_003766 were pre-designed and validated by QIAGEN (QuantiTect Primers, QIAGEN) and the reference gene for GAPDH was designed and validated in the lab:
F-TGTTCGACAGTCAGCCGCATCTTC
R-CAGAGTTAAAAGCAGCCCTGGTGAC

A master mix was prepared for each primer set containing the appropriate volume of SSO Advanced Universal SYBR Green PCR Supermix (Biorad), primers and template cDNA. All reactions were performed in duplicate and according to the manufacturer's recommendations: 95°C for 30 sec, followed by 45 cycles at 95°C for 5 sec, 58°C for 15 sec and 0.5ºC increment for starting at 65ºC at each 5 sec/step up to 95ºC. The amplification efficiency for each primer pair and the threshold values for threshold cycle determination (Ct) were determined automatically by the StepOne Software v2.3 (Applied Biosystems). The mRNA fold change with respect to control samples was determined by the Pfaffl method, taking into consideration different amplification efficiencies of all genes.

2.3.10- Statistical analysis

Statistical computations were performed using GraphPad Prism version 5.0, GraphPad Software, La Jolla, CA, USA, www.graphpad.com. Statistical significance between groups was determined by unpaired Student t-test or one-way ANOVA for multiple comparisons, followed by Bonferroni test for selected pairs comparison. P-values <0.05 were considered as statistically significant; $p<0.01$ very significant; and $p<0.001$ extremely significant.

2.4-Results

2.4.1-Establishment and characterization of primary human skin fibroblast cultures

Skin explants were obtained from healthy individuals and MJD patients followed at the Coimbra University Hospital Centre and cultured as previously described (Normand and Karasek, 1995; Rittie and Fisher, 2005; Takashima, 2001) taking advantage of the outgrowing property of fibroblasts from skin, which enabled a high cell yield in a short period time. Five days post-cultured fibroblasts presented the characteristic spindle-shape morphology, with elongated cell bodies, single oval nucleus and linear alignment of cellular distribution as previously described (Hayflick and Moorhead, 1961) (Fig. 2.1A). Migration of fibroblasts from the cultured skin explant and cellularity were similar for both MJD and healthy control samples and no correlation was found with donor age (Schneider and Mitsui, 1976).

Once confluent (Fig. 2.1B), fibroblast cultures surrounding the pieces of skin were further expanded (Fig. 2.1C) and observed under vimentin and TE-7 immunostaining. All the cells were positive for vimentin, a common marker for mesodermal-derived tissues as dermis and for TE-7, a specific marker for fibroblasts (Pilling et al., 2009). Together these results confirm the purity of the established fibroblast cultures.

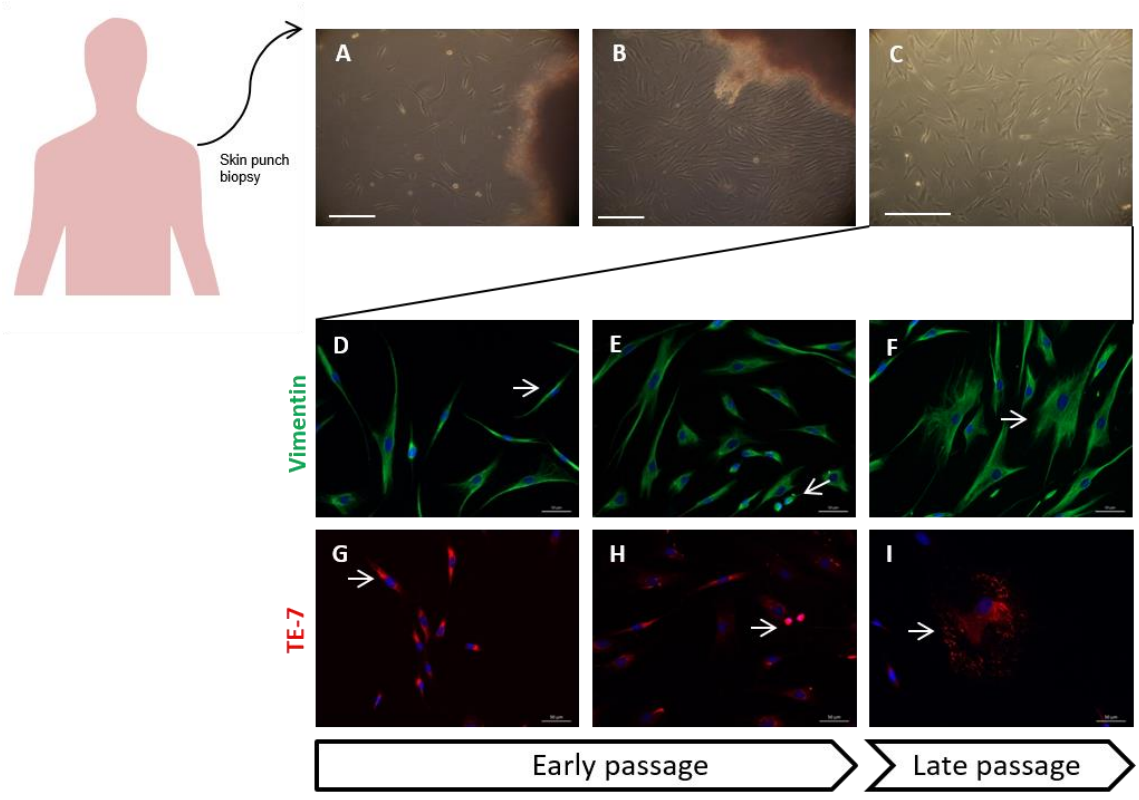

Figure 2.1- Fibroblasts primary cultures were derived directly from excised skin as explants.

Fibroblasts cultures started to grow from the minced fragments in 5 days (A). After a week the cells reached confluency (B) and were detached enzymatically and plated for further expansion on passage P1 (C). Scale 250 µm. Immunostaining of fibroblasts with vimentin (green), TE-7 (red) and DAPI (blue). Starting cultures of fibroblasts and early passages were mainly composed/enriched in fusiform cells and bright cells, capable of division, (D,E,G and H) late passages instead display senescent cells in star-like shape (F and I).

Early passages of fibroblasts were mainly composed by fusiform (Fig. 2.1D and E, arrows) and dividing cells (Fig. 2.1F and G, arrows); in contrast, late passages were progressively enriched in non-dividing star-like shaped senescent cells (Fig. 2.1H and I, arrows) as a result of replicative senescence, regardless of the genotype, gender and age of the donor.

In agreement with previous reports (Chen et al., 2013), fibroblast cultures presented a normal diploid karyotype with no aberrant modifications (Fig. 2.2).

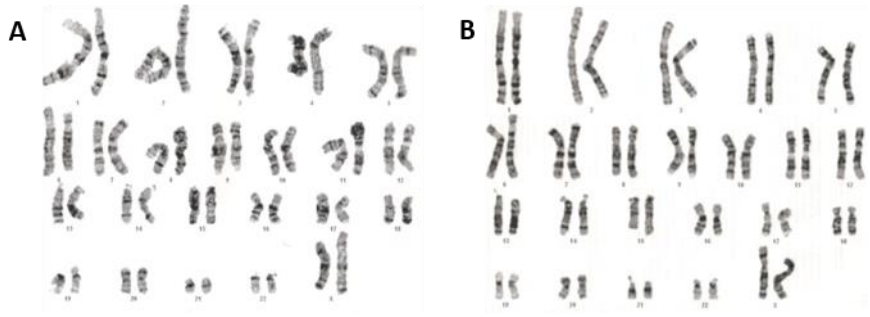

Figure 2.2- Chromosome analysis of fibroblast primary cultures.

Representative aligned karyotype of CTRL and MJD primary fibroblasts (A and B, respectively). The results revealed a normal diploid karyotype of 2n=46 for all the established cultures of primary fibroblasts.

We further performed genetic characterization through DNA sequencing for the *ATXN3* gene, and we found that normal non-expanded CAG repeats in control and MJD fibroblast cultures varied similarly from 14 to 23, whereas the expanded allele ranged from 70 to 80 (Table I).

Interestingly, the subjects exhibiting a severe phenotype of the disease, based on SARA scores and clinical evaluation, also presented the highest number of CAG repetitions reinforcing the correlation between CAG expansion size and disease severity previously described (Maciel et al., 1995). We also analyzed the exon and intron 10 of *ATXN3* gene for the presence of the 3 flanking single-nucleotide polymorphisms (SNPs) associated to the $(CAG)_n$ region namely $\underline{C}^{987}GG/\underline{G}^{987}GG$ (SNP rs12895357), $TA\underline{A}^{1118}/TA\underline{C}^{1118}$ (SNP rs7158733) and C^{1178}/A^{1178} (SNP rs3092822) (Maciel et al., 1999; Martins et al., 2007). We found the ACA and GGC haplotypes (related to Flores and São Miguel island, respectively) in the MJD patients in study.

Table I

		Clinical data					Genetic data			
		Age	Gender	Age of onset	SARA score	Ataxia severity	PolyQ expansion	SNP rs12895357	SNP rs7158733	SNP rs3092822
								$\underline{G}^{887}GG/\underline{C}^{887}GG$	$TA\underline{C}^{1118}/TA\underline{A}^{1118}$	A^{1178}/C^{1178}
CTRL	CTRL 1	44	F	n/a	n/a	n/a	19/14	G	C	A
	CTRL 2	67	F	n/a	n/a	n/a	23/14	G	C	A
	CTRL 3	52	F	n/a	n/a	n/a	23/22	G	C	A
	CTRL 4	47	M	n/a	n/a	n/a	23/22	G	C	A
MJD	MJD 1	31	F	22	35	severe	79/18	**C**	**A**	**C**
	MJD 2	25	F	20	5	severe	77/22	**C**	**A**	**C**
	MJD 3	22	M	18	10	severe	80/23	**C**	**A**	**C**
	MJD 4	42	M	34	5	mild	74/20	G	C	A
	MJD 5	69	M	55	17	mild	70/14	G	C	A

Table I- Clinical and genetic data of healthy individuals and MJD patients included in the study.
Fibroblasts were obtained from five MJD patients who came from four families (patients MJD 2 and MJD 3 are siblings) and healthy individuals, with no history of neurological disease, related (CTRL 3 is the non-affected sister of MJD1) or not related with MJD patients. The ataxia severity was evaluated based on symptoms and scores on the Scale for the Assessment and Rating of Ataxia (SARA, range: 0 – 40). n/a-not applicable.

2.4.2-Assessment of ataxin-3 levels in human fibroblasts cultures

To clarify whether MJD would modify the subcellular localization and levels of ataxin-3 in control and patient fibroblasts we analyzed cultures by immunofluorescence and western blot. We found that ataxin-3 was predominantly located in the cytoplasm of cells, in granular and fibrillar form (Fig. 2.3A) as previously described (Trottier et al., 1998; Wang et al., 1997). The subcellular location of ataxin-3 was similar in control and MJD fibroblast cultures, with 16% ± 0.003 of nuclear ataxin-3 in control fibroblasts and 20% ± 0.019 in MJD fibroblasts. Ataxin-3 was located mainly in the cytoplasm and no aggregates or inclusions were found (Fig. 2.3B). The presence of ataxin-3 in a non-neuronal cell type as fibroblasts confirms the ubiquous expression of ataxin-3 (Paulson et al., 1997a).

Levels of wild-type and mutant ataxin-3 were then analyzed by RT-PCR (Fig. 2.3C) and western blot (Fig. 2.3D-F). All patient cells were derived from heterozygous MJD patients and therefore exhibited expression of both mutant and wild-type ataxin-3. As expected we found that the sum of wild-type and mutant ataxin-3 protein levels in MJD fibroblasts was similar to the levels of wild-type ataxin-3 in healthy controls (Fig. 2.3E) and that the levels of wild-type ataxin-3 in patient cells were half those found in controls. qPCR analysis of mRNA levels of ataxin-3 further confirmed that the levels of ataxin-3 were similar in both groups (Fig. 2.3G).

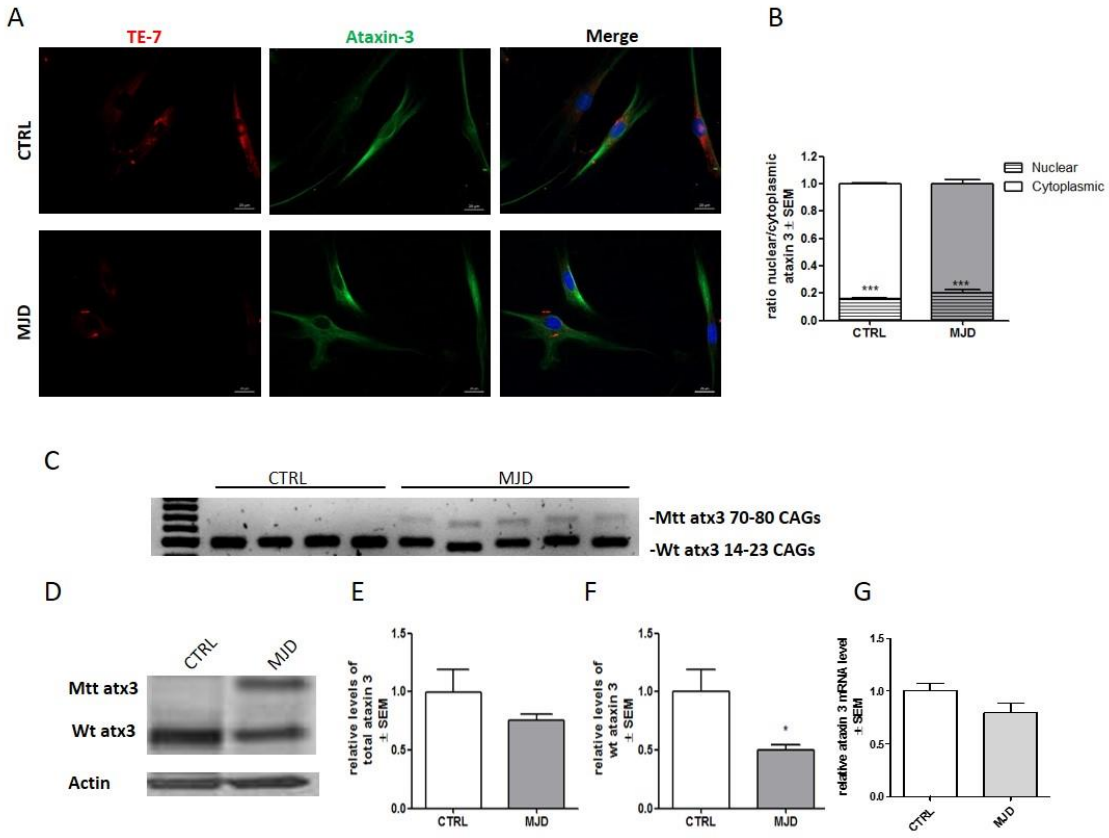

Figure 2.3- Ataxin-3 is predominantly a cytoplasmic protein for CTRL and MJD fibroblasts with similar total levels.

Immunostaining of cultured fibroblasts obtained from skin biopsies with TE-7 (red), ataxin-3 (green), and DAPI (blue) (A). Quantification of nuclear and cytoplasmic ataxin-3, based on ataxin-3 immunoreactivity (B). Levels of nuclear ataxin-3 were significantly lower than cytoplasmic ones (Student t-test n=3/n=3 ***p=0.001). RT-PCR analysis of transcripts from control and MJD fibroblast cultures (C). Representative Western of wild-type (44kDa) and mutant ataxin-3 (64 KDa) in CTRL and MJD fibroblasts (D). Densitometric quantification of total ataxin-3 (E) and wild type ataxin-3 (F) relative to actin (Student t-test n=3/n=5 *p=0,05). qRT-PCR analysis of total level of ataxin-3 relative to GAPDH (n=3/n=5) (G).

2.4.3-Defining MJD autophagic dysfunction phenotype: autophagy is impaired in MJD fibroblasts

In order to investigate whether the MJD genotype was associated with a cellular dysfunction in patient fibroblasts we evaluated the levels of Beclin-1, as previous described (Nascimento-Ferreira et al., 2011) and two crucial autophagic flux related proteins: p62/SQSTM1 and LC3-II.

Protein and mRNA levels of Beclin-1 were significantly decreased in MJD condition (Fig. 2.4 A-C), which suggests an impairment on the early step of vesicle nucleation of autophagic pathway (Levine and Kroemer, 2008). We did not find a significant difference in protein levels of Beclin-1, p62/SQSTM1 and LC3-II (Fig. 2.4D, E, F and G) in MJD group as compared with the control group in basal untreated conditions. Nevertheless, a tendency

for abnormal accumulation of p62 and decrease of LC3 II was observed in basal autophagic flux state, as verified by comparing control and MJD untreated conditions (untreated conditions - UNT). This tendency was already suggestive of an autophagy defective phenotype (Klionsky et al., 2012).

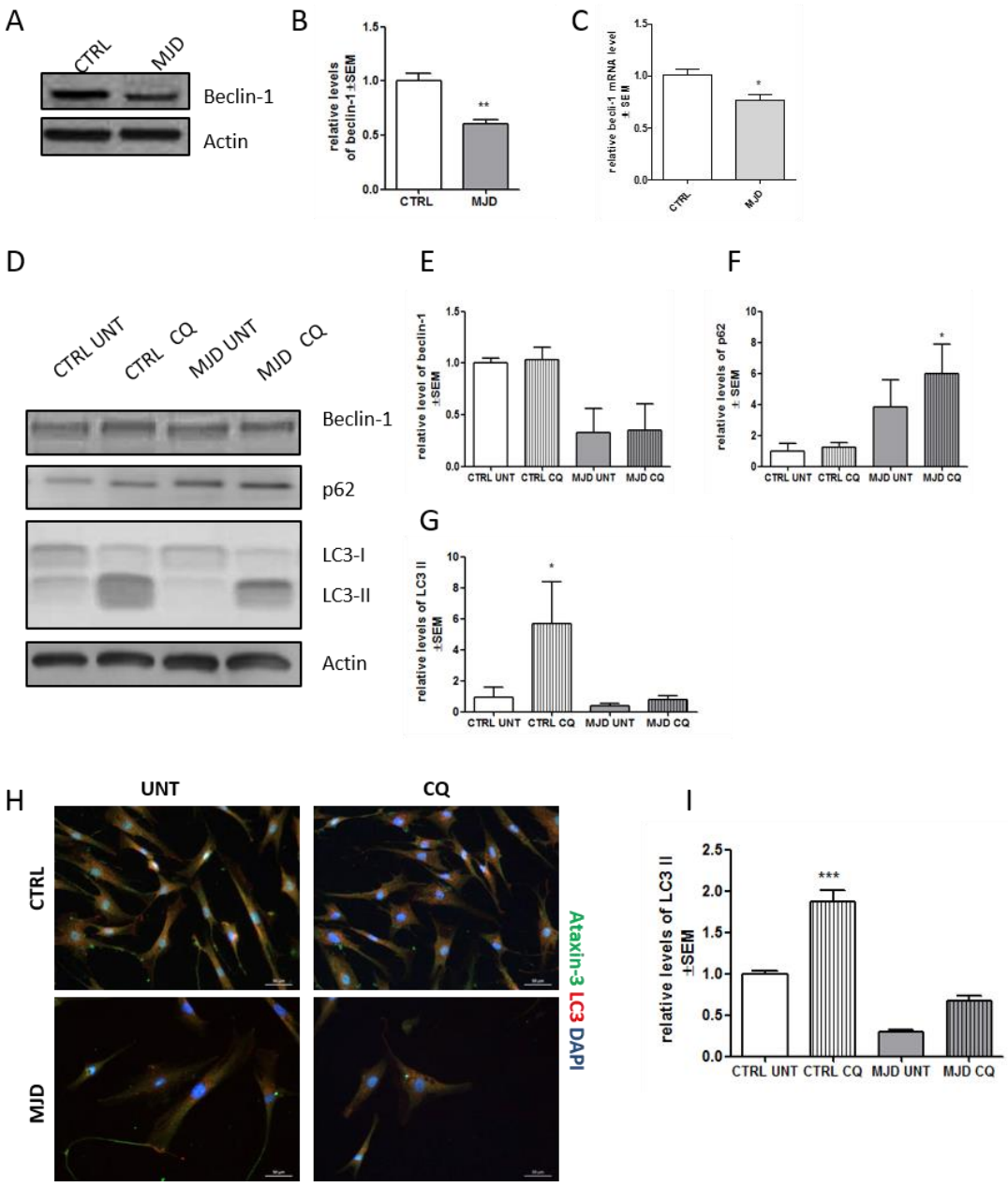

Figure 2.4- Defining MJD autophagic dysfunction phenotype.

Representative western blot of Beclin-1 (61 kDa) (Student t-test n=3/n=4 **p=0.01) in human fibroblasts (A and B) and qRT-PCR analysis of Beclin-1 (Student t-test n=3/n=4 *p=0.05 (C). Representative western blots (D) of beclin-1 (E) (61 kDa), p62 (F) (60 kDa), LC3-I and LC3-II (14 and 16 kDa) levels (G), normalized with actin in human fibroblasts after treatment with chloroquine (CQ). 1way ANOVA with Bonferroni post test (*p<0.05; **p< 0.01) n=3/n=3. Immunostaining of cultured fibroblasts obtained from skin biopsies with ataxin-3 (green), LC3 (red), and DAPI (blue) (H). Quantification of LC3-II, based on LC3-II immunoreactivity, normalized for CTRL UNT condition. Levels of LC3-II were significantly higher after chloroquine treatment in CTRL (I) (1 way ANOVA n=3/n=3***p=0.001).

We next sought to further investigate the putative autophagic dysfunction related with the MJD genotype by treating both MJD and control fibroblasts with chloroquine, an autophagic inhibitor which prevents autophagosome-lysosome fusion and subsequent proteolysis by raising the lysosomal pH (Shintani and Klionsky, 2004) (Klionsky et al., 2012; Klionsky et al., 2008). Levels of beclin-1 (Fig 2.4E) remained similar for both control and MJD conditions, in presence or absence of chloroquine. On the contrary P62/SQSTM1, an autophagy substrate, presented significantly increased levels in MJD samples treated with chloroquine as compared to control cells under the same treatment (Fig. 2.4F). This accumulation of p62/SQSTM1 in MJD fibroblasts upon chloroquine treatment indicates an impairment in autophagic flux.

The levels of LC3-II, a protein found on both the lumenal and cytosolic surfaces of mature autophagosomes, and the conversion of LC3-I in LC3-II were also investigated for both MJD and control fibroblasts in the presence and absence of chloroquine, as a way to analyze the autophagic flux dynamics in the presence of a blocker of fusion of autophagosomes with the lysosomes. In the chloroquine condition, MJD fibroblasts presented drastically reduced levels of LC3-II/Actin when compared with control fibroblasts suggesting incapacity to properly activate autophagy (Fig. 2.4D and G). These results indicate that the reduction of LC3-II levels is due to an impaired generation of autophagosomes. We further confirmed by immunostaining for LC3 II that the levels of LC3 are abnormally decreased in MJD fibroblasts (Fig 2.4 H and I).

Together these results indicate that autophagy is impaired in MJD fibroblasts and suggest that the underlying mechanism is the reduced synthesis of autophagosomes.

2.5-Discussion

In this work we found an autophagy impairment phenotype associated with MJD in dermal fibroblasts obtained from patient's biopsies. We also verified that this phenotype is MJD specific and a consequence of defective generation of autophagosomes.

We established MJD human primary cultures of fibroblasts, with preserved diploid karyotype characteristic from the tissue of origin (Fig. 2.2) and we provided its characterization in terms of disease genotype (Table I) and autophagy related phenotype. The standardization of the conditions for explantation and subcultivation of the skin fibroblast cultures were observed (Campisi, 2001), as both MJD and control groups of skin fibroblast cultures presented similar characteristics regarding cell growth, cellularity and normal karyotype (Fig. 2.1 and Fig. 2.2).

Interestingly, we found the ACA haplotype (Maciel et al., 1999) in patients with most severe clinical outcome, as measured by SARA score (Table 1) and we also found for these patients a correlation between increased CAG expansion size and earlier age of onset, as previously described (Maciel et al., 1995). The C variant for the mutant allele is the most common (Gaspar et al., 1996; Gaspar et al., 2001) and it is a distinctive feature that allows the use of allele-specific siRNA silencing (Alves et al., 2008a; Nobrega et al., 2013) and other gene editing strategies in neuronal *in vitro* models derived from MJD fibroblast, as therapeutic strategies for MJD.

Distribution and levels of mutant ataxin-3 are important for the manifestation of the neurodegenerative phenotype and the presence of protein aggregates in the nucleus of neuronal cells in the form of NIIs (neuronal ubiquitinated intranuclear inclusion bodies) is considered a hallmark of MJD (Bichelmeier et al., 2007; Fujigasaki et al., 2000; Paulson et al., 1997b; Schmidt et al., 1998). In our study, we found that ataxin-3 distributed predominantly in the cytoplasm of the fibroblasts as described previously for both neural and non-neural tissues (Trottier et al., 1998). In MJD fibroblasts, ataxin-3 was also found in the nucleus (Fig. 2.3A), but not in the ubiquitinated form (data not shown) as reported for neurons targeted by the disease (Paulson et al., 1997b; Trottier et al., 1998). We found similar levels of total ataxin-3 for both control and MJD fibroblasts (Fig. 2.3D and E), but as expected the levels of wild-type ataxin-3 in MJD fibroblasts were decreased by 50% (Fig. 2.3F).

It has been reported that reduced autophagy induction, altered cargo recognition, inefficient autophagosome/lysosome fusion or inefficient degradation of the autophagic cargo in lysosomes were potential defects underlying autophagy malfunction in neurodegenerative diseases (Caballero and Coto-Montes, 2012; Hara et al., 2006; Holmberg et al., 2004; Komatsu et al., 2006; Levine and Kroemer, 2008). In this study, we

addressed the general cellular effects of mutant ataxin-3 on autophagic flux, using three different markers to qualify the underlying malfunction: Beclin-1 levels, p62/SQSTM1degradation (Bjorkoy et al., 2005) and the levels of LC3-II and (Mizushima, 2007). Cellular levels of Beclin-1 are often correlated with autophagic activity as the reduced expression in neurodegenerative diseases is linked to autophagy impairment (Pickford et al., 2008). Also the accumulation of p62/SQSTM1 is a reliable indicator of autophagy suppression when used in combination with LC3-II turnover (Klionsky et al., 2012), a marker closely correlated with the number of autophagosomes and thus with autophagosome formation.

We found reduced levels of Beclin-1 in MJD fibroblasts (Fig. 2.4A-C), as described before (Nascimento-Ferreira et al., 2011). In order to estimate the dynamics of autophagic flux in MJD fibroblasts and to confirm the autophagy-defective phenotype, we added a new study condition, by blocking fusion of autophagosomes with lysosomes with chloroquine. We found unaltered levels of beclin-1 after chloroquine treatment in both control and MJD fibroblasts (Fig. 2.4E) which was expected, given that this protein is not a substrate in the autophagic pathway and rather plays a role in its early step of autophagy initiation (Rami, 2009). On the contrary, P62/ SQSTM1 was accumulated in chloroquine condition. Having in mind that p62 is a substrate degraded during the course of autophagic flux, this accumulation corroborates the indication of autophagy impairment (Fig. 2.4F). Simultaneouslly, in control fibroblasts LC3-II levels were increased due to the expected autophagosome accumulation in a situation of uncompromised autophagic flux. Importantly, in MJD fibroblasts the defective autophagic machinery was unable to produce the expected increase in LC3-II levels observed in control fibroblasts.

These results indicate that the autophagic flux is compromised in MJD fibroblasts based on data from basal and dynamic autophagic flux. Moreover, our results suggest that the possible underlying mechanism is the reduced autophagosome synthesis based on LC3-II levels (Fig. 2.4G and I).

Altogether our results suggest that fibroblasts can be used as a MJD *in vitro* model for initial tests of drug screening targeting autophagy impairments and gene repair therapies that can be applied in *in vitro* neuronal models, speeding up clinical translation.

Chapter 3

Generation and characterization of MJD human induced pluripotent stem (iPS) cells

3.1-Abstract

Machado-Joseph Disease is the most common autosomal dominant subtype of cerebellar ataxia worldwide. It is a neurodegenerative disorder of late onset caused by an abnormal expansion of a CAG trinucleotide repeat within the coding sequence of the *ATXN3* gene, that leads into a mutated ataxin-3 protein.

With the development of induced pluripotent stem (iPS) cell technology, the study of the pathology of MJD is no longer restricted to artificial disease modeling systems such as animal models or cell lines, which present limitations as models of human neurogenetic disorders. Human iPS cells are a powerful tool in the context of disease modeling and patient-specific iPS cells represent invaluable *in vitro* models for degenerative disorders, such as MJD.

Here we describe the generation and full characterization of induced pluripotent (iPS) cell lines derived from MJD patient's dermal fibroblasts through the induced expression of the four reprogramming factors OCT3/4, SOX2, KLF4 and c-MYC using a lentiviral vector.

The high quality of those cells was evaluated by their robust expansion in culture, maintenance of the disease genotype and fulfillment of all the morphological, molecular and functional pluripotency assays as regular morphology, reprogramming vector silencing, acquisition of pluripotency markers expression, normal diploid karyotype and *in vitro* and *in vivo* differentiation in the three germ layers: endoderm, mesoderm and ectoderm.

The derived MJD-specific iPS cell lines offer an unparalleled opportunity to create a novel human disease model, bringing new insights in disease mechanisms and pathology, complementing other established disease models and allowing drug screening.

3.2-Introduction

MJD is a monogenic neurodegenerative disorder mapped to chromosome 14q32.1(Kawaguchi et al., 1994; Takiyama et al., 1993) and genetically inherited in an autosomal dominant pattern (Coutinho and Andrade, 1978). The CAG trinucleotide repeat expansion in the *ATXN3* gene causes the expression of mutant ataxin-3 responsible for the neuropathological manifestation of the disease (Schmidt et al., 1998; Schols et al., 1997; Sudarsky and Coutinho, 1995).

Being MJD a monogenic disease makes it a perfect candidate for the generation of iPS cells to study the correlation between the mutation and the associated disease specific phenotype (Koch et al., 2011). This connection has been shown previously for other iPSC-based neurogenetic disease models, such as ALS (Dimos et al., 2008), HD (Camnasio et al., 2012; Park et al., 2008a), FD (Lee et al., 2009), SMA (Boulting et al., 2011; Ebert et al., 2009), Rett syndrome (Marchetto et al., 2010), Friedreich Ataxia (Ku et al., 2010) and Fragile X syndrome (Urbach et al., 2010).

As reprogramming method, the delivery of the 4 Yamanaka factors (OCT3/4, SOX2, KLF4 and c-MYC) (Takahashi et al., 2007; Takahashi and Yamanaka, 2006) by an integrative mediated strategy offers the possibility of robustly reprogramming human adult and mature somatic cells (Maherali and Hochedlinger, 2008) and also polycistronic vector constructs help to achieve higher reprogramming efficiencies by enabling the favorable stoichiometry of expression of the 4 reprogramming factors (Papapetrou et al., 2009). The use of small molecules (Feng et al., 2009; Xu et al., 2008), as chromatin modifiers (Huangfu et al., 2008a), player molecules in pluripotency pathways (Lin et al., 2009) or antioxidant compounds (Esteban et al., 2010) is also a common approach to enhance the low reprogramming efficiencies (0.02% to 0.002%) reported for human cells (Maherali et al., 2008; Takahashi et al., 2007; Yu et al., 2007) and also a way to improve the stochastic process (Hanna et al., 2009; Yamanaka, 2009).

iPS cells pluripotency is commonly verified by a broad range of morphological, molecular and functional key criteria, often by comparing with the physiological equivalent, hES cells, considered to be the so called “gold standard” (Hochedlinger and Plath, 2009). Tightly packed and flat colonies, exhibiting large nuclei and a high ratio of nucleus to cytoplasm with high self-renewal capability (Thomson et al., 1998) are the first morphological criteria to check in iPS cells cultures (Takahashi et al., 2007; Yu et al., 2007).

The sequential acquisition of several molecular pluripotency markers (Brambrink et al., 2008), as transgene silencing, alkaline phosphatase activity, expression of cell surface markers, such as SSEA4 (Przyborski, 2001) and TRA-1-60 (Schopperle and DeWolf,

2007), expression of the nuclear transcription factor Nanog (Chambers et al., 2003; Chambers and Smith, 2004; International Stem Cell et al., 2007) and steady and high expression of pluripotency related genes (Chan et al., 2009) are important molecular events to verify. Also the fulfillment of functional assays to prove the differentiation potential *in vitro* and *in vivo* in representatives of the three germ layers (endoderm, mesoderm and ectoderm) and the maintenance of normal diploid karyotype during prolonged time in culture are very important criteria to validate the high quality of the iPS cells generated (Maherali and Hochedlinger, 2008) with implications in further use of those cells for differentiation into cell-type patient-specific cells for disease modeling, drug screening and cell therapies (Daley et al., 2009).

Here we report the successful establishment of iPS cell lines from fibroblasts of 4 MJD patients and 3 controls. These cells were fully pluripotent meeting all the criteria in pluripotency assays and conserved the expression of mutant ataxin-3, with no interference of the reprogramming strategy. This unique stem cell resource will be a valuable tool to generate high quality neurons to study MJD phenotype.

3.3-Material and Methods

3.3.1- Vector production and lentiviral transduction

The lentiviral vector encoding for the 4 reprogramming factors and dTomato fluorescent protein (Warlich et al., 2011) was produced in HEK 293T cells with a four plasmid system, as previously described (de Almeida et al., 2001). Briefly, 3×10^6 cells underwent transfection with the lentiviral vector plasmid, the packaging plasmids pCMVDR-8.92 (expressing HIV-1 *gag/pol*) and pRSV-Rev (expressing the HIV-1 *rev*), and the VSV-G protein envelope plasmid pMD.G (encoding the vesicular stomatitis virus glycoprotein) using the calcium phosphate DNA precipitation method.

Supernatants were harvested 48 hours after transfection, filtered and concentrated using ultracentrifugation. The lentiviral particles were resuspended in 1% bovine serum albumin (BSA) in phosphate-buffered saline (PBS) and viral stocks were stored at -80ºC until use. The viral particle content of batches was determined by either by assessing HIV-1 p24 antigen levels (pg p24/ml) by an ELISA assay (RETROtek, Gentaur, Paris, France) or by the number of transducing units (TU/ml) (Geraerts et al., 2006). Lentiviral titration was performed in fibroblasts 5 days after transduction as previously described (Ramezani and Hawley, 2002) and dTomato fluorescence was measured via microscopy. The MOI (multiplicity of infection) was calculated using the following equation:

$$\mathrm{MOI} = \frac{\text{total number of cells} \times \%\text{ of transduced cells}}{\text{viral volume}} \times 1000$$

To produce iPSCs, 10,000 human fibroblasts, on early passage (P5), were transduced at a MOI of 0.1–1 with virus encoding for the 4 reprogramming factors in fibroblast culture medium (DMEM (Gibco, Invitrogen), supplemented with 10% FBS (Gibco, Invitrogen), 2mM L-Glu (Gibco, Invitrogen), 1% penicillin/streptomycin (Gibco, Invitrogen) and 1% NEAA (Sigma)).

Fibroblasts were incubated with virus for 12 h before medium was changed to standard fibroblast medium for 48 h. Cells were subsequently cultured in standard hESC culture medium during the course of reprogramming.

3.3.2- Reprogramming

To function as feeder layers, MEFs (GlobalStem) were grown to confluence in fibroblast culture medium (DMEM (Gibco, Invitrogen), supplemented with 10% FBS (Gibco,

Invitrogen), 2mM L-Glu (Gibco, Invitrogen), 1% penicillin/streptomycin (Gibco, Invitrogen) and 1% NEAA (Sigma-Aldrich) and inactivated with 10 ug/ml mitomycin C (Roche).

Transduced fibroblasts were harvested via trypsinization and transferred onto mitomycin C-treated MEF feeders 3 days after transduction and thereafter cultured in hES cells medium composed by DMEM F-12 (Gibco, Invitrogen), 20% Knock-out serum replacement (KOSR), 1 mmol/l L-glutamine (Gibco, Invitrogen), 0.1 mmol/l nonessential amino acids (Sigma-Aldrich), 100 umol/l β-mercaptoethanol (Sigma-Aldrich), 100 units/ml penicillin/100 ug/ml streptomycin (Gibco, Invitrogen) and 10 ng/mL of bFGF (Peprotech).

At the time of appearance of ESC-like colonies, single colonies were picked based on morphology and expanded on MEF feeder cells. hES cells culture medium was replaced every 1–3 days, depending on the cell density and iPSCs were splitted by manual dissection (1:4) every 3–4 days. For compound treatment, the cells were cultured in the reprogramming medium and were treated with the combination of PD0325901(Axon Medchem) (0.5 µM from day 3-14 and 1 µM from day 14-21) and SB431542 (Axon Medchem) (2 µM from day 3-14 and 1 µM from day 14-21)(Lin et al., 2009) or with Vit C (Sigma-Aldrich) (from day 3-21) and VPA (Sigma-Aldrich) (from day 7-14) (Esteban et al., 2010).

3.3.3- Alkaline phosphatase staining

Alkaline phosphatase activity was detected in live cultures using the Leukocyte Alkaline Phosphatase kit (Sigma-Aldrich) according to the manufacturer's instructions.

3.3.4- Immunocytochemistry

Cells were briefly fixed in 4% PFA for 10 min at room temperature and then blocked in PBS containing 0.3% Triton X-100 and 5% FBS for 1 h before incubation with primary antibodies overnight, in PBS containing 0.3% Triton X-100 and 1% BSA. Pluripotency markers and three-germ layer immunostainings used in this study were SSEA-4 (1:400, Cell Signaling), TRA1-60 (1:400, Cell Signaling), Nanog (1:400, Cell Signaling), AFP (1:500, DAKO), Desmin (1:500, Invitrogen) and βIII-Tubulin (clone 38F4 1:1000, Invitrogen). After three washes with PBS, cells were incubated with Alexa Fluor® 488 and 594 secondary antibodies (Invitrogen 1:200) for 2 hr at room temperature. Additionally, cells were stained with DAPI in order to visualize cell nuclei and, after washing, mounted in Fluoroshield (Sigma Aldrich). Fluorescent signals were detected using a Zeiss inverted microscope (Zeiss Axio Observer Z1).

3.3.5- Protein isolation and western blot

For protein isolation, cells were lysed with RIPA buffer (50 mM Tris-Cl, pH 7.5, 150 mM NaCl, 1% Nonidet P-40, 0.5% sodium deoxycholate and 0.1% SDS, 1 mM PMSF and 1mM DTT) supplemented with a protease inhibitor cocktail (Roche), triturated and centrifuged at 12,000 rpm for 20 min at 4ºC. The cell lysates were collected after centrifugation. The protein concentration in the lysates was determined using the Bradford protein assay reagent (Bio-Rad). Approximately 30 ug of protein were separated on SDS-PAGE gels (4% stacking and 10% running) and transferred to a PVDF membrane (Immobilon®-P, Millipore). The blots were then incubated with primary antibodies against ataxin-3 (clone 1H9 1:3000, Millipore) and tubulin (clone SAP.4G5, 1:15000, Sigma). The protein bands were visualized by using the corresponding alkaline phosphatase-linked secondary antibodies and ECF substrate (GE Healthcare) in a chemifluorescence device (VersaDoc Imaging System Model 3000, Bio-Rad). For semiquantitative analysis, a partition ratio with actin or tubulin was calculated following quantification with Quantity-one 1-D image analysis software version 4.5.

3.3.6- RNA extraction and cDNA synthesis

Total RNA was isolated using the RNeasy Mini Kit (QIAGEN) according to the manufacturer's instructions. Total amount of RNA was quantified by optical density (OD) using a Nanodrop 2000 Spectrophotometer (Thermo Scientific) and the purity was evaluated by measuring the ratio of OD at 260 and 280 nm. Purification of RNA and first strand cDNA synthesis was performed using the DNA-free Kit (Ambion) and the SuperScript™III Reverse Transcriptase Kit (Invitrogen), respectively and according to the manufacturer's instructions.

3.3.7- Quantitative real-time polymerase chain reaction (qRT-PCR)

Quantitative PCR was performed in an iQ5 thermocycler (Bio-Rad) using iQ SyBr Green Supermix-Bio-Rad Mix (Bio-Rad). A master mix was prepared for each primer set containing the appropriate volume of 25 uL SYBR Green PCR Master Mix (Bio-Rad), primers and template cDNA. All reactions were performed in duplicate and according to the manufacturer's recommendations: 95°C for 10 min, followed by 40 cycles at 95°C for 15 sec, 60°C for 1 min and 0.5ºC increment for starting at 55ºC at each 10 sec/step up to 95ºC.

The amplification efficiency for each primer pair and the threshold values for threshold cycle determination (Ct) were determined automatically by the iQ5 Optical System Software (Bio-Rad).

Quantitative levels for all genes were normalized to endogenous GAPDH. For pluripotency genes, mRNA levels were expressed relative to the levels in hES cell line HuES-1. The mRNA fold increase or fold decrease with respect to control samples was determined by the Pfaffl method. Standard curves were run to ensure equal efficiency of all primers.

Reference gene

GADPH F	TGTTCGACAGTCAGCCGCATCTTC
GADPH R	CAGAGTTAAAAGCAGCCCTGGTGAC

Vector silencing

C-MYC VIRAL dT-4RF F	TACGCCCTGTTGAAGCTGGCTG
C-MYC VIRAL dT-4RF R	TGCACCGAGTCGTAGTCGAGGT
SOX2 VIRAL dT-4RF F	GCATGACCAGCAGCCAGACCTA
SOX2 VIRAL dT-4RF R	TCTTGACCACGCTGCCCATGCT
OCT4 VIRAL dT-4RF F	AACCCCGAGGAAAGCCAGGACA
OCT4 VIRAL dT-4RF R	ACAGCACGCCCAGTGTCAGT
KLF4 VIRAL dT-4RF F	TGGAAGTTCGCCAGAAGCGACG
KLF4 VIRAL dT-4RF R	TTCATGTGCAGAGCCAGGTGGT
dTomato F	TGAAGATGCGCGGCACCAACT
dTomato R	TGGTGGATCTCGCCCTTCAGCA

Pluripotency genes

SOX2 ENDO F	CGAGGGAAATGGGAGGGGTGC
SOX2 ENDO R	TGCAGCTGTCATTTGCTGTGGGT
NANOG ENDO F	GCCTGTGATTTGTGGGCCTGA
NANOG ENDO R	GTGGAAGAATCAGGGCTGTCCTG
OCT4 ENDO F	TGTCTCCGTCACCACTCTGGGC
OCT4 ENDO R	CCCAAAAACCCTGGCACAAACTCCA
TERT F	GAACAGCCTCCAGACGGTGTGC
TERT R	GGAGGCCGTGTCAGAGATGACG
DNMT3B F	CTCCTGGTGGCCCGCCATG
DNMT3B R	ACAGCCCCAGTGCCACCAGT
REX1 F	ACAAATGTACTGAGGCTGGAGCCTG
REX1 R	TCAACCACCTCCAGGCAGTAGTGA
ABCG2 F	CGTACTGGGACTGGTTATAGGTGCC
ABCG2 R	TCCACGGCTGAAACACTGCTGA
GDF3 F	GGGCGTCCGCGGGAATGTAC
GDF3 R	TCCCTTTCTTTGATGGCAGACAGGT
TDGF1 F	TGCGCAAAGAGAACTGTGGGTCTG
TDGF1 R	GGTGCTCATCCATCACAAGGCCA

3 germ layer differentiation	
PAX6 F	GCTGTGACAACCAGAAAGGATGCCT
PAX6 R	GGGGCTCGAATATGGGGCTCTGA
NES F	AGCCTGGAGGTGGCCACGTA
NES R	CGGCCCTCTGGGGTCCTAGG
SOX17 F	GAGCCAAGGGCGAGTCCCGTAT
SOX17 R	TCCACGACTTGCCCAGCATCTTGC
DES F	CCTGCTCAACGTGAAGATGGCCC
DES R	TGCTCAGGGCTGGTTTCTCGGA
EOMES F	TGTGCAACCGGCCTCTGTGGC
EOMES R	GTGGGCAGTGGGATTGAGTCCGT
T F	TACCCCAGCCCCTATGCTCATCG
T R	TGCTGGGATGGGCAGGCATTC
AFP F	ACTATTGGCCTGTGGCGAGGGA
AFP R	GAAGCATGGCCTCCTGTTGGCA
SOX1 F	CCAGGACCGGGTCAAACGGC
SOX1 R	ACCTTCCACTCGGCCCCCAG

3.3.8- Spontaneous *in vitro* three-germ layer differentiation

Whole stem cell colonies were isolated using 1mg/mL of collagenase IV (Gibco, Invitrogen) and plated in suspension in low-cluster 6-well plates (Corning) in hES cell culture medium without bFGF. Cells aggregated to form embryoid bodies (EBs) within 24 h and culture medium was replaced every 48 h. On day 14, EBs were trypsin and/or mechanically dissociated and plated on gelatin-coated culture plates for another 5 days of adherent culture conditions before fixation and staining (Itskovitz-Eldor et al., 2000; Takahashi et al., 2007).

3.3.9- Teratoma formation assay

All mouse procedures were conducted under local ethical guidelines and permission from the animal facility under an experimental protocol approved by ORBEA (Orgão Responsável pelo Bem-estar Animal) and the Portuguese authorities (Direcção Geral de Veterinária).

Seven weeks old NOD.Cg-Prkdc^{scid} Il2rg^{tm1Wjl}/SzJ JAX mice (Jackson Labs, USA) were used for transplantation. In all experiments, the mice were anesthetized by an intraperitoneal injection of 75 mg/Kg ketamine and 1 mg/Kg medetomidine for transplantation procedures and reverted by atipamezole 1mg/Kg.

For subcutaneous injection of hiPS cells, cells were harvested and dissociated into a single cell suspension using 1mg/mL of collagenase IV and kept in ice cold PBS supplemented with 30% Matrigel (Prokhorova et al., 2009). To ensure a single cell

suspension, the cells were drawn into 1-mL syringe immediately before injection. Mice were injected in the dorso-lateral area into the subcutaneous space on both sides with approximately 1×10^6 cells in 50 µL/ site of injection. For negative controls, vehicle (PBS+30%Matrigel) and 1×10^6 human adult fibroblasts were transplanted.

Animals were observed daily for changes in appearance and behavior and the injection site for tumor growth, for about 6–12 weeks till the predetermined experimental endpoint when the tumor was palpable (Wesselschmidt, 2011) and about 1 cm^3 in size. When the endpoint for tumor growth was met, the mice were euthanized and tumors surgically removed.

3.3.10- Immunohistochemistry

The procedure was performed according to a standard avidin-biotin peroxidase complex using the Ultra Vision Kit (Thermo-Scientific).

Paraffin-embedded teratomas were cut into 4-µm serial sections and floated placed on coated slides to dry overnight. After deparaffinization and rehydration, antigen unmasking was performed using citrate buffer for 25 min at pH 6 and endogenous peroxidase activity was quenched by incubating 15 min with 3% diluted hydrogen peroxide (H_2O_2). For blocking non-specific binding of primary antibodies Ultra V Block was used.

Cells were incubated with monoclonal mouse anti-human antibodies against Oct4 (1:100, clone N1NK, Novocastra), TTF1 (1:100, clone SP724, Novocastra) Cdx2 (ready to use, clone AMT28, Leica) s100 (1:1000, Dako) NSE (1:400 Dako) Cytokeratin 5.6 (1:150, clone MNF116), α-SMA (1:100, clone 1A4, Cell Marque), at room temperature. After washing with PBS, slides were incubated with a biotin-labelled secondary antibody for 15min. Primary antibody binding was localized in cells using peroxidase-conjugated streptavidin and 3,3-diaminobenzidine tetrahydrochloride as the chromogen according to manufacturer's instructions. Slides were counterstained with hematoxylin and then dehydrated and mounted. Known positive and negative controls were performed in parallel (Sousa et al., 2011; Val et al., 2015)

3.3.11- Karyotypic analysis

In order to purify hiPS cells from the co-culture with MEFs feed-layer, the cells were plated in gelatin coated culture flasks and cultured in MEF conditioned medium (Papapetrou and Sadelain, 2011) a week before DNA extraction.

DNA was extracted from cell cultures using the High Pure PCR Template Preparation Kit (Roche Applied Science, Indianapolis, USA) according to the manufacturer's instructions.

The karyotype analysis was performed using standard G-banding techniques (Rooney DE, 1992). Cells cultured in a T25 flask were treated with 0.2 µg/ml colcemid for up to 3 hours, followed by dissociation with trypsin/EDTA. The cells were pelleted via centrifugation and re-suspended in pre-warmed 0.05M KCl hypotonic solution and incubated for 20 minutes. Following centrifugations the cells were re-suspended in fixative. Metaphase spreads were prepared on glass microscope slides and GTG-banded by brief exposure to trypsin and stained with Giemsa. A minimum of 20 metaphase spreads were analysed for the iPS cells and a minimum of 10 metaphase spreads were analysed for the fibroblasts. Karyotypes were established according to the International System for Human Cytogenetic Nomenclature (ISCN) 2013(Shaffer LG, 2013).

3.3.12- Statistical analysis

Statistical computations were performed using GraphPad Prism version 5.0, GraphPad Software, La Jolla, CA, USA, www.graphpad.com. Statistical significance between groups was determined by. one-way ANOVA or two-way ANOVA for multiple comparisons, followed by Bonferroni test for selected pairs comparison. P-values <0.05 were considered as statistically significant; $p<0.01$ very significant; and $p<0.001$ extremely significant.

3.4 Results

3.4.1- Generation of iPSCs from MJD patients and healthy controls adult dermal fibroblasts

We used a polycistronic lentiviral vector to induce pluripotency of adult human fibroblasts (Warlich et al., 2011). This vector encoded for the reprogramming cassete, comprising the 4 Yamanaka factors (OCT4, SOX2, KLF4 and c-MYC) and a red fluorescent protein (dTomato) under the promoter SFFV (Fig 3.1). This promotor is sensitive to epigenetic modifications and is silenced when the embryonic like stem cell state is achieved, which allowed us to follow the time course of reprogramming (Fig 3.2A).

Figure 3.1-Schematic representation of the lentiviral vector construction used for the generation of iPS cells.
The vector expressed the four codon-optimized reprogramming factors (OCT4, KLF4, SOX2 and c-MYC), under the SFFV promotor and via 2A self-cleavage sites (E2A, equine rhinitis A virus 2A; P2A, porcine teschovirus 2A and T2A, thosea asigna virus 2A). The fluorescent marker, dTomato is linked via IRES site to the reprogramming cassette, enabling coexpression of reprogramming factors and the fluorescent marker in a single polycistronic transcript.

Fibroblasts expressed dTomato three days after transduction (Fig 3.2B), and this expression was maintained even when the first morphological alterations were observed (Fig 3.2C). We named those first colonies as pre-iPS cells because despite the morphological change, the pluripotency was still dependent of the expression of the ectopic reprogramming factors, as the vector expression was active. The maturation of those colonies was completed when the compact flat final morphology was met and the vector was silenced, achieving the maintenance of the pluripotency network. (Fig 3.2D)

To further enhance the efficiency of reprogramming we used a combination of VPA, an HDAC inhibitor (Huangfu et al., 2008a; Huangfu et al., 2008b) and Vit C, an antioxidant compound (Esteban et al., 2010) and the PD0325901+ SB431542 combination (Lin et al., 2009). Interestingly, even though the VPA condition induced higher expression levels of pluripotency-related genes (Fig 3.2E) it also caused more death in cultures as compared with the other conditions. The VPA+Vc condition was the most efficient condition, conjugating the improved kinetics associated with VPA treatment and the alleviation of oxidative stress (Shi et al., 2010).

The combination of the MEK-ERK pathway antagonist PD0325901 and TGF-β receptor antagonist SB431542 also helped in cell survival and favorable kinetics as compared with the untreated condition. The double MOI of 2 (Fig 3.2F) did not bring any

positive outcome on reprogramming and this result supports the careful choice of the MOI in order to balance the best reprogramming efficiency with avoidance of genetic instability caused by insertional mutagenesis (Somers et al., 2010). We found no difference in reprogramming efficiencies between control and MJD fibroblasts.

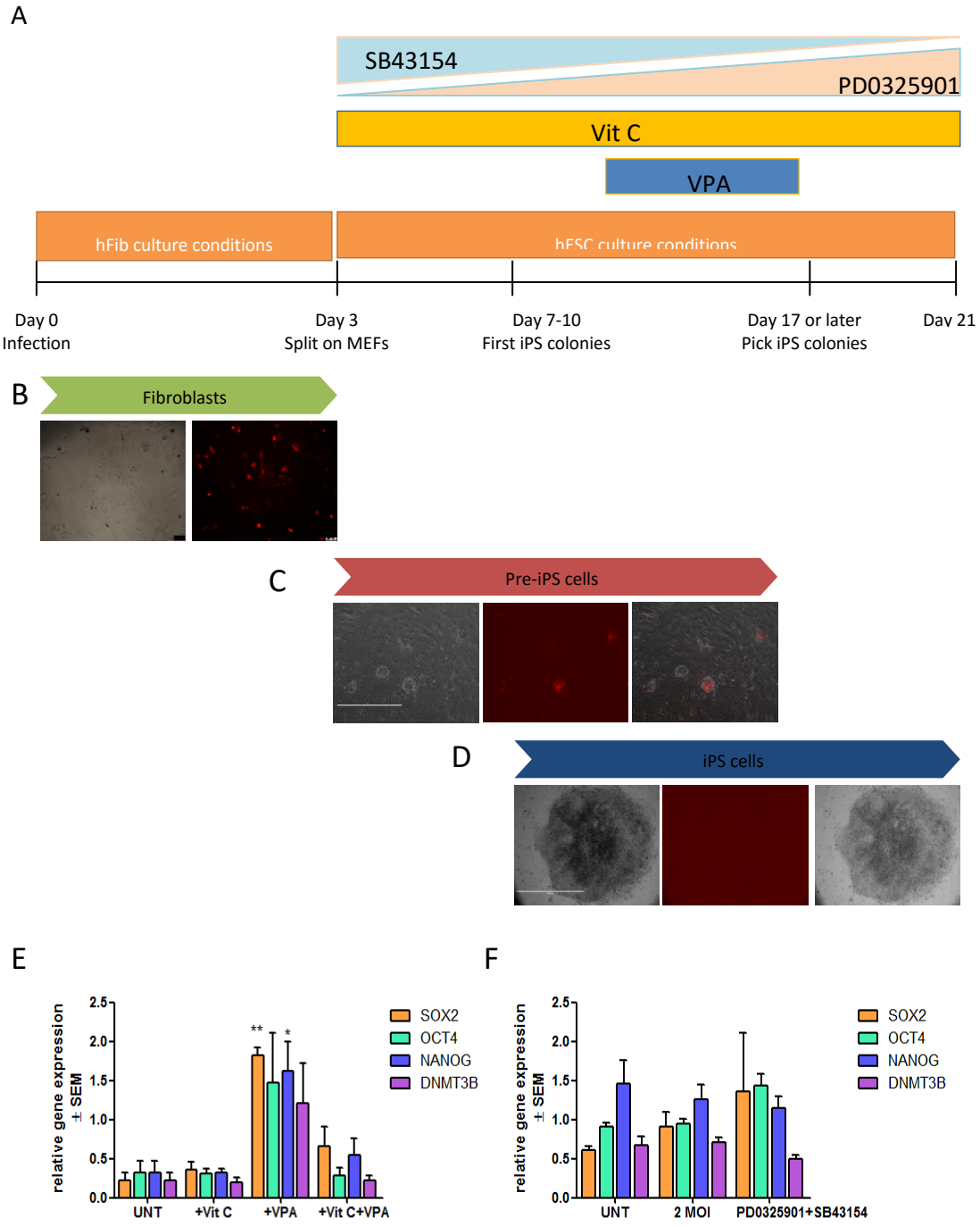

Figure 3.2-Time schedule of human iPS cells generation and reprogramming strategy scheme.

The combination of small molecules was used to promote reprogramming efficiency: SB431542 (ALK5 inhibitor) + PD0325901 (MEK inhibitor or) or VPA (chromatin modifier) + Vit C (antioxidant) (A) Three days after transduction, the red fluorescent expression is detected (scale 100 µm) (B) and also along the time of pre-iPS cells colonies emergence on culture, indicating active lentiviral gene expression (scale 1mm) (C). iPS cells display hESC like compact colony and the red fluorescence is no longer detected (scale 1mm) (D). Treatments with compounds were effective in reprogramming as the levels of pluripotency related genes are increased as compared with the untreated condition for VPA condition (E) and was similar for 2 MOI and PD0325901+SB431542 conditions (1way ANOVA with Dunnett's multiple comparison post test, *p<0.05 and **p<0.01) (F).

IPS cell lines derived from the initial cohort of adult dermal fibroblast cultures obtained from three healthy controls and four MJD patients showed expression of mutant ataxin-3 (Fig 3.3A), with similar levels of total ataxin-3 for both protein and mRNA (Fig 3.3B and D) and a decrease of wild-type ataxin-3 (Fig 3.3C) in MJD iPS cell lines, as previously shown in fibroblasts.

This result confirms that patient-derived iPS cells preserved the genetic mutation carried by the corresponding patient and that the reprogramming process did not affect the disease genetic background.

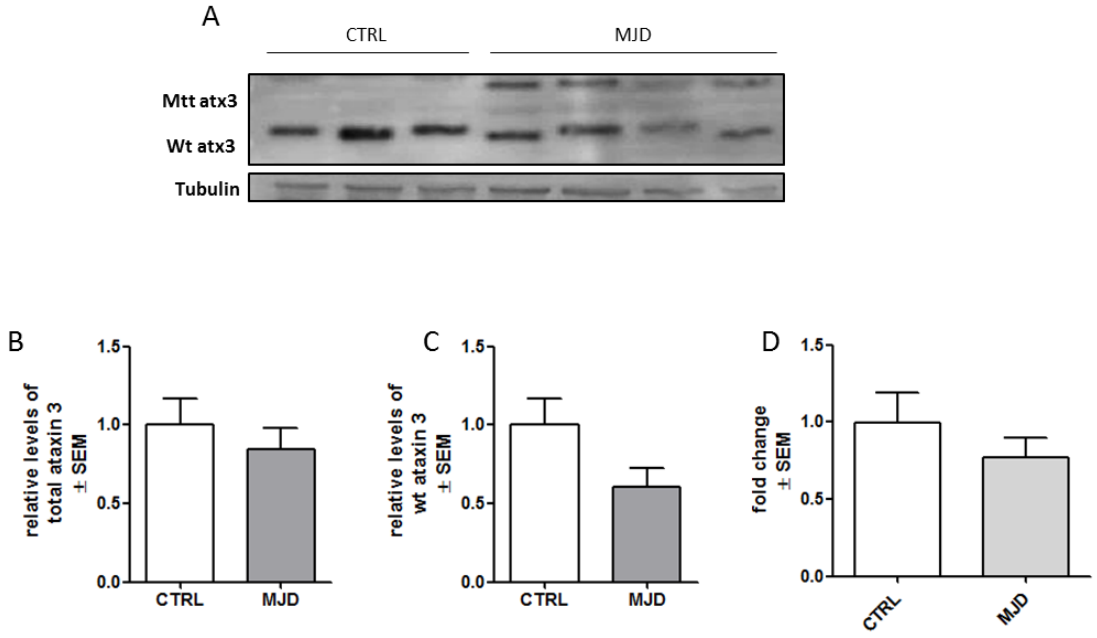

Figure 3.3- Ataxin-3 protein expression on iPS cell lines derived from the initial cohort of fibroblasts

Representative western blot of wild-type and mutant ataxin-3 (A). Levels of total ataxin-3 were similar for both control and MJD conditions, when analyzed by western blot and qRT-PCR (B and D, respectively) and wild-type ataxin-3 was found decreased in MJD condition (C). Protein densiometric quantification of ataxin-3 was performed using tubulin as loading control (n=3/n=4) and qRT-PCR quantification was performed using GAPDH as reference gene (n=3/n=4).

3.4.2- Pluripotency characterization of iPS cells: molecular markers

3.4.2.1- Morphology and vector silencing

Examination and isolation of hiPS cell colonies based on the distinct morphology of hES cells colonies is the first step to establish the cell culture and also the first criteria to assess pluripotency of hiPS cells (Lowry et al., 2008; Takahashi et al., 2007; Yu et al., 2007). Typically hES cells and hiPS cells are small cells characterized by a high nuclear to cytoplasm ratio and prominent nucleoli (Blum and Benvenisty, 2009) and grow in tightly

packed flat colonies (Fig 3.4B). All the picked hiPS colonies met this first key criterion of pluripotency.

Next, and in order to evaluate if the reprogramming process was complete and successful we evaluated the pluripotency-associated transcriptional network of the derived iPS cells. We evaluated whether it was supported by the ectopic expression of the reprogramming factors or by the activation of the pluripotency-associated transcriptional network.

We found a pronounced silencing of the transcription factors encoded by the lentiviral vectors (Fig 3.4C) in all the iPS cells (Fig 3.4B) as compared with pre-iPS cells (Fig 3.3A). The codon-optimization of the reprogramming factors (Moreno-Carranza et al., 2009; Ng et al., 2010) and the synthetic origin of dTomato (Shaner et al., 2004) allowed us to study the down-regulation of the lentiviral cassete with no interference from the expression of endogenous equivalents. All the ectopic genes showed similar levels of expression, corroborating the expected 1:1:1:1:1 stoichiometry of expression from the polycistronic vector.

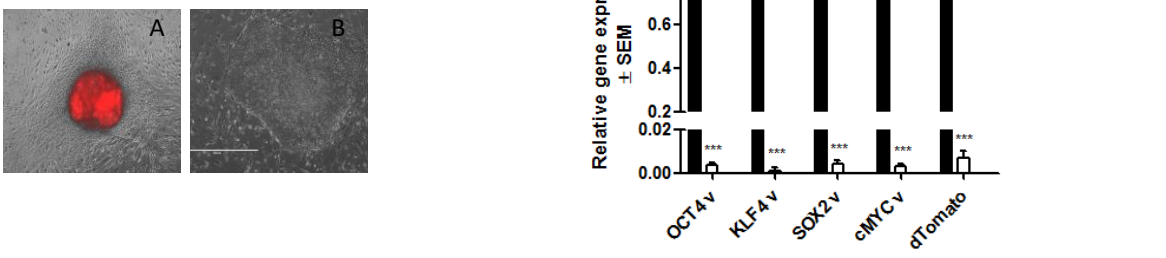

Figure 3.4- Silencing of the 4 reprogramming factors encoded by the polycistronic lentiviral vector in iPS cell lines.

Representative images of pre-iPS cell (A) and iPS cell colonies (B) considered to analyse the vector expression silencing (scale 1mm). qRT-PCR analysis derived iPS cells, using GAPDH as reference gene and pre-iPS cells as positive control for active lentiviral transduction; all the genes were silenced in iPS cell lines n=8/n=8 (C) (2 way ANOVA with Bonferroni post test, ***p<0.001).

3.4.2.2- Pluripotency markers expression

One of the earliest markers for the undifferentiated status of pluripotent stem cells is the high activity of alkaline phosphatase (O'Connor et al., 2008), which is also a reliable indicator of the sequential activation of the successive pluripotency markers (Brambrink et al., 2008; Wernig et al., 2007). Several clones from the hiPS cells generated (Fig 3.5A) exhibited alkaline phosphatase activity (Fig 3.5B) as well as immunoreactivity for the cell surface markers SSEA4 (Fig 5C) and TRA-1-60 (Fig 3.5D) (Hockemeyer et al., 2008; Lowry et al., 2008).

We also observed expression of the transcription factor Nanog (Fig 3.5E) since its expression is supported by the sustained endogenous expression of other transcription

factors OCT4 and SOX2 (Loh et al., 2006; Rodda et al., 2005) responsible for maintenance of pluripotency (International Stem Cell et al., 2007).

Finally, we assessed by qPCR the mRNA levels of the core trascritption factors OCT4, SOX2 and NANOG and other pluripotency related genes (Fig 3.5F) considered to be the *bona fide* markers to distinguish fully reprogrammed iPS cells: REX1 (reduced expressed 1), DNMT3B (DNA (cytosine-5-)-methyltransferase 3 beta), ABCG2 (ATP-binding cassette sub-family G member 2), TERT (telomerase reverse transcriptase), GDF3 (growth and differentiation factor 3) and TDGF1 (Teratocarcinoma-derived growth factor 1) (Boulting et al., 2011; Chan et al., 2009; Takahashi et al., 2007). We found that both normal and MJD iPS cell lines had similar gene expression levels with hES cell line HuES1.

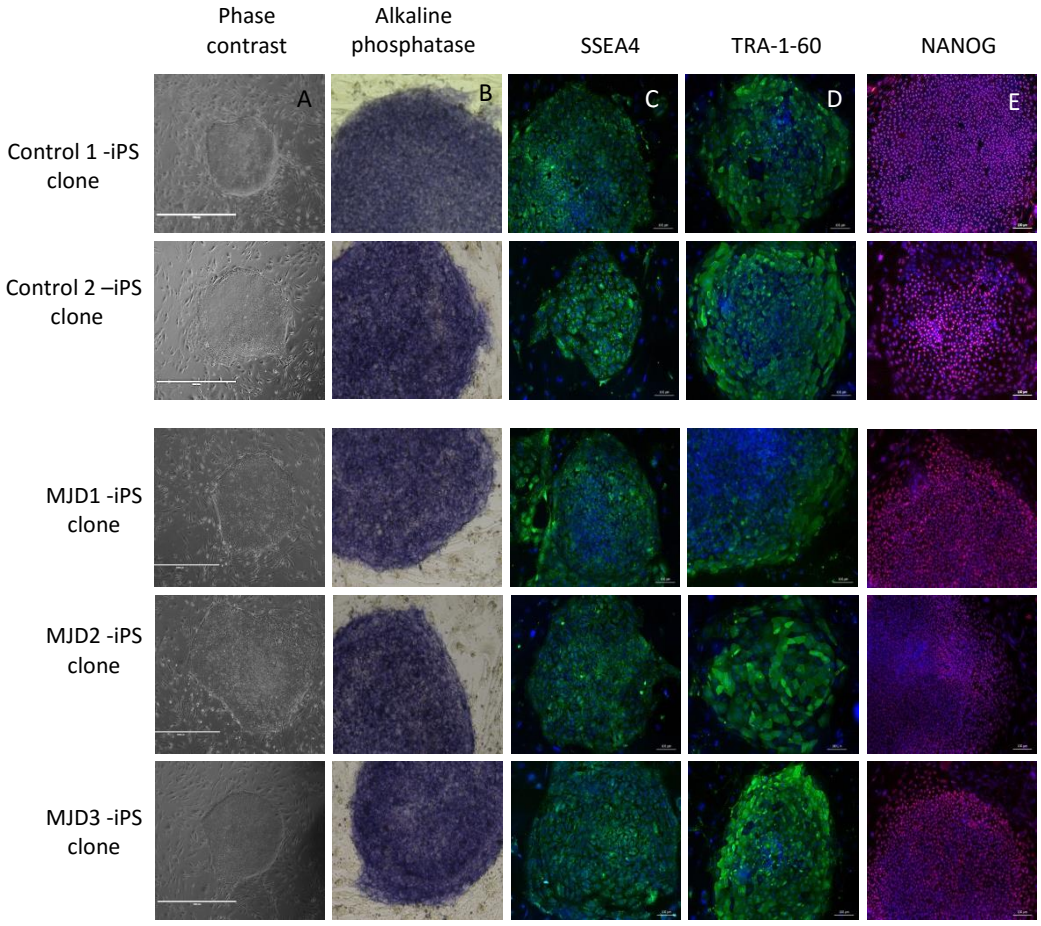

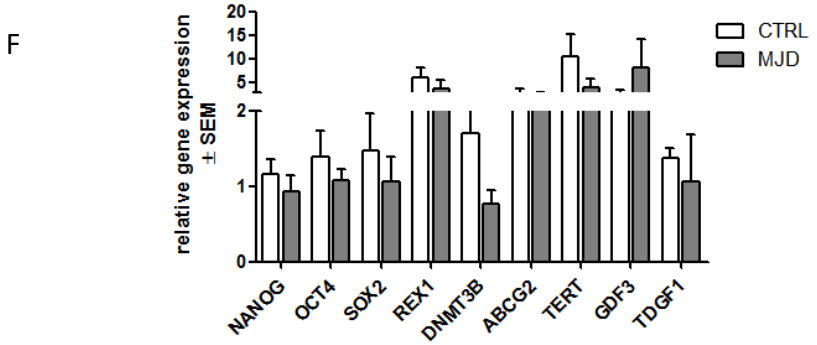

Figure 3.5- Expression of pluripotency markers in iPS cell lines.

Representative phase contrast images of iPS cell colonies, scale 1mm (A), alkaline phosphatase positive staining (B), SSEA4 (C), TRA-1-60(D) and Nanog(E) scale 100 µm. qRT-PCR analysis of pluripotency related genes in derived iPS cells, using GAPDH as reference gene and HuES1 as pluripotency standard, n= 8/n=8 (F)

3.4.2.3- Genetic stability

Human pluripotent stem cells, ES cells and iPS cells, are prone to epigenetic and transcriptional aberrations mainly due to the prolonged and extensive *in vitro* culture (Baker et al., 2007). We did not find any abnormalities related with the somatic cell type of origin or secondary to the reprogramming method, as shown by the matched normal diploid karyotypes of fibroblasts and the derived iPS cell line (Fig 3.6A and B) (Ben-David and Benvenisty, 2011; Ma et al., 2014).

We also found that all the human iPS cell lines generated retained diploid karyotypes with no detectable numerical or structural chromosomal abnormalities (Fig 3.6B and C), except for one clone, which exhibited a partial translocation of chromosome 2 into chromosome 3, in a mosaic culture (Fig 3.6D). This clone was not used for differentiation.

Taken together, these data suggest that the generated iPS cells are genetically stable and adequate for further functional assays.

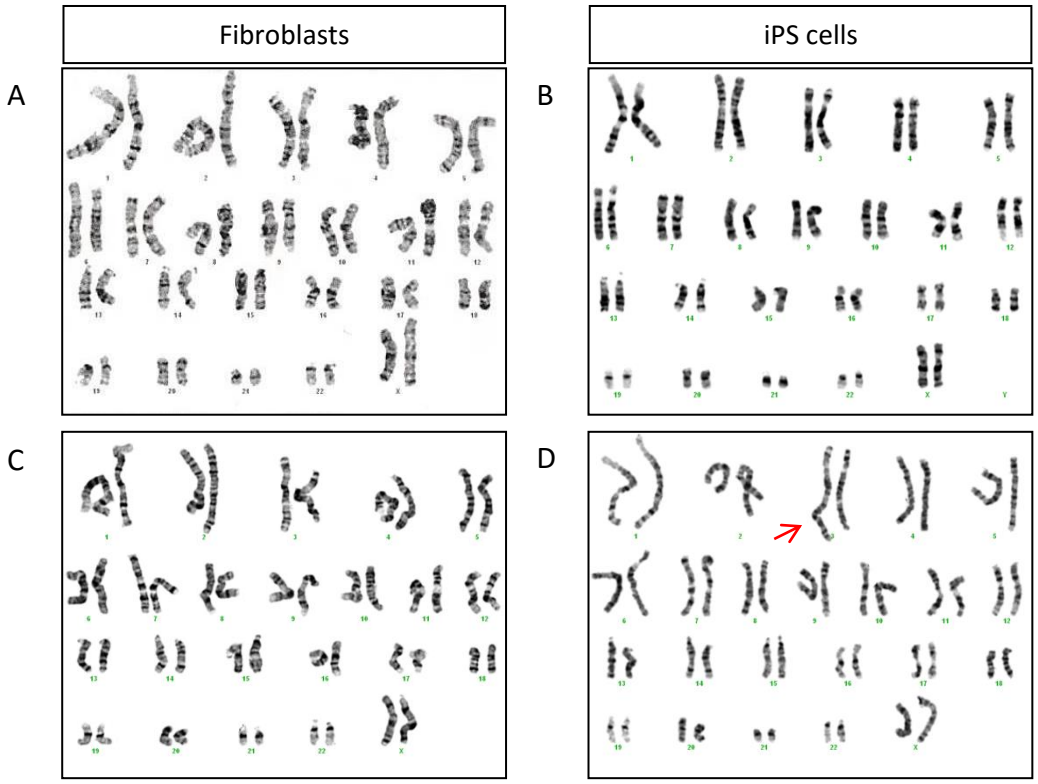

Figure 3.6- Representative metaphase spreads of aligned karyotypes of fibroblasts and matched-derived iPS cell lines.

Normal diploid karyotype of MJD fibroblasts (A) and the matched iPS cell line derived (B). All the derived iPS cell lines derived presented a normal diploid karyotype but one clone from a CTRL-iPS cell line (D), with a chromosomal translocation between chromosomes 2 and 3. This chromosomal anomaly was not present in the fibroblast culture of origin (C).

3.4.3- Pluripotency characterization of iPS cells: functional assays

3.4.3.1- *In vitro* differentiation potential

The formation and random differentiation of EBs (embryoid bodies) is a useful assay to evaluate pluripotency of human pluripotent stem cells (Itskovitz-Eldor et al., 2000; Sheridan et al., 2012). An increase in number and size of EBs was observed over time (Pekkanen-Mattila et al., 2010) and similar growth and morphology among the different cell lines from MJD and controls (Fig 3.7A).

In order to evaluate the spontaneous differentiation into cells of all three germ layers we plated EBs in adherent conditions for a week allowing the differentiation into more mature cell types (Keller, 2005; Keller, 1995). The resulting cultures were then studied for the expression of germ layer-specific genes. We used a typical set of markers for endoderm including Sox17 (Vassilieva et al., 2012) and AFP (alpha-fetoprotein); EOMES (Eomesodermin) (Teo et al., 2011), T (Brachyury), (Bernemann et al., 2011) and DES (desmin), (Karbanova and Mokry, 2002) for mesoderm; and NES (Nestin) (Fuchs and Weber, 1994), PAX-6 and SOX-1 (Suter et al., 2009) for ectoderm. EBs derived from both control and MJD iPS cell lines expressed three germ layer-specific genes (Fig 3.7B) and also stained positively for proteins specific of the three germ layers (Fig 3.7C) demonstrating the completeness of differentiation.

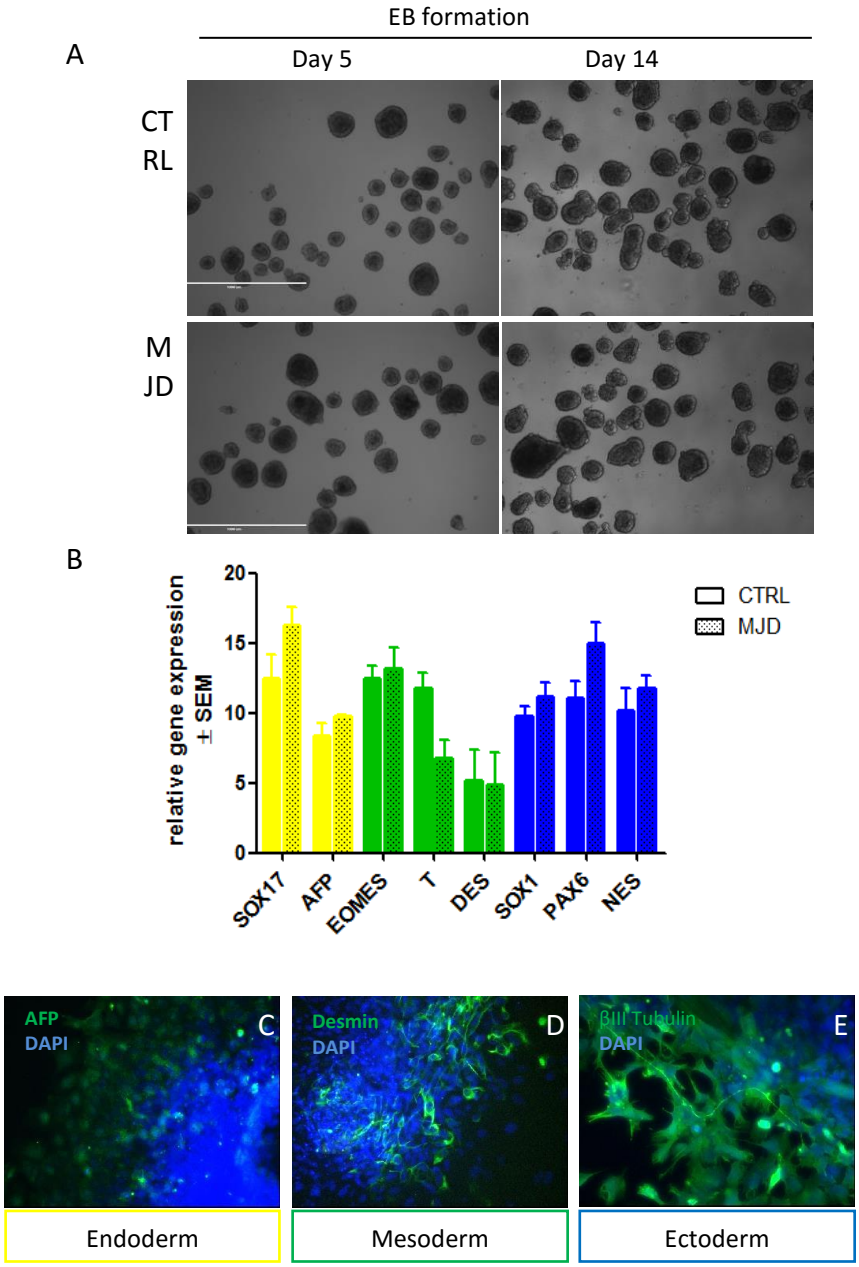

Figure 3.7- Spontaneous *in vitro* differentiation of iPS cell lines in EBs and cells representing the three germ layers

CTRL and MJD iPS cell lines presented similar early developmental competence during EB formation (A), as presented by representative phase-contrast images of EBs at 5 days and 14 days of differentiation (scale 1 mm). Both CTRL and MJD EBs expressed similar levels of endoderm, mesoderm and ectoderm related genes (B) and the derived cultures stained positively for mature cell types from endoderm (AFP marker), mesoderm (desmin marker) and ectoderm (βIII Tubulin marker) (C-E), scale 100 µm. qRT-PCR was performed using GAPDH as reference gene (n=8/n=8).

3.4.3.2- *In vivo* differentiation potential

The generation of teratomas is the most stringent assay to assess pluripotency of human pluripotent stem cells (Gropp et al., 2012; Muller et al., 2010) and it is considered the "gold standard" for pluripotency. Teratomas are solid and nonmalignant defined tumors composed by highly organized differentiated cells and tissues containing representatives of the three developmental germ layers.

We injected subcutaneously undifferentiated iPS cells in seven weeks old NOD.Cg-Prkdc^{scid} Il2rg^{tm1Wjl}/SzJ JAX mice and after 12 weeks we removed surgically the developed teratomas to analyze the tissue composition. We obtained mixed teratomas, containing both solid and cystic parts (due to the presence of secretory epithelial cells). The solid parts of all analyzed teratomas had similar histological composition and displayed tissues belonging to all three germ layers (Fig 3.8). We could observe several distinct types of epithelia (Fig 3.8A and B) (endoderm), muscle, bone and cartilage (Fig 3.8C and D) (mesoderm) and neural rosettes and epidermis (Fig 3.8E and F) (ectoderm).

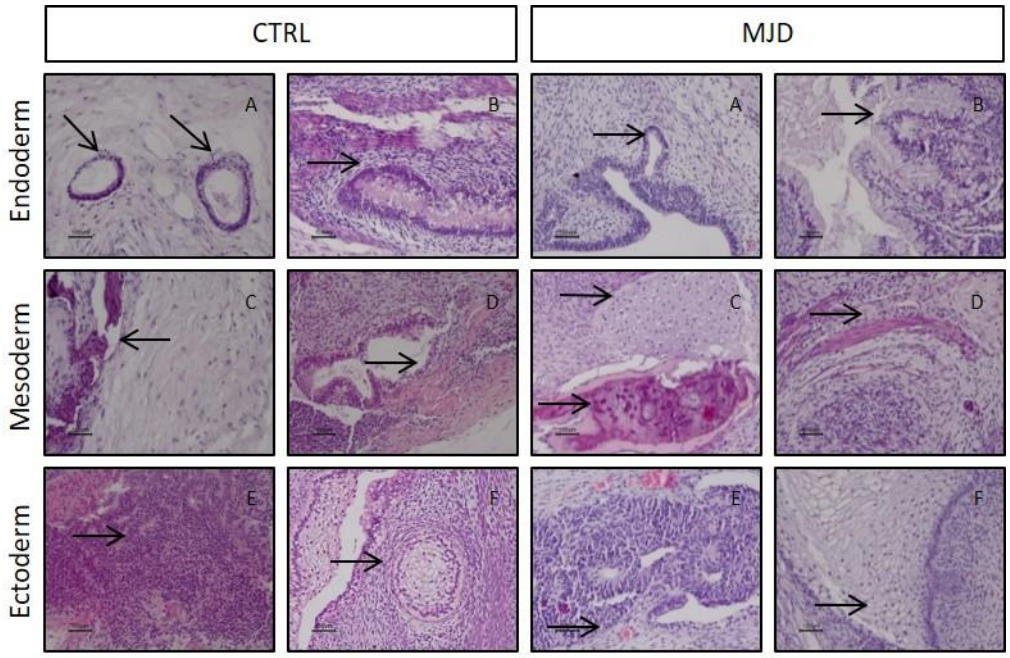

Figure 3.8- *In vivo* differentiation of iPS cell lines in tissues representing the three germ layers after teratoma formation.

All CTRL and MJD iPS cell lines were able to generate teratomas and presented typical structures of endoderm as glands (A) and goblet cells (B) (arrows), cartilage/bone (C) and muscle(D) (mesoderm panel with arrows) and neural rosettes (E) and epidermis (F) (ectoderm panel with arrows). Representative hematoxylin and eosin staining of teratoma sections, scale 100 µm.

Teratomas, depending on the maturation level, can present small portions of undifferentiated tissues. We analyzed the expression of Oct4 (Fig 3.9 A) to address this question and we found a discrete expression in some teratomas, revealing the overall high maturity level of the developed teratomas. The differentiated tissues stained positively for specific markers of well-defined mature structures as the respiratory epithelium-TTF1 (Boggaram, 2009), glandular epithelium-Cdx2 (Silberg et al., 2000) (Fig 3.9 B), cartilage and bone-s100 (Donato et al., 2013), smooth muscle- α-SMA (Fuchs and Weber, 1994) (Fig 3.9 C), neural rosettes-NSE (Yuan et al., 2011) and epidermis-CK 5/6 (Fuchs and Weber, 1994) (Fig 3.9 D).

Taken together these results further confirm the pluripotency of the iPS cell lines under study and its capability to generate mature tissues and terminally differentiated cells.

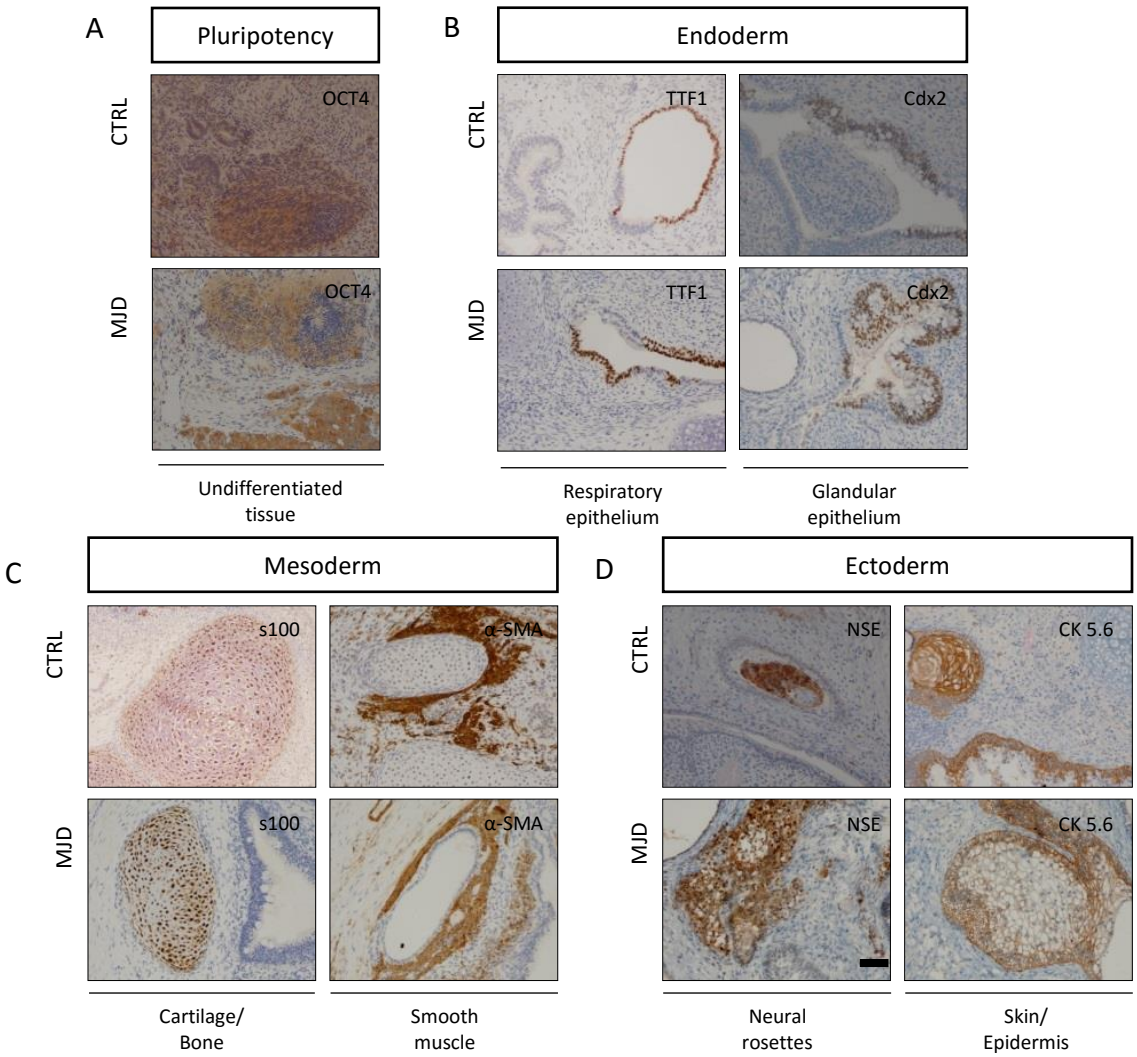

Figure 3.9- Immunohistochemistry of iPS cells derived teratomas for specific markers of immature tissues and endoderm, mesoderm and ectoderm.

Minor regions of teratomas stained positively for OCT4 (A), a marker for immature tissues as the major area of the tumors were composed by more mature tissues related to endoderm as respiratory and glandular epithelium, stained positively for TTF1 and Cdx2, respectively (B); to mesoderm as cartilage/bone and smooth muscle , stained positively for s100 and α-SMA, repectively (C) and to ectoderm as neural rosettes and skin/epidermis structures, stained positively for NSE and CK 5.6, repectively (D).All teratomas presented similar composition regardless the genotype of the iPS cell line of origin (scale bar 100 µm).

3.5-Discussion

In this work we generated and characterized a set of MJD iPS cell lines, with preserved expression of mutant ataxin-3. All the iPS cell lines met the key aspects of pluripotency as flat colony morphology, acquisition of molecular pluripotency markers (transgene silencing, alkaline phosphatase activity, expression of cell surface markers and high expression of pluripotency related genes), maintenance of normal diploid karyotype and also fulfilled the differentiation potential assays, both *in vitro* and *in vivo*

The generation of iPS cells, pioneered by Shinya Yamanaka and colleagues (Takahashi et al., 2007; Takahashi and Yamanaka, 2006) used retroviral vectors to overexpress the 4 reprogramming factors into somatic cells, with a reported low efficiency. With the development of the technique, lentiviral vectors were introduced (Stadtfeld et al., 2008b; Yu et al., 2007), with more favorable designs, as polycistronic vectors (Carey et al., 2009; Sommer et al., 2009) and with “stem cell cassetes” (Papapetrou and Sadelain, 2011; Somers et al., 2010; Sommer et al., 2010), increasing the transduction efficiency and safety by reducing the number of viral integrations.

We used a polycistronic lentiviral vector (Fig 3.1A) in our work in order to achieve higher efficiencies in the reprogramming process (Warlich et al., 2011). The expression of the 4 factors simultaneously in a stoichiometry of equal parts enabled a favorable kinetics and was highly effective in reprogramming (Carey et al., 2009; Papapetrou et al., 2009; Warlich et al., 2011) allowing the emergence of early iPS colonies during the first week of reprogramming. This vector, also encoding for a fluorescence protein (dTomato) along with the 4 reprogramming factors, allowed us to follow the course of reprogramming (Fig 3.2A) and to choose the precise time to select full-reprogrammed iPS cells (Fig 3.2D).

To resolve the issue of slowness and inefficiency of the reprogramming process we also used specific chemical compounds and signaling molecules (Feng et al., 2009). Interestingly, we found that although the VPA treatment (Fig 3.2E) was the most effective in increasing the expression of pluripotency genes, it also contributed to cell death. The combination of VPA+Vc and PD0325901+ SB431542 (Fig 2E) allowed the most successful conditions, resulting in both improved kinetics and cell survival. Also, the absolute levels of expression of the 4 reprogramming are vital in successful reprogramming and the use of a defined MOI in the correct stoichiometry during a defined time frame is highly effective and must be determined in order to avoid additional insertional mutagenesis. The need of high MOI is overcome by using the single polycistronic vector (Chinnasamy et al., 2006) and it not only influences on the reprogramming process (Fig 3.2F) but also the further use of the iPS cell lines in differentiation protocols.

We confirmed the presence of mutant ataxin-3 protein in the derived iPS cell lines (Fig 3.3) as previously described by Koch P and col. (Koch et al., 2011) and this result ensures the use of MJD iPS cell lines as the source of neurons to study MJD pathogenesis.

As the most important test for success of the reprogramming process is the quality of the derived iPS cells, we then sought to validate the pluripotency of those cells. We followed a well-characterized set of assays to perform the characterization of iPS cells (Boulting et al., 2011; Chan et al., 2009) using standard methods and techniques and a hES cell line to perform comparative analysis (Maherali and Hochedlinger, 2008; Maherali et al., 2007). Our cells resembled hES cells (Fig 4A) and silenced effectively the ectopic gene expression of the 4 reprogramming factors, confirming the fulfillment of the morphological criteria (Fig 3.4B). We also verified the activity of alkaline phosphatase enzyme, the expression of cell surface markers (Fig 3.5B-D) and nuclear transcription factors, as Nanog (Fig 3.5E), that together with Oct4 and Sox2 are considered the core transcription factors that regulate the ground state of pluripotency (Silva et al., 2009). We confirmed the high expression of this trio by qPCR and other pluripotency related genes (Fig 3.5F). The high expression of hTERT (Agarwal et al., 2010) is a fundamental feature of iPS cells that supports the acquisition of the indefinite self-renewal capacity observed in our cultures. We did not find differences on morphological and functional pluripotency features regarding MJD genotype.

In order to provide differentiated cells for several applications the continuous maintenance of undifferentiated and genetically stable iPS cells for long periods in culture is required (Baker et al., 2007; Stadtfeld and Hochedlinger, 2010). However, chromosomal stability during extended passaging cannot be guaranteed, as aneuploidies may arise within a few passages in culture (Ben-David and Benvenisty, 2011). Based on this evidence, iPS cell lines must be analyzed as close as possible to their actual use in experiments, and re-evaluated during continued culture (Ben-David et al., 2010). In our study we analyzed the karyotype of iPS cells just before the differentiation assays, as an abnormal karyotype could compromise the differentiation performance of those cells (Blum and Benvenisty, 2009). We did not find aberrations originated from the parental somatic cell or from the reprogramming method by itself (Fig 3.6A and B), confirming the genetic safety of our reprogramming strategy.

We also did not find the most frequent karyotypic changes observed in human pluripotent stem cells due to culture adaptation such as the duplication of chromosomes 12, 17 or X (Draper et al., 2004; Mayshar et al., 2010; Spits et al., 2008), suggesting that good routine culture techniques were followed (Ben-David et al., 2010). Interestingly, we found one singular chromosomal aberration in mosaic for one clone, the translocation between chromosome 2 and 3 that so far was not reported as a common aneuploidy related with human iPS cells. This type of aneuploidy suggests an in-between transformation, possibly malignant (Na et al., 2014) that shall be verified in further cell passages.

For the *in vitro* differentiation assay, we generated EBs, which are three-dimensional aggregates that contain an amalgam of cells from the three developmental

germ layers (endoderm, mesoderm and ectoderm) obtained from the suspension culture of iPSCs in the absence of bFGF. We observed varied EB morphology and size (Fig 3.7A), with no clear correlation with MJD genotype or differentiation patterns. All the tested iPS cell lines differentiated in the 3 germ layers (Fig 3.7B and C), matured (Kim et al., 2007) confirming the *in vitro* developmental competence. This assay provided an exceptional insight on the intrinsic differentiation properties of iPS cell line, predicting a neuronal differentiation taking in account the high levels of SOX1, PAX6 and NESTIN expression (Lappalainen et al., 2010).

Teratoma formation is known as the most stringent assay to confirm the pluripotency of human cells (International Stem Cell Banking, 2009; Maherali and Hochedlinger, 2008). In the case of iPS cells, its validity is definite only when the other criteria of pluripotency are met because it was reported that partially reprogrammed iPS cells can form teratomas (Dolgin, 2010). In our study, all the generated iPS cell lines met the previous criteria of pluripotency and were able to form teratomas composed by representative tissues of the three germ layers (Fig 3.8 and 3.9B-D). It is also known that teratomas formed by pluripotent stem cells resemble type I GCTs (Cunningham et al., 2012) and can be composed by undifferentiated tissue. Interestingly we found that some teratomas stained weakly for Oct4 protein as described for these tumors (Looijenga et al., 2003) (Fig 3.9A). The presence of only small parts of undifferentiated tissue and the large composition in fully differentiated tissues on those teratomas allowed us to classify them in mature teratomas and distinguish it from teratocarcinomas (Solter, 2006). Also, the full body necropsy following animal sacrifice did not reveal presence of teratomas or other tumors within the peritoneal cavity or elsewhere within the animal, confirming that the presence of c-MYC in the reprogramming cocktail did not stimulate the emergence of tumors (Lee et al., 2013; Miura et al., 2009).

In conclusion, in this study, we generated high quality patient-derived iPS cells, preserving mutant ataxin-3 expression. These iPS cells can be differentiated into human neurons, contributing to the establishment of a novel MJD *in vitro* model.

Chapter 4

Early MJD phenotype in human iPS derived neurons

4.1-Abstract

Machado-Joseph disease also called SCA3 is a dominantly inherited late-onset neurodegenerative disease caused by the polyQ tract in *ATXN3* gene that results in the translation of an expanded CAG repetition in ataxin-3 protein, leading to a toxic gain of function of this protein. The accumulation of mutant ataxin-3 in ubiquitinated neuronal intranuclear inclusions is a hallmark of neurodegeneration in the brains of MJD patients and it is linked to the pattern of observed neurodegeneration.

Here we describe the successful generation of human MJD neurons derived from 2 actual patients and we recapitulate the MJD early disease phenotype *in vitro*. We found that autophagy is impaired in early stages of MJD neuronal cultures (21 days), contributing to the defective clearance mechanisms observed in MJD neurons. We also demonstrate that after exposition to increased intracellular levels of Ca^{2+}, ataxin-3 migrates to the nucleus and forms small aggregates in MJD neurons, contributing to the development of a robust phenotype. Together these data suggest that the pathogenesis of the disease occurs in earlier stages than the development of ubiquitinated intranuclear inclusions and that survival pathways are affected.

Finally, we demonstrate that our model of iPS cells-derived patient neurons allows the study of MJD as a late onset neurodegenerative disease and provides a new tool for further pathogenesis studies and development of therapies.

4.2-Introduction

MJD is an autosomal-dominant progressive neurodegenerative disease, characterized by progressive cerebellar ataxia, external progressive ophthalmoplegia, pyramidal signs, and extra-pyramidal signs, as dystonia and peripheral amyotrophy (Lima and Coutinho, 1980; Rosenberg, 1992). MJD is a monogenic disease caused by an unstable expansion of a CAG repeat in exon 10 of the *ATXN3* gene that translates in an abnormal polyglutamine tract in ataxin-3 (Kawaguchi et al., 1994; Takiyama et al., 1993). The neuropathology involves aggregation of mutant ataxin-3 in ubiquitinated intranuclear inclusions accompanied by neuronal loss in specific brain regions as cerebellum, substantia nigra, striatum and cortex (Alves et al., 2008b; Rub et al., 2008; Yamada et al., 2001). The pathogenic mechanisms that lead to neurodegeneration in MJD are still not well understood, since current experimental MJD models fail to fully recapitulate the human neuropathological features of the disease.

Recently, human iPS cells technology (Takahashi and Yamanaka, 2006) has emerged as a promising powerful tool for research into the pathogenesis of many diseases, including late onset neurodegenerative diseases, as Parkinson's disease (Nguyen et al., 2011) and Alzheimer's disease (Israel et al., 2012; Sproul et al., 2014) making possible to analyze human living disease-specific neurons *in vitro*. Generation of polyQ disease specific iPS cells from patients and derived neuronal models has also been reported for Huntington's disease (Camnasio et al., 2012; Consortium, 2012), MJD/SCA3 (Koch et al., 2011), SCA2 (Xia et al., 2013), SCA7 (Luo et al., 2012) and SBMA (Grunseich et al., 2014; Nihei et al., 2013) illustrating the importance and usefulness of this technique in understanding the disease pathogenesis.

Neurogenesis and neuronal terminal differentiation of iPS cells recapitulates *in vivo* neurodevelopment with similar differentiation profiles and potencies of hES cells (Hu et al., 2010; Reubinoff et al., 2001; Zhang et al., 2001), enabling the use of small molecules that mimic morphogens involved in regionalization and patterning of the central nervous system (Okada et al., 2008; Okano and Temple, 2009; Temple, 2001). One of the most used strategies to promote neural induction *in vitro* is the dual-SMAD signaling inhibition (dSMADi) that consists in the inhibition of TGF-β and BMP signaling pathways (Chambers et al., 2009) and enables a rapid and synchronous neural conversion of iPS cells with a broad spectrum of terminally differentiated neurons, ranging from a more anterior patterning, as cortical neurons (Shi et al., 2012) to a more posterior fate, as in motor neurons (Boulting et al., 2011; Dimos et al., 2008; Ebert et al., 2009) and also more ventral neuronal populations as in striatal interneurons (Delli Carri et al., 2013b) and substantia nigra dopaminergic neurons (Chambers et al., 2011; Kriks et al., 2011). In this study we

used the combination of retinoids (retinoic acid) and shh agonists (purmorphamine) to promote both caudal and ventral fates (Blumberg et al., 1997; Lai et al., 2003).

The precise assessment of mature and functional properties of the terminally differentiated neuronal subtype and the characterization of the disease genetic identity is extremely important to the correlation of the disease pathogenesis, in the special case of monogenic diseases, such as MJD, where the CAG repeat length correlates with the disease onset (Maciel et al., 1995; Matsumura et al., 1996a). The CAG repetition in polyQ iPS cells-derived models as in the SBMA,DRPLA, MJD and HD models has been reported to be stable (Koch et al., 2011; Nihei et al., 2013; Zhang et al., 2010), or unstable in the form of an expansion of CAG repetition in a different the HD model (Consortium, 2012). This later finding could be related with the two clinical features common to polyQ disorders: anticipation and the somatic CAG mosaicism (Ito et al., 1998; Maciel et al., 1997; Shelbourne et al., 2007; Zhang et al., 1994). The chromatin remodeling during cell reprogramming could recapitulate the anticipation process similar to those that take place during meiosis and gametogenesis (Xu et al., 2011) or could represent the somatic mosaicism of fibroblast cultures.

It has been reported that autophagy modulates pathological processes that occur in different neurodegenerative diseases (Hara et al., 2006; Komatsu et al., 2006; Nixon, 2013) and the impairment of this specific pathway contributes to the accumulation of abnormal misfolded proteins as in the case of MJD and mutant ataxin-3 (Nascimento-Ferreira et al., 2011). Therefore, in this study we verified the contribution of this phenotype as an early event of MJD pathogenesis in our human *in vitro* neuronal model.

Using late cultures of MJD-specific iPSC-derived neurons, Koch and col. 2011 revealed that glutamate-induced excitation was critical for proteolysis and aberrant insoluble aggregation of ataxin-3. In this study we used a similar approach to increase the intracellular Ca^{2+} levels but mediated by the inhibition of calcium uptake by the endoplasmic reticulum (Berridge, 1998), activated by thapsigargin (Lytton et al., 1991). We sought to investigate whether the triggered proteolysis of cytoplasmic ataxin-3 and the translocation of fragments to the nucleus was an early contributing event for the development of the MJD phenotype.

Here, we report the derivation and functional characterization of neurons derived from MJD iPS cells that retained the patient genetic complexity and allowed to study the progressive nature of MJD neurodegeneration, based on early events in the pathogenesis of the disease, specifically autophagy impairment and translocation of mutant ataxin-3 to the nucleus. We expect that this model will contribute to a better knowledge of the MJD pathogenesis MJD, providing new insights and functioning as a plataform for development of new therapies.

4.3-Material and Methods

4.3.1-Generation of iPSC-derived NSC lines

iPS cell colonies were treated with 1mg/mL Collagenase IV (Gibco, Invitrogen) to separate colonies from the feeder layer and were cultured as EBs (Takahashi et al., 2007) for 4 days. On day 5, EBs were switched to neural induction medium (NIM), composed by DMEM F12 (Invitrogen), 1x N2 supplement (Gibco, Invitrogen), 10 uM SB431542 (Axon), 1uM Dorsomorphin (Sigma-Aldrich), 1% NEAA (Sigma-Aldrich) and 1% Penicillin/streptomycin (Gibco, Invitrogen).

After one week in neutralizing conditions, the EBs were transferred to poly-ornithin/laminin (Sigma-Aldrich) coated plates and the culture medium was changed to neural expansion medium (NEM), composed by DMEM F12 (Invitrogen), 2x B27 (Gibco, Invitrogen), 20 ng/mL EGF (Peprotech), 20 ng/mL bFGF (Peprotech) and 5 ug/mL heparin (Sigma-Aldrich). In the following days, neural rosettes started to emerge and were carefully picked and kept in suspension as neurospheres (free-floating spherical aggregates of neural stem cells (NSCs)), in NEM. Neurospheres were expanded and passaged weekly with a chopping technique.

4.3.2-Neuronal differentiation from NSCs

To initiate differentiation, NSCs were manually dissociated with a pipette in small aggregates and plated in poly-ornithin/laminin (Sigma-Aldrich) coated plates as small droplets. The next day, culture medium was changed to neuronal differentiation medium (NDM), composed by DMEM F12 supplemented with 1x N2: Neurobasal supplemented with 2x B27 in 1:1 mixture, 1% L-Glu, 0.2 mM ascorbic acid (Sigma-Aldrich)1% penicillin/streptomycin, (Gibco, Invitrogen) 10 uM of forskolin, 1uM of retinoic acid (Sigma-Aldrich), 0.5 mM dbcAMP (Sigma-Aldrich), 2uM purmorphamin (Merck-Millipore),10 ng/mL of BDNF (Peprotech) and 10 ng/mL of GDNF (Peprotech) in adequate working volume. Neurons were kept in this neuronal medium, allowing maturing till the experiments timepoints (Gupta et al., 2013; Koch et al., 2009). Medium was half-changed twice per week or as needed.

4.3.3-Cell treatment: autophagy inhibition and Ca $^{2+}$-mediated excitotoxicity

To assess the effects of cellular stressors in neuronal cultures, 21 days neurons were treated with 100 uM of Chloroquine diphosphate (Sigma Aldrich), diluted in NDM without growth factors overnight for autophagy inhibition. Without any disturbance, 12hr later, cells were either fixed with 4% PFA and analyzed using immunohistochemistry or western blot for levels of LC3.

We used 1 uM of thapsigargin (Sigma-Aldrich) to block Ca^{2+} uptake by the ER in 21 day neuronal cultures. The compound was diluted with NDM without growth factors at the desired final concentration and added to each well. Without any disturbance, 12hr later, cells were fixed with 4% PFA and analyzed using immunocytochemistry.

4.3.4-Single Cell Calcium Analysis

Variations of free intracellular calcium levels ($[Ca2+]_i$) were evaluated in single cells obtained from neurospheres following an adaptation of the protocol from (Barreto-Chang and Dolmetsch, 2009; De Melo Reis et al., 2011).

Neurospheres were differentiated as described before in coated coverslips to allow the formation of a mixed culture containing glia and neurons and were analysed at 3 time points 7, 14 and 21 days.

These cultures were loaded for 40 min with 5 µM Fura-2/AM (Takahashi et al., 1999) (Molecular Probes), 0.1% fatty acid-free bovine serum albumin (BSA), and 0.02% pluronic acid F-127 (Molecular Probes) in Krebs solution (142 mM NaCl, 4 mM KCl, 1 mM $MgCl_2$, 1 mM $CaCl_2$, 10 mM glucose, 10 mM HEPES and 10 mM $NaHCO_3$, pH 7.4), in an incubator with 5% CO_2 at 37°C.

After a 10 min post-loading period at room temperature in Krebs solution, to obtain a complete hydrolysis of the probe, the glass coverslip with the cells was mounted on an RC-20 chamber in a PH3 platform (Warner Instruments, Hamden, CT) on the stage of an inverted fluorescence microscope (Axiovert 200; CarlZeiss).

Cells were continuously perfused with Krebs solution and stimulated following the protocol: 4 min in Krebs solution, 2 min in 50 mM K^+, 4 min in Krebs solution, 2 min in histamine and 4 min in Krebs solution. Solutions were added to the cells manually:
50 mM K^+ solution (96 mM NaCl, 50 mM KCl, 1 mM $MgCl_2$, 1 mM $CaCl_2$, 10 mM glucose, 10 mM HEPES and 10 mM $NaHCO_3$, pH 7.4) and 100 µM histamine (Sigma-Aldrich) in Krebs solution.

The variations in ($[Ca2+]_i$) were evaluated by quantifying the ratio of the fluorescence emitted at 510 nm following alternate excitation (750 ms) at 340 and 380 nm,

using a Lambda DG4 apparatus (Sutter Instrument, Novato, CA) and a 510 nm long-pass filter (Carl Zeiss) before fluorescence acquisition with a 40x objective.

Acquired values were processed using the MetaFluor software (Universal Imaging Corp., West Chester, PA). Values for Fura-2 fluorescence ratio were calculated based on a cut-off of 10% increase in the ($[Ca2+]_i$) level induced by the stimulus. Single cell calcium variation profiles were then matched with the cell phenotype by immunolabeling to determine the functional differentiation pattern of neurospheres.

4.3.5-Immunocytochemistry

Cells were briefly fixed in 4% PFA for 10 min at room temperature and then blocked in PBS containing 0.3% Triton X-100 and 5% FBS for 1 hr before incubation with primary antibodies overnight, in PBS containing 0.3% Triton X-100 and 1% BSA. Primary antibodies used in this study were mouse βIII Tubulin (clone 38F4 1:1,000, Invitrogen), rabbit Nestin (Millipore, 1:500), chicken MAP2 (1:5000, Abcam), rabbit NeuN (1:500, Millipore), rabbit GFAP (1:500, Dako), rabbit GABA (1:1000, Sigma-Aldrich) rabbit GluR1 (1:1000, Millipore), rabbit GABA γ2 (1:500, Synaptic Systems), mouse Ataxin-3 (clone 1H9, Millipore, 1:1000), rabbit LC3 (1:400, Cell Signaling) and rabbit ubiquitin (1:1000, Dako). After three washes with PBS, cells were incubated with Alexa Fluor® 488,568 and 647 secondary antibodies (1:200, Invitrogen) for 2 hr at room temperature. Additionally, cells were stained with DAPI in order to visualize cell nuclei and, after washing, mounted in Fluoroshield (Sigma Aldrich). Fluorescent signals were detected using a Zeiss inverted microscope (Zeiss Axio Observer Z1).

4.3.6-Protein isolation and western blot

For protein isolation, cells were lysed with RIPA buffer (50 mM Tris-Cl, pH 7.5, 150 mM NaCl, 1% Nonidet P-40, 0.5% sodium deoxycholate and 0.1% SDS, 1 mM PMSF and 1mM DTT) supplemented with a protease inhibitor cocktail (Roche), triturated and centrifuged at 12,000 rpm for 20 min at 4ºC. The cell lysates were collected after centrifugation. The protein concentration in the lysates was determined using the Bradford protein assay reagent (Bio-Rad). Approximately 30 ug of protein were separated on SDS-PAGE gels (4% stacking and 10-12% running) and transferred to a PVDF membrane (Immobilon®-P, Millipore). The blots were then incubated with primary antibodies against ataxin-3 (clone 1H9 1:1000, Millipore), rabbit p62 (1:1000 Cell Signaling), rabbit LC3-B

(1:1000, Cell Signaling) and mouse tubulin (clone SAP.4G5, 1:15000, Sigma) at 4 °C overnight.

The protein bands were visualized by using the corresponding alkaline phosphatase-linked secondary antibodies and ECF substrate (GE Healthcare) in a chemifluorescence device (VersaDoc Imaging System Model 3000, Bio-Rad).

For semiquantitative analysis, a partition ratio with tubulin was calculated following quantification with Quantity-one 1-D image analysis software version 4.5.

4.3.7- DNA extraction and CAG repeat sizing

Genomic DNA was isolated from fibroblasts, iPS cells and neuronal cultures using the Quick-gDNA Miniprep Genomic DNA Purification kit (Zymo® Research Corporation). All DNA samples were considered pure regarding the A260/A280 ratio that was comprised between1.8–2.0. Two fragments of approximately 473 base pairs (bp) were generated by PCR reaction for allele 1 and allele 2, with customized primers for exon 10 of *ATXN3* gene. Those fragments were resolved in an agarose gel and further purified using the MiniElute Gel Extraction Kit (Qiagen).

A cloning reaction of the PCR fragments was performed with Zero Blunt® TOPO® PCR Cloning kit for Sequencing (Invitrogen) following the manufacturer indications. After transformation of competent *E. coli* cells, the resulting colonies were selected and analysed by colony PCR using the universal primers of the vector (M13 forward and T3 or alternatively M13 reverse and T7). Positive colonies were sent to sequence (Eurofins MWG Operon, Germany). Information regarding primers and PCR parameters used will be provided upon request.

4.3.8-RNA extraction and cDNA synthesis

Total RNA was isolated using NucleoSpin RNA II kit (Macherey-Nagel) from all primary fibroblast cultures at early and later cell passages, according to the manufacturer's instructions. Total amount of RNA was quantified by optical density (OD) using a Nanodrop 2000 Spectrophotometer (Thermo Scientific) and the purity was evaluated by measuring the ratio of OD at 260 and 280 nm. 1 ug of DNAse-I treated RNA was converted to cDNA by iScript cDNA synthesis kit (BioRad) following the manufacturer's instructions and stored at -20ºC. A portion of the RT reaction (1/20 volume) was used to amplify the various genes with specific primer sets.

4.3.9-Quantitative real-time polymerase chain reaction (qRT-PCR)

Quantitative PCR was performed in a thermocycler (StepOne Plus Real Time PCR System, Applied Biosystems) using the SSO Advanced Universal SYBR Green PCR Supermix (Biorad). The primers for OCT4 viral (F-ACCCCGAGGAAAGCCAGGACA and R-ACAGCACGCCCAGTGTCAGT) and for the reference gene GAPDH (F-TGTTCGACAGTCAGCCGCATCTTC and R- CAGAGTTAAAAGCAGCCCTGGTGAC) were used to assess the transgene expression in neuronal cultures.

A master mix was prepared for each primer set containing the appropriate volume of SSO Advanced Universal SYBR Green PCR Supermix (Biorad), primers and template cDNA. All reactions were performed in duplicate and according to the manufacturer's recommendations: 95°C for 30 sec, followed by 45 cycles at 95°C for 5 sec, 58°C for 15 sec and 0.5ºC increment for starting at 65ºC at each 5 sec/step up to 95ºC. The amplification efficiency for each primer pair and the threshold values for threshold cycle determination (Ct) were determined automatically by the StepOne Software v2.3 (Applied Biosystems). The mRNA fold change with respect to control samples was determined by the Pfaffl method, taking into consideration different amplification efficiencies of all genes.

4.3.10-Cell counts and quantification of ataxin-3, ubiquitin and LC3-II

Ataxin-3, ubiquitin and LC3-II fluorescence were measured using a semi automated image-analysis software package (Zen Observer, Germany). At least 100 cells for each condition were analyzed, using an x40 objective.

4.3.11-Statistical analysis

Statistical significance between groups was determined by unpaired Student t-test or one-way ANOVA for multiple comparisons, followed by Bonferroni test for selected pairs comparison. P-values <0.05 were considered as statistically significant; $p<0.01$ very significant; and $p<0.001$ extremely significant.

4.4-Results

4.4.1- Generation of MJD-iPS cells derived neurons

Neuronal differentiation of MJD patient-specific iPS cells enables *in vitro* modeling of the disease pathogenesis. For the direct differentiation of iPS cells towards neurons we used a 41-day protocol based on the exogenous application of patterning factors and morphogens that mimics *in vivo* CNS mammalian development (Okada et al., 2008; Okano and Temple, 2009; Temple, 2001) as schematically represented (Fig 4.1 A).

Briefly, iPS cells (Fig 4.1B) were dissociated and cultured in suspension as EBs (Fig 4.1C), which contain progenitor cells of the three germ layers and then EBs were dissociated and cultured using the dual-SMAD signaling inhibition approach (Stuart et al., 2009). The spontaneously appearing neural rosette structures (Fig 4.1D), an intermediate neural stem cell population (Chambers et al., 2011; Falk et al., 2012) with high rate of proliferation, enabled picking of these structures and culture in suspension as neurospheres (Fig 4.1E), free-floating aggregates of neural stem cells (NSCs). Neural stem cells were then differentiated into mature neurons in adherent conditions (Fig 4.1F).

We confirmed the neuralization of the EBs cultures and derived neuroepithelium by the expression of the typical neural stem cell marker Nestin (Fig 4.1G-I) and the neuronal differentiation progress by the expression of neuron-specific class III β-tubulin (Fig 4.1J). We did not find significant differences in neural differentiation profiles of control and MJD patient iPS cell lines and the alteration of cell morphologies and number of neuronal structures obtained were similar along the neuronal differentiation process for both conditions.

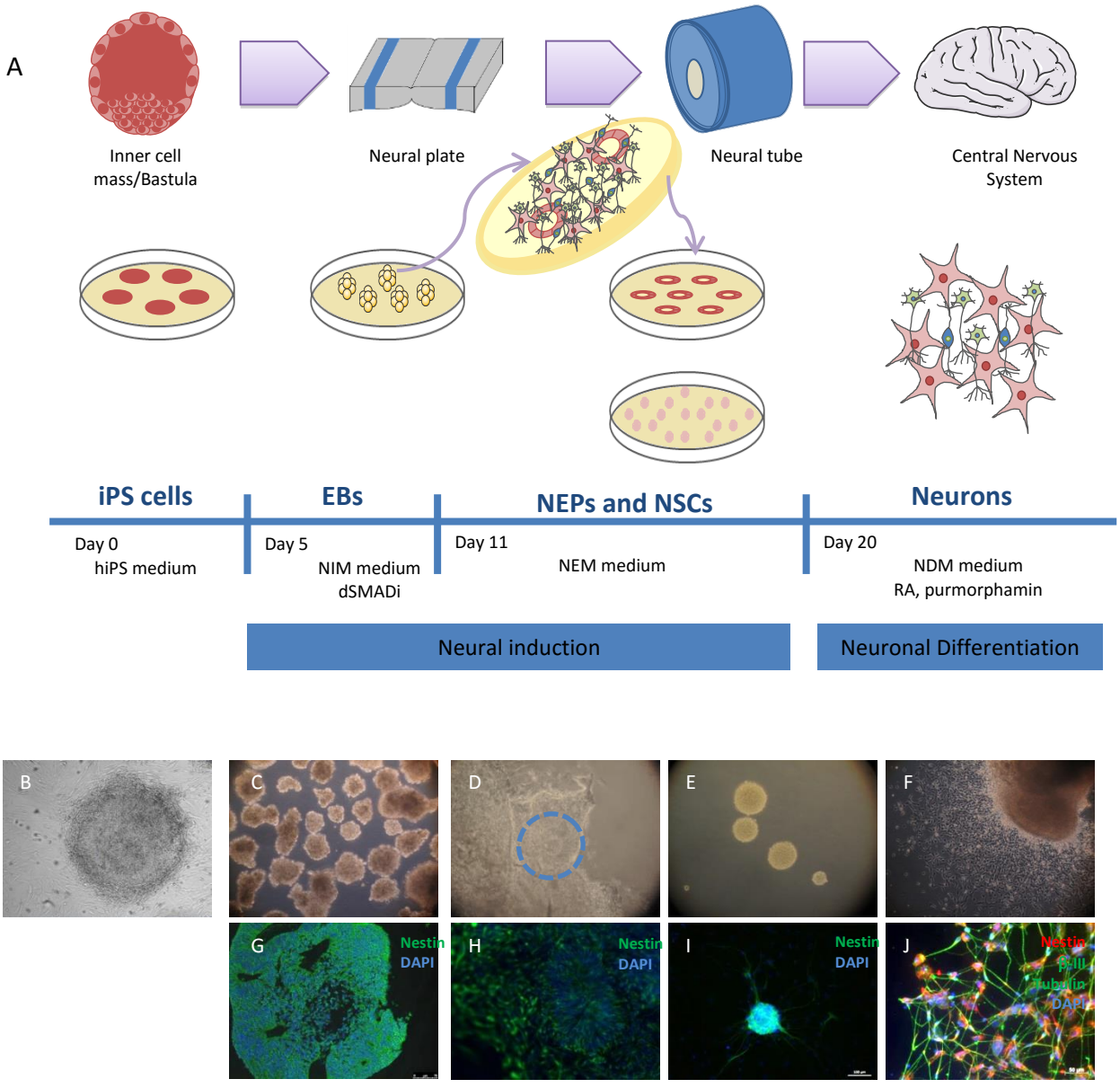

Figure 4.1- Schematic in vivo neurodevelopment is recapitulated by *in vitro* neuronalization

The development events of neuralization and neuronal differentitaion were recapitulated *in vitro* by using suspended aggregate methods (EBs and NSCs) and adherent conditions and in the presence of morphogens (A).iPS cells (B) were cultured in suspension as EBs (C) in dSMADi conditions, which contributed to the neuralization of these structures, as verified by the positive Nestin staining for neural precusors (G). EBs were plated and neuroepithelial cells emerged (D), staining for Nestin (H), establishing a paralell with in vivo neurodevelopment and the formation of neurotube. Neuroepithelial cells were cultured in suspension (E, I) as neurospheres that after plating (F) and in the presence of morphogens differentiated in neurons, staining positively for βIII-Tubulin (J).

4.4.2-Neuronal characterization and genetic assessment of MJD neuronal cultures

We next sought to evaluate whether the neurons generated by our *in vitro* system were functional. We used the single cell calcium imaging (SCCI) technique for assessment of neural network dynamics *in vitro* by measuring intracellular Ca^{2+} signals along time in culture and to evaluate the differentiation and maturation of neurons derived from neural progenitors (Barreto-Chang and Dolmetsch, 2009; De Melo Reis et al., 2011; Grienberger and Konnerth, 2012).

Neurospheres were allowed to differentiate for 3 weeks and every week and the differentiated cultures (Fig 4.2 A) were subjected to the stimulation protocol (Fig 4.2 B) based on the response to K^+ (neurons) or histamine (neural progenitors) (Grade et al., 2013). We found an enrichment of neuronal cells in cultures along time, as result of neuronal differentiation and this finding was further confirmed by correlating cell response with cell identity (Fig 4.2D). The number of neurons stained with βIII-Tubulin increased in culture as the number of neural progenitors stained with Nestin decreased as result of differentiation (Fig 4.2E).

Some cells did not respond to either K^+ or histamine in the SCCI assay, indicating a typical non-responsive profile of astrocytes. In fact, we found that our 21 day cultures were mixed cultures, composed by neurons and astrocytes, staining positively for βIII-Tubulin and GFAP (Fig 4.2F). Those cultures presented mature neurons, staining positively for the late neuronal markers MAP2 and NeuN (Fig 4.2 G-I).

Taken together these results allow us to define the composition of the obtained cultures as a mix culture of neurons and astrocytes, enriched in mature neurons (Fig 4.2J-L).

In order to further identify the neuronal population under study after the treatment with posterior and ventralizing morphogens, we performed immunostaining against γ-aminobutiric acid (GABA), a marker for cortical and striatal interneurons (Delli Carri et al., 2013b; Maroof et al., 2013) and we found that most of the population was GABAergic (Fig4.3A and D) (with discrete TH^+ neurons, data not shown) with expression of glutamate and GABA receptors (Fig 4.3 B and C). This result suggest a ventral identity of the generated interneurons, although they failed to co-stain for parvalbumin, a late marker for ventral interneurons (Delli Carri et al., 2013b).

We also analyzed vector silencing in theses cultures as the epigenetic alterations can potentially reactivate the vector expression and interfere in the study of the MJD phenotype. We found that the reprogramming factors used for iPS cells generation were silenced (Fig 4.3 E).

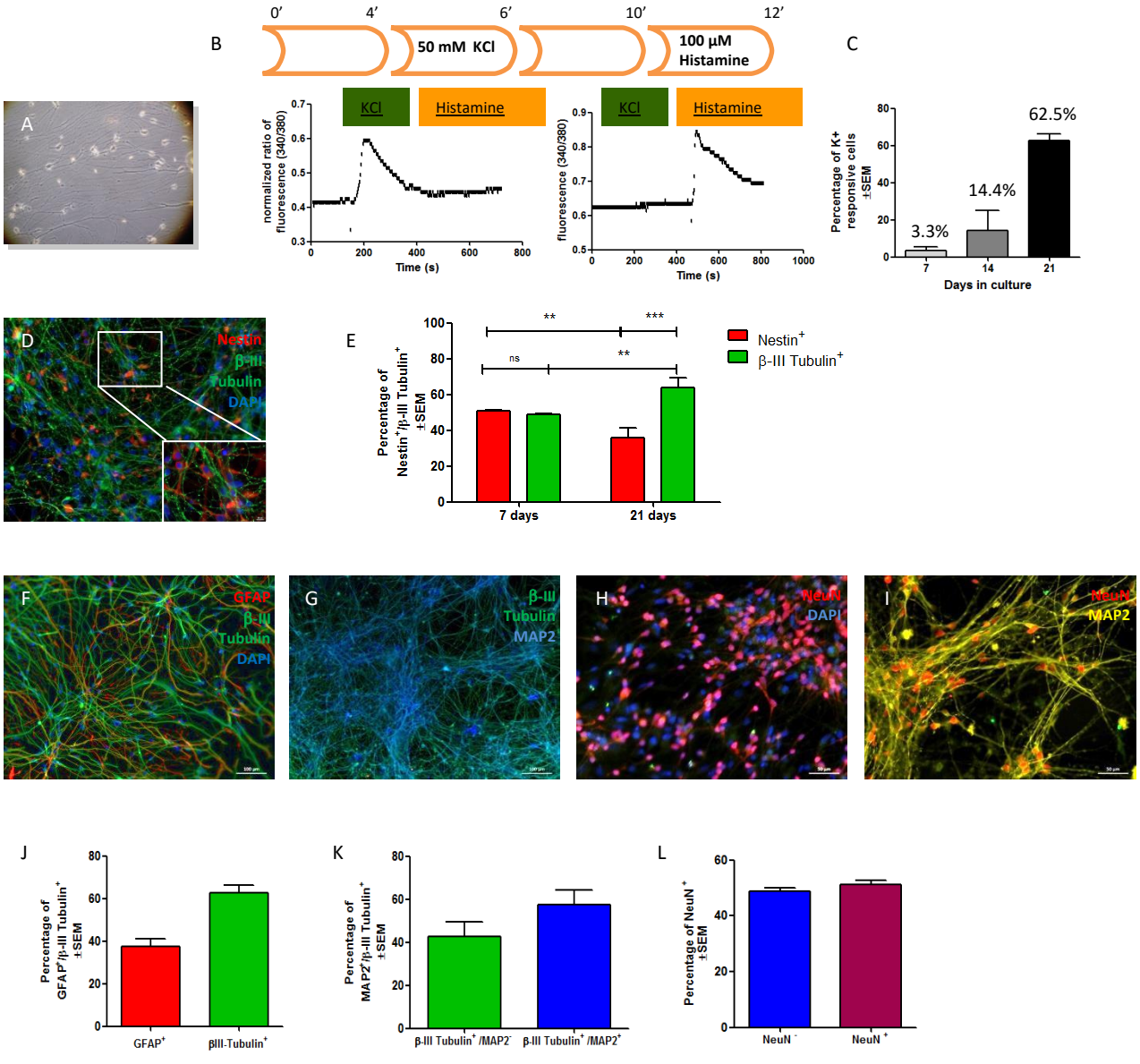

Figure 4.2- Functional evaluation of neuronal phenotypes presented in neuronal cultures derived from iPS cells.

Neuronal cultures (A) were analyzed by SSCI using a protocol of K^+ and histamine stimulation (B), along 3 weeks, showing a progressive enrichment in cells responsive to K^+ (C), neurons, as confirmed by immunostaining for βIII-Tubulin and nestin (D). The number of neurons increased as the number of progenitors decreased, along time (E) (Student's t test *p<0.05 **p<0.01 ***p<0.001 n=3/n=3). At 21 days the cultures were analyzed for neuronal and glial markers. The neuronal cultures were mixed cultures, with astrocytes (GFAP staining) (F and J), and with mature neurons as verified by the MAP2 (G and K) and NeuN (H and L) positive stainings. The co-staining for both late neuronal markers indicates neuronal maturation of the cultures at 21 days(I).

It has been reported that CAG repeats in iPS cell lines can be unstable for some polyQ disorders (Consortium, 2012) and for the derived differentiated neurons. Here we studied 2 different MJD iPS cells and derived neurons. We observed that iPS cell lines as

well neurons retain the CAG repeat expansion size present in the parental fibroblasts (Fig 4.3F), and also the associated SNPs (data not shown), excluding the influence of reprogramming process and somatic mosaicism in the MJD genotype presented in cultures. Finally, we verified the expression of mutant ataxin-3 in MJD neurons (Fig 4.3 G-I) and we found that mutant ataxin-3 was expressed in cultures.

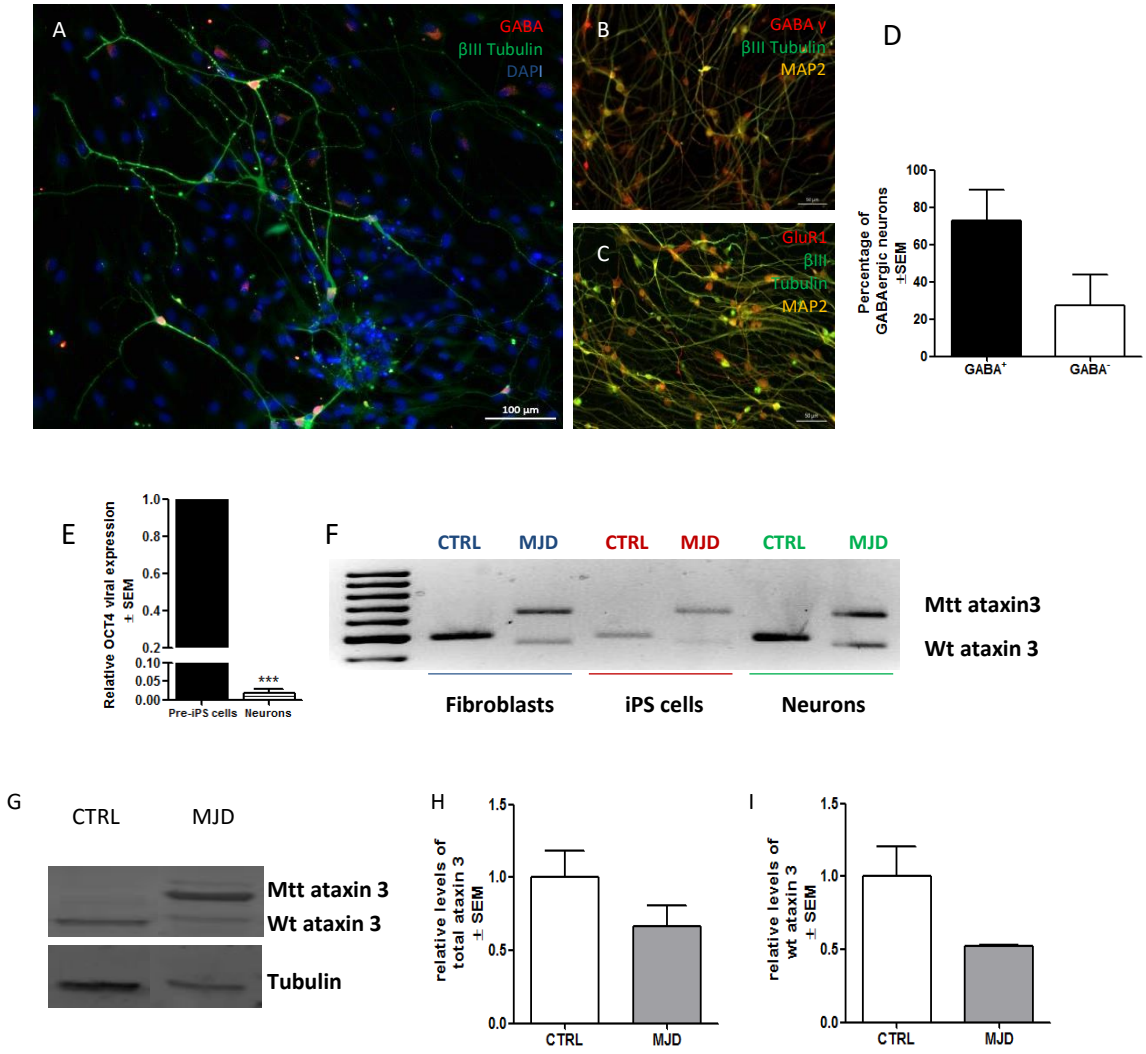

Figure 4.3- Genetic characterization of MJD derived neurons.

Neurons differentiated from iPS cells (A) were mostly GABAergic (C), expresssing receptors for GABA (B) and glutamate (C), scale 100 um and 50 um. Both CTRL and MJD neuronal cultures (2 cell lines each) did not express viral transgenes used for reprogramming (E) as verified by qRT-PCR, using GAPDH as refrence gene and pre-iPS cells as positive control for active lentiviral transduction, n=3/n=3 (Student's t test ***p<0.001). The number of CAGs was stable during reprogramming and differentiation as represented in RT-PCR analysis of transcripts (F), neuronal cultures contained the same number of CAG repetitions as the parental fibroblasts (CTRL-22/23 CAGs and MJD-23/80 CAGs). Representative western-blot of wild-type and mutant ataxin-3 in CTRL and MJD neurons (G) and densiometric quantification of total ataxin-3 (H) and wild-type ataxin-3 (I) relative to tubulin (n=3/n=3).

4.4.3-Autophagy is impaired in early human neuronal cultures of MJD

We next sought to investigate if autophagy was impaired in MJD human neurons as described previously for a MJD mouse model developed in our group (Nascimento-Ferreira et al., 2011).

We found decreased levels of Beclin-1 in our neuronal cultures (Fig 4.4 A and B), which suggest an impairment of the autophagic pathway in its first stage of initiation. In order to access the autophagic flux in basal and dynamic conditions we treated neuronal cultures with chloroquine, an autophagy inhibitor which prevents autophagosome-lysosome fusion and we found increased levels of p62 (Fig 4.4C and D) and LC3-II (Fig 4.4 E) for both control and MJD conditions as expected, but with more pronounced levels for MJD condition, which suggest an impairment on the autophagic flux. This autophagic compromise has been reported for other polyQ and neurodegenerative neuronal disease models derived from iPS cells (Camnasio et al., 2012; Sanchez-Danes et al., 2012) supporting our findings as a MJD related phenotype.

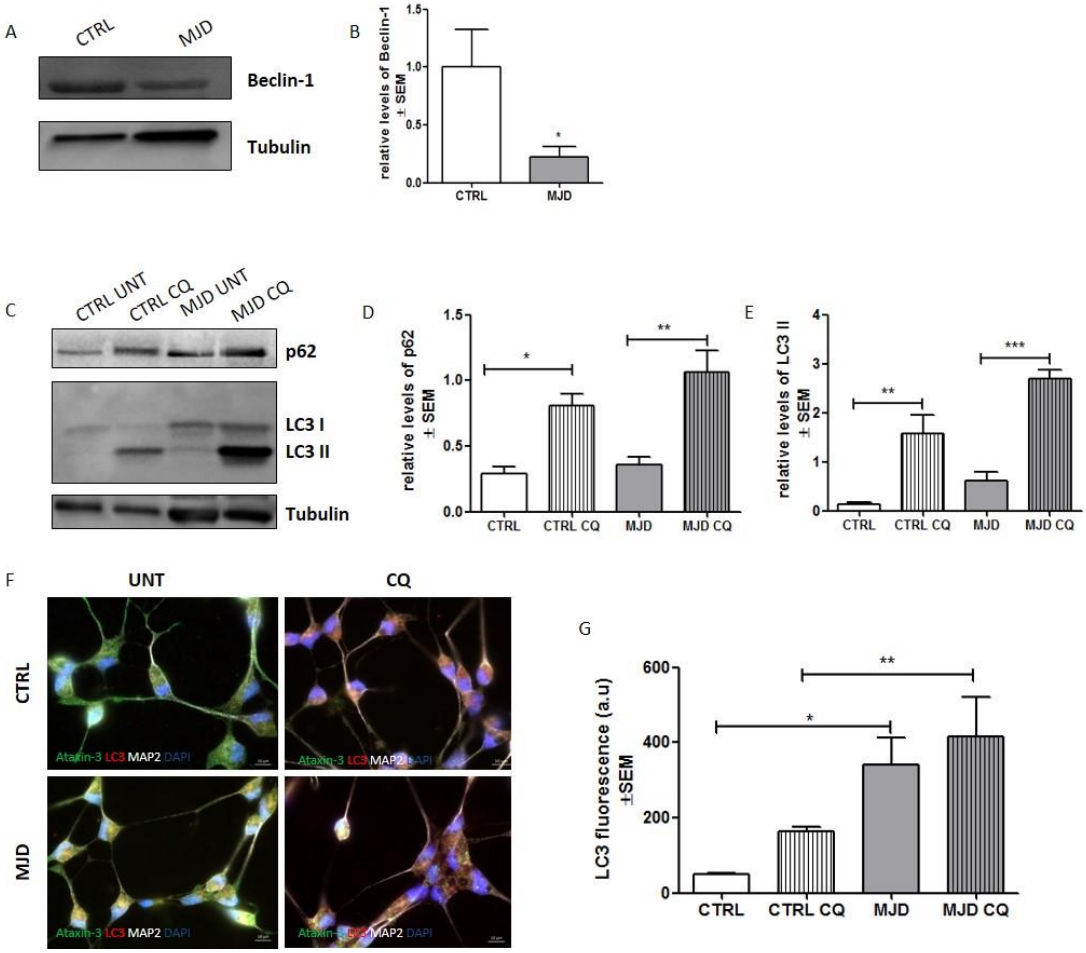

Figure 4.4- Autophagy is impaired in early human neuronal cultures of MJD.

Representative western blot of beclin-1 (61 kDa)in neuronal cultures (A and B) (t student n=3/n=3 *p<0.05). Representative western blots of p62 (62 kDa) and LC3-I and LC3-II (14 and 16 kDa) (C)in neuronal cultures after treatment with chloroquine (CQ). Quantification of p62 (D) and LC3-II (E), one-way ANOVA with Bonferroni post test (*p<0.05; **p<0.01; ***p<0.001, n=3/n=3). Immunostaining of neuronal cultures with ataxin-3 (green), LC3 (red), MAP2 (white) and DAPI (blue) (F), scale 10 um. Quantification of LC3, based on LC3 immunoreactivity (1 way ANOVA with Bonferroni post test n=3/n=3 *p<0.05; **p<0.01).

As our cultures were mix cultures of neurons and astrocytes we also investigated the actual contribution of neurons in this result to confirm the previous results obtained by western blot (Nguyen et al., 2011). We found that control neurons differentiated from Ctrl-iPS cells showed a diffuse cytoplasmic LC3 staining with very few autophagosomes (LC3-positive puncta) in contrast with a marked increase in LC3-positive puncta (in red) evident in untreated MJD neurons differentiated from MJD iPS cells (Fig 4.4F and G). The fact that autophagosomes were evident even in the absence of chloroquine in these neurons suggests a clear compromise in the clearance mechanisms related to MJD phenotype and confirm the contribution of the neuronal population in the western blot result.

4.4.4-Ataxin-3 translocates to the nucleus in early human neuronal cultures of MJD

Nuclear localization of ataxin-3 in the form of ubiquitinated aggregates is an hallmark of MJD pathogenesis(Paulson et al., 1997b) In order to study the phenomenon of ataxin-3 aggregation and accumulation in the nucleus of neurons we used a strategy to increase the intracellular Ca^{2+} levels and promote Ca^{2+} dependent proteolysis of cytoplasmic ataxin-3.

Our 21 days MJD neuronal cultures presented a diffuse cytoplasmic accumulation of ataxin-3 with no aggregates or inclusions as described previously by Koch and colleagues (2011) for both control and MJD neuronal cultures (Fig 4.5A). We used thapsigargin, a compound that blocks the Ca^{2+}uptake by the ER and promotes the increase of intracellular Ca^{2+} levels in our early neuronal cultures. After treatment we found a different distribution of ataxin-3 in control and MJD neurons: while in control cultures ataxin-3 accumulated in the cytoplasm in perinuclear localization (Fig 4.5 B), in MJD cultures ataxin-3 was found in the nucleus in punctuated form (Fig 4.5 C).

We then tried to find if the accumulation of ataxin-3 in the nucleus corresponded to the ubiquitinated form. We found increased levels of ataxin-3 in the nucleus of MJD neurons as compared with controls (Fig4.5E) and also an accumulation of ubiquitin after

thapsigargin treatment (Fig4.5F), but with a discrete co-localization of both proteins in the nucleus and in the cytoplasm (Fig4.5D, arrows).

This data suggests that a switch in the localization of ataxin-3 from the cytoplasm to the nucleus in the form of microaggregates or oligomeric structures may be one of the early steps of MJD pathogenesis.

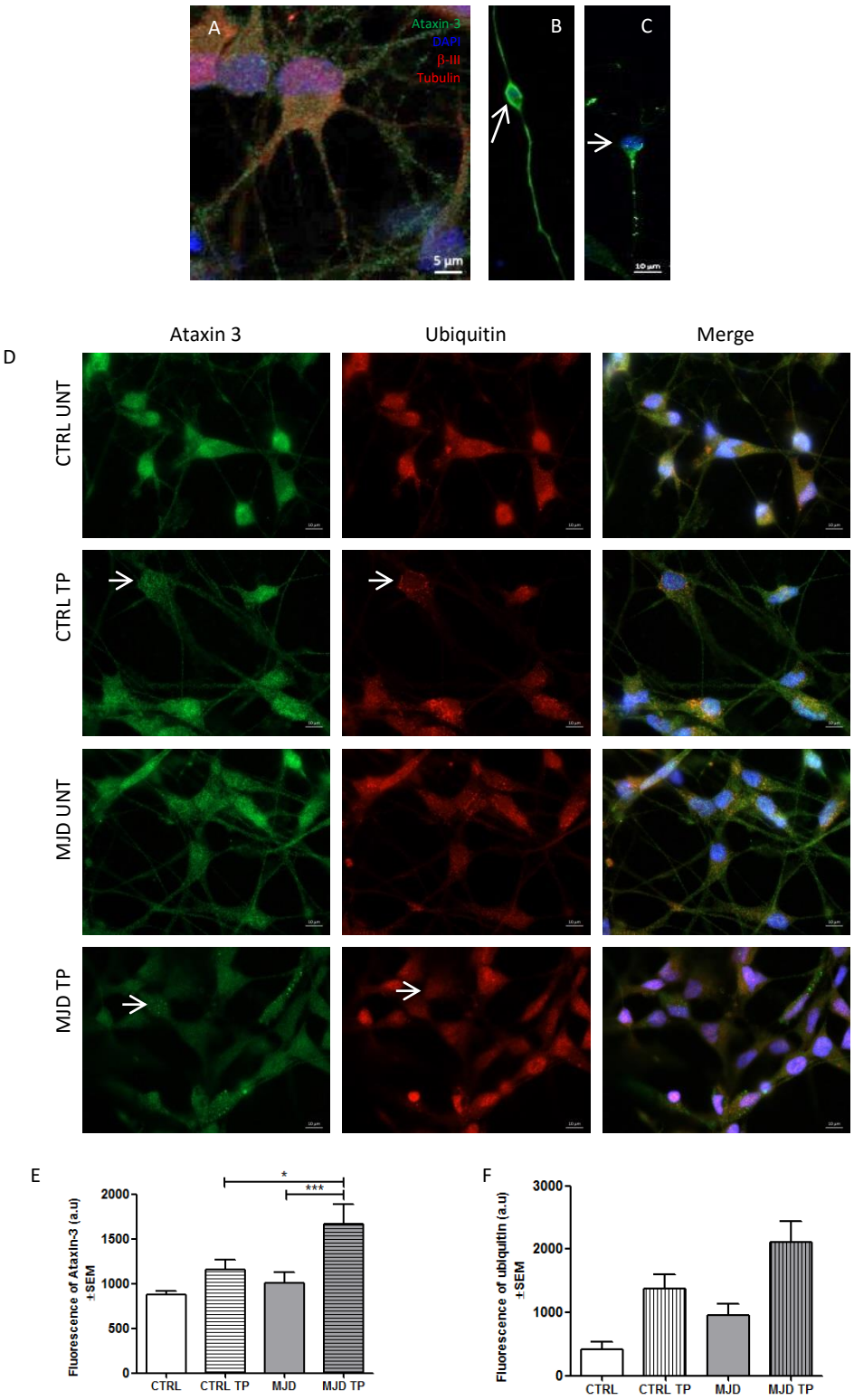

Figure 4.5- Ataxin-3 translocates to the nucleus in early human neuronal cultures of MJD

Both CTRL and MJD neuronal cultures presented a diffuse cytoplasmic staining for ataxin-3 (green) (A), with perinuclear localization for CTRL neuronal cultures (B) and nuclear localization for MJD cultures (C) (Confocal pictures, scale bar 10µm and 5 µm). Neuronal cultures were treated with thapsigargin (TP) (D). Levels of ataxin-3 in the nucleus of neurons were increased after treatment with TP (arrows), with significant expression for MJD neurons (E) and also ubiquitin levels were increased (arrows) (F) (one-way ANOVA n=3/n=3 *p<0.05; ***p<0.001).

4.5-Discussion

In this work we have generated a neuronal iPS cell-based model for MJD that recapitulates key pathological features of MJD such as autophagy impairment and neuronal intranuclear ataxin-3 accumulation.

Our neuronal differentiation strategy (Fig 4.1) enabled generation of fully functional neurons, responsive to K^+ (Fig 4.2 B and C) and displaying depolarizing membrane properties. This neuronal population was also mature staining positively for late neuronal maturation markers, namely MAP2 and NeuN, and a low number of progenitor cells, Nestin positive cells. We worked with 21 days neuronal cultures, as an early neuronal culture, balancing the mature and functional characteristics of the neurons and the late onset disease being modeled (Hayden, 2011). Our cultures were mixed cultures, with a contribution of glial cells, which add cellular complexity to the culture and mimics the actual composition of the nervous system.

We found that we had a major population of GABAergic neurons, belonging to the ventral region of the brain and that contribute for the composition of striatum, one of the most affected regions in MJD (Alves et al., 2008b; Rub et al., 2008). It is important to fully characterize the neuronal subtype in culture in order to relate with the physiological type *in vivo* and with the phenotype. We also confirmed the silencing of the lentiviral reprogramming factors in those cultures, which proved that the lentiviral mediated reprogramming strategy did not affect the differentiation protocol and can be used to generate fully functional and mature *in vitro* neuronal models. Our early neuronal cultures differentiated from MJD-iPS cells also displayed CAG repeat stability, conserving the same number of CAGs and SNPs observed in the starting fibroblast cultures, which proved our iPS cell based cellular model can capture MJD genetic complexity, allowing study of MJD pathogenesis and testing genetic strategies in neurons, the final MJD disease-relevant cell type. MJD neuronal cultures obtained from iPS cells presented expression of mutant ataxin-3 as described for the *in vitro* model developed by Koch and colleagues, but this feature was not enough to uncover a clear MJD phenotype.

In order to confirm and support previous results of an autophagy impairment phenotype related to MJD (Nascimento-Ferreira et al., 2011) we analyzed our cultures for common markers of autophagic flux, such as beclin-1, p62 and LC3. We found decreased levels of Beclin-1, a protein related to the first step of autophagy process which suggests an impairment of autophagy. This finding in our human *in vitro* model supported the observations in the MJD animal model and also provided the opportunity to study the mechanism behind the autophagy impairment. Accordingly, we treated our cultures with chloroquine, an autophagy blocker and we found increased levels of p62 and LC3 for both control and MJD cultures, being this accumulation more pronounced and significative in

MJD cultures, which suggests failure in clearance mechanism as reported for other neurodegenerative in iPS cell derived *in vitro* models (Sanchez-Danes et al., 2012). This result was also confirmed by studying the contribution of the neuronal population for this result and interestingly we found both neurons (Fig 4.4 F) as well astrocytes contributed for the phenotype as a mixed neuronal culture. Neurons present increased levels of LC3 II even in the absence of chloroquine, which supports the defective clearance mechanism as a crucial player for the abnormal accumulation of misfolded proteins and MJD neurodegenerative phenotype. Together these results suggest that autophagy impairment is one early contributor for MJD pathogenesis.

We then wondered whether the abnormal Ca^{2+} signaling played a role in the early events of MJD pathogenesis (Chen et al., 2008a). In non-treated cells we found no ataxin-3 aggregates in the nucleus or the cytoplasm of MJD neurons, but in the presence of increased intracellular levels of Ca^{2+} mediated by the treatment of the cultures with thapsigargin we observed formation of small inclusions of ataxin-3 in the nucleus of neurons as compared with control neurons. The increased levels of ataxin-3 in the nucleus corroborates the shift of ataxin-3 from the cytoplasm to the nucleus promoted by the activation of Ca^{2+} dependent proteases, which suggest that the translocation of a cleaved form of ataxin-3 to the nucleus is an early event of pathogenesis and the formation of small aggregates in the nucleus (Bichelmeier et al., 2007; Schmidt et al., 1998; Simoes et al., 2012). In spite of the increased levels of ubiquitin we did not find a clear pattern of co-localization, which suggest that the formed aggregates/ inclusions of ataxin-3 were not fully ubiquitinated. This result suggests that the formation of ubiquitinated inclusions is a later step in the pathogenesis and can be correlated with formation of insoluble aggregates, found in later neuronal cultures (Koch et al., 2011).

Our results are in accordance with previous evidence of soluble aggregates and intrinsic capacity of ataxin-3 to misfold (Ellisdon et al., 2006), and suggest that the early mechanism of MJD pathogenesis involves the formation of inclusions (both cytoplasmic an nuclear) and the migration to the nucleus, where it can impair mechanisms of transcription. Importantly, the accumulation and aggregation of mutant ataxin-3 in iPS-derived neurons provides a read-out that can be used in medium- to high-throughput analysis platforms enabling a more efficient pathway analysis and disease-modifying drug screening.

Altogether our results indicate that both failure in clearance mechanisms and formation of oligomeric or soluble structures of ataxin-3 as the primary species are early events in the MJD pathogenesis. These results provide an insight in the pathogenesis but further studies are required to confirm the temporal line/kinetics of events and also the susceptibility of other subtypes of neurons affected by the disease, such as cerebellar neurons, the most affected by the disease both in normal and stress conditions (Jessica et

al., 2015) and the consequences of the verified changes in ataxin-3 migration and autophagy impairment in disease mechanism and progression.

It is still a challenge to model late onset diseases, as age-dependent processes play a critical role in recapitulating pathological features such as the complex process of protein aggregation that involves several kinds of intermediates and aggregates/inclusions (Ross and Poirier, 2004). Nevertheless, the human *in vitro* models derived from iPS cells are a formidable tool to uncover the mechanisms of pathogenesis in the early steps of disease.

Chapter 5

Final conclusions and perspectives

5- Final conclusions and perspectives

The main goal of this thesis was to generate and study a relevant neuronal human *in vitro* model of MJD derived from patient iPS cells, capable of recapitulating the pathogenesis of the disease and reproduce the specific cellular and molecular hallmarks of the disease as observed *in vivo* in patient neurons. Our model proved valuable by enlightening the early steps of MJD pathogenesis, providing evidence that autophagy is impaired and that ataxin-3 translocates to the nucleus under elevated intracellular Ca^{2+} condition.

Being MJD a monogenic progressive neurodegenerative disease, caused by a single genetic mutation, the expansion of a CAG repeat, coding for polyglutamine within ataxin-3 protein, makes it an attractive disease to be modeled by iPS cells technology (Takahashi and Yamanaka, 2006). As for other human progressive neurodegenerative disorders, MJD is among the most difficult diseases to study, in particular because of the inability to readily obtain patient neurons. Neurons are particularly inaccessible through patient biopsies. By using reprogrammed cells from patients, it has become possible to produce neurons carrying the precise genetic variants that caused neurodegeneration in a given individual allowing experiments that until recently would have been inconceivable (Bellin et al., 2012).

The discovery that dermal fibroblasts from an adult human can be reprogrammed back to their embryonic stage and then differentiated to produce neurons in culture opened an opportunity to study the neurodegenerative disease pathogenesis in these two somatic cell types, enabling the correlation of tissue/cell type specificity with a phenotype found in fibroblasts and in neurons (Auburger et al., 2012; Grunewald et al., 2010; Mazzola and Sirover, 2001; Schwartz et al., 2014). We found that autophagy is impaired in MJD fibroblasts and neurons, despite differences in the underlying autophagic impairment. Our data suggests a defective autophagosome formation in MJD fibroblasts and impaired clearance in MJD neurons (chapter 2 and 4). This result is particularly significant by revealing that primary cells can be used to screen compounds that affect the autophagy pathway by targeting its activation, correcting the verified phenotype and alleviating MJD phenotype (Nascimento-Ferreira et al., 2011).

Our data regarding the MJD genetic characterization of CAG repetition and SNPs revealed a conserved MJD genotype in both starting fibroblast populations and end neuronal population (chapters 2 and 4), which enables the study of perfect matched genotypes in different cell types/phenotypes and the use of the starting population as a good platform to validate gene editing therapies such as TALENs and CRISP/Cas9 (Boch et al., 2009; Cong et al., 2013) and its further application in human MJD neurons.

We used a lentiviral-mediated strategy to deliver of the 4 Yamanaka factors taking advantage of the high efficiency provided by this method in the generation of iPS cells. However insertional mutagenesis and transgene activation are associated drawbacks and together with mutations accumulated in the somatic cell prior to reprogramming (Gore et al., 2011; Young et al., 2012) are major contributors to the variability between the generated iPS cell lines, affecting the pluripotency and differentiation potential (Boulting et al., 2011). In order to avoid the risk of reactivation of oncogenic reprogramming factors we used a 4-in one polycistronic vector at the lowest MOI capable of inducing pluripotency, reducing the load of lentiviral integrations (Papapetrou et al., 2009; Warlich et al., 2011). Our strategy proved to be successful as all the iPS cell lines and derived neurons presented full silencing of the reprogramming transgenes (chapter 3 and 4). Also, all the iPS cell lines presented similar differentiation propensities as verified in *in vitro* and *in vivo* differentiation assays and overall, iPS cell lines generated from MJD patients or from healthy individuals were indistinguishable in all tests performed (chapter 3). The verification of the best practices (Hyun et al., 2008; Maherali and Hochedlinger, 2008) for establishment and evaluation of iPS cell lines allowed the elimination of atypical cell lines with discordant behavior that could confound disease modeling results.

Given the prolonged timeframe for functional maturation of human cells, which resembles the timing of normal human brain development, disorders with late onset, and age-related degeneration as MJD are more difficult to model than those with early developmental phenotypes. In spite of the extraordinary development of neuronal differentiation protocols the current differentiation strategies for hiPSCs yield differentiated cell types that most closely resemble embryonic or fetal stages of development and our ability to control the maturation state and age of resulting pluripotent-derived lineages remains incipient. Also, the heterogeneity in the state of functional maturation and the presence of neural progenitors in neuronal cultures represent a particular obstacle when neurons must be cultured for long periods of time to allow maturation of phenotypes, which warn for the careful assessment of the contribution of these cells ($Nestin^+$ population) in the final culture (chapter 4). The use of antimitotic agents can reduce the production of immature neurons by inhibiting progenitor cell proliferation but may have mild cytotoxic consequences (Miller et al., 2013). We used an alternative strategy to speed up the timing of neural cell-fate acquisition and maturation of neurons by combining the dSMADi (Chambers et al., 2009) and the the co-culture of neurons with astrocytes that proved to accelerate electrophysiological maturation of iPS cells-derived neurons (Bardy et al., 2015).

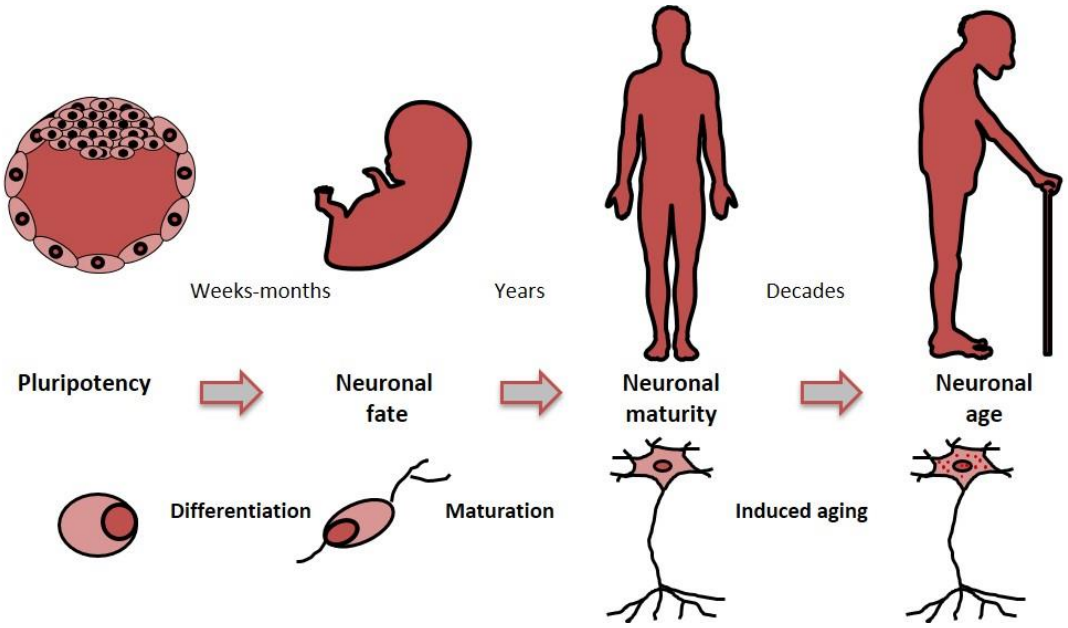

Figure 5.1-The cellular age in pluripotent-derived neurons.

The three stages of developmental timing: cell-fate specification, maturation and aging *in vivo* correlates with *in vitro* differentiation of iPS cells to neuronal lineages. MJD iPS cells-derived neurons represent immature neurons that are functional and whose maturation and aging is essential to study events that occur later in pathogenesis such as the formation and accumulation of large-scale protein inclusions.

However, there is no clear relation that can be made between time in culture and "age" of a neuronal type *in vivo* (Dong et al., 2014; Mattson and Magnus, 2006) and therefore it is difficult to predict the time to wait before a degenerative phenotype emerges. Neuronal dysfunction and death resulting from chronic cellular stress induced by misfolded or misprocecessed proteins are the most relevant phenotype to many neurodegenerative diseases (Matus et al., 2011; Wong and Cuervo, 2010a), as well for MJD but it is still a challenge to mimic in culture, maturation and age, as from a chronic perspective, cell specification, maturation and aging represent contiguous temporal ages for cells (Fig 5.1).

Despite the age mismatch, many studies have successfully modeled aspects of human neurodegenerative disease in the context of disease susceptibility rather than normal disease or disease progression. Modeling disease susceptibility can be very powerful for studying biochemical changes directly dependent on a genetic defect. In our model we took advantage of calcium dysregulation as a stressor, to try to reproduce environmental influences and age-related degeneration and to accelerate the MJD disease process, enabling the study in a shorter time frame (Cooper et al., 2012a; Jeon et al., 2012). With this approach we could verify the migration of ataxin-3 to the nucleus in MJD neurons as reported previously for other MJD models (Bichelmeier et al., 2007; Schmidt et al., 1998; Simoes et al., 2012). However to obtain conclusive results about the nature of the migrating fragment it is important to perform more studies in successive time-points to

evaluate phenotype and to further investigate the role of Ca^{2+} signaling in MJD pathogenesis (Chen et al., 2008a). Also remains to be investigated if those structures further evolve to ubiquitinated intranuclear inclusions contributing to cell death, revealing intrinsic differences between vulnerable and resistant neurons (Double et al., 2010; Paulson et al., 1997b; Yamada et al., 2001). The use of multiple neuronal subtypes derived from large cohorts of patient specific iPS cell lines can also contribute to reveal subtle variations in the identity of resistant and vulnerable neurons providing novel mechanistic insights.

Enthusiasm for the use of *in vitro* disease modeling has developed at rapid pace and recent works have shown the feasibility of creating functional three-dimensional (3D) cerebral organoids (Lancaster and Knoblich, 2014; Lancaster et al., 2013) using iPS cells-derived neurons, which could be of particular benefit in modelling diseases that involve multiple types of neurons as in MJD (Durr et al., 1996; Matsumura et al., 1996a; Paulson et al., 1997a). Because of their cellular and organizational complexity, organoid cultures may improve differentiation schemes by providing appropriate niche signaling and by mimicking different brain regions. So far cerebral organoids successfully modeled microencephaly (Lancaster et al., 2013) and more recently Alzheimer disease (Choi et al., 2014), opening the exciting opportunity to provide a more complex and complete *in vitro* system to study neurodegenerative diseases and be in the very verge of clinical translation…the final frontier!

In conclusion, our iPS cell derived neuronal model offers the opportunity to evaluate the early pathogenesis of MJD and is expected to further enlarge our understanding of the disease mechanism. Moreover, the observed MJD defects regarding translocation of ataxin-3 to the nucleus and autophagy impairment provide a valuable readout to the identification of effective therapies that are desperately needed.

References

References

Aasen, T., Raya, A., Barrero, M.J., Garreta, E., Consiglio, A., Gonzalez, F., Vassena, R., Bilic, J., Pekarik, V., Tiscornia, G.*, et al.* (2008). Efficient and rapid generation of induced pluripotent stem cells from human keratinocytes. Nat Biotechnol *26*, 1276-1284.

Agarwal, S., Loh, Y.H., McLoughlin, E.M., Huang, J., Park, I.H., Miller, J.D., Huo, H., Okuka, M., Dos Reis, R.M., Loewer, S.*, et al.* (2010). Telomere elongation in induced pluripotent stem cells from dyskeratosis congenita patients. Nature *464*, 292-296.

Albrecht, M., Golatta, M., Wullner, U., and Lengauer, T. (2004). Structural and functional analysis of ataxin-2 and ataxin-3. European journal of biochemistry / FEBS *271*, 3155-3170.

Albrecht, M., Hoffmann, D., Evert, B.O., Schmitt, I., Wullner, U., and Lengauer, T. (2003). Structural modeling of ataxin-3 reveals distant homology to adaptins. Proteins *50*, 355-370.

Almeida, S., Gascon, E., Tran, H., Chou, H.J., Gendron, T.F., Degroot, S., Tapper, A.R., Sellier, C., Charlet-Berguerand, N., Karydas, A.*, et al.* (2013). Modeling key pathological features of frontotemporal dementia with C9ORF72 repeat expansion in iPSC-derived human neurons. Acta Neuropathol *126*, 385-399.

Almeida, S., Zhang, Z., Coppola, G., Mao, W., Futai, K., Karydas, A., Geschwind, M.D., Tartaglia, M.C., Gao, F., Gianni, D.*, et al.* (2012). Induced pluripotent stem cell models of progranulin-deficient frontotemporal dementia uncover specific reversible neuronal defects. Cell Rep *2*, 789-798.

Altmann, C.R., and Brivanlou, A.H. (2001). Neural patterning in the vertebrate embryo. International review of cytology *203*, 447-482.

Alves, S., Nascimento-Ferreira, I., Auregan, G., Hassig, R., Dufour, N., Brouillet, E., Pedroso de Lima, M.C., Hantraye, P., Pereira de Almeida, L., and Deglon, N. (2008a). Allele-specific RNA silencing of mutant ataxin-3 mediates neuroprotection in a rat model of Machado-Joseph disease. PLoS One *3*, e3341.

Alves, S., Nascimento-Ferreira, I., Dufour, N., Hassig, R., Auregan, G., Nobrega, C., Brouillet, E., Hantraye, P., Pedroso de Lima, M.C., Deglon, N.*, et al.* (2010). Silencing ataxin-3 mitigates degeneration in a rat model of Machado-Joseph disease: no role for wild-type ataxin-3? Hum Mol Genet *19*, 2380-2394.

Alves, S., Regulier, E., Nascimento-Ferreira, I., Hassig, R., Dufour, N., Koeppen, A., Carvalho, A.L., Simoes, S., de Lima, M.C., Brouillet, E.*, et al.* (2008b). Striatal and nigral pathology in a lentiviral rat model of Machado-Joseph disease. Hum Mol Genet *17*, 2071-2083.

Amoroso, M.W., Croft, G.F., Williams, D.J., O'Keeffe, S., Carrasco, M.A., Davis, A.R., Roybon, L., Oakley, D.H., Maniatis, T., Henderson, C.E.*, et al.* (2013). Accelerated high-yield generation of limb-innervating motor neurons from human stem cells. J Neurosci *33*, 574-586.

An, M.C., Zhang, N., Scott, G., Montoro, D., Wittkop, T., Mooney, S., Melov, S., and Ellerby, L.M. (2012). Genetic correction of Huntington's disease phenotypes in induced pluripotent stem cells. Cell Stem Cell *11*, 253-263.

Anokye-Danso, F., Trivedi, C.M., Juhr, D., Gupta, M., Cui, Z., Tian, Y., Zhang, Y., Yang, W., Gruber, P.J., Epstein, J.A.*, et al.* (2011). Highly efficient miRNA-mediated reprogramming of mouse and human somatic cells to pluripotency. Cell Stem Cell *8*, 376-388.

Antonini, A., Leenders, K.L., Spiegel, R., Meier, D., Vontobel, P., Weigell-Weber, M., Sanchez-Pernaute, R., de Yebenez, J.G., Boesiger, P., Weindl, A.*, et al.* (1996). Striatal glucose

metabolism and dopamine D2 receptor binding in asymptomatic gene carriers and patients with Huntington's disease. Brain *119 (Pt 6)*, 2085-2095.

Antony, P.M., Mantele, S., Mollenkopf, P., Boy, J., Kehlenbach, R.H., Riess, O., and Schmidt, T. (2009). Identification and functional dissection of localization signals within ataxin-3. Neurobiol Dis *36*, 280-292.

Araujo, J., Breuer, P., Dieringer, S., Krauss, S., Dorn, S., Zimmermann, K., Pfeifer, A., Klockgether, T., Wuellner, U., and Evert, B.O. (2011). FOXO4-dependent upregulation of superoxide dismutase-2 in response to oxidative stress is impaired in spinocerebellar ataxia type 3. Hum Mol Genet *20*, 2928-2941.

Arrasate, M., Mitra, S., Schweitzer, E.S., Segal, M.R., and Finkbeiner, S. (2004). Inclusion body formation reduces levels of mutant huntingtin and the risk of neuronal death. Nature *431*, 805-810.

Aubry, L., Bugi, A., Lefort, N., Rousseau, F., Peschanski, M., and Perrier, A.L. (2008). Striatal progenitors derived from human ES cells mature into DARPP32 neurons in vitro and in quinolinic acid-lesioned rats. Proc Natl Acad Sci U S A *105*, 16707-16712.

Auburger, G., Klinkenberg, M., Drost, J., Marcus, K., Morales-Gordo, B., Kunz, W.S., Brandt, U., Broccoli, V., Reichmann, H., Gispert, S.*, et al.* (2012). Primary skin fibroblasts as a model of Parkinson's disease. Mol Neurobiol *46*, 20-27.

Baker, D.E., Harrison, N.J., Maltby, E., Smith, K., Moore, H.D., Shaw, P.J., Heath, P.R., Holden, H., and Andrews, P.W. (2007). Adaptation to culture of human embryonic stem cells and oncogenesis in vivo. Nat Biotechnol *25*, 207-215.

Ban, H., Nishishita, N., Fusaki, N., Tabata, T., Saeki, K., Shikamura, M., Takada, N., Inoue, M., Hasegawa, M., Kawamata, S.*, et al.* (2011). Efficient generation of transgene-free human induced pluripotent stem cells (iPSCs) by temperature-sensitive Sendai virus vectors. Proc Natl Acad Sci U S A *108*, 14234-14239.

Barbeau, A., Roy, M., Cunha, L., de Vincente, A.N., Rosenberg, R.N., Nyhan, W.L., MacLeod, P.L., Chazot, G., Langston, L.B., Dawson, D.M.*, et al.* (1984). The natural history of Machado-Joseph disease. An analysis of 138 personally examined cases. The Canadian journal of neurological sciences Le journal canadien des sciences neurologiques *11*, 510-525.

Bardy, C., van den Hurk, M., Eames, T., Marchand, C., Hernandez, R.V., Kellogg, M., Gorris, M., Galet, B., Palomares, V., Brown, J.*, et al.* (2015). Neuronal medium that supports basic synaptic functions and activity of human neurons in vitro. Proc Natl Acad Sci U S A *112*, E2725-2734.

Barreto-Chang, O.L., and Dolmetsch, R.E. (2009). Calcium imaging of cortical neurons using Fura-2 AM. J Vis Exp.

Bauer, P.O., Wong, H.K., Oyama, F., Goswami, A., Okuno, M., Kino, Y., Miyazaki, H., and Nukina, N. (2009). Inhibition of Rho kinases enhances the degradation of mutant huntingtin. J Biol Chem *284*, 13153-13164.

Bellin, M., Marchetto, M.C., Gage, F.H., and Mummery, C.L. (2012). Induced pluripotent stem cells: the new patient? Nat Rev Mol Cell Biol *13*, 713-726.

Belo, J.A., Bouwmeester, T., Leyns, L., Kertesz, N., Gallo, M., Follettie, M., and De Robertis, E.M. (1997). Cerberus-like is a secreted factor with neutralizing activity expressed in the anterior primitive endoderm of the mouse gastrula. Mechanisms of development *68*, 45-57.

Ben-David, U., and Benvenisty, N. (2011). The tumorigenicity of human embryonic and induced pluripotent stem cells. Nat Rev Cancer *11*, 268-277.

Ben-David, U., Benvenisty, N., and Mayshar, Y. (2010). Genetic instability in human induced pluripotent stem cells: Classification of causes and possible safeguards. Cell Cycle *9*, 4603-4604.

Berke, S.J., Schmied, F.A., Brunt, E.R., Ellerby, L.M., and Paulson, H.L. (2004). Caspase-mediated proteolysis of the polyglutamine disease protein ataxin-3. J Neurochem *89*, 908-918.

Bernemann, C., Greber, B., Ko, K., Sterneckert, J., Han, D.W., Arauzo-Bravo, M.J., and Scholer, H.R. (2011). Distinct developmental ground states of epiblast stem cell lines determine different pluripotency features. Stem Cells *29*, 1496-1503.

Berridge, M.J. (1998). Neuronal calcium signaling. Neuron *21*, 13-26.

Bettencourt, C., and Lima, M. (2011). Machado-Joseph Disease: from first descriptions to new perspectives. Orphanet J Rare Dis *6*, 35.

Bettencourt, C., Raposo, M., Ros, R., Montiel, R., Bruges-Armas, J., and Lima, M. (2013). Transcript diversity of Machado-Joseph disease gene (ATXN3) is not directly determined by SNPs in exonic or flanking intronic regions. J Mol Neurosci *49*, 539-543.

Bettencourt, C., Santos, C., Montiel, R., Costa Mdo, C., Cruz-Morales, P., Santos, L.R., Simoes, N., Kay, T., Vasconcelos, J., Maciel, P.*, et al.* (2010). Increased transcript diversity: novel splicing variants of Machado-Joseph disease gene (ATXN3). Neurogenetics *11*, 193-202.

Bevivino, A.E., and Loll, P.J. (2001). An expanded glutamine repeat destabilizes native ataxin-3 structure and mediates formation of parallel beta -fibrils. Proc Natl Acad Sci U S A *98*, 11955-11960.

Bezprozvanny, I. (2009). Calcium signaling and neurodegenerative diseases. Trends Mol Med *15*, 89-100.

Bezprozvanny, I. (2010). Inositol 1,4,5-tripshosphate receptor, calcium signaling, and polyglutamine expansion disorders. Current topics in membranes *66*, 323-341.

Bichelmeier, U., Schmidt, T., Hubener, J., Boy, J., Ruttiger, L., Habig, K., Poths, S., Bonin, M., Knipper, M., Schmidt, W.J.*, et al.* (2007). Nuclear localization of ataxin-3 is required for the manifestation of symptoms in SCA3: in vivo evidence. J Neurosci *27*, 7418-7428.

Bilican, B., Serio, A., Barmada, S.J., Nishimura, A.L., Sullivan, G.J., Carrasco, M., Phatnani, H.P., Puddifoot, C.A., Story, D., Fletcher, J.*, et al.* (2012). Mutant induced pluripotent stem cell lines recapitulate aspects of TDP-43 proteinopathies and reveal cell-specific vulnerability. Proc Natl Acad Sci U S A *109*, 5803-5808.

Bjorkoy, G., Lamark, T., Brech, A., Outzen, H., Perander, M., Overvatn, A., Stenmark, H., and Johansen, T. (2005). p62/SQSTM1 forms protein aggregates degraded by autophagy and has a protective effect on huntingtin-induced cell death. J Cell Biol *171*, 603-614.

Blum, B., and Benvenisty, N. (2009). The tumorigenicity of diploid and aneuploid human pluripotent stem cells. Cell Cycle *8*, 3822-3830.

Blumberg, B., Bolado, J., Jr., Moreno, T.A., Kintner, C., Evans, R.M., and Papalopulu, N. (1997). An essential role for retinoid signaling in anteroposterior neural patterning. Development *124*, 373-379.

Boch, J., Scholze, H., Schornack, S., Landgraf, A., Hahn, S., Kay, S., Lahaye, T., Nickstadt, A., and Bonas, U. (2009). Breaking the code of DNA binding specificity of TAL-type III effectors. Science *326*, 1509-1512.

Bock, C., Kiskinis, E., Verstappen, G., Gu, H., Boulting, G., Smith, Z.D., Ziller, M., Croft, G.F., Amoroso, M.W., Oakley, D.H.*, et al.* (2011). Reference Maps of human ES and iPS cell variation enable high-throughput characterization of pluripotent cell lines. Cell *144*, 439-452.

Boggaram, V. (2009). Thyroid transcription factor-1 (TTF-1/Nkx2.1/TITF1) gene regulation in the lung. Clinical science *116*, 27-35.

Boulting, G.L., Kiskinis, E., Croft, G.F., Amoroso, M.W., Oakley, D.H., Wainger, B.J., Williams, D.J., Kahler, D.J., Yamaki, M., Davidow, L.*, et al.* (2011). A functionally characterized test set of human induced pluripotent stem cells. Nat Biotechnol *29*, 279-286.

Boy, J., Schmidt, T., Wolburg, H., Mack, A., Nuber, S., Bottcher, M., Schmitt, I., Holzmann, C., Zimmermann, F., Servadio, A.*, et al.* (2009). Reversibility of symptoms in a conditional mouse model of spinocerebellar ataxia type 3. Hum Mol Genet *18*, 4282-4295.

Boyer, L.A., Lee, T.I., Cole, M.F., Johnstone, S.E., Levine, S.S., Zucker, J.P., Guenther, M.G., Kumar, R.M., Murray, H.L., Jenner, R.G.*, et al.* (2005). Core transcriptional regulatory circuitry in human embryonic stem cells. Cell *122*, 947-956.

Brambrink, T., Foreman, R., Welstead, G.G., Lengner, C.J., Wernig, M., Suh, H., and Jaenisch, R. (2008). Sequential expression of pluripotency markers during direct reprogramming of mouse somatic cells. Cell Stem Cell *2*, 151-159.

Breuer, P., Haacke, A., Evert, B.O., and Wullner, U. (2010). Nuclear aggregation of polyglutamine-expanded ataxin-3: fragments escape the cytoplasmic quality control. J Biol Chem *285*, 6532-6537.

Briggs, R., and King, T.J. (1952). Transplantation of Living Nuclei From Blastula Cells into Enucleated Frogs' Eggs. Proc Natl Acad Sci U S A *38*, 455-463.

Brouillet, E., Hantraye, P., Ferrante, R.J., Dolan, R., Leroy-Willig, A., Kowall, N.W., and Beal, M.F. (1995). Chronic mitochondrial energy impairment produces selective striatal degeneration and abnormal choreiform movements in primates. Proc Natl Acad Sci U S A *92*, 7105-7109.

Buhmann, C., Bussopulos, A., and Oechsner, M. (2003). Dopaminergic response in Parkinsonian phenotype of Machado-Joseph disease. Movement disorders : official journal of the Movement Disorder Society *18*, 219-221.

Burkhardt, M.F., Martinez, F.J., Wright, S., Ramos, C., Volfson, D., Mason, M., Garnes, J., Dang, V., Lievers, J., Shoukat-Mumtaz, U.*, et al.* (2013). A cellular model for sporadic ALS using patient-derived induced pluripotent stem cells. Molecular and cellular neurosciences *56*, 355-364.

Burnett, B., Li, F., and Pittman, R.N. (2003). The polyglutamine neurodegenerative protein ataxin-3 binds polyubiquitylated proteins and has ubiquitin protease activity. Hum Mol Genet *12*, 3195-3205.

Burnett, B.G., and Pittman, R.N. (2005). The polyglutamine neurodegenerative protein ataxin 3 regulates aggresome formation. Proc Natl Acad Sci U S A *102*, 4330-4335.

Byers, B., Cord, B., Nguyen, H.N., Schule, B., Fenno, L., Lee, P.C., Deisseroth, K., Langston, J.W., Pera, R.R., and Palmer, T.D. (2011). SNCA triplication Parkinson's patient's iPSC-derived DA neurons accumulate alpha-synuclein and are susceptible to oxidative stress. PLoS One *6*, e26159.

Caballero, B., and Coto-Montes, A. (2012). An insight into the role of autophagy in cell responses in the aging and neurodegenerative brain. Histology and histopathology *27*, 263-275.

Camnasio, S., Delli Carri, A., Lombardo, A., Grad, I., Mariotti, C., Castucci, A., Rozell, B., Lo Riso, P., Castiglioni, V., Zuccato, C*., et al.* (2012). The first reported generation of several induced pluripotent stem cell lines from homozygous and heterozygous Huntington's disease patients demonstrates mutation related enhanced lysosomal activity. Neurobiol Dis *46*, 41-51.

Campisi, J. (2001). From cells to organisms: can we learn about aging from cells in culture? Experimental Gerontology *36*, 607-618.

Camus, A., Perea-Gomez, A., Moreau, A., and Collignon, J. (2006). Absence of Nodal signaling promotes precocious neural differentiation in the mouse embryo. Dev Biol *295*, 743-755.

Carey, B.W., Markoulaki, S., Hanna, J., Saha, K., Gao, Q., Mitalipova, M., and Jaenisch, R. (2009). Reprogramming of murine and human somatic cells using a single polycistronic vector. Proc Natl Acad Sci U S A *106*, 157-162.

Caviston, J.P., Ross, J.L., Antony, S.M., Tokito, M., and Holzbaur, E.L. (2007). Huntingtin facilitates dynein/dynactin-mediated vesicle transport. Proc Natl Acad Sci U S A *104*, 10045-10050.

Chai, Y., Berke, S.S., Cohen, R.E., and Paulson, H.L. (2004). Poly-ubiquitin binding by the polyglutamine disease protein ataxin-3 links its normal function to protein surveillance pathways. J Biol Chem *279*, 3605-3611.

Chai, Y., Koppenhafer, S.L., Shoesmith, S.J., Perez, M.K., and Paulson, H.L. (1999). Evidence for proteasome involvement in polyglutamine disease: localization to nuclear inclusions in SCA3/MJD and suppression of polyglutamine aggregation in vitro. Hum Mol Genet *8*, 673-682.

Chai, Y., Shao, J., Miller, V.M., Williams, A., and Paulson, H.L. (2002). Live-cell imaging reveals divergent intracellular dynamics of polyglutamine disease proteins and supports a sequestration model of pathogenesis. Proc Natl Acad Sci U S A *99*, 9310-9315.

Chambers, I., Colby, D., Robertson, M., Nichols, J., Lee, S., Tweedie, S., and Smith, A. (2003). Functional expression cloning of Nanog, a pluripotency sustaining factor in embryonic stem cells. Cell *113*, 643-655.

Chambers, I., and Smith, A. (2004). Self-renewal of teratocarcinoma and embryonic stem cells. Oncogene *23*, 7150-7160.

Chambers, S.M., Fasano, C.A., Papapetrou, E.P., Tomishima, M., Sadelain, M., and Studer, L. (2009). Highly efficient neural conversion of human ES and iPS cells by dual inhibition of SMAD signaling. Nat Biotechnol *27*, 275-280.

Chambers, S.M., Mica, Y., Studer, L., and Tomishima, M.J. (2011). Converting human pluripotent stem cells to neural tissue and neurons to model neurodegeneration. Methods in molecular biology *793*, 87-97.

Chambers, S.M., Qi, Y., Mica, Y., Lee, G., Zhang, X.J., Niu, L., Bilsland, J., Cao, L., Stevens, E., Whiting, P*., et al.* (2012). Combined small-molecule inhibition accelerates developmental timing and converts human pluripotent stem cells into nociceptors. Nat Biotechnol *30*, 715-720.

Chan, E.M., Ratanasirintrawoot, S., Park, I.H., Manos, P.D., Loh, Y.H., Huo, H., Miller, J.D., Hartung, O., Rho, J., Ince, T.A*., et al.* (2009). Live cell imaging distinguishes bona fide human iPS cells from partially reprogrammed cells. Nat Biotechnol *27*, 1033-1037.

Chang, W.H., Tien, C.L., Chen, T.J., Nukina, N., and Hsieh, M. (2009). Decreased protein synthesis of Hsp27 associated with cellular toxicity in a cell model of Machado-Joseph disease. Neurosci Lett *454*, 152-156.

Chen, H., Li, Y., and Tollefsbol, T.O. (2013). Cell senescence culturing methods. Methods in molecular biology *1048*, 1-10.

Chen, H., Qian, K., Du, Z., Cao, J., Petersen, A., Liu, H., Blackbourn, L.W.t., Huang, C.L., Errigo, A., Yin, Y.*, et al.* (2014). Modeling ALS with iPSCs reveals that mutant SOD1 misregulates neurofilament balance in motor neurons. Cell Stem Cell *14*, 796-809.

Chen, S., Berthelier, V., Yang, W., and Wetzel, R. (2001). Polyglutamine aggregation behavior in vitro supports a recruitment mechanism of cytotoxicity. J Mol Biol *311*, 173-182.

Chen, X., Tang, T.S., Tu, H., Nelson, O., Pook, M., Hammer, R., Nukina, N., and Bezprozvanny, I. (2008a). Deranged calcium signaling and neurodegeneration in spinocerebellar ataxia type 3. J Neurosci *28*, 12713-12724.

Chen, X., Xu, H., Yuan, P., Fang, F., Huss, M., Vega, V.B., Wong, E., Orlov, Y.L., Zhang, W., Jiang, J.*, et al.* (2008b). Integration of external signaling pathways with the core transcriptional network in embryonic stem cells. Cell *133*, 1106-1117.

Chinnasamy, D., Milsom, M.D., Shaffer, J., Neuenfeldt, J., Shaaban, A.F., Margison, G.P., Fairbairn, L.J., and Chinnasamy, N. (2006). Multicistronic lentiviral vectors containing the FMDV 2A cleavage factor demonstrate robust expression of encoded genes at limiting MOI. Virol J *3*, 14.

Cho, H.J., Lee, C.S., Kwon, Y.W., Paek, J.S., Lee, S.H., Hur, J., Lee, E.J., Roh, T.Y., Chu, I.S., Leem, S.H.*, et al.* (2010). Induction of pluripotent stem cells from adult somatic cells by protein-based reprogramming without genetic manipulation. Blood *116*, 386-395.

Choi, S.H., Kim, Y.H., Hebisch, M., Sliwinski, C., Lee, S., D'Avanzo, C., Chen, H., Hooli, B., Asselin, C., Muffat, J.*, et al.* (2014). A three-dimensional human neural cell culture model of Alzheimer's disease. Nature *515*, 274-278.

Chou, A.H., Chen, S.Y., Yeh, T.H., Weng, Y.H., and Wang, H.L. (2011). HDAC inhibitor sodium butyrate reverses transcriptional downregulation and ameliorates ataxic symptoms in a transgenic mouse model of SCA3. Neurobiol Dis *41*, 481-488.

Chou, A.H., Yeh, T.H., Ouyang, P., Chen, Y.L., Chen, S.Y., and Wang, H.L. (2008). Polyglutamine-expanded ataxin-3 causes cerebellar dysfunction of SCA3 transgenic mice by inducing transcriptional dysregulation. Neurobiol Dis *31*, 89-101.

Christopherson, K.S., Ullian, E.M., Stokes, C.C., Mullowney, C.E., Hell, J.W., Agah, A., Lawler, J., Mosher, D.F., Bornstein, P., and Barres, B.A. (2005). Thrombospondins are astrocyte-secreted proteins that promote CNS synaptogenesis. Cell *120*, 421-433.

Ciechanover, A., and Brundin, P. (2003). The ubiquitin proteasome system in neurodegenerative diseases: sometimes the chicken, sometimes the egg. Neuron *40*, 427-446.

Clowry, G., Molnar, Z., and Rakic, P. (2010). Renewed focus on the developing human neocortex. J Anat *217*, 276-288.

Cong, L., Ran, F.A., Cox, D., Lin, S., Barretto, R., Habib, N., Hsu, P.D., Wu, X., Jiang, W., Marraffini, L.A.*, et al.* (2013). Multiplex genome engineering using CRISPR/Cas systems. Science *339*, 819-823.

Connolly, G.P. (1998). Fibroblast models of neurological disorders: fluorescence measurement studies. Trends Pharmacol Sci *19*, 171-177.

Consortium, H.D.i. (2012). Induced pluripotent stem cells from patients with Huntington's disease show CAG-repeat-expansion-associated phenotypes. Cell Stem Cell *11*, 264-278.

Cooper, O., Hallett, P., and Isacson, O. (2012a). Using stem cells and iPS cells to discover new treatments for Parkinson's disease. Parkinsonism & Related Disorders *18*, S14-S16.

Cooper, O., Seo, H., Andrabi, S., Guardia-Laguarta, C., Graziotto, J., Sundberg, M., McLean, J.R., Carrillo-Reid, L., Xie, Z., Osborn, T.*, et al.* (2012b). Pharmacological rescue of mitochondrial deficits in iPSC-derived neural cells from patients with familial Parkinson's disease. Sci Transl Med *4*, 141ra190.

Corti, S., Nizzardo, M., Simone, C., Falcone, M., Nardini, M., Ronchi, D., Donadoni, C., Salani, S., Riboldi, G., Magri, F.*, et al.* (2012). Genetic correction of human induced pluripotent stem cells from patients with spinal muscular atrophy. Sci Transl Med *4*, 165ra162.

Costa, M.C., Gomes-da-Silva, J., Miranda, C.J., Sequeiros, J., Santos, M.M., and Maciel, P. (2004). Genomic structure, promoter activity, and developmental expression of the mouse homologue of the Machado-Joseph disease (MJD) gene. Genomics *84*, 361-373.

Costa Mdo, C., and Paulson, H.L. (2012). Toward understanding Machado-Joseph disease. Prog Neurobiol *97*, 239-257.

Coutinho, P., and Andrade, C. (1978). Autosomal dominant system degeneration in Portuguese families of the Azores Islands. A new genetic disorder involving cerebellar, pyramidal, extrapyramidal and spinal cord motor functions. Neurology *28*, 703-709.

Coutinho, P., and Sequeiros, J. (1981). [Clinical, genetic and pathological aspects of Machado-Joseph disease]. Journal de genetique humaine *29*, 203-209.

Cunningham, J.J., Ulbright, T.M., Pera, M.F., and Looijenga, L.H. (2012). Lessons from human teratomas to guide development of safe stem cell therapies. Nat Biotechnol *30*, 849-857.

D'Abreu, A., Franca, M.C., Jr., Paulson, H.L., and Lopes-Cendes, I. (2010). Caring for Machado-Joseph disease: current understanding and how to help patients. Parkinsonism Relat Disord *16*, 2-7.

Daley, G.Q., Lensch, M.W., Jaenisch, R., Meissner, A., Plath, K., and Yamanaka, S. (2009). Broader implications of defining standards for the pluripotency of iPSCs. Cell Stem Cell *4*, 200-201; author reply 202.

David, G., Abbas, N., Stevanin, G., Durr, A., Yvert, G., Cancel, G., Weber, C., Imbert, G., Saudou, F., Antoniou, E.*, et al.* (1997). Cloning of the SCA7 gene reveals a highly unstable CAG repeat expansion. Nat Genet *17*, 65-70.

de Almeida, L.P., Zala, D., Aebischer, P., and Deglon, N. (2001). Neuroprotective effect of a CNTF-expressing lentiviral vector in the quinolinic acid rat model of Huntington's disease. Neurobiol Dis *8*, 433-446.

De Melo Reis, R.A., Schitine, C.S., Kofalvi, A., Grade, S., Cortes, L., Gardino, P.F., Malva, J.O., and de Mello, F.G. (2011). Functional identification of cell phenotypes differentiating from mice retinal neurospheres using single cell calcium imaging. Cell Mol Neurobiol *31*, 835-846.

Delli Carri, A., Onorati, M., Castiglioni, V., Faedo, A., Camnasio, S., Toselli, M., Biella, G., and Cattaneo, E. (2013a). Human pluripotent stem cell differentiation into authentic striatal projection neurons. Stem Cell Rev *9*, 461-474.

Delli Carri, A., Onorati, M., Lelos, M.J., Castiglioni, V., Faedo, A., Menon, R., Camnasio, S., Vuono, R., Spaiardi, P., Talpo, F.*, et al.* (2013b). Developmentally coordinated extrinsic signals drive human pluripotent stem cell differentiation toward authentic DARPP-32+ medium-sized spiny neurons. Development *140*, 301-312.

Desponts, C., and Ding, S. (2010). Using small molecules to improve generation of induced pluripotent stem cells from somatic cells. Methods in molecular biology *636*, 207-218.

Devine, M.J., Ryten, M., Vodicka, P., Thomson, A.J., Burdon, T., Houlden, H., Cavaleri, F., Nagano, M., Drummond, N.J., Taanman, J.W.*, et al.* (2011). Parkinson's disease induced pluripotent stem cells with triplication of the alpha-synuclein locus. Nat Commun *2*, 440.

Diez del Corral, R., Olivera-Martinez, I., Goriely, A., Gale, E., Maden, M., and Storey, K. (2003). Opposing FGF and retinoid pathways control ventral neural pattern, neuronal differentiation, and segmentation during body axis extension. Neuron *40*, 65-79.

DiFiglia, M., Sapp, E., Chase, K.O., Davies, S.W., Bates, G.P., Vonsattel, J.P., and Aronin, N. (1997). Aggregation of huntingtin in neuronal intranuclear inclusions and dystrophic neurites in brain. Science *277*, 1990-1993.

Dimos, J.T., Rodolfa, K.T., Niakan, K.K., Weisenthal, L.M., Mitsumoto, H., Chung, W., Croft, G.F., Saphier, G., Leibel, R., Goland, R.*, et al.* (2008). Induced pluripotent stem cells generated from patients with ALS can be differentiated into motor neurons. Science *321*, 1218-1221.

do Carmo Costa, M., Bajanca, F., Rodrigues, A.J., Tome, R.J., Corthals, G., Macedo-Ribeiro, S., Paulson, H.L., Logarinho, E., and Maciel, P. (2010). Ataxin-3 plays a role in mouse myogenic differentiation through regulation of integrin subunit levels. PLoS One *5*, e11728.

Dolgin, E. (2010). Putting stem cells to the test. Nat Med *16*, 1354-1357.

Dolmetsch, R., and Geschwind, D.H. (2011). The human brain in a dish: the promise of iPSC-derived neurons. Cell *145*, 831-834.

Donaldson, K.M., Li, W., Ching, K.A., Batalov, S., Tsai, C.C., and Joazeiro, C.A. (2003). Ubiquitin-mediated sequestration of normal cellular proteins into polyglutamine aggregates. Proc Natl Acad Sci U S A *100*, 8892-8897.

Donato, R., Cannon, B.R., Sorci, G., Riuzzi, F., Hsu, K., Weber, D.J., and Geczy, C.L. (2013). Functions of S100 proteins. Curr Mol Med *13*, 24-57.

Dong, C.M., Wang, X.L., Wang, G.M., Zhang, W.J., Zhu, L., Gao, S., Yang, D.J., Qin, Y., Liang, Q.J., Chen, Y.L.*, et al.* (2014). A stress-induced cellular aging model with postnatal neural stem cells. Cell Death Dis *5*, e1116.

Donnelly, C.J., Zhang, P.W., Pham, J.T., Haeusler, A.R., Mistry, N.A., Vidensky, S., Daley, E.L., Poth, E.M., Hoover, B., Fines, D.M.*, et al.* (2013). RNA toxicity from the ALS/FTD C9ORF72 expansion is mitigated by antisense intervention. Neuron *80*, 415-428.

Doss-Pepe, E.W., Stenroos, E.S., Johnson, W.G., and Madura, K. (2003). Ataxin-3 interactions with rad23 and valosin-containing protein and its associations with ubiquitin chains and the proteasome are consistent with a role in ubiquitin-mediated proteolysis. Mol Cell Biol *23*, 6469-6483.

Double, K.L., Reyes, S., Werry, E.L., and Halliday, G.M. (2010). Selective cell death in neurodegeneration: why are some neurons spared in vulnerable regions? Prog Neurobiol *92*, 316-329.

Draper, J.S., Smith, K., Gokhale, P., Moore, H.D., Maltby, E., Johnson, J., Meisner, L., Zwaka, T.P., Thomson, J.A., and Andrews, P.W. (2004). Recurrent gain of chromosomes 17q and 12 in cultured human embryonic stem cells. Nat Biotechnol *22*, 53-54.

Driesch, H. (1891). Entwicklungsmechanische Studien: I. Der Werth der beiden ersten Furchungszellen in der Echinodermenentwicklung. Z wiss Zool *53*, 160-178.

Durr, A., Stevanin, G., Cancel, G., Duyckaerts, C., Abbas, N., Didierjean, O., Chneiweiss, H., Benomar, A., Lyon-Caen, O., Julien, J.*, et al.* (1996). Spinocerebellar ataxia 3 and Machado-Joseph disease: clinical, molecular, and neuropathological features. Ann Neurol *39*, 490-499.

Ebert, A.D., and Svendsen, C.N. (2010). Human stem cells and drug screening: opportunities and challenges. Nat Rev Drug Discov *9*, 367-372.

Ebert, A.D., Yu, J., Rose, F.F., Jr., Mattis, V.B., Lorson, C.L., Thomson, J.A., and Svendsen, C.N. (2009). Induced pluripotent stem cells from a spinal muscular atrophy patient. Nature *457*, 277-280.

Egawa, N., Kitaoka, S., Tsukita, K., Naitoh, M., Takahashi, K., Yamamoto, T., Adachi, F., Kondo, T., Okita, K., Asaka, I.*, et al.* (2012). Drug screening for ALS using patient-specific induced pluripotent stem cells. Sci Transl Med *4*, 145ra104.

Ellisdon, A.M., Thomas, B., and Bottomley, S.P. (2006). The two-stage pathway of ataxin-3 fibrillogenesis involves a polyglutamine-independent step. J Biol Chem *281*, 16888-16896.

Emerit, J., Edeas, M., and Bricaire, F. (2004). Neurodegenerative diseases and oxidative stress. Biomedicine & pharmacotherapy = Biomedecine & pharmacotherapie *58*, 39-46.

Erceg, S., Lukovic, D., Moreno-Manzano, V., Stojkovic, M., and Bhattacharya, S.S. (2012). Derivation of cerebellar neurons from human pluripotent stem cells. Curr Protoc Stem Cell Biol *Chapter 1*, Unit 1H 5.

Erceg, S., Ronaghi, M., Zipancic, I., Lainez, S., Rosello, M.G., Xiong, C., Moreno-Manzano, V., Rodriguez-Jimenez, F.J., Planells, R., Alvarez-Dolado, M.*, et al.* (2010). Efficient differentiation of human embryonic stem cells into functional cerebellar-like cells. Stem Cells Dev *19*, 1745-1756.

Eriksson, P.S., Perfilieva, E., Bjork-Eriksson, T., Alborn, A.M., Nordborg, C., Peterson, D.A., and Gage, F.H. (1998). Neurogenesis in the adult human hippocampus. Nat Med *4*, 1313-1317.

Espuny-Camacho, I., Michelsen, K.A., Gall, D., Linaro, D., Hasche, A., Bonnefont, J., Bali, C., Orduz, D., Bilheu, A., Herpoel, A.*, et al.* (2013). Pyramidal neurons derived from human pluripotent stem cells integrate efficiently into mouse brain circuits in vivo. Neuron *77*, 440-456.

Esteban, M.A., Wang, T., Qin, B., Yang, J., Qin, D., Cai, J., Li, W., Weng, Z., Chen, J., Ni, S.*, et al.* (2010). Vitamin C enhances the generation of mouse and human induced pluripotent stem cells. Cell Stem Cell *6*, 71-79.

Evans, M.J., and Kaufman, M.H. (1981). Establishment in culture of pluripotential cells from mouse embryos. Nature *292*, 154-156.

Evers, M.M., Toonen, L.J., and van Roon-Mom, W.M. (2014). Ataxin-3 protein and RNA toxicity in spinocerebellar ataxia type 3: current insights and emerging therapeutic strategies. Mol Neurobiol *49*, 1513-1531.

Evert, B.O., Araujo, J., Vieira-Saecker, A.M., de Vos, R.A., Harendza, S., Klockgether, T., and Wullner, U. (2006). Ataxin-3 represses transcription via chromatin binding, interaction with histone deacetylase 3, and histone deacetylation. J Neurosci *26*, 11474-11486.

Evert, B.O., Vogt, I.R., Kindermann, C., Ozimek, L., de Vos, R.A., Brunt, E.R., Schmitt, I., Klockgether, T., and Wullner, U. (2001). Inflammatory genes are upregulated in expanded ataxin-3-expressing cell lines and spinocerebellar ataxia type 3 brains. J Neurosci *21*, 5389-5396.

Evert, B.O., Vogt, I.R., Vieira-Saecker, A.M., Ozimek, L., de Vos, R.A., Brunt, E.R., Klockgether, T., and Wullner, U. (2003). Gene expression profiling in ataxin-3 expressing cell lines reveals distinct effects of normal and mutant ataxin-3. J Neuropathol Exp Neurol *62*, 1006-1018.

Falk, A., Koch, P., Kesavan, J., Takashima, Y., Ladewig, J., Alexander, M., Wiskow, O., Tailor, J., Trotter, M., Pollard, S.*, et al.* (2012). Capture of neuroepithelial-like stem cells from pluripotent stem cells provides a versatile system for in vitro production of human neurons. PLoS One *7*, e29597.

Federation, A.J., Bradner, J.E., and Meissner, A. (2014). The use of small molecules in somatic-cell reprogramming. Trends Cell Biol *24*, 179-187.

Feng, B., Ng, J.H., Heng, J.C., and Ng, H.H. (2009). Molecules that promote or enhance reprogramming of somatic cells to induced pluripotent stem cells. Cell Stem Cell *4*, 301-312.

Franca, M.C., Jr., D'Abreu, A., Nucci, A., and Lopes-Cendes, I. (2008). Muscle excitability abnormalities in Machado-Joseph disease. Arch Neurol *65*, 525-529.

Freeman, W., and Wszolek, Z. (2005). Botulinum toxin type A for treatment of spasticity in spinocerebellar ataxia type 3 (Machado-Joseph disease). Movement disorders : official journal of the Movement Disorder Society *20*, 644.

Fuchs, E., and Weber, K. (1994). Intermediate filaments: structure, dynamics, function, and disease. Annu Rev Biochem *63*, 345-382.

Fujigasaki, H., Uchihara, T., Koyano, S., Iwabuchi, K., Yagishita, S., Makifuchi, T., Nakamura, A., Ishida, K., Toru, S., Hirai, S.*, et al.* (2000). Ataxin-3 is translocated into the nucleus for the formation of intranuclear inclusions in normal and Machado-Joseph disease brains. Exp Neurol *165*, 248-256.

Fujikake, N., Nagai, Y., Popiel, H.A., Okamoto, Y., Yamaguchi, M., and Toda, T. (2008). Heat shock transcription factor 1-activating compounds suppress polyglutamine-induced neurodegeneration through induction of multiple molecular chaperones. J Biol Chem *283*, 26188-26197.

Fusaki, N., Ban, H., Nishiyama, A., Saeki, K., and Hasegawa, M. (2009). Efficient induction of transgene-free human pluripotent stem cells using a vector based on Sendai virus, an RNA virus that does not integrate into the host genome. Proceedings of the Japan Academy, Series B *85*, 348-362.

Gage, F.H., and Temple, S. (2013). Neural stem cells: generating and regenerating the brain. Neuron *80*, 588-601.

Gaspar, C., Lopes-Cendes, I., DeStefano, A.L., Maciel, P., Silveira, I., Coutinho, P., MacLeod, P., Sequeiros, J., Farrer, L.A., and Rouleau, G.A. (1996). Linkage disequilibrium analysis in Machado-Joseph disease patients of different ethnic origins. Hum Genet *98*, 620-624.

Gaspar, C., Lopes-Cendes, I., Hayes, S., Goto, J., Arvidsson, K., Dias, A., Silveira, I., Maciel, P., Coutinho, P., Lima, M.*, et al.* (2001). Ancestral origins of the Machado-Joseph disease mutation: a worldwide haplotype study. Am J Hum Genet *68*, 523-528.

Gaspard, N., Bouschet, T., Hourez, R., Dimidschstein, J., Naeije, G., van den Ameele, J., Espuny-Camacho, I., Herpoel, A., Passante, L., Schiffmann, S.N.*, et al.* (2008). An intrinsic mechanism of corticogenesis from embryonic stem cells. Nature *455*, 351-357.

Gatchel, J.R., and Zoghbi, H.Y. (2005). Diseases of unstable repeat expansion: mechanisms and common principles. Nature reviews Genetics *6*, 743-755.

Gearhart, J. (1998). New potential for human embryonic stem cells. Science *282*, 1061-1062.

Geraerts, M., Willems, S., Baekelandt, V., Debyser, Z., and Gijsbers, R. (2006). Comparison of lentiviral vector titration methods. BMC Biotechnol *6*, 34.

Giorgetti, A., Montserrat, N., Aasen, T., Gonzalez, F., Rodriguez-Piza, I., Vassena, R., Raya, A., Boue, S., Barrero, M.J., Corbella, B.A.*, et al.* (2009). Generation of induced pluripotent stem cells from human cord blood using OCT4 and SOX2. Cell Stem Cell *5*, 353-357.

Giudice, A., and Trounson, A. (2008). Genetic modification of human embryonic stem cells for derivation of target cells. Cell Stem Cell *2*, 422-433.

Goncalves, N., Simoes, A.T., Cunha, R.A., and de Almeida, L.P. (2013). Caffeine and adenosine A(2A) receptor inactivation decrease striatal neuropathology in a lentiviral-based model of Machado-Joseph disease. Ann Neurol *73*, 655-666.

Gore, A., Li, Z., Fung, H.L., Young, J.E., Agarwal, S., Antosiewicz-Bourget, J., Canto, I., Giorgetti, A., Israel, M.A., Kiskinis, E.*, et al.* (2011). Somatic coding mutations in human induced pluripotent stem cells. Nature *471*, 63-67.

Goti, D., Katzen, S.M., Mez, J., Kurtis, N., Kiluk, J., Ben-Haiem, L., Jenkins, N.A., Copeland, N.G., Kakizuka, A., Sharp, A.H.*, et al.* (2004). A mutant ataxin-3 putative-cleavage fragment in brains of Machado-Joseph disease patients and transgenic mice is cytotoxic above a critical concentration. J Neurosci *24*, 10266-10279.

Goto, J., Watanabe, M., Ichikawa, Y., Yee, S.B., Ihara, N., Endo, K., Igarashi, S., Takiyama, Y., Gaspar, C., Maciel, P.*, et al.* (1997). Machado-Joseph disease gene products carrying different carboxyl termini. Neuroscience research *28*, 373-377.

Goulburn, A.L., Stanley, E.G., Elefanty, A.G., and Anderson, S.A. (2012). Generating GABAergic cerebral cortical interneurons from mouse and human embryonic stem cells. Stem Cell Res *8*, 416-426.

Grade, S., Bernardino, L., and Malva, J.O. (2013). Oligodendrogenesis from neural stem cells: perspectives for remyelinating strategies. Int J Dev Neurosci *31*, 692-700.

Grienberger, C., and Konnerth, A. (2012). Imaging calcium in neurons. Neuron *73*, 862-885.

Gropp, M., Shilo, V., Vainer, G., Gov, M., Gil, Y., Khaner, H., Matzrafi, L., Idelson, M., Kopolovic, J., Zak, N.B.*, et al.* (2012). Standardization of the teratoma assay for analysis of pluripotency of human ES cells and biosafety of their differentiated progeny. PLoS One *7*, e45532.

Grskovic, M., Javaherian, A., Strulovici, B., and Daley, G.Q. (2011). Induced pluripotent stem cells--opportunities for disease modelling and drug discovery. Nat Rev Drug Discov *10*, 915-929.

Grunewald, A., Voges, L., Rakovic, A., Kasten, M., Vandebona, H., Hemmelmann, C., Lohmann, K., Orolicki, S., Ramirez, A., Schapira, A.H.*, et al.* (2010). Mutant Parkin impairs mitochondrial function and morphology in human fibroblasts. PLoS One *5*, e12962.

Grunseich, C., Zukosky, K., Kats, I.R., Ghosh, L., Harmison, G.G., Bott, L.C., Rinaldi, C., Chen, K.L., Chen, G., Boehm, M.*, et al.* (2014). Stem cell-derived motor neurons from spinal and bulbar muscular atrophy patients. Neurobiol Dis *70*, 12-20.

Gunawardena, S., Her, L.S., Brusch, R.G., Laymon, R.A., Niesman, I.R., Gordesky-Gold, B., Sintasath, L., Bonini, N.M., and Goldstein, L.S. (2003). Disruption of axonal transport by loss of huntingtin or expression of pathogenic polyQ proteins in Drosophila. Neuron *40*, 25-40.

Gupta, K., Hardingham, G.E., and Chandran, S. (2013). NMDA receptor-dependent glutamate excitotoxicity in human embryonic stem cell-derived neurons. Neurosci Lett *543*, 95-100.

Gurdon, J.B. (1962). The developmental capacity of nuclei taken from intestinal epithelium cells of feeding tadpoles. J Embryol Exp Morphol *10*, 622-640.

Gurdon, J.B., Elsdale, T.R., and Fischberg, M. (1958). Sexually mature individuals of Xenopus laevis from the transplantation of single somatic nuclei. Nature *182*, 64-65.

Haacke, A., Broadley, S.A., Boteva, R., Tzvetkov, N., Hartl, F.U., and Breuer, P. (2006). Proteolytic cleavage of polyglutamine-expanded ataxin-3 is critical for aggregation and sequestration of non-expanded ataxin-3. Hum Mol Genet *15*, 555-568.

Haacke, A., Hartl, F.U., and Breuer, P. (2007). Calpain inhibition is sufficient to suppress aggregation of polyglutamine-expanded ataxin-3. J Biol Chem *282*, 18851-18856.

Hackam, D.G., and Redelmeier, D.A. (2006). Translation of research evidence from animals to humans. Jama *296*, 1731-1732.

Han, S.S., Williams, L.A., and Eggan, K.C. (2011). Constructing and deconstructing stem cell models of neurological disease. Neuron *70*, 626-644.

Hanna, J., Saha, K., Pando, B., van Zon, J., Lengner, C.J., Creyghton, M.P., van Oudenaarden, A., and Jaenisch, R. (2009). Direct cell reprogramming is a stochastic process amenable to acceleration. Nature *462*, 595-601.

Hara, T., Nakamura, K., Matsui, M., Yamamoto, A., Nakahara, Y., Suzuki-Migishima, R., Yokoyama, M., Mishima, K., Saito, I., Okano, H.*, et al.* (2006). Suppression of basal autophagy in neural cells causes neurodegenerative disease in mice. Nature *441*, 885-889.

Hargus, G., Cooper, O., Deleidi, M., Levy, A., Lee, K., Marlow, E., Yow, A., Soldner, F., Hockemeyer, D., Hallett, P.J.*, et al.* (2010). Differentiated Parkinson patient-derived induced pluripotent stem cells grow in the adult rodent brain and reduce motor asymmetry in Parkinsonian rats. Proc Natl Acad Sci U S A *107*, 15921-15926.

Harris, G.M., Dodelzon, K., Gong, L., Gonzalez-Alegre, P., and Paulson, H.L. (2010). Splice isoforms of the polyglutamine disease protein ataxin-3 exhibit similar enzymatic yet different aggregation properties. PLoS One *5*, e13695.

Havel, L.S., Li, S., and Li, X.J. (2009). Nuclear accumulation of polyglutamine disease proteins and neuropathology. Mol Brain *2*, 21.

Hayden, E.C. (2011). Stem cells: The growing pains of pluripotency. Nature *473*, 272-274.

Hayflick, L., and Moorhead, P.S. (1961). The serial cultivation of human diploid cell strains. Exp Cell Res *25*, 585-621.

Heldin, C.H., Miyazono, K., and ten Dijke, P. (1997). TGF-beta signalling from cell membrane to nucleus through SMAD proteins. Nature *390*, 465-471.

Hemmati-Brivanlou, A., Kelly, O.G., and Melton, D.A. (1994). Follistatin, an antagonist of activin, is expressed in the Spemann organizer and displays direct neuralizing activity. Cell *77*, 283-295.

Hemmati-Brivanlou, A., and Melton, D.A. (1994). Inhibition of activin receptor signaling promotes neuralization in Xenopus. Cell *77*, 273-281.

Hersch, S.M., Gevorkian, S., Marder, K., Moskowitz, C., Feigin, A., Cox, M., Como, P., Zimmerman, C., Lin, M., Zhang, L.*, et al.* (2006). Creatine in Huntington disease is safe, tolerable, bioavailable in brain and reduces serum 8OH2'dG. Neurology *66*, 250-252.

Hester, M.E., Murtha, M.J., Song, S., Rao, M., Miranda, C.J., Meyer, K., Tian, J., Boulting, G., Schaffer, D.V., Zhu, M.X.*, et al.* (2011). Rapid and efficient generation of functional motor neurons from human pluripotent stem cells using gene delivered transcription factor codes. Mol Ther *19*, 1905-1912.

Hick, A., Wattenhofer-Donze, M., Chintawar, S., Tropel, P., Simard, J.P., Vaucamps, N., Gall, D., Lambot, L., Andre, C., Reutenauer, L.*, et al.* (2013). Neurons and cardiomyocytes derived from induced pluripotent stem cells as a model for mitochondrial defects in Friedreich's ataxia. Dis Model Mech *6*, 608-621.

Hochedlinger, K., and Plath, K. (2009). Epigenetic reprogramming and induced pluripotency. Development *136*, 509-523.

Hockemeyer, D., Soldner, F., Cook, E.G., Gao, Q., Mitalipova, M., and Jaenisch, R. (2008). A drug-inducible system for direct reprogramming of human somatic cells to pluripotency. Cell Stem Cell *3*, 346-353.

Hockemeyer, D., Wang, H., Kiani, S., Lai, C.S., Gao, Q., Cassady, J.P., Cost, G.J., Zhang, L., Santiago, Y., Miller, J.C.*, et al.* (2011). Genetic engineering of human pluripotent cells using TALE nucleases. Nat Biotechnol *29*, 731-734.

Holmberg, C.I., Staniszewski, K.E., Mensah, K.N., Matouschek, A., and Morimoto, R.I. (2004). Inefficient degradation of truncated polyglutamine proteins by the proteasome. EMBO J *23*, 4307-4318.

Hossini, A.M., Megges, M., Prigione, A., Lichtner, B., Toliat, M.R., Wruck, W., Schroter, F., Nuernberg, P., Kroll, H., Makrantonaki, E.*, et al.* (2015). Induced pluripotent stem cell-derived neuronal cells from a sporadic Alzheimer's disease donor as a model for investigating AD-associated gene regulatory networks. BMC Genomics *16*, 84.

Hou, P., Li, Y., Zhang, X., Liu, C., Guan, J., Li, H., Zhao, T., Ye, J., Yang, W., Liu, K.*, et al.* (2013). Pluripotent stem cells induced from mouse somatic cells by small-molecule compounds. Science *341*, 651-654.

Hu, B.Y., Weick, J.P., Yu, J., Ma, L.X., Zhang, X.Q., Thomson, J.A., and Zhang, S.C. (2010). Neural differentiation of human induced pluripotent stem cells follows developmental principles but with variable potency. Proc Natl Acad Sci U S A *107*, 4335-4340.

Hu, B.Y., and Zhang, S.C. (2009). Differentiation of spinal motor neurons from pluripotent human stem cells. Nat Protoc *4*, 1295-1304.

Hu, J., Gagnon, K.T., Liu, J., Watts, J.K., Syeda-Nawaz, J., Bennett, C.F., Swayze, E.E., Randolph, J., Chattopadhyaya, J., and Corey, D.R. (2011). Allele-selective inhibition of ataxin-3 (ATX3) expression by antisense oligomers and duplex RNAs. Biological chemistry *392*, 315-325.

Huang, S.M., Mishina, Y.M., Liu, S., Cheung, A., Stegmeier, F., Michaud, G.A., Charlat, O., Wiellette, E., Zhang, Y., Wiessner, S.*, et al.* (2009). Tankyrase inhibition stabilizes axin and antagonizes Wnt signalling. Nature *461*, 614-620.

Huangfu, D., Maehr, R., Guo, W., Eijkelenboom, A., Snitow, M., Chen, A.E., and Melton, D.A. (2008a). Induction of pluripotent stem cells by defined factors is greatly improved by small-molecule compounds. Nat Biotechnol *26*, 795-797.

Huangfu, D., Osafune, K., Maehr, R., Guo, W., Eijkelenboom, A., Chen, S., Muhlestein, W., and Melton, D.A. (2008b). Induction of pluripotent stem cells from primary human fibroblasts with only Oct4 and Sox2. Nat Biotechnol *26*, 1269-1275.

Hubener, J., Weber, J.J., Richter, C., Honold, L., Weiss, A., Murad, F., Breuer, P., Wullner, U., Bellstedt, P., Paquet-Durand, F.*, et al.* (2013). Calpain-mediated ataxin-3 cleavage in the molecular pathogenesis of spinocerebellar ataxia type 3 (SCA3). Hum Mol Genet *22*, 508-518.

Huntington Study Group Pre, C.I., Hyson, H.C., Kieburtz, K., Shoulson, I., McDermott, M., Ravina, B., de Blieck, E.A., Cudkowicz, M.E., Ferrante, R.J., Como, P.*, et al.* (2010). Safety and tolerability of high-dosage coenzyme Q10 in Huntington's disease and healthy subjects. Movement disorders : official journal of the Movement Disorder Society *25*, 1924-1928.

Hyun, I., Lindvall, O., Ahrlund-Richter, L., Cattaneo, E., Cavazzana-Calvo, M., Cossu, G., De Luca, M., Fox, I.J., Gerstle, C., Goldstein, R.A.*, et al.* (2008). New ISSCR guidelines underscore major principles for responsible translational stem cell research. Cell Stem Cell *3*, 607-609.

Ichikawa, Y., Goto, J., Hattori, M., Toyoda, A., Ishii, K., Jeong, S.Y., Hashida, H., Masuda, N., Ogata, K., Kasai, F.*, et al.* (2001). The genomic structure and expression of MJD, the Machado-Joseph disease gene. J Hum Genet *46*, 413-422.

Igarashi, S., Takiyama, Y., Cancel, G., Rogaeva, E.A., Sasaki, H., Wakisaka, A., Zhou, Y.X., Takano, H., Endo, K., Sanpei, K.*, et al.* (1996). Intergenerational instability of the CAG repeat of the gene for Machado-Joseph disease (MJD1) is affected by the genotype of the normal chromosome: implications for the molecular mechanisms of the instability of the CAG repeat. Hum Mol Genet *5*, 923-932.

Ikeda, H., Yamaguchi, M., Sugai, S., Aze, Y., Narumiya, S., and Kakizuka, A. (1996). Expanded polyglutamine in the Machado-Joseph disease protein induces cell death in vitro and in vivo. Nat Genet *13*, 196-202.

Imaizumi, Y., Okada, Y., Akamatsu, W., Koike, M., Kuzumaki, N., Hayakawa, H., Nihira, T., Kobayashi, T., Ohyama, M., Sato, S.*, et al.* (2012). Mitochondrial dysfunction associated with increased oxidative stress and alpha-synuclein accumulation in PARK2 iPSC-derived neurons and postmortem brain tissue. Mol Brain *5*, 35.

Imbert, G., Saudou, F., Yvert, G., Devys, D., Trottier, Y., Garnier, J.M., Weber, C., Mandel, J.L., Cancel, G., Abbas, N.*, et al.* (1996). Cloning of the gene for spinocerebellar ataxia 2 reveals a locus with high sensitivity to expanded CAG/glutamine repeats. Nat Genet *14*, 285-291.

Incardona, J.P., Gaffield, W., Lange, Y., Cooney, A., Pentchev, P.G., Liu, S., Watson, J.A., Kapur, R.P., and Roelink, H. (2000). Cyclopamine inhibition of Sonic hedgehog signal transduction is not mediated through effects on cholesterol transport. Dev Biol *224*, 440-452.

International Stem Cell Banking, I. (2009). Consensus guidance for banking and supply of human embryonic stem cell lines for research purposes. Stem Cell Rev *5*, 301-314.

International Stem Cell, I., Adewumi, O., Aflatoonian, B., Ahrlund-Richter, L., Amit, M., Andrews, P.W., Beighton, G., Bello, P.A., Benvenisty, N., Berry, L.S.*, et al.* (2007). Characterization of human embryonic stem cell lines by the International Stem Cell Initiative. Nat Biotechnol *25*, 803-816.

Israel, M.A., Yuan, S.H., Bardy, C., Reyna, S.M., Mu, Y., Herrera, C., Hefferan, M.P., Van Gorp, S., Nazor, K.L., Boscolo, F.S.*, et al.* (2012). Probing sporadic and familial Alzheimer's disease using induced pluripotent stem cells. Nature *482*, 216-220.

Ito, Y., Tanaka, F., Yamamoto, M., Doyu, M., Nagamatsu, M., Riku, S., Mitsuma, T., and Sobue, G. (1998). Somatic mosaicism of the expanded CAG trinucleotide repeat in mRNAs for the responsible gene of Machado-Joseph disease (MJD), dentatorubral-pallidoluysian atrophy (DRPLA), and spinal and bulbar muscular atrophy (SBMA). Neurochem Res *23*, 25-32.

Itskovitz-Eldor, J., Schuldiner, M., Karsenti, D., Eden, A., Yanuka, O., Amit, M., Soreq, H., and Benvenisty, N. (2000). Differentiation of human embryonic stem cells into embryoid bodies

compromising the three embryonic germ layers. Molecular medicine (Cambridge, Mass) *6*, 88-95.

Jaenisch, R., and Young, R. (2008). Stem cells, the molecular circuitry of pluripotency and nuclear reprogramming. Cell *132*, 567-582.

Jana, N.R., Dikshit, P., Goswami, A., Kotliarova, S., Murata, S., Tanaka, K., and Nukina, N. (2005). Co-chaperone CHIP associates with expanded polyglutamine protein and promotes their degradation by proteasomes. J Biol Chem *280*, 11635-11640.

Jang, J., Quan, Z., Yum, Y.J., Song, H.S., Paek, S., and Kang, H.C. (2014). Induced pluripotent stem cells for modeling of pediatric neurological disorders. Biotechnol J *9*, 871-881.

Jeon, I., Lee, N., Li, J.Y., Park, I.H., Park, K.S., Moon, J., Shim, S.H., Choi, C., Chang, D.J., Kwon, J.*, et al.* (2012). Neuronal properties, in vivo effects, and pathology of a Huntington's disease patient-derived induced pluripotent stem cells. Stem Cells *30*, 2054-2062.

Jiang, H., Ren, Y., Yuen, E.Y., Zhong, P., Ghaedi, M., Hu, Z., Azabdaftari, G., Nakaso, K., Yan, Z., and Feng, J. (2012). Parkin controls dopamine utilization in human midbrain dopaminergic neurons derived from induced pluripotent stem cells. Nat Commun *3*, 668.

Jinek, M., Chylinski, K., Fonfara, I., Hauer, M., Doudna, J.A., and Charpentier, E. (2012). A programmable dual-RNA-guided DNA endonuclease in adaptive bacterial immunity. Science *337*, 816-821.

Johnson, M.A., Weick, J.P., Pearce, R.A., and Zhang, S.C. (2007). Functional neural development from human embryonic stem cells: accelerated synaptic activity via astrocyte coculture. J Neurosci *27*, 3069-3077.

Jung, J., Xu, K., Lessing, D., and Bonini, N.M. (2009). Preventing Ataxin-3 protein cleavage mitigates degeneration in a Drosophila model of SCA3. Hum Mol Genet *18*, 4843-4852.

Juopperi, T.A., Kim, W.R., Chiang, C.H., Yu, H., Margolis, R.L., Ross, C.A., Ming, G.L., and Song, H. (2012). Astrocytes generated from patient induced pluripotent stem cells recapitulate features of Huntington's disease patient cells. Mol Brain *5*, 17.

Kaji, K., Norrby, K., Paca, A., Mileikovsky, M., Mohseni, P., and Woltjen, K. (2009). Virus-free induction of pluripotency and subsequent excision of reprogramming factors. Nature *458*, 771-775.

Kamao, H., Mandai, M., Okamoto, S., Sakai, N., Suga, A., Sugita, S., Kiryu, J., and Takahashi, M. (2014). Characterization of human induced pluripotent stem cell-derived retinal pigment epithelium cell sheets aiming for clinical application. Stem Cell Reports *2*, 205-218.

Kanai, K., Kuwabara, S., Arai, K., Sung, J.Y., Ogawara, K., and Hattori, T. (2003). Muscle cramp in Machado-Joseph disease: altered motor axonal excitability properties and mexiletine treatment. Brain *126*, 965-973.

Karbanova, J., and Mokry, J. (2002). Histological and histochemical analysis of embryoid bodies. Acta Histochem *104*, 361-365.

Karumbayaram, S., Novitch, B.G., Patterson, M., Umbach, J.A., Richter, L., Lindgren, A., Conway, A.E., Clark, A.T., Goldman, S.A., Plath, K.*, et al.* (2009). Directed differentiation of human-induced pluripotent stem cells generates active motor neurons. Stem Cells *27*, 806-811.

Kawaguchi, Y., Okamoto, T., Taniwaki, M., Aizawa, M., Inoue, M., Katayama, S., Kawakami, H., Nakamura, S., Nishimura, M., Akiguchi, I.*, et al.* (1994). CAG expansions in a novel gene for Machado-Joseph disease at chromosome 14q32.1. Nat Genet *8*, 221-228.

Kawasaki, H., Mizuseki, K., Nishikawa, S., Kaneko, S., Kuwana, Y., Nakanishi, S., Nishikawa, S.I., and Sasai, Y. (2000). Induction of midbrain dopaminergic neurons from ES cells by stromal cell-derived inducing activity. Neuron *28*, 31-40.

Kaye, J.A., and Finkbeiner, S. (2013). Modeling Huntington's disease with induced pluripotent stem cells. Molecular and cellular neurosciences *56*, 50-64.

Kayed, R., Head, E., Thompson, J.L., McIntire, T.M., Milton, S.C., Cotman, C.W., and Glabe, C.G. (2003). Common structure of soluble amyloid oligomers implies common mechanism of pathogenesis. Science *300*, 486-489.

Kazachkova, N., Raposo, M., Montiel, R., Cymbron, T., Bettencourt, C., Silva-Fernandes, A., Silva, S., Maciel, P., and Lima, M. (2013). Patterns of mitochondrial DNA damage in blood and brain tissues of a transgenic mouse model of Machado-Joseph disease. Neuro-degenerative diseases *11*, 206-214.

Keller, G. (2005). Embryonic stem cell differentiation: emergence of a new era in biology and medicine. Genes Dev *19*, 1129-1155.

Keller, G.M. (1995). In vitro differentiation of embryonic stem cells. Current opinion in cell biology *7*, 862-869.

Khan, L.A., Bauer, P.O., Miyazaki, H., Lindenberg, K.S., Landwehrmeyer, B.G., and Nukina, N. (2006). Expanded polyglutamines impair synaptic transmission and ubiquitin-proteasome system in Caenorhabditis elegans. J Neurochem *98*, 576-587.

Kieling, C., Prestes, P.R., Saraiva-Pereira, M.L., and Jardim, L.B. (2007). Survival estimates for patients with Machado-Joseph disease (SCA3). Clin Genet *72*, 543-545.

Kim, D., Kim, C.H., Moon, J.I., Chung, Y.G., Chang, M.Y., Han, B.S., Ko, S., Yang, E., Cha, K.Y., Lanza, R.*, et al.* (2009a). Generation of human induced pluripotent stem cells by direct delivery of reprogramming proteins. Cell Stem Cell *4*, 472-476.

Kim, J., Chu, J., Shen, X., Wang, J., and Orkin, S.H. (2008a). An extended transcriptional network for pluripotency of embryonic stem cells. Cell *132*, 1049-1061.

Kim, J.B., Greber, B., Arauzo-Bravo, M.J., Meyer, J., Park, K.I., Zaehres, H., and Scholer, H.R. (2009b). Direct reprogramming of human neural stem cells by OCT4. Nature *461*, 649-643.

Kim, J.B., Zaehres, H., Wu, G., Gentile, L., Ko, K., Sebastiano, V., Arauzo-Bravo, M.J., Ruau, D., Han, D.W., Zenke, M.*, et al.* (2008b). Pluripotent stem cells induced from adult neural stem cells by reprogramming with two factors. Nature *454*, 646-650.

Kim, S.E., Kim, B.K., Gil, J.E., Kim, S.K., and Kim, J.H. (2007). Comparative analysis of the developmental competence of three human embryonic stem cell lines in vitro. Mol Cells *23*, 49-56.

Kirkeby, A., Grealish, S., Wolf, D.A., Nelander, J., Wood, J., Lundblad, M., Lindvall, O., and Parmar, M. (2012). Generation of regionally specified neural progenitors and functional neurons from human embryonic stem cells under defined conditions. Cell Rep *1*, 703-714.

Kiskinis, E., Sandoe, J., Williams, L.A., Boulting, G.L., Moccia, R., Wainger, B.J., Han, S., Peng, T., Thams, S., Mikkilineni, S.*, et al.* (2014). Pathways disrupted in human ALS motor neurons identified through genetic correction of mutant SOD1. Cell Stem Cell *14*, 781-795.

Klionsky, D.J., Abdalla, F.C., Abeliovich, H., Abraham, R.T., Acevedo-Arozena, A., Adeli, K., Agholme, L., Agnello, M., Agostinis, P., Aguirre-Ghiso, J.A.*, et al.* (2012). Guidelines for the use and interpretation of assays for monitoring autophagy. Autophagy *8*, 445-544.

Klionsky, D.J., Abeliovich, H., Agostinis, P., Agrawal, D.K., Aliev, G., Askew, D.S., Baba, M., Baehrecke, E.H., Bahr, B.A., Ballabio, A.*, et al.* (2008). Guidelines for the use and interpretation of assays for monitoring autophagy in higher eukaryotes. Autophagy *4*, 151-175.

Klockgether, T., Lüdtke, R., Kramer, B., Abele, M., Bürk, K., Schöls, L., Riess, O., Laccone, F., Boesch, S., Lopes-Cendes, I.*, et al.* (1998). The natural history of degenerative ataxia: a retrospective study in 466 patients. Brain : a journal of neurology *121 (Pt 4)*, 589-600.

Koch, P., Breuer, P., Peitz, M., Jungverdorben, J., Kesavan, J., Poppe, D., Doerr, J., Ladewig, J., Mertens, J., Tuting, T.*, et al.* (2011). Excitation-induced ataxin-3 aggregation in neurons from patients with Machado-Joseph disease. Nature *480*, 543-546.

Koch, P., Opitz, T., Steinbeck, J.A., Ladewig, J., and Brustle, O. (2009). A rosette-type, self-renewing human ES cell-derived neural stem cell with potential for in vitro instruction and synaptic integration. Proc Natl Acad Sci U S A *106*, 3225-3230.

Koide, R., Ikeuchi, T., Onodera, O., Tanaka, H., Igarashi, S., Endo, K., Takahashi, H., Kondo, R., Ishikawa, A., Hayashi, T.*, et al.* (1994). Unstable expansion of CAG repeat in hereditary dentatorubral-pallidoluysian atrophy (DRPLA). Nat Genet *6*, 9-13.

Komatsu, M., Waguri, S., Chiba, T., Murata, S., Iwata, J., Tanida, I., Ueno, T., Koike, M., Uchiyama, Y., Kominami, E.*, et al.* (2006). Loss of autophagy in the central nervous system causes neurodegeneration in mice. Nature *441*, 880-884.

Kondo, T., Asai, M., Tsukita, K., Kutoku, Y., Ohsawa, Y., Sunada, Y., Imamura, K., Egawa, N., Yahata, N., Okita, K.*, et al.* (2013). Modeling Alzheimer's disease with iPSCs reveals stress phenotypes associated with intracellular Abeta and differential drug responsiveness. Cell Stem Cell *12*, 487-496.

Kriks, S., Shim, J.W., Piao, J., Ganat, Y.M., Wakeman, D.R., Xie, Z., Carrillo-Reid, L., Auyeung, G., Antonacci, C., Buch, A.*, et al.* (2011). Dopamine neurons derived from human ES cells efficiently engraft in animal models of Parkinson's disease. Nature *480*, 547-551.

Ku, S., Soragni, E., Campau, E., Thomas, E.A., Altun, G., Laurent, L.C., Loring, J.F., Napierala, M., and Gottesfeld, J.M. (2010). Friedreich's ataxia induced pluripotent stem cells model intergenerational GAATTC triplet repeat instability. Cell Stem Cell *7*, 631-637.

Kuemmerle, S., Gutekunst, C.A., Klein, A.M., Li, X.J., Li, S.H., Beal, M.F., Hersch, S.M., and Ferrante, R.J. (1999). Huntington aggregates may not predict neuronal death in Huntington's disease. Ann Neurol *46*, 842-849.

Kukekov, V.G., Laywell, E.D., Suslov, O., Davies, K., Scheffler, B., Thomas, L.B., O'Brien, T.F., Kusakabe, M., and Steindler, D.A. (1999). Multipotent stem/progenitor cells with similar properties arise from two neurogenic regions of adult human brain. Exp Neurol *156*, 333-344.

La Spada, A.R., Wilson, E.M., Lubahn, D.B., Harding, A.E., and Fischbeck, K.H. (1991). Androgen receptor gene mutations in X-linked spinal and bulbar muscular atrophy. Nature *352*, 77-79.

Laco, M.N., Cortes, L., Travis, S.M., Paulson, H.L., and Rego, A.C. (2012a). Valosin-containing protein (VCP/p97) is an activator of wild-type ataxin-3. PLoS One *7*, e43563.

Laco, M.N., Oliveira, C.R., Paulson, H.L., and Rego, A.C. (2012b). Compromised mitochondrial complex II in models of Machado-Joseph disease. Biochim Biophys Acta *1822*, 139-149.

Lai, K., Kaspar, B.K., Gage, F.H., and Schaffer, D.V. (2003). Sonic hedgehog regulates adult neural progenitor proliferation in vitro and in vivo. Nat Neurosci *6*, 21-27.

Lako, M., Armstrong, L., and Stojkovic, M. (2010). Induced pluripotent stem cells : it looks simple but can looks deceive? Stem Cells *28*, 845-850.

Lancaster, M.A., and Knoblich, J.A. (2014). Generation of cerebral organoids from human pluripotent stem cells. Nat Protoc *9*, 2329-2340.

Lancaster, M.A., Renner, M., Martin, C.A., Wenzel, D., Bicknell, L.S., Hurles, M.E., Homfray, T., Penninger, J.M., Jackson, A.P., and Knoblich, J.A. (2013). Cerebral organoids model human brain development and microcephaly. Nature *501*, 373-379.

Lappalainen, R.S., Salomaki, M., Yla-Outinen, L., Heikkila, T.J., Hyttinen, J.A., Pihlajamaki, H., Suuronen, R., Skottman, H., and Narkilahti, S. (2010). Similarly derived and cultured hESC lines show variation in their developmental potential towards neuronal cells in long-term culture. Regen Med *5*, 749-762.

Le Dreau, G., and Marti, E. (2012). Dorsal-ventral patterning of the neural tube: a tale of three signals. Dev Neurobiol *72*, 1471-1481.

Lee, G., Papapetrou, E.P., Kim, H., Chambers, S.M., Tomishima, M.J., Fasano, C.A., Ganat, Y.M., Menon, J., Shimizu, F., Viale, A.*, et al.* (2009). Modelling pathogenesis and treatment of familial dysautonomia using patient-specific iPSCs. Nature *461*, 402-406.

Lee, G., Ramirez, C.N., Kim, H., Zeltner, N., Liu, B., Radu, C., Bhinder, B., Kim, Y.J., Choi, I.Y., Mukherjee-Clavin, B.*, et al.* (2012a). Large-scale screening using familial dysautonomia induced pluripotent stem cells identifies compounds that rescue IKBKAP expression. Nat Biotechnol *30*, 1244-1248.

Lee, J., Xia, Y., Son, M.Y., Jin, G., Seol, B., Kim, M.J., Son, M.J., Do, M., Lee, M., Kim, D.*, et al.* (2012b). A novel small molecule facilitates the reprogramming of human somatic cells into a pluripotent state and supports the maintenance of an undifferentiated state of human pluripotent stem cells. Angewandte Chemie *51*, 12509-12513.

Lee, M.O., Moon, S.H., Jeong, H.C., Yi, J.Y., Lee, T.H., Shim, S.H., Rhee, Y.H., Lee, S.H., Oh, S.J., Lee, M.Y.*, et al.* (2013). Inhibition of pluripotent stem cell-derived teratoma formation by small molecules. Proc Natl Acad Sci U S A *110*, E3281-3290.

Lenzi, J., De Santis, R., de Turris, V., Morlando, M., Laneve, P., Calvo, A., Caliendo, V., Chio, A., Rosa, A., and Bozzoni, I. (2015). ALS mutant FUS proteins are recruited into stress granules in induced pluripotent stem cell-derived motoneurons. Dis Model Mech *8*, 755-766.

Levine, B., and Kroemer, G. (2008). Autophagy in the pathogenesis of disease. Cell *132*, 27-42.

Li, F., Macfarlan, T., Pittman, R.N., and Chakravarti, D. (2002). Ataxin-3 is a histone-binding protein with two independent transcriptional corepressor activities. J Biol Chem *277*, 45004-45012.

Li, W., and Ding, S. (2010). Small molecules that modulate embryonic stem cell fate and somatic cell reprogramming. Trends Pharmacol Sci *31*, 36-45.

Li, W., Wei, W., Zhu, S., Zhu, J., Shi, Y., Lin, T., Hao, E., Hayek, A., Deng, H., and Ding, S. (2009a). Generation of rat and human induced pluripotent stem cells by combining genetic reprogramming and chemical inhibitors. Cell Stem Cell *4*, 16-19.

Li, W., Zhou, H., Abujarour, R., Zhu, S., Young Joo, J., Lin, T., Hao, E., Scholer, H.R., Hayek, A., and Ding, S. (2009b). Generation of human-induced pluripotent stem cells in the absence of exogenous Sox2. Stem Cells *27*, 2992-3000.

Li, X.J., Zhang, X., Johnson, M.A., Wang, Z.B., Lavaute, T., and Zhang, S.C. (2009c). Coordination of sonic hedgehog and Wnt signaling determines ventral and dorsal telencephalic neuron types from human embryonic stem cells. Development *136*, 4055-4063.

Li, Y., Polak, U., Bhalla, A.D., Rozwadowska, N., Butler, J.S., Lynch, D.R., Dent, S.Y., and Napierala, M. (2015). Excision of Expanded GAA Repeats Alleviates the Molecular Phenotype of Friedreich's Ataxia. Mol Ther *23*, 1055-1065.

Liem, K.F., Jr., Tremml, G., and Jessell, T.M. (1997). A role for the roof plate and its resident TGFbeta-related proteins in neuronal patterning in the dorsal spinal cord. Cell *91*, 127-138.

Liem, K.F., Jr., Tremml, G., Roelink, H., and Jessell, T.M. (1995). Dorsal differentiation of neural plate cells induced by BMP-mediated signals from epidermal ectoderm. Cell *82*, 969-979.

Lima, L., and Coutinho, P. (1980). Clinical criteria for diagnosis of Machado-Joseph disease: report of a non-Azorena Portuguese family. Neurology *30*, 319-322.

Lima, M., Costa, M.C., Montiel, R., Ferro, A., Santos, C., Silva, C., Bettencourt, C., Sousa, A., Sequeiros, J., Coutinho, P.*, et al.* (2005). Population genetics of wild-type CAG repeats in the Machado-Joseph disease gene in Portugal. Human heredity *60*, 156-163.

Lima, M., Mayer, F.M., Coutinho, P., and Abade, A. (1998). Origins of a mutation: population genetics of Machado-Joseph disease in the Azores (Portugal). Hum Biol *70*, 1011-1023.

Lin, T., Ambasudhan, R., Yuan, X., Li, W., Hilcove, S., Abujarour, R., Lin, X., Hahm, H.S., Hao, E., Hayek, A.*, et al.* (2009). A chemical platform for improved induction of human iPSCs. Nat Methods *6*, 805-808.

Lin, X., Antalffy, B., Kang, D., Orr, H.T., and Zoghbi, H.Y. (2000). Polyglutamine expansion down-regulates specific neuronal genes before pathologic changes in SCA1. Nat Neurosci *3*, 157-163.

Liu, G.H., Ding, Z., and Izpisua Belmonte, J.C. (2012). iPSC technology to study human aging and aging-related disorders. Current opinion in cell biology *24*, 765-774.

Liu, J., Verma, P.J., Evans-Galea, M.V., Delatycki, M.B., Michalska, A., Leung, J., Crombie, D., Sarsero, J.P., Williamson, R., Dottori, M.*, et al.* (2011). Generation of induced pluripotent stem cell lines from Friedreich ataxia patients. Stem Cell Rev *7*, 703-713.

Loh, Y.H., Agarwal, S., Park, I.H., Urbach, A., Huo, H., Heffner, G.C., Kim, K., Miller, J.D., Ng, K., and Daley, G.Q. (2009). Generation of induced pluripotent stem cells from human blood. Blood *113*, 5476-5479.

Loh, Y.H., Wu, Q., Chew, J.L., Vega, V.B., Zhang, W., Chen, X., Bourque, G., George, J., Leong, B., Liu, J.*, et al.* (2006). The Oct4 and Nanog transcription network regulates pluripotency in mouse embryonic stem cells. Nat Genet *38*, 431-440.

Looijenga, L.H., Stoop, H., de Leeuw, H.P., de Gouveia Brazao, C.A., Gillis, A.J., van Roozendaal, K.E., van Zoelen, E.J., Weber, R.F., Wolffenbuttel, K.P., van Dekken, H.*, et al.* (2003). POU5F1 (OCT3/4) identifies cells with pluripotent potential in human germ cell tumors. Cancer Res *63*, 2244-2250.

Lowry, W.E., Richter, L., Yachechko, R., Pyle, A.D., Tchieu, J., Sridharan, R., Clark, A.T., and Plath, K. (2008). Generation of human induced pluripotent stem cells from dermal fibroblasts. Proc Natl Acad Sci U S A *105*, 2883-2888.

Luo, Y., Fan, Y., Zhou, B., Xu, Z., Chen, Y., and Sun, X. (2012). Generation of induced pluripotent stem cells from skin fibroblasts of a patient with olivopontocerebellar atrophy. Tohoku J Exp Med *226*, 151-159.

Lyashenko, N., Winter, M., Migliorini, D., Biechele, T., Moon, R.T., and Hartmann, C. (2011). Differential requirement for the dual functions of beta-catenin in embryonic stem cell self-renewal and germ layer formation. Nat Cell Biol *13*, 753-761.

Lytton, J., Westlin, M., and Hanley, M.R. (1991). Thapsigargin inhibits the sarcoplasmic or endoplasmic reticulum Ca-ATPase family of calcium pumps. J Biol Chem *266*, 17067-17071.

Ma, H., Morey, R., O'Neil, R.C., He, Y., Daughtry, B., Schultz, M.D., Hariharan, M., Nery, J.R., Castanon, R., Sabatini, K.*, et al.* (2014). Abnormalities in human pluripotent cells due to reprogramming mechanisms. Nature *511*, 177-183.

MacDonald, M.E., Ambrose, C.M., Duyao, M.P., Myers, R.H., Lin, C., Srinidhi, L., Barnes, G., Taylor, S.A., James, M., and Groot, N. (1993). A novel gene containing a trinucleotide repeat that is expanded and unstable on Huntington's disease chromosomes. Cell *72*, 971-983.

Maciel, P., Costa, M.C., Ferro, A., Rousseau, M., Santos, C.S., Gaspar, C., Barros, J., Rouleau, G.A., Coutinho, P., and Sequeiros, J. (2001). Improvement in the molecular diagnosis of Machado-Joseph disease. Arch Neurol *58*, 1821-1827.

Maciel, P., Gaspar, C., DeStefano, A.L., Silveira, I., Coutinho, P., Radvany, J., Dawson, D.M., Sudarsky, L., Guimaraes, J., Loureiro, J.E.*, et al.* (1995). Correlation between CAG repeat length and clinical features in Machado-Joseph disease. Am J Hum Genet *57*, 54-61.

Maciel, P., Gaspar, C., Guimaraes, L., Goto, J., Lopes-Cendes, I., Hayes, S., Arvidsson, K., Dias, A., Sequeiros, J., Sousa, A.*, et al.* (1999). Study of three intragenic polymorphisms in the Machado-Joseph disease gene (MJD1) in relation to genetic instability of the (CAG)n tract. Eur J Hum Genet *7*, 147-156.

Maciel, P., Lopes-Cendes, I., Kish, S., Sequeiros, J., and Rouleau, G.A. (1997). Mosaicism of the CAG repeat in CNS tissue in relation to age at death in spinocerebellar ataxia type 1 and Machado-Joseph disease patients. *60*, 993-996.

Maden, M. (2002). Retinoid signalling in the development of the central nervous system. Nat Rev Neurosci *3*, 843-853.

Maden, M. (2007). Retinoic acid in the development, regeneration and maintenance of the nervous system. Nat Rev Neurosci *8*, 755-765.

Mahairaki, V., Ryu, J., Peters, A., Chang, Q., Li, T., Park, T.S., Burridge, P.W., Talbot, C.C., Jr., Asnaghi, L., Martin, L.J.*, et al.* (2014). Induced pluripotent stem cells from familial Alzheimer's disease patients differentiate into mature neurons with amyloidogenic properties. Stem Cells Dev *23*, 2996-3010.

Maherali, N., Ahfeldt, T., Rigamonti, A., Utikal, J., Cowan, C., and Hochedlinger, K. (2008). A high-efficiency system for the generation and study of human induced pluripotent stem cells. Cell Stem Cell *3*, 340-345.

Maherali, N., and Hochedlinger, K. (2008). Guidelines and techniques for the generation of induced pluripotent stem cells. Cell Stem Cell *3*, 595-605.

Maherali, N., Sridharan, R., Xie, W., Utikal, J., Eminli, S., Arnold, K., Stadtfeld, M., Yachechko, R., Tchieu, J., Jaenisch, R.*, et al.* (2007). Directly reprogrammed fibroblasts show global epigenetic remodeling and widespread tissue contribution. Cell Stem Cell *1*, 55-70.

Mali, P., Chou, B.K., Yen, J., Ye, Z., Zou, J., Dowey, S., Brodsky, R.A., Ohm, J.E., Yu, W., Baylin, S.B.*, et al.* (2010). Butyrate greatly enhances derivation of human induced pluripotent stem cells by promoting epigenetic remodeling and the expression of pluripotency-associated genes. Stem Cells *28*, 713-720.

Mali, P., Yang, L., Esvelt, K.M., Aach, J., Guell, M., DiCarlo, J.E., Norville, J.E., and Church, G.M. (2013). RNA-guided human genome engineering via Cas9. Science *339*, 823-826.

Marchetto, M.C., Carromeu, C., Acab, A., Yu, D., Yeo, G.W., Mu, Y., Chen, G., Gage, F.H., and Muotri, A.R. (2010). A model for neural development and treatment of Rett syndrome using human induced pluripotent stem cells. Cell *143*, 527-539.

Mariani, J., Simonini, M.V., Palejev, D., Tomasini, L., Coppola, G., Szekely, A.M., Horvath, T.L., and Vaccarino, F.M. (2012). Modeling human cortical development in vitro using induced pluripotent stem cells. Proc Natl Acad Sci U S A *109*, 12770-12775.

Maroof, A.M., Keros, S., Tyson, J.A., Ying, S.W., Ganat, Y.M., Merkle, F.T., Liu, B., Goulburn, A., Stanley, E.G., Elefanty, A.G.*, et al.* (2013). Directed differentiation and functional maturation of cortical interneurons from human embryonic stem cells. Cell Stem Cell *12*, 559-572.

Martins, S., Calafell, F., Gaspar, C., Wong, V.C., Silveira, I., Nicholson, G.A., Brunt, E.R., Tranebjaerg, L., Stevanin, G., Hsieh, M.*, et al.* (2007). Asian origin for the worldwide-spread mutational event in Machado-Joseph disease. Arch Neurol *64*, 1502-1508.

Martins, S., Calafell, F., Wong, V.C., Sequeiros, J., and Amorim, A. (2006). A multistep mutation mechanism drives the evolution of the CAG repeat at MJD/SCA3 locus. Eur J Hum Genet *14*, 932-940.

Maruyama, H., Nakamura, S., Matsuyama, Z., Sakai, T., Doyu, M., Sobue, G., Seto, M., Tsujihata, M., Oh-i, T., Nishio, T.*, et al.* (1995). Molecular features of the CAG repeats and clinical manifestation of Machado-Joseph disease. Hum Mol Genet *4*, 807-812.

Masino, L., Musi, V., Menon, R.P., Fusi, P., Kelly, G., Frenkiel, T.A., Trottier, Y., and Pastore, A. (2003). Domain architecture of the polyglutamine protein ataxin-3: a globular domain followed by a flexible tail. FEBS Lett *549*, 21-25.

Mateizel, I., De Temmerman, N., Ullmann, U., Cauffman, G., Sermon, K., Van de Velde, H., De Rycke, M., Degreef, E., Devroey, P., Liebaers, I.*, et al.* (2006). Derivation of human embryonic stem cell lines from embryos obtained after IVF and after PGD for monogenic disorders. Hum Reprod *21*, 503-511.

Matsumoto, M., Yada, M., Hatakeyama, S., Ishimoto, H., Tanimura, T., Tsuji, S., Kakizuka, A., Kitagawa, M., and Nakayama, K.I. (2004). Molecular clearance of ataxin-3 is regulated by a mammalian E4. EMBO J *23*, 659-669.

Matsumura, R., Takayanagi, T., Fujimoto, Y., Murata, K., Mano, Y., Horikawa, H., and Chuma, T. (1996a). The relationship between trinucleotide repeat length and phenotypic variation in Machado-Joseph disease. Journal of the neurological sciences *139*, 52-57.

Matsumura, R., Takayanagi, T., Murata, K., Futamura, N., Hirano, M., and Ueno, S. (1996b). Relationship of (CAG)nC configuration to repeat instability of the Machado-Joseph disease gene. Hum Genet *98*, 643-645.

Mattis, V.B., Tom, C., Akimov, S., Saeedian, J., Ostergaard, M.E., Southwell, A.L., Doty, C.N., Ornelas, L., Sahabian, A., Lenaeus, L.*, et al.* (2015). HD iPSC-derived neural progenitors accumulate in culture and are susceptible to BDNF withdrawal due to glutamate toxicity. Hum Mol Genet *24*, 3257-3271.

Mattson, M.P. (2007). Calcium and neurodegeneration. Aging Cell *6*, 337-350.

Mattson, M.P., and Magnus, T. (2006). Ageing and neuronal vulnerability. Nat Rev Neurosci *7*, 278-294.

Matus, S., Glimcher, L.H., and Hetz, C. (2011). Protein folding stress in neurodegenerative diseases: a glimpse into the ER. Current opinion in cell biology *23*, 239-252.

Mauri, P.L., Riva, M., Ambu, D., De Palma, A., Secundo, F., Benazzi, L., Valtorta, M., Tortora, P., and Fusi, P. (2006). Ataxin-3 is subject to autolytic cleavage. The FEBS journal *273*, 4277-4286.

Mayshar, Y., Ben-David, U., Lavon, N., Biancotti, J.C., Yakir, B., Clark, A.T., Plath, K., Lowry, W.E., and Benvenisty, N. (2010). Identification and classification of chromosomal aberrations in human induced pluripotent stem cells. Cell Stem Cell *7*, 521-531.

Mazzola, J.L., and Sirover, M.A. (2001). Reduction of glyceraldehyde-3-phosphate dehydrogenase activity in Alzheimer's disease and in Huntington's disease fibroblasts. J Neurochem *76*, 442-449.

Mazzucchelli, S., De Palma, A., Riva, M., D'Urzo, A., Pozzi, C., Pastori, V., Comelli, F., Fusi, P., Vanoni, M., Tortora, P*., et al.* (2009). Proteomic and biochemical analyses unveil tight interaction of ataxin-3 with tubulin. Int J Biochem Cell Biol *41*, 2485-2492.

McCampbell, A., Taylor, J.P., Taye, A.A., Robitschek, J., Li, M., Walcott, J., Merry, D., Chai, Y., Paulson, H., Sobue, G*., et al.* (2000). CREB-binding protein sequestration by expanded polyglutamine. Hum Mol Genet *9*, 2197-2202.

Meno, C., Gritsman, K., Ohishi, S., Ohfuji, Y., Heckscher, E., Mochida, K., Shimono, A., Kondoh, H., Talbot, W.S., Robertson, E.J*., et al.* (1999). Mouse Lefty2 and zebrafish antivin are feedback inhibitors of nodal signaling during vertebrate gastrulation. Mol Cell *4*, 287-298.

Menzies, F.M., Huebener, J., Renna, M., Bonin, M., Riess, O., and Rubinsztein, D.C. (2010). Autophagy induction reduces mutant ataxin-3 levels and toxicity in a mouse model of spinocerebellar ataxia type 3. Brain *133*, 93-104.

Menzies, F.M., Moreau, K., Puri, C., Renna, M., and Rubinsztein, D.C. (2012). Measurement of autophagic activity in mammalian cells. Curr Protoc Cell Biol *Chapter 15*, Unit 15 16.

Merkle, F.T., and Eggan, K. (2013). Modeling human disease with pluripotent stem cells: from genome association to function. Cell Stem Cell *12*, 656-668.

Mertens, J., Stuber, K., Wunderlich, P., Ladewig, J., Kesavan, J.C., Vandenberghe, R., Vandenbulcke, M., van Damme, P., Walter, J., Brustle, O*., et al.* (2013). APP processing in human pluripotent stem cell-derived neurons is resistant to NSAID-based gamma-secretase modulation. Stem Cell Reports *1*, 491-498.

Miller, J.D., Ganat, Y.M., Kishinevsky, S., Bowman, R.L., Liu, B., Tu, E.Y., Mandal, P.K., Vera, E., Shim, J.W., Kriks, S*., et al.* (2013). Human iPSC-based modeling of late-onset disease via progerin-induced aging. Cell Stem Cell *13*, 691-705.

Miller, V.M., Nelson, R.F., Gouvion, C.M., Williams, A., Rodriguez-Lebron, E., Harper, S.Q., Davidson, B.L., Rebagliati, M.R., and Paulson, H.L. (2005). CHIP suppresses polyglutamine aggregation and toxicity in vitro and in vivo. J Neurosci *25*, 9152-9161.

Miller, V.M., Xia, H., Marrs, G.L., Gouvion, C.M., Lee, G., Davidson, B.L., and Paulson, H.L. (2003). Allele-specific silencing of dominant disease genes. Proc Natl Acad Sci U S A *100*, 7195-7200.

Mitne-Neto, M., Machado-Costa, M., Marchetto, M.C., Bengtson, M.H., Joazeiro, C.A., Tsuda, H., Bellen, H.J., Silva, H.C., Oliveira, A.S., Lazar, M*., et al.* (2011). Downregulation of VAPB expression in motor neurons derived from induced pluripotent stem cells of ALS8 patients. Hum Mol Genet *20*, 3642-3652.

Miura, K., Okada, Y., Aoi, T., Okada, A., Takahashi, K., Okita, K., Nakagawa, M., Koyanagi, M., Tanabe, K., Ohnuki, M.*, et al.* (2009). Variation in the safety of induced pluripotent stem cell lines. Nat Biotechnol *27*, 743-745.

Miyoshi, K., Tsuji, D., Kudoh, K., Satomura, K., Muto, T., Itoh, K., and Noma, T. (2010). Generation of human induced pluripotent stem cells from oral mucosa. Journal of bioscience and bioengineering *110*, 345-350.

Miyoshi, N., Ishii, H., Nagano, H., Haraguchi, N., Dewi, D.L., Kano, Y., Nishikawa, S., Tanemura, M., Mimori, K., Tanaka, F.*, et al.* (2011). Reprogramming of mouse and human cells to pluripotency using mature microRNAs. Cell Stem Cell *8*, 633-638.

Mizushima, N. (2007). How to Interpret LC3 Immunoblotting. Autophagy *3*, 542-545.

Monte, T.L., Rieder, C.R., Tort, A.B., Rockenback, I., Pereira, M.L., Silveira, I., Ferro, A., Sequeiros, J., and Jardim, L.B. (2003). Use of fluoxetine for treatment of Machado-Joseph disease: an open-label study. Acta neurologica Scandinavica *107*, 207-210.

Moreno-Carranza, B., Gentsch, M., Stein, S., Schambach, A., Santilli, G., Rudolf, E., Ryser, M.F., Haria, S., Thrasher, A.J., Baum, C.*, et al.* (2009). Transgene optimization significantly improves SIN vector titers, gp91phox expression and reconstitution of superoxide production in X-CGD cells. Gene Ther *16*, 111-118.

Morizane, A., Doi, D., and Takahashi, J. (2013). Neural induction with a dopaminergic phenotype from human pluripotent stem cells through a feeder-free floating aggregation culture. Methods in molecular biology *1018*, 11-19.

Muchowski, P.J., Schaffar, G., Sittler, A., Wanker, E.E., Hayer-Hartl, M.K., and Hartl, F.U. (2000). Hsp70 and hsp40 chaperones can inhibit self-assembly of polyglutamine proteins into amyloid-like fibrils. Proc Natl Acad Sci U S A *97*, 7841-7846.

Muller, F.J., Goldmann, J., Loser, P., and Loring, J.F. (2010). A call to standardize teratoma assays used to define human pluripotent cell lines. Cell Stem Cell *6*, 412-414.

Munoz-Sanjuan, I., and Brivanlou, A.H. (2002). Neural induction, the default model and embryonic stem cells. Nat Rev Neurosci *3*, 271-280.

Murashov, A.K., Pak, E.S., Hendricks, W.A., Owensby, J.P., Sierpinski, P.L., Tatko, L.M., and Fletcher, P.L. (2005). Directed differentiation of embryonic stem cells into dorsal interneurons. FASEB journal : official publication of the Federation of American Societies for Experimental Biology *19*, 252-254.

Murry, C.E., and Keller, G. (2008). Differentiation of embryonic stem cells to clinically relevant populations: lessons from embryonic development. Cell *132*, 661-680.

Myers, R.H., Madden, J.J., Teague, J.L., and Falek, A. (1982). Factors related to onset age of Huntington disease. Am J Hum Genet *34*, 481-488.

Na, J., Baker, D., Zhang, J., Andrews, P.W., and Barbaric, I. (2014). Aneuploidy in pluripotent stem cells and implications for cancerous transformation. Protein Cell *5*, 569-579.

Nagafuchi, S., Yanagisawa, H., Sato, K., Shirayama, T., Ohsaki, E., Bundo, M., Takeda, T., Tadokoro, K., Kondo, I., Murayama, N.*, et al.* (1994). Dentatorubral and pallidoluysian atrophy expansion of an unstable CAG trinucleotide on chromosome 12p. Nat Genet *6*, 14-18.

Nagai, Y., Fujikake, N., Popiel, H.A., and Wada, K. (2010). Induction of molecular chaperones as a therapeutic strategy for the polyglutamine diseases. Current pharmaceutical biotechnology *11*, 188-197.

Nagai, Y., Inui, T., Popiel, H.A., Fujikake, N., Hasegawa, K., Urade, Y., Goto, Y., Naiki, H., and Toda, T. (2007). A toxic monomeric conformer of the polyglutamine protein. Nat Struct Mol Biol *14*, 332-340.

Nakagawa, M., Koyanagi, M., Tanabe, K., Takahashi, K., Ichisaka, T., Aoi, T., Okita, K., Mochiduki, Y., Takizawa, N., and Yamanaka, S. (2008). Generation of induced pluripotent stem cells without Myc from mouse and human fibroblasts. Nat Biotechnol *26*, 101-106.

Nakamura, K., Jeong, S.Y., Uchihara, T., Anno, M., Nagashima, K., Nagashima, T., Ikeda, S., Tsuji, S., and Kanazawa, I. (2001). SCA17, a novel autosomal dominant cerebellar ataxia caused by an expanded polyglutamine in TATA-binding protein. Hum Mol Genet *10*, 1441-1448.

Nakano, K.K., Dawson, D.M., and Spence, A. (1972). Machado disease. A hereditary ataxia in Portuguese emigrants to Massachusetts. Neurology *22*, 49-55.

Narsinh, K.H., Jia, F., Robbins, R.C., Kay, M.A., Longaker, M.T., and Wu, J.C. (2011). Generation of adult human induced pluripotent stem cells using nonviral minicircle DNA vectors. Nat Protoc *6*, 78-88.

Nascimento-Ferreira, I., Nobrega, C., Vasconcelos-Ferreira, A., Onofre, I., Albuquerque, D., Aveleira, C., Hirai, H., Deglon, N., and Pereira de Almeida, L. (2013). Beclin 1 mitigates motor and neuropathological deficits in genetic mouse models of Machado-Joseph disease. Brain *136*, 2173-2188.

Nascimento-Ferreira, I., Santos-Ferreira, T., Sousa-Ferreira, L., Auregan, G., Onofre, I., Alves, S., Dufour, N., Colomer Gould, V.F., Koeppen, A., Deglon, N.*, et al.* (2011). Overexpression of the autophagic beclin-1 protein clears mutant ataxin-3 and alleviates Machado-Joseph disease. Brain *134*, 1400-1415.

Ng, Y.Y., Baert, M.R., Pike-Overzet, K., Rodijk, M., Brugman, M.H., Schambach, A., Baum, C., Hendriks, R.W., van Dongen, J.J., and Staal, F.J. (2010). Correction of B-cell development in Btk-deficient mice using lentiviral vectors with codon-optimized human BTK. Leukemia *24*, 1617-1630.

Nguyen, H.N., Byers, B., Cord, B., Shcheglovitov, A., Byrne, J., Gujar, P., Kee, K., Schule, B., Dolmetsch, R.E., Langston, W.*, et al.* (2011). LRRK2 mutant iPSC-derived DA neurons demonstrate increased susceptibility to oxidative stress. Cell Stem Cell *8*, 267-280.

Nicastro, G., Menon, R.P., Masino, L., Knowles, P.P., McDonald, N.Q., and Pastore, A. (2005). The solution structure of the Josephin domain of ataxin-3: structural determinants for molecular recognition. Proc Natl Acad Sci U S A *102*, 10493-10498.

Nicholas, C.R., Chen, J., Tang, Y., Southwell, D.G., Chalmers, N., Vogt, D., Arnold, C.M., Chen, Y.J., Stanley, E.G., Elefanty, A.G.*, et al.* (2013). Functional maturation of hPSC-derived forebrain interneurons requires an extended timeline and mimics human neural development. Cell Stem Cell *12*, 573-586.

Nicoleau, C., Varela, C., Bonnefond, C., Maury, Y., Bugi, A., Aubry, L., Viegas, P., Bourgois-Rocha, F., Peschanski, M., and Perrier, A.L. (2013). Embryonic stem cells neural differentiation qualifies the role of Wnt/beta-Catenin signals in human telencephalic specification and regionalization. Stem Cells *31*, 1763-1774.

Nie, B., Wang, H., Laurent, T., and Ding, S. (2012). Cellular reprogramming: a small molecule perspective. Current opinion in cell biology *24*, 784-792.

Nihei, Y., Ito, D., Okada, Y., Akamatsu, W., Yagi, T., Yoshizaki, T., Okano, H., and Suzuki, N. (2013). Enhanced aggregation of androgen receptor in induced pluripotent stem cell-derived neurons from spinal and bulbar muscular atrophy. J Biol Chem *288*, 8043-8052.

Nishimura, K., Sano, M., Ohtaka, M., Furuta, B., Umemura, Y., Nakajima, Y., Ikehara, Y., Kobayashi, T., Segawa, H., Takayasu, S*., et al.* (2011). Development of defective and persistent Sendai virus vector: a unique gene delivery/expression system ideal for cell reprogramming. J Biol Chem *286*, 4760-4771.

Nishimura, R., Hata, K., Ikeda, F., Matsubara, T., Yamashita, K., Ichida, F., and Yoneda, T. (2003). The role of Smads in BMP signaling. Frontiers in bioscience : a journal and virtual library *8*, s275-284.

Nixon, R.A. (2013). The role of autophagy in neurodegenerative disease. Nat Med *19*, 983-997.

Nizzardo, M., Simone, C., Falcone, M., Locatelli, F., Riboldi, G., Comi, G.P., and Corti, S. (2010). Human motor neuron generation from embryonic stem cells and induced pluripotent stem cells. Cell Mol Life Sci *67*, 3837-3847.

Nóbrega, C., and de Almeida, L.P. (2012). Machado-Joseph Disease/Spinocerebellar Ataxia Type 3. SPINOCEREBELLAR ATAXIA, Chapter 6.

Nobrega, C., Nascimento-Ferreira, I., Onofre, I., Albuquerque, D., Deglon, N., and de Almeida, L.P. (2014). RNA interference mitigates motor and neuropathological deficits in a cerebellar mouse model of Machado-Joseph disease. PLoS One *9*, e100086.

Nobrega, C., Nascimento-Ferreira, I., Onofre, I., Albuquerque, D., Hirai, H., Deglon, N., and de Almeida, L.P. (2013). Silencing mutant ataxin-3 rescues motor deficits and neuropathology in Machado-Joseph disease transgenic mice. PLoS One *8*, e52396.

Normand, J., and Karasek, M.A. (1995). A method for the isolation and serial propagation of keratinocytes, endothelial cells, and fibroblasts from a single punch biopsy of human skin. In Vitro Cell Dev Biol Anim *31*, 447-455.

Nucifora, F.C., Jr., Sasaki, M., Peters, M.F., Huang, H., Cooper, J.K., Yamada, M., Takahashi, H., Tsuji, S., Troncoso, J., Dawson, V.L*., et al.* (2001). Interference by huntingtin and atrophin-1 with cbp-mediated transcription leading to cellular toxicity. Science *291*, 2423-2428.

O'Connor, M.D., Kardel, M.D., Iosfina, I., Youssef, D., Lu, M., Li, M.M., Vercauteren, S., Nagy, A., and Eaves, C.J. (2008). Alkaline phosphatase-positive colony formation is a sensitive, specific, and quantitative indicator of undifferentiated human embryonic stem cells. Stem Cells *26*, 1109-1116.

Oberheim, N.A., Wang, X., Goldman, S., and Nedergaard, M. (2006). Astrocytic complexity distinguishes the human brain. Trends Neurosci *29*, 547-553.

Okada, Y., Matsumoto, A., Shimazaki, T., Enoki, R., Koizumi, A., Ishii, S., Itoyama, Y., Sobue, G., and Okano, H. (2008). Spatiotemporal recapitulation of central nervous system development by murine embryonic stem cell-derived neural stem/progenitor cells. Stem Cells *26*, 3086-3098.

Okano, H., and Temple, S. (2009). Cell types to order: temporal specification of CNS stem cells. Curr Opin Neurobiol *19*, 112-119.

Okita, K., Matsumura, Y., Sato, Y., Okada, A., Morizane, A., Okamoto, S., Hong, H., Nakagawa, M., Tanabe, K., Tezuka, K*., et al.* (2011). A more efficient method to generate integration-free human iPS cells. Nat Methods *8*, 409-412.

Okita, K., Nakagawa, M., Hyenjong, H., Ichisaka, T., and Yamanaka, S. (2008). Generation of mouse induced pluripotent stem cells without viral vectors. Science *322*, 949-953.

Okita, K., and Yamanaka, S. (2011). Induced pluripotent stem cells: opportunities and challenges. Philos Trans R Soc Lond B Biol Sci *366*, 2198-2207.

Orenstein, S.J., Kuo, S.H., Tasset, I., Arias, E., Koga, H., Fernandez-Carasa, I., Cortes, E., Honig, L.S., Dauer, W., Consiglio, A.*, et al.* (2013). Interplay of LRRK2 with chaperone-mediated autophagy. Nat Neurosci *16*, 394-406.

Orr, H.T., Chung, M.Y., Banfi, S., Kwiatkowski, T.J., Jr., Servadio, A., Beaudet, A.L., McCall, A.E., Duvick, L.A., Ranum, L.P., and Zoghbi, H.Y. (1993). Expansion of an unstable trinucleotide CAG repeat in spinocerebellar ataxia type 1. Nat Genet *4*, 221-226.

Padiath, Q.S., Srivastava, A.K., Roy, S., Jain, S., and Brahmachari, S.K. (2005). Identification of a novel 45 repeat unstable allele associated with a disease phenotype at the MJD1/SCA3 locus. American journal of medical genetics Part B, Neuropsychiatric genetics : the official publication of the International Society of Psychiatric Genetics *133B*, 124-126.

Pankevich, D.E., Altevogt, B.M., Dunlop, J., Gage, F.H., and Hyman, S.E. (2014). Improving and accelerating drug development for nervous system disorders. Neuron *84*, 546-553.

Papapetrou, E.P., and Sadelain, M. (2011). Generation of transgene-free human induced pluripotent stem cells with an excisable single polycistronic vector. Nat Protoc *6*, 1251-1273.

Papapetrou, E.P., Tomishima, M.J., Chambers, S.M., Mica, Y., Reed, E., Menon, J., Tabar, V., Mo, Q., Studer, L., and Sadelain, M. (2009). Stoichiometric and temporal requirements of Oct4, Sox2, Klf4, and c-Myc expression for efficient human iPSC induction and differentiation. Proc Natl Acad Sci U S A *106*, 12759-12764.

Pappano, W.N., Scott, I.C., Clark, T.G., Eddy, R.L., Shows, T.B., and Greenspan, D.S. (1998). Coding sequence and expression patterns of mouse chordin and mapping of the cognate mouse chrd and human CHRD genes. Genomics *52*, 236-239.

Park, I.H., Arora, N., Huo, H., Maherali, N., Ahfeldt, T., Shimamura, A., Lensch, M.W., Cowan, C., Hochedlinger, K., and Daley, G.Q. (2008a). Disease-specific induced pluripotent stem cells. Cell *134*, 877-886.

Park, I.H., Zhao, R., West, J.A., Yabuuchi, A., Huo, H., Ince, T.A., Lerou, P.H., Lensch, M.W., and Daley, G.Q. (2008b). Reprogramming of human somatic cells to pluripotency with defined factors. Nature *451*, 141-146.

Paulson, H. (2012). Machado-Joseph disease/spinocerebellar ataxia type 3. Handb Clin Neurol *103*, 437-449.

Paulson, H.L., Das, S.S., Crino, P.B., Perez, M.K., Patel, S.C., Gotsdiner, D., Fischbeck, K.H., and Pittman, R.N. (1997a). Machado-Joseph disease gene product is a cytoplasmic protein widely expressed in brain. Ann Neurol *41*, 453-462.

Paulson, H.L., Perez, M.K., Trottier, Y., Trojanowski, J.Q., Subramony, S.H., Das, S.S., Vig, P., Mandel, J.L., Fischbeck, K.H., and Pittman, R.N. (1997b). Intranuclear inclusions of expanded polyglutamine protein in spinocerebellar ataxia type 3. Neuron *19*, 333-344.

Pekkanen-Mattila, M., Pelto-Huikko, M., Kujala, V., Suuronen, R., Skottman, H., Aalto-Setala, K., and Kerkela, E. (2010). Spatial and temporal expression pattern of germ layer markers during human embryonic stem cell differentiation in embryoid bodies. Histochem Cell Biol *133*, 595-606.

Perez, M.K., Paulson, H.L., Pendse, S.J., Saionz, S.J., Bonini, N.M., and Pittman, R.N. (1998). Recruitment and the role of nuclear localization in polyglutamine-mediated aggregation. J Cell Biol *143*, 1457-1470.

Perrier, A.L., Tabar, V., Barberi, T., Rubio, M.E., Bruses, J., Topf, N., Harrison, N.L., and Studer, L. (2004). Derivation of midbrain dopamine neurons from human embryonic stem cells. Proc Natl Acad Sci U S A *101*, 12543-12548.

Perutz, M.F. (1999). Glutamine repeats and neurodegenerative diseases. Brain Res Bull *50*, 467.

Perutz, M.F., Johnson, T., Suzuki, M., and Finch, J.T. (1994). Glutamine repeats as polar zippers: their possible role in inherited neurodegenerative diseases. Proc Natl Acad Sci U S A *91*, 5355-5358.

Petros, T.J., Tyson, J.A., and Anderson, S.A. (2011). Pluripotent stem cells for the study of CNS development. Front Mol Neurosci *4*, 30.

Pickford, F., Masliah, E., Britschgi, M., Lucin, K., Narasimhan, R., Jaeger, P.A., Small, S., Spencer, B., Rockenstein, E., Levine, B.*, et al.* (2008). The autophagy-related protein beclin 1 shows reduced expression in early Alzheimer disease and regulates amyloid beta accumulation in mice. J Clin Invest *118*, 2190-2199.

Pilling, D., Fan, T., Huang, D., Kaul, B., and Gomer, R.H. (2009). Identification of markers that distinguish monocyte-derived fibrocytes from monocytes, macrophages, and fibroblasts. PLoS One *4*, e7475.

Pozzi, C., Valtorta, M., Tedeschi, G., Galbusera, E., Pastori, V., Bigi, A., Nonnis, S., Grassi, E., and Fusi, P. (2008). Study of subcellular localization and proteolysis of ataxin-3. Neurobiol Dis *30*, 190-200.

Prokhorova, T.A., Harkness, L.M., Frandsen, U., Ditzel, N., Schroder, H.D., Burns, J.S., and Kassem, M. (2009). Teratoma formation by human embryonic stem cells is site dependent and enhanced by the presence of Matrigel. Stem Cells Dev *18*, 47-54.

Przyborski, S.A. (2001). Isolation of human embryonal carcinoma stem cells by immunomagnetic sorting. Stem Cells *19*, 500-504.

Pulst, S.M., Nechiporuk, A., Nechiporuk, T., Gispert, S., Chen, X.N., Lopes-Cendes, I., Pearlman, S., Starkman, S., Orozco-Diaz, G., Lunkes, A.*, et al.* (1996). Moderate expansion of a normally biallelic trinucleotide repeat in spinocerebellar ataxia type 2. Nat Genet *14*, 269-276.

Purves, D. (2004). Neuroscience, Vol 1, 3rd edn (Sunderland, Mass.: Sinauer Associates, Publishers).

Rakovic, A., Shurkewitsch, K., Seibler, P., Grunewald, A., Zanon, A., Hagenah, J., Krainc, D., and Klein, C. (2013). Phosphatase and tensin homolog (PTEN)-induced putative kinase 1 (PINK1)-dependent ubiquitination of endogenous Parkin attenuates mitophagy: study in human primary fibroblasts and induced pluripotent stem cell-derived neurons. J Biol Chem *288*, 2223-2237.

Ramezani, A., and Hawley, R.G. (2002). Generation of HIV-1-based lentiviral vector particles. Curr Protoc Mol Biol *Chapter 16*, Unit 16 22.

Rami, A. (2009). Review: autophagy in neurodegeneration: firefighter and/or incendiarist? Neuropathol Appl Neurobiol *35*, 449-461.

Ravikumar, B., Vacher, C., Berger, Z., Davies, J.E., Luo, S., Oroz, L.G., Scaravilli, F., Easton, D.F., Duden, R., O'Kane, C.J.*, et al.* (2004). Inhibition of mTOR induces autophagy and reduces toxicity of polyglutamine expansions in fly and mouse models of Huntington disease. Nat Genet *36*, 585-595.

Reina, C.P., Zhong, X., and Pittman, R.N. (2010). Proteotoxic stress increases nuclear localization of ataxin-3. Hum Mol Genet *19*, 235-249.

Reinhardt, P., Schmid, B., Burbulla, L.F., Schondorf, D.C., Wagner, L., Glatza, M., Hoing, S., Hargus, G., Heck, S.A., Dhingra, A.*, et al.* (2013). Genetic correction of a LRRK2 mutation in

human iPSCs links parkinsonian neurodegeneration to ERK-dependent changes in gene expression. Cell Stem Cell *12*, 354-367.

Ren, Y., Jiang, H., Hu, Z., Fan, K., Wang, J., Janoschka, S., Wang, X., Ge, S., and Feng, J. (2014). Parkin mutations reduce the complexity of neuronal processes in iPSC-derived human neurons. Stem Cells *33*, 68-78.

Reubinoff, B.E., Itsykson, P., Turetsky, T., Pera, M.F., Reinhartz, E., Itzik, A., and Ben-Hur, T. (2001). Neural progenitors from human embryonic stem cells. Nat Biotechnol *19*, 1134-1140.

Reynolds, B.A., and Weiss, S. (1992). Generation of neurons and astrocytes from isolated cells of the adult mammalian central nervous system. Science *255*, 1707-1710.

Riess, O., Rub, U., Pastore, A., Bauer, P., and Schols, L. (2008). SCA3: neurological features, pathogenesis and animal models. Cerebellum *7*, 125-137.

Rittie, L., and Fisher, G.J. (2005). Isolation and culture of skin fibroblasts. Methods Mol Med *117*, 83-98.

Robinton, D.A., and Daley, G.Q. (2012). The promise of induced pluripotent stem cells in research and therapy. Nature *481*, 295-305.

Rodda, D.J., Chew, J.L., Lim, L.H., Loh, Y.H., Wang, B., Ng, H.H., and Robson, P. (2005). Transcriptional regulation of nanog by OCT4 and SOX2. J Biol Chem *280*, 24731-24737.

Rodrigues, A.J., do Carmo Costa, M., Silva, T.L., Ferreira, D., Bajanca, F., Logarinho, E., and Maciel, P. (2010). Absence of ataxin-3 leads to cytoskeletal disorganization and increased cell death. Biochim Biophys Acta *1803*, 1154-1163.

Rodrigues, A.J., Neves-Carvalho, A., Teixeira-Castro, A., Rokka, A., Corthals, G., Logarinho, E., and Maciel, P. (2011). Absence of ataxin-3 leads to enhanced stress response in C. elegans. PLoS One *6*, e18512.

Romanul, F.C., Fowler, H.L., Radvany, J., Feldman, R.G., and Feingold, M. (1977). Azorean disease of the nervous system. N Engl J Med *296*, 1505-1508.

Rooney DE, C.B. (1992). Human Cytogenetics: A Practical Approach. Oxford University Press.

Rosenberg, R.N. (1992). Machado-Joseph disease: an autosomal dominant motor system degeneration. Movement disorders : official journal of the Movement Disorder Society *7*, 193-203.

Rosenberg, R.N., Nyhan, W.L., Bay, C., and Shore, P. (1976). Autosomal dominant striatonigral degeneration. A clinical, pathologic, and biochemical study of a new genetic disorder. Neurology *26*, 703-714.

Ross, C.A., and Akimov, S.S. (2014). Human-induced pluripotent stem cells: potential for neurodegenerative diseases. Hum Mol Genet *23*, R17-26.

Ross, C.A., and Poirier, M.A. (2004). Protein aggregation and neurodegenerative disease. Nat Med *10 Suppl*, S10-17.

Ross, C.A., and Poirier, M.A. (2005). Opinion: What is the role of protein aggregation in neurodegeneration? Nat Rev Mol Cell Biol *6*, 891-898.

Ross, C.A., Wood, J.D., Schilling, G., Peters, M.F., Nucifora, F.C., Jr., Cooper, J.K., Sharp, A.H., Margolis, R.L., and Borchelt, D.R. (1999). Polyglutamine pathogenesis. Philos Trans R Soc Lond B Biol Sci *354*, 1005-1011.

Rub, U., Brunt, E.R., and Deller, T. (2008). New insights into the pathoanatomy of spinocerebellar ataxia type 3 (Machado-Joseph disease). Current opinion in neurology *21*, 111-116.

Rub, U., de Vos, R.A., Brunt, E.R., Sebesteny, T., Schols, L., Auburger, G., Bohl, J., Ghebremedhin, E., Gierga, K., Seidel, K.*, et al.* (2006). Spinocerebellar ataxia type 3 (SCA3): thalamic neurodegeneration occurs independently from thalamic ataxin-3 immunopositive neuronal intranuclear inclusions. Brain Pathol *16*, 218-227.

Ryan, S.D., Dolatabadi, N., Chan, S.F., Zhang, X., Akhtar, M.W., Parker, J., Soldner, F., Sunico, C.R., Nagar, S., Talantova, M.*, et al.* (2013). Isogenic human iPSC Parkinson's model shows nitrosative stress-induced dysfunction in MEF2-PGC1alpha transcription. Cell *155*, 1351-1364.

Sakai, T., and Kawakami, H. (1996). Machado-Joseph disease: A proposal of spastic paraplegic subtype. Neurology *46*, 846-847.

Salero, E., and Hatten, M.E. (2007). Differentiation of ES cells into cerebellar neurons. Proc Natl Acad Sci U S A *104*, 2997-3002.

Sanchez-Danes, A., Richaud-Patin, Y., Carballo-Carbajal, I., Jimenez-Delgado, S., Caig, C., Mora, S., Di Guglielmo, C., Ezquerra, M., Patel, B., Giralt, A.*, et al.* (2012). Disease-specific phenotypes in dopamine neurons from human iPS-based models of genetic and sporadic Parkinson's disease. EMBO Mol Med *4*, 380-395.

Sanchez, I., Mahlke, C., and Yuan, J. (2003). Pivotal role of oligomerization in expanded polyglutamine neurodegenerative disorders. Nature *421*, 373-379.

Sanders, L.H., Laganiere, J., Cooper, O., Mak, S.K., Vu, B.J., Huang, Y.A., Paschon, D.E., Vangipuram, M., Sundararajan, R., Urnov, F.D.*, et al.* (2014). LRRK2 mutations cause mitochondrial DNA damage in iPSC-derived neural cells from Parkinson's disease patients: reversal by gene correction. Neurobiol Dis *62*, 381-386.

Sandoe, J., and Eggan, K. (2013). Opportunities and challenges of pluripotent stem cell neurodegenerative disease models. Nat Neurosci *16*, 780-789.

Sanpei, K., Takano, H., Igarashi, S., Sato, T., Oyake, M., Sasaki, H., Wakisaka, A., Tashiro, K., Ishida, Y., Ikeuchi, T.*, et al.* (1996). Identification of the spinocerebellar ataxia type 2 gene using a direct identification of repeat expansion and cloning technique, DIRECT. Nat Genet *14*, 277-284.

Sareen, D., Ebert, A.D., Heins, B.M., McGivern, J.V., Ornelas, L., and Svendsen, C.N. (2012). Inhibition of apoptosis blocks human motor neuron cell death in a stem cell model of spinal muscular atrophy. PLoS One *7*, e39113.

Sasai, Y., Lu, B., Steinbeisser, H., Geissert, D., Gont, L.K., and De Robertis, E.M. (1994). Xenopus chordin: a novel dorsalizing factor activated by organizer-specific homeobox genes. Cell *79*, 779-790.

Saudou, F., Finkbeiner, S., Devys, D., and Greenberg, M.E. (1998). Huntingtin acts in the nucleus to induce apoptosis but death does not correlate with the formation of intranuclear inclusions. Cell *95*, 55-66.

Saute, J.A.M., and Jardim, L.B. (2015). Machado Joseph disease: clinical and genetic aspects, and current treatment. Expert Opinion on Orphan Drugs *3*, 517-535.

Scaffidi, P., and Misteli, T. (2006). Lamin A-dependent nuclear defects in human aging. Science *312*, 1059-1063.

Scannell, J.W., Blanckley, A., Boldon, H., and Warrington, B. (2012). Diagnosing the decline in pharmaceutical R&D efficiency. Nat Rev Drug Discov *11*, 191-200.

Schaffar, G., Breuer, P., Boteva, R., Behrends, C., Tzvetkov, N., Strippel, N., Sakahira, H., Siegers, K., Hayer-Hartl, M., and Hartl, F.U. (2004). Cellular toxicity of polyglutamine expansion proteins: mechanism of transcription factor deactivation. Mol Cell *15*, 95-105.

Scherzinger, E., Lurz, R., Turmaine, M., Mangiarini, L., Hollenbach, B., Hasenbank, R., Bates, G.P., Davies, S.W., Lehrach, H., and Wanker, E.E. (1997). Huntingtin-encoded polyglutamine expansions form amyloid-like protein aggregates in vitro and in vivo. Cell *90*, 549-558.

Schmidt, T., Landwehrmeyer, G.B., Schmitt, I., Trottier, Y., Auburger, G., Laccone, F., Klockgether, T., Volpel, M., Epplen, J.T., Schols, L.*, et al.* (1998). An isoform of ataxin-3 accumulates in the nucleus of neuronal cells in affected brain regions of SCA3 patients. Brain Pathol *8*, 669-679.

Schmidt, T., Lindenberg, K.S., Krebs, A., Schols, L., Laccone, F., Herms, J., Rechsteiner, M., Riess, O., and Landwehrmeyer, G.B. (2002). Protein surveillance machinery in brains with spinocerebellar ataxia type 3: redistribution and differential recruitment of 26S proteasome subunits and chaperones to neuronal intranuclear inclusions. Ann Neurol *51*, 302-310.

Schmitt, I., Linden, M., Khazneh, H., Evert, B.O., Breuer, P., Klockgether, T., and Wuellner, U. (2007). Inactivation of the mouse Atxn3 (ataxin-3) gene increases protein ubiquitination. Biochem Biophys Res Commun *362*, 734-739.

Schneider, E.L., and Mitsui, Y. (1976). The relationship between in vitro cellular aging and in vivo human age. Proceedings of the National Academy of Sciences *73*, 3584-3588.

Schols, L., Amoiridis, G., Buttner, T., Przuntek, H., Epplen, J.T., and Riess, O. (1997). Autosomal dominant cerebellar ataxia: phenotypic differences in genetically defined subtypes? Ann Neurol *42*, 924-932.

Schols, L., Bauer, P., Schmidt, T., Schulte, T., and Riess, O. (2004). Autosomal dominant cerebellar ataxias: clinical features, genetics, and pathogenesis. The Lancet Neurology *3*, 291-304.

Schöls, L., Vieira-Saecker, A.M.M., Schöls, S., Przuntek, H., Epplen, J.T., and Riess, O. (1995). Trinucleotide expansion within the MJD1 gene presents clinically as spinocerebellar ataxia and occurs most frequently in German SCA patients. Human Molecular Genetics *4*, 1001-1005.

Schopperle, W.M., and DeWolf, W.C. (2007). The TRA-1-60 and TRA-1-81 human pluripotent stem cell markers are expressed on podocalyxin in embryonal carcinoma. Stem Cells *25*, 723-730.

Schwartz, J.C., Podell, E.R., Han, S.S., Berry, J.D., Eggan, K.C., and Cech, T.R. (2014). FUS is sequestered in nuclear aggregates in ALS patient fibroblasts. Mol Biol Cell *25*, 2571-2578.

Seibler, P., Graziotto, J., Jeong, H., Simunovic, F., Klein, C., and Krainc, D. (2011). Mitochondrial Parkin recruitment is impaired in neurons derived from mutant PINK1 induced pluripotent stem cells. J Neurosci *31*, 5970-5976.

Seidel, K., den Dunnen, W.F., Schultz, C., Paulson, H., Frank, S., de Vos, R.A., Brunt, E.R., Deller, T., Kampinga, H.H., and Rub, U. (2010). Axonal inclusions in spinocerebellar ataxia type 3. Acta Neuropathol *120*, 449-460.

Seki, T., Yuasa, S., Oda, M., Egashira, T., Yae, K., Kusumoto, D., Nakata, H., Tohyama, S., Hashimoto, H., Kodaira, M.*, et al.* (2010). Generation of induced pluripotent stem cells from human terminally differentiated circulating T cells. Cell Stem Cell *7*, 11-14.

Sergiu, P.P., Georgia, P., and Ricardo, E.D. (2014). Generating Human Neurons In Vitro and Using Them to Understand Neuropsychiatric Disease. Neuroscience *37*, 479-501.

Sermon, K.D., Simon, C., Braude, P., Viville, S., Borstlap, J., and Veiga, A. (2009). Creation of a registry for human embryonic stem cells carrying an inherited defect: joint collaboration between ESHRE and hESCreg. Hum Reprod *24*, 1556-1560.

Shaffer LG, S.M., Campbell LJ (2013). An International System for Human Cytogenetic Nomenclature- Recommendations of the International Standing Committee on Human Cytogenetic Nomenclature. S Karger.

Shaner, N.C., Campbell, R.E., Steinbach, P.A., Giepmans, B.N., Palmer, A.E., and Tsien, R.Y. (2004). Improved monomeric red, orange and yellow fluorescent proteins derived from Discosoma sp. red fluorescent protein. Nat Biotechnol *22*, 1567-1572.

Shao, J., and Diamond, M.I. (2007). Polyglutamine diseases: emerging concepts in pathogenesis and therapy. Hum Mol Genet *16 Spec No. 2*, R115-123.

Shelbourne, P.F., Keller-McGandy, C., Bi, W.L., Yoon, S.R., Dubeau, L., Veitch, N.J., Vonsattel, J.P., Wexler, N.S., Group, U.S.-V.C.R., Arnheim, N.*, et al.* (2007). Triplet repeat mutation length gains correlate with cell-type specific vulnerability in Huntington disease brain. Hum Mol Genet *16*, 1133-1142.

Sheridan, S.D., Surampudi, V., and Rao, R.R. (2012). Analysis of embryoid bodies derived from human induced pluripotent stem cells as a means to assess pluripotency. Stem Cells Int *2012*, 738910.

Shi, Y., Kirwan, P., Smith, J., Robinson, H.P., and Livesey, F.J. (2012). Human cerebral cortex development from pluripotent stem cells to functional excitatory synapses. Nature neuroscience *15*, 477.

Shi, Y., Zhao, Y., and Deng, H. (2010). Powering reprogramming with vitamin C. Cell Stem Cell *6*, 1-2.

Shintani, T., and Klionsky, D.J. (2004). Autophagy in health and disease: a double-edged sword. Science *306*, 990-995.

Si-Tayeb, K., Noto, F.K., Sepac, A., Sedlic, F., Bosnjak, Z.J., Lough, J.W., and Duncan, S.A. (2010). Generation of human induced pluripotent stem cells by simple transient transfection of plasmid DNA encoding reprogramming factors. BMC developmental biology *10*, 81.

Silberg, D.G., Swain, G.P., Suh, E.R., and Traber, P.G. (2000). Cdx1 and cdx2 expression during intestinal development. Gastroenterology *119*, 961-971.

Silva, J., Nichols, J., Theunissen, T.W., Guo, G., van Oosten, A.L., Barrandon, O., Wray, J., Yamanaka, S., Chambers, I., and Smith, A. (2009). Nanog is the gateway to the pluripotent ground state. Cell *138*, 722-737.

Simoes, A.T., Goncalves, N., Koeppen, A., Deglon, N., Kugler, S., Duarte, C.B., and Pereira de Almeida, L. (2012). Calpastatin-mediated inhibition of calpains in the mouse brain prevents mutant ataxin 3 proteolysis, nuclear localization and aggregation, relieving Machado-Joseph disease. Brain *135*, 2428-2439.

Simoes, A.T., Goncalves, N., Nobre, R.J., Duarte, C.B., and Pereira de Almeida, L. (2014). Calpain inhibition reduces ataxin-3 cleavage alleviating neuropathology and motor impairments in mouse models of Machado-Joseph disease. Hum Mol Genet *23*, 4932-4944.

Sinha, S., and Chen, J.K. (2006). Purmorphamine activates the Hedgehog pathway by targeting Smoothened. Nat Chem Biol *2*, 29-30.

Skogh, C., Eriksson, C., Kokaia, M., Meijer, X.C., Wahlberg, L.U., Wictorin, K., and Campbell, K. (2001). Generation of regionally specified neurons in expanded glial cultures derived from the mouse and human lateral ganglionic eminence. Molecular and cellular neurosciences *17*, 811-820.

Skovronsky, D.M., Lee, V.M., and Trojanowski, J.Q. (2006). Neurodegenerative diseases: new concepts of pathogenesis and their therapeutic implications. Annu Rev Pathol *1*, 151-170.

Slow, E.J., Graham, R.K., Osmand, A.P., Devon, R.S., Lu, G., Deng, Y., Pearson, J., Vaid, K., Bissada, N., Wetzel, R.*, et al.* (2005). Absence of behavioral abnormalities and neurodegeneration in vivo despite widespread neuronal huntingtin inclusions. Proc Natl Acad Sci U S A *102*, 11402-11407.

Smith, J.R., Vallier, L., Lupo, G., Alexander, M., Harris, W.A., and Pedersen, R.A. (2008). Inhibition of Activin/Nodal signaling promotes specification of human embryonic stem cells into neuroectoderm. Dev Biol *313*, 107-117.

Smith, W.C., and Harland, R.M. (1992). Expression cloning of noggin, a new dorsalizing factor localized to the Spemann organizer in Xenopus embryos. Cell *70*, 829-840.

Soldner, F., Hockemeyer, D., Beard, C., Gao, Q., Bell, G.W., Cook, E.G., Hargus, G., Blak, A., Cooper, O., Mitalipova, M.*, et al.* (2009). Parkinson's disease patient-derived induced pluripotent stem cells free of viral reprogramming factors. Cell *136*, 964-977.

Soldner, F., Laganiere, J., Cheng, A.W., Hockemeyer, D., Gao, Q., Alagappan, R., Khurana, V., Golbe, L.I., Myers, R.H., Lindquist, S.*, et al.* (2011). Generation of isogenic pluripotent stem cells differing exclusively at two early onset Parkinson point mutations. Cell *146*, 318-331.

Solter, D. (2006). From teratocarcinomas to embryonic stem cells and beyond: a history of embryonic stem cell research. Nature reviews Genetics *7*, 319-327.

Somers, A., Jean, J.C., Sommer, C.A., Omari, A., Ford, C.C., Mills, J.A., Ying, L., Sommer, A.G., Jean, J.M., Smith, B.W.*, et al.* (2010). Generation of transgene-free lung disease-specific human induced pluripotent stem cells using a single excisable lentiviral stem cell cassette. Stem Cells *28*, 1728-1740.

Sommer, C.A., Sommer, A.G., Longmire, T.A., Christodoulou, C., Thomas, D.D., Gostissa, M., Alt, F.W., Murphy, G.J., Kotton, D.N., and Mostoslavsky, G. (2010). Excision of reprogramming transgenes improves the differentiation potential of iPS cells generated with a single excisable vector. Stem Cells *28*, 64-74.

Sommer, C.A., Stadtfeld, M., Murphy, G.J., Hochedlinger, K., Kotton, D.N., and Mostoslavsky, G. (2009). Induced pluripotent stem cell generation using a single lentiviral stem cell cassette. Stem Cells *27*, 543-549.

Sonntag, K.C., Pruszak, J., Yoshizaki, T., van Arensbergen, J., Sanchez-Pernaute, R., and Isacson, O. (2007). Enhanced yield of neuroepithelial precursors and midbrain-like dopaminergic neurons from human embryonic stem cells using the bone morphogenic protein antagonist noggin. Stem Cells *25*, 411-418.

Sousa, V., Espirito Santo, J., Silva, M., Cabral, T., Alarcao, A.M., Gomes, A., Couceiro, P., and Carvalho, L. (2011). EGFR/erB-1, HER2/erB-2, CK7, LP34, Ki67 and P53 expression in preneoplastic lesions of bronchial epithelium: an immunohistochemical and genetic study. Virchows Archiv : an international journal of pathology *458*, 571-581.

Spits, C., Mateizel, I., Geens, M., Mertzanidou, A., Staessen, C., Vandeskelde, Y., Van der Elst, J., Liebaers, I., and Sermon, K. (2008). Recurrent chromosomal abnormalities in human embryonic stem cells. Nat Biotechnol *26*, 1361-1363.

Sproul, A.A., Jacob, S., Pre, D., Kim, S.H., Nestor, M.W., Navarro-Sobrino, M., Santa-Maria, I., Zimmer, M., Aubry, S., Steele, J.W.*, et al.* (2014). Characterization and molecular profiling of PSEN1 familial Alzheimer's disease iPSC-derived neural progenitors. PLoS One *9*, e84547.

Sridhar, S., Botbol, Y., Macian, F., and Cuervo, A.M. (2012). Autophagy and disease: always two sides to a problem. J Pathol *226*, 255-273.

Srikanth, P., and Young-Pearse, T.L. (2014). Stem cells on the brain: modeling neurodevelopmental and neurodegenerative diseases using human induced pluripotent stem cells. J Neurogenet *28*, 5-29.

St George-Hyslop, P., Rogaeva, E., Huterer, J., Tsuda, T., Santos, J., Haines, J.L., Schlumpf, K., Rogaev, E.I., Liang, Y., and McLachlan, D.R. (1994). Machado-Joseph disease in pedigrees of Azorean descent is linked to chromosome 14. American journal of human genetics *55*, 120-125.

Stadtfeld, M., Brennand, K., and Hochedlinger, K. (2008a). Reprogramming of pancreatic beta cells into induced pluripotent stem cells. Curr Biol *18*, 890-894.

Stadtfeld, M., and Hochedlinger, K. (2010). Induced pluripotency: history, mechanisms, and applications. Genes & Development *24*.

Stadtfeld, M., Maherali, N., Breault, D.T., and Hochedlinger, K. (2008b). Defining molecular cornerstones during fibroblast to iPS cell reprogramming in mouse. Cell Stem Cell *2*, 230-240.

Stadtfeld, M., Nagaya, M., Utikal, J., Weir, G., and Hochedlinger, K. (2008c). Induced pluripotent stem cells generated without viral integration. Science *322*, 945-949.

Sterneckert, J.L., Reinhardt, P., and Scholer, H.R. (2014). Investigating human disease using stem cell models. Nature reviews Genetics *15*, 625-639.

Stuart, M.C., Christopher, A.F., Eirini, P.P., Mark, T., Michel, S., and Lorenz, S. (2009). Highly efficient neural conversion of human ES and iPS cells by dual inhibition of SMAD signaling. Nature Biotechnology *27*.

Studer, L., Vera, E., and Cornacchia, D. (2015). Programming and Reprogramming Cellular Age in the Era of Induced Pluripotency. Cell Stem Cell *16*, 591-600.

Su, Y.C., and Qi, X. (2013). Inhibition of excessive mitochondrial fission reduced aberrant autophagy and neuronal damage caused by LRRK2 G2019S mutation. Hum Mol Genet *22*, 4545-4561.

Subramanyam, D., Lamouille, S., Judson, R.L., Liu, J.Y., Bucay, N., Derynck, R., and Blelloch, R. (2011). Multiple targets of miR-302 and miR-372 promote reprogramming of human fibroblasts to induced pluripotent stem cells. Nat Biotechnol *29*, 443-448.

Sudarsky, L., and Coutinho, P. (1995). Machado-Joseph disease. Clinical neuroscience *3*, 17-22.

Sun, N., Panetta, N.J., Gupta, D.M., Wilson, K.D., Lee, A., Jia, F., Hu, S., Cherry, A.M., Robbins, R.C., Longaker, M.T.*, et al.* (2009). Feeder-free derivation of induced pluripotent stem cells from adult human adipose stem cells. Proc Natl Acad Sci U S A *106*, 15720-15725.

Suter, D.M., Tirefort, D., Julien, S., and Krause, K.H. (2009). A Sox1 to Pax6 switch drives neuroectoderm to radial glia progression during differentiation of mouse embryonic stem cells. Stem Cells *27*, 49-58.

Swistowski, A., Peng, J., Liu, Q., Mali, P., Rao, M.S., Cheng, L., and Zeng, X. (2010). Efficient generation of functional dopaminergic neurons from human induced pluripotent stem cells under defined conditions. Stem Cells *28*, 1893-1904.

Switonski, P.M., Fiszer, A., Kazmierska, K., Kurpisz, M., Krzyzosiak, W.J., and Figiel, M. (2011). Mouse ataxin-3 functional knock-out model. Neuromolecular medicine *13*, 54-65.

Tait, D. (1998). Ataxin-3 is transported into the nucleus and associates with the nuclear matrix. Human Molecular Genetics *7*, 991-997.

Takahashi, A., Camacho, P., Lechleiter, J.D., and Herman, B. (1999). Measurement of intracellular calcium. Physiol Rev *79*, 1089-1125.

Takahashi, K., Tanabe, K., Ohnuki, M., Narita, M., Ichisaka, T., Tomoda, K., and Yamanaka, S. (2007). Induction of pluripotent stem cells from adult human fibroblasts by defined factors. Cell *131*, 861-872.

Takahashi, K., and Yamanaka, S. (2006). Induction of pluripotent stem cells from mouse embryonic and adult fibroblast cultures by defined factors. Cell *126*, 663-676.

Takahashi, T., Kikuchi, S., Katada, S., Nagai, Y., Nishizawa, M., and Onodera, O. (2008). Soluble polyglutamine oligomers formed prior to inclusion body formation are cytotoxic. Hum Mol Genet *17*, 345-356.

Takashima, A. (2001). Establishment of fibroblast cultures. Curr Protoc Cell Biol *Chapter 2*, Unit 2 1.

Takiyama, Y., Nishizawa, M., Tanaka, H., Kawashima, S., Sakamoto, H., Karube, Y., Shimazaki, H., Soutome, M., Endo, K., Ohta, S*., et al.* (1993). The gene for Machado-Joseph disease maps to human chromosome 14q. Nat Genet *4*, 300-304.

Takiyama, Y., Sakoe, K., Nakano, I., and Nishizawa, M. (1997). Machado-Joseph disease: cerebellar ataxia and autonomic dysfunction in a patient with the shortest known expanded allele (56 CAG repeat units) of the MJD1 gene. Neurology *49*, 604-606.

Teixeira-Castro, A., Ailion, M., Jalles, A., Brignull, H.R., Vilaca, J.L., Dias, N., Rodrigues, P., Oliveira, J.F., Neves-Carvalho, A., Morimoto, R.I*., et al.* (2011). Neuron-specific proteotoxicity of mutant ataxin-3 in C. elegans: rescue by the DAF-16 and HSF-1 pathways. Hum Mol Genet *20*, 2996-3009.

Temple, S. (2001). The development of neural stem cells. Nature *414*, 112-117.

Teo, A.K., Arnold, S.J., Trotter, M.W., Brown, S., Ang, L.T., Chng, Z., Robertson, E.J., Dunn, N.R., and Vallier, L. (2011). Pluripotency factors regulate definitive endoderm specification through eomesodermin. Genes Dev *25*, 238-250.

Thomson, J.A., Itskovitz-Eldor, J., Shapiro, S.S., Waknitz, M.A., Swiergiel, J.J., Marshall, V.S., and Jones, J.M. (1998). Embryonic stem cell lines derived from human blastocysts. Science *282*, 1145-1147.

Tiscornia, G., Vivas, E.L., and Izpisua Belmonte, J.C. (2011). Diseases in a dish: modeling human genetic disorders using induced pluripotent cells. Nat Med *17*, 1570-1576.

Trottier, Y., Cancel, G., An-Gourfinkel, I., Lutz, Y., Weber, C., Brice, A., Hirsch, E., and Mandel, J.L. (1998). Heterogeneous intracellular localization and expression of ataxin-3. Neurobiol Dis *5*, 335-347.

Tuite, P.J., Rogaeva, E.A., St George-Hyslop, P.H., and Lang, A.E. (1995). Dopa-responsive parkinsonism phenotype of Machado-Joseph disease: confirmation of 14q CAG expansion. Ann Neurol *38*, 684-687.

Urbach, A., Bar-Nur, O., Daley, G.Q., and Benvenisty, N. (2010). Differential modeling of fragile X syndrome by human embryonic stem cells and induced pluripotent stem cells. Cell Stem Cell *6*, 407-411.

Val, M.M., Mendes, L.A., Alarcao, A., Carvalho, L., Carreira, I., Rodrigues, C.F., and Alpoim, M.C. (2015). Senescent bronchial fibroblasts induced to senescence by Cr(VI) promote epithelial-mesenchymal transition when co-cultured with bronchial epithelial cells in the presence of Cr(VI). Mutagenesis *30*, 277-286.

Valenzuela, D.M., Economides, A.N., Rojas, E., Lamb, T.M., Nunez, L., Jones, P., Lp, N.Y., Espinosa, R., 3rd, Brannan, C.I., Gilbert, D.J.*, et al.* (1995). Identification of mammalian noggin and its expression in the adult nervous system. J Neurosci *15*, 6077-6084.

van Alfen, N., Sinke, R.J., Zwarts, M.J., Gabreels-Festen, A., Praamstra, P., Kremer, B.P., and Horstink, M.W. (2001). Intermediate CAG repeat lengths (53,54) for MJD/SCA3 are associated with an abnormal phenotype. Ann Neurol *49*, 805-807.

van der Worp, H.B., Howells, D.W., Sena, E.S., Porritt, M.J., Rewell, S., O'Collins, V., and Macleod, M.R. (2010). Can animal models of disease reliably inform human studies? PLoS medicine *7*, e1000245.

Vassilieva, S., Goh, H.N., Lau, K.X., Hughes, J.N., Familari, M., Rathjen, P.D., and Rathjen, J. (2012). A system to enrich for primitive streak-derivatives, definitive endoderm and mesoderm, from pluripotent cells in culture. PLoS One *7*, e38645.

Vera, E., and Studer, L. (2015). When rejuvenation is a problem: challenges of modeling late-onset neurodegenerative disease. Development *142*, 3085-3089.

Wainger, B.J., Kiskinis, E., Mellin, C., Wiskow, O., Han, S.S., Sandoe, J., Perez, N.P., Williams, L.A., Lee, S., Boulting, G.*, et al.* (2014). Intrinsic membrane hyperexcitability of amyotrophic lateral sclerosis patient-derived motor neurons. Cell Rep *7*, 1-11.

Wang, G., Ide, K., Nukina, N., Goto, J., Ichikawa, Y., Uchida, K., Sakamoto, T., and Kanazawa, I. (1997). Machado-Joseph disease gene product identified in lymphocytes and brain. Biochem Biophys Res Commun *233*, 476-479.

Wang, Q., Xu, X., Li, J., Liu, J., Gu, H., Zhang, R., Chen, J., Kuang, Y., Fei, J., Jiang, C.*, et al.* (2011). Lithium, an anti-psychotic drug, greatly enhances the generation of induced pluripotent stem cells. Cell research *21*, 1424-1435.

Wang, S., Wang, B., Pan, N., Fu, L., Wang, C., Song, G., An, J., Liu, Z., Zhu, W., Guan, Y.*, et al.* (2015). Differentiation of human induced pluripotent stem cells to mature functional Purkinje neurons. Sci Rep *5*, 9232.

Ward, R.J., Zucca, F.A., Duyn, J.H., Crichton, R.R., and Zecca, L. (2014). The role of iron in brain ageing and neurodegenerative disorders. The Lancet Neurology *13*, 1045-1060.

Warlich, E., Kuehle, J., Cantz, T., Brugman, M.H., Maetzig, T., Galla, M., Filipczyk, A.A., Halle, S., Klump, H., Scholer, H.R.*, et al.* (2011). Lentiviral vector design and imaging approaches to visualize the early stages of cellular reprogramming. Mol Ther *19*, 782-789.

Warrick, J.M., Chan, H.Y., Gray-Board, G.L., Chai, Y., Paulson, H.L., and Bonini, N.M. (1999). Suppression of polyglutamine-mediated neurodegeneration in Drosophila by the molecular chaperone HSP70. Nat Genet *23*, 425-428.

Warrick, J.M., Morabito, L.M., Bilen, J., Gordesky-Gold, B., Faust, L.Z., Paulson, H.L., and Bonini, N.M. (2005). Ataxin-3 suppresses polyglutamine neurodegeneration in Drosophila by a ubiquitin-associated mechanism. Mol Cell *18*, 37-48.

Watanabe, K., Kamiya, D., Nishiyama, A., Katayama, T., Nozaki, S., Kawasaki, H., Watanabe, Y., Mizuseki, K., and Sasai, Y. (2005). Directed differentiation of telencephalic precursors from embryonic stem cells. Nat Neurosci *8*, 288-296.

Weber, J.J., Sowa, A.S., Binder, T., and Hubener, J. (2014). From pathways to targets: understanding the mechanisms behind polyglutamine disease. BioMed research international *2014*, 701758.

Weismann, A. (1885). Die Continuitat des Keimplasmas als Grundlage einer Theorie der Vererbung. Jena (Gustav Fisher).

Wellington, C.L., Ellerby, L.M., Hackam, A.S., Margolis, R.L., Trifiro, M.A., Singaraja, R., McCutcheon, K., Salvesen, G.S., Propp, S.S., Bromm, M.*, et al.* (1998). Caspase cleavage of gene products associated with triplet expansion disorders generates truncated fragments containing the polyglutamine tract. J Biol Chem *273*, 9158-9167.

Wernig, M., Meissner, A., Cassady, J.P., and Jaenisch, R. (2008). c-Myc is dispensable for direct reprogramming of mouse fibroblasts. Cell Stem Cell *2*, 10-12.

Wernig, M., Meissner, A., Foreman, R., Brambrink, T., Ku, M., Hochedlinger, K., Bernstein, B.E., and Jaenisch, R. (2007). In vitro reprogramming of fibroblasts into a pluripotent ES-cell-like state. Nature *448*, 318-324.

Wesselschmidt, R.L. (2011). The teratoma assay: an in vivo assessment of pluripotency. Methods in molecular biology *767*, 231-241.

Williams, A.J., and Paulson, H.L. (2008). Polyglutamine neurodegeneration: protein misfolding revisited. Trends Neurosci *31*, 521-528.

Wilmut, I., Schnieke, A.E., McWhir, J., Kind, A.J., and Campbell, K.H. (1997). Viable offspring derived from fetal and adult mammalian cells. Nature *385*, 810-813.

Wilmut, I., Sullivan, G., and Chambers, I. (2011). The evolving biology of cell reprogramming. Philos Trans R Soc Lond B Biol Sci *366*, 2183-2197.

Wilson, P.A., Lagna, G., Suzuki, A., and Hemmati-Brivanlou, A. (1997). Concentration-dependent patterning of the Xenopus ectoderm by BMP4 and its signal transducer Smad1. Development *124*, 3177-3184.

Winborn, B.J., Travis, S.M., Todi, S.V., Scaglione, K.M., Xu, P., Williams, A.J., Cohen, R.E., Peng, J., and Paulson, H.L. (2008). The deubiquitinating enzyme ataxin-3, a polyglutamine disease protein, edits Lys63 linkages in mixed linkage ubiquitin chains. J Biol Chem *283*, 26436-26443.

Wong, E., and Cuervo, A.M. (2010a). Autophagy gone awry in neurodegenerative diseases. Nat Neurosci *13*, 805-811.

Wong, E., and Cuervo, A.M. (2010b). Integration of clearance mechanisms: the proteasome and autophagy. Cold Spring Harb Perspect Biol *2*, a006734.

Woods, B.T., and Schaumburg, H.H. (1972). Nigro-spino-dentatal degeneration with nuclear ophthalmoplegia. A unique and partially treatable clinico-pathological entity. J Neurol Sci *17*, 149-166.

Wray, S., Self, M., Consortium, N.P.s.D.i., Consortium, N.H.s.D.i., Consortium, N.A.i., Lewis, P.A., Taanman, J.W., Ryan, N.S., Mahoney, C.J., Liang, Y.*, et al.* (2012). Creation of an open-access, mutation-defined fibroblast resource for neurological disease research. PLoS One *7*, e43099.

Xia, G., Santostefano, K., Hamazaki, T., Liu, J., Subramony, S.H., Terada, N., and Ashizawa, T. (2013). Generation of human-induced pluripotent stem cells to model spinocerebellar ataxia type 2 in vitro. J Mol Neurosci *51*, 237-248.

Xu, X., Pantakani, D.V., Luhrig, S., Tan, X., Khromov, T., Nolte, J., Dressel, R., Zechner, U., and Engel, W. (2011). Stage-specific germ-cell marker genes are expressed in all mouse pluripotent cell types and emerge early during induced pluripotency. PLoS One *6*, e22413.

Xu, Y., Shi, Y., and Ding, S. (2008). A chemical approach to stem-cell biology and regenerative medicine. Nature *453*, 338-344.

Yagi, T., Ito, D., Okada, Y., Akamatsu, W., Nihei, Y., Yoshizaki, T., Yamanaka, S., Okano, H., and Suzuki, N. (2011). Modeling familial Alzheimer's disease with induced pluripotent stem cells. Hum Mol Genet *20*, 4530-4539.

Yakubov, E., Rechavi, G., Rozenblatt, S., and Givol, D. (2010). Reprogramming of human fibroblasts to pluripotent stem cells using mRNA of four transcription factors. Biochem Biophys Res Commun *394*, 189-193.

Yamada, M., Hayashi, S., Tsuji, S., and Takahashi, H. (2001). Involvement of the cerebral cortex and autonomic ganglia in Machado-Joseph disease. Acta Neuropathol *101*, 140-144.

Yamanaka, S. (2009). Elite and stochastic models for induced pluripotent stem cell generation. Nature *460*, 49-52.

Yan, X., Qin, H., Qu, C., Tuan, R.S., Shi, S., and Huang, G.T. (2010). iPS cells reprogrammed from human mesenchymal-like stem/progenitor cells of dental tissue origin. Stem Cells Dev *19*, 469-480.

Yan, Y., Yang, D., Zarnowska, E.D., Du, Z., Werbel, B., Valliere, C., Pearce, R.A., Thomson, J.A., and Zhang, S.C. (2005). Directed differentiation of dopaminergic neuronal subtypes from human embryonic stem cells. Stem Cells *23*, 781-790.

Yang, W., Dunlap, J.R., Andrews, R.B., and Wetzel, R. (2002). Aggregated polyglutamine peptides delivered to nuclei are toxic to mammalian cells. Hum Mol Genet *11*, 2905-2917.

Yoshida, H., Yoshizawa, T., Shibasaki, F., Shoji, S., and Kanazawa, I. (2002). Chemical chaperones reduce aggregate formation and cell death caused by the truncated Machado-Joseph disease gene product with an expanded polyglutamine stretch. Neurobiol Dis *10*, 88-99.

Yoshioka, N., Gros, E., Li, H.R., Kumar, S., Deacon, D.C., Maron, C., Muotri, A.R., Chi, N.C., Fu, X.D., Yu, B.D.*, et al.* (2013). Efficient generation of human iPSCs by a synthetic self-replicative RNA. Cell Stem Cell *13*, 246-254.

Young, M.A., Larson, D.E., Sun, C.W., George, D.R., Ding, L., Miller, C.A., Lin, L., Pawlik, K.M., Chen, K., Fan, X.*, et al.* (2012). Background mutations in parental cells account for most of the genetic heterogeneity of induced pluripotent stem cells. Cell Stem Cell *10*, 570-582.

Yu, J., Hu, K., Smuga-Otto, K., Tian, S., Stewart, R., Slukvin, II, and Thomson, J.A. (2009a). Human induced pluripotent stem cells free of vector and transgene sequences. Science *324*, 797-801.

Yu, J., Vodyanik, M.A., Smuga-Otto, K., Antosiewicz-Bourget, J., Frane, J.L., Tian, S., Nie, J., Jonsdottir, G.A., Ruotti, V., Stewart, R.*, et al.* (2007). Induced pluripotent stem cell lines derived from human somatic cells. Science *318*, 1917-1920.

Yu, Y.C., Kuo, C.L., Cheng, W.L., Liu, C.S., and Hsieh, M. (2009b). Decreased antioxidant enzyme activity and increased mitochondrial DNA damage in cellular models of Machado-Joseph disease. J Neurosci Res *87*, 1884-1891.

Yuan, S.H., Martin, J., Elia, J., Flippin, J., Paramban, R.I., Hefferan, M.P., Vidal, J.G., Mu, Y., Killian, R.L., Israel, M.A.*, et al.* (2011). Cell-surface marker signatures for the isolation of neural stem cells, glia and neurons derived from human pluripotent stem cells. PLoS One *6*, e17540.

Zaehres, H., and Scholer, H.R. (2007). Induction of pluripotency: from mouse to human. Cell *131*, 834-835.

Zeng, H., Guo, M., Martins-Taylor, K., Wang, X., Zhang, Z., Park, J.W., Zhan, S., Kronenberg, M.S., Lichtler, A., Liu, H.X.*, et al.* (2010). Specification of region-specific neurons including forebrain glutamatergic neurons from human induced pluripotent stem cells. PLoS One *5*, e11853.

Zhang, L., Leeflang, E.P., Yu, J., and Arnheim, N. (1994). Studying human mutations by sperm typing: instability of CAG trinucleotide repeats in the human androgen receptor gene. Nat Genet *7*, 531-535.

Zhang, N., An, M.C., Montoro, D., and Ellerby, L.M. (2010). Characterization of Human Huntington's Disease Cell Model from Induced Pluripotent Stem Cells. PLoS Curr *2*, RRN1193.

Zhang, S.C. (2006). Neural subtype specification from embryonic stem cells. Brain Pathol *16*, 132-142.

Zhang, S.C., Wernig, M., Duncan, I.D., Brustle, O., and Thomson, J.A. (2001). In vitro differentiation of transplantable neural precursors from human embryonic stem cells. Nat Biotechnol *19*, 1129-1133.

Zhang, W. (2014). Teratoma formation: A tool for monitoring pluripotency in stem cell research. StemBook.

Zhou, H., Wu, S., Joo, J.Y., Zhu, S., Han, D.W., Lin, T., Trauger, S., Bien, G., Yao, S., Zhu, Y., *et al.* (2009). Generation of induced pluripotent stem cells using recombinant proteins. Cell Stem Cell *4*, 381-384.

Zhou, J., Su, P., Li, D., Tsang, S., Duan, E., and Wang, F. (2010). High-efficiency induction of neural conversion in human ESCs and human induced pluripotent stem cells with a single chemical inhibitor of transforming growth factor beta superfamily receptors. Stem Cells *28*, 1741-1750.

Zhou, L., Wang, H., Wang, P., Ren, H., Chen, D., Ying, Z., and Wang, G. (2013). Ataxin-3 protects cells against H2O2-induced oxidative stress by enhancing the interaction between Bcl-X(L) and Bax. Neuroscience *243*, 14-21.

Zhou, W., and Freed, C.R. (2009). Adenoviral gene delivery can reprogram human fibroblasts to induced pluripotent stem cells. Stem Cells *27*, 2667-2674.

Zhu, S., Li, W., Zhou, H., Wei, W., Ambasudhan, R., Lin, T., Kim, J., Zhang, K., and Ding, S. (2010). Reprogramming of human primary somatic cells by OCT4 and chemical compounds. Cell Stem Cell *7*, 651-655.

Zhuchenko, O., Bailey, J., Bonnen, P., Ashizawa, T., Stockton, D.W., Amos, C., Dobyns, W.B., Subramony, S.H., Zoghbi, H.Y., and Lee, C.C. (1997). Autosomal dominant cerebellar ataxia

(SCA6) associated with small polyglutamine expansions in the alpha 1A-voltage-dependent calcium channel. Nat Genet *15*, 62-69.

Zou, J., Maeder, M.L., Mali, P., Pruett-Miller, S.M., Thibodeau-Beganny, S., Chou, B.K., Chen, G., Ye, Z., Park, I.H., Daley, G.Q.*, et al.* (2009). Gene targeting of a disease-related gene in human induced pluripotent stem and embryonic stem cells. Cell Stem Cell *5*, 97-110.